

32nd International Gemmological Conference IGC

July 2011
Interlaken, Switzerland

32nd International Gemmological Conference IGC

July 2011

Interlaken, Switzerland

Dear Participant of the 32nd IGC Conference in Interlaken, Switzerland

Two years after the last IGC Conference - organised by John Saul and his family in Arusha, Tanzania - it is our great pleasure to now host this event in Switzerland, 39 years after the last IGC Conference was held in Switzerland in 1972.

The IGC has always been a platform to present and discuss the latest research in gemmology. But apart from this, it has also been a great opportunity to meet old and new friends and to share not only science, but also friendship during the meeting.

In this spirit, I wish you in the name of the whole organising team an exciting and inspiring IGC Conference with lots of gemmological inputs for your own gemmological research and work.

June 2011

Michael S. Krzemnicki, SSEF

About the organising Committee for the 32nd IGC Conference:

Organisers

Michael S. Krzemnicki, Swiss Gemmological Institute SSEF
Laurent Cartier, Swiss Gemmological Institute SSEF
George Bosshart
Anne Bosshart
Walter Balmer
Henry A. Hänni, Swiss Gemmological Institute SSEF & GemExpert
Michael Hügi, Swiss Gemmological Society SGS
Thomas Frieden, Swiss Gemmological Society SGS, Frieden AG

Local planning & Social programme:

Walter Balmer

Abstract Review Board:

George Bosshart,
Henry A. Hänni, Swiss Gemmological Institute SSEF & GemExpert,

Layout & Editing & Website:

Laurent Cartier, Swiss Gemmological Institute

Organising an IGC Conference is only possible with a strong and committed team. I would like to thank my colleagues for their support, which has made this conference possible.

Special thanks go to:

- George Bosshart for his tremendous work finalizing the abstract versions for the Conference Proceedings and Henry A. Hänni for reviewing the submitted abstracts.
- Anne Bosshart for setting up a spectacular Accompanying programme in the heart of Switzerland.
- Walter Balmer, who with his local „network“ in Interlaken (see also sponsors!) has been a great support for me, actually from the first moment when the decision was taken during the last IGC in Tanzania 2009 to host this Conference in Switzerland.

Finally, I also would like to thank Laurent Cartier very much for his assistance in organising the Conference and the excursions, communicating with the participants, and layouting and editing the website and these Conference proceedings.

June 2011

Michael. S. Krzemnicki

About the IGC Executive Board

In 2009, four new members (Jayshree Panjekar, George Bosshart, Hanco Zwaan, and Michael S. Krzemnicki) joined the IGC Executive Board replacing long-standing Board members Dr. Jan Kanis, Mr. Alan Jobbins, Prof. Ichiro Sunagawa, and Prof. Hermann Bank, who were awarded the honorary membership of the IGC in acknowledging the contributions they made to IGC in the past.



Photo of the new IGC Executive Board, taken in October 2009 in Arusha:

(From left to right) Hanco Zwaan, Jayshree Panjekar, George Bosshart, Emmanuel Fritsch, Tay Thye Sun, Gamini Zoysa, Michael S. Krzemnicki, John Saul, together with Mark Saul (standing). Not on the photo: John Koivula and Henry A. Hänni.

Pre-conference excursion: 11-13 July 2011. Bern, Ticino and Swiss Alps.

Conference: 13-17 July 2011. Interlaken, Switzerland.

Post-conference excursion: 18-20 July 2011. Bernese Alps, Binn valley, Zermatt.

Guest programme: 13-16 July 2011. Frutigen, Bern, Ballenberg, Lauterbrunnen, Schilthorn.

About the venue

Interlaken

Interlaken is a small town in the heart of Switzerland, beautifully located between the lakes of Brienz and Thun, and surrounded by the Swiss Alps, among them the famous Eiger, Mönch and Jungfrau with the train station „Top of Europe“ in the midst of glaciers.

We have chosen Interlaken not only because of the conference infrastructure it offers, but mainly, because of the spectacular setting with plenty of possibilities to enjoy the Swiss nature and culture.

The organising committee has planned a number of social activities, which include a visit to the Harder Kulm and the Gala Dinner at the Hotel Giessbach close to the famous Giessbach falls, not to mention a traditional Swiss folklore night with the hope to make you this Conference a lasting souvenir.

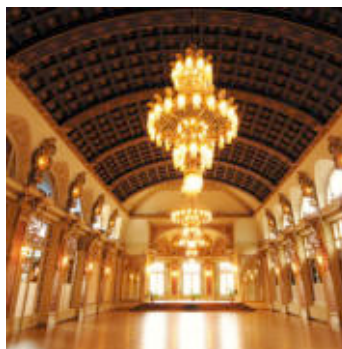


Spectacular view on Interlaken and the Eiger, Mönch and Jungfrau summits.



The Conference Venue

The Conference will be held at the Interlaken Congress centre, perfectly equipped to host the 32nd IGC Conference. We have at our disposition the Ballsaal (dancing room), where all presentations will be given. At the back of the Ballsaal, the posters will be presented, together with a few product presentations of our sponsors. In the adjacent Rondell, the Interlaken Congress centre Catering will offer small snacks and coffee during coffee breaks and lunch during lunch breaks.



About the Sponsors

The organisers would like to thank the following sponsors, which have kindly contributed with their sponsorship to organise the IGC Conference in Interlaken.

Bödeli www.kabel-tv-boedeli.ch/

GemExpert www.gemexpert.ch

Swiss Gemmological Institute SSEF www.ssef.ch

Polytec GmbH www.polytec.de

Bruker Switzerland www.bruker.ch

System Eickhorst www.eickhorst



IGC 2011 Programme

Interlaken, Switzerland 13-17 July 2011

Wednesday 13 July

18.00-20.30 IGC Welcome reception in Interlaken at the Grand Hotel Victoria Jungfrau
20.30-22.00 Executive Committee (EXECO) reunion

Thursday 14 July

Coloured Stones

9.00-9.20 Opening ceremony and Announcements

9.20-10.05 Invited lecture by Prof. T. Armbruster, University of Berne, Switzerland :
Gemmology at the Interface between Mineralogy and Crystallography

Tourmaline, Garnet, Spodumene, Spinel, Turquoise (Chairman John Koivula)

10.05-10.25 Karl Schmetzer et al : Trapiche tourmaline from Zambia –chemical and structural zoning

10.25-10.45 Federico Pezzotta et al: Gem tourmaline from Elba Island, Italy

10.45-11.05 Coffee break

11.05-11.25 Ulrich Henn et al: Mn-bearing grossular garnet

11.25-11.45 George Bosshart et al: Colorimetric investigation of unstable and stable spodumene colours

11.45-12.05 Furuya Masaki Colouring agents and their spectra in blue spinel

12.05-12.25 Jean Marie Dereppe et al : EPR of turquoise and some of its imitations

12.25-14.00 Lunch

Quartz, Opals (Chairman Lin Sutherland)

- 14.00-14.20 Jorgen Schnellrath et al.: Quartz cat's eyes with unusual fibre distribution patterns
- 14.20-14.40 Claudio Milisenda et al : Irradiated blue common opal from Brazil
- 14.40-15.00 Benjamin Rondeau et al : Play-of-colour opal from Wollo, Ethiopia: a new pedogenetic model for gem opal formation
- 15.00-16.00 Poster session (see below)
- 15.40-16.00 Coffee break

Beryls

- 16.00-16.20 Henry Hänni : Beryl – 30 years later
- 16.20-16.40 Liu Shang-l et al: Study of an extraordinary Cs- and Li-rich beryl from Madagascar
- 16.40-17.00 Hanco Zwaan et al. : Preliminary report on emeralds from the Fazenda Bonfim region, Rio Grande do Norte, Brazil
- 17.00 Conference closes
- 19.00 Meeting point Kursaal entrance for walk to Harder Kulm train station
- 19.30-22.00 Dinner at Harder Kulm Restaurant

Friday 15 July**Pearls / Diamonds**

- 8.00-8.45 EXECO reunion

Pearls (Chairman Hanco Zwaan)

- 9.00-9.20 Elisabeth Strack : An overview of production techniques for Chinese freshwater cultured pearls
- 9.20- 9.40 Michael Krzemnicki et al.: External and internal structures of Tokki pearls: additional cultured pearls formed during pearl cultivation

- 9.40-10.00 Nick Sturman et al. Cultured Queen Conch pearls – A comparison to natural Queen Conch pearls
- 10.00-10.20 Federico Bärlocher : The natural Melo pearls from the Andaman Sea, Myanmar
- 10.20-10.40 Coffee break

Diamonds (Chairman Karl Schmetzer)

- 10.40-11.00 Laurent Cartier Diamond production in Sierra Leone since 1930
- 11.00- 11.20 N. N. Zudina, et al.: Orange diamonds from the Siberian placers: the features of structural defects
- 11.20-11.40 Thomas Hainschwang et al.: Photoluminescence spectroscopy and imaging of type Ib diamonds
- 11.40-12.00 Emmanuel Fritsch et al.: "Birefringence" in diamond: a useful tool to separate natural from synthetic diamond
- 12.00-12.05 Announcements
- 12.05-13.30 Lunch
- 13.30-14.20 Poster session (see below)

Diamonds (Chairman Tay Thye Sun)

- 14.20-14.40 Yuri Shelementiev et al.: Distinction between well and poorly cut diamonds on the basis of dark zone analysis
- 14.40-15.00 Joe Yuan et al.: Using synchrotron radiation to analyse diamond crystal structure
- 15.00-15.20 Israel Eliezri: From Rough to Report – Use of Technology
- 15.20 Conference day closes
- 17.00 Meeting point Kursaal entrance for walk to boat pier Interlaken East
- 17.30 Boat leaves for Giessbach
- 19.00 Conference photograph will be taken with all participants at Giessbach
- 19.30-22.00 Gala Dinner at Giessbach Hotel

Saturday 16 July

Coloured Stones

Corundum, Heat treatment (Chairman Ulrich Henn)

- 9.00-9.20 Walter Balmer et al.: Re-assessment of the characterisation of UV-Vis spectra for rubies from marble-hosted deposits
- 9.20- 9.40 Jayshree Panjekar et al.: Importance of various "feather type" inclusions in the identification of natural, treated, synthetic and treated-synthetic yellow sapphire
- 09.40-10.00 John Koivula: High temperature fusion of corundum mimics so-called residues in heat treated rubies and sapphires
- 10.00-10.20 Visut Pisutha-Arnond et al.: Blue coloration of heat-treated zircon
- 10.20-10.40 Coffee break

Corundum (Chairlady Francine Payette)

- 10.40-11.00 John Saul: Emplacement of deposits of coloured gemstones at the intersection of faults with the perimeters of large circular structures
- 11.00-11.20 Lore Kiefert: Sapphires from exotic sources: Azad Kashmir and New Zealand
- 11.20-11.40 Lin Sutherland et al.: The New England, New South Wales, Australia gem field: geographic typing of a world class giant gem deposit of basaltic placer origin
- 11.40-12.00 Nguyen Ngoc Khoi et al.: Three main types of corundum gem deposits in Vietnam
- 12.00-12.20 Terry Coldham : Basaltic corundum. A case for the promotion of increased cooperation between gemmological researchers and gemstone producers ?
- 12.20-12.25 Announcements
- 12.25-14.00 Lunch

Olivine, Jadeite (Chairlady Jayshree Panjekar)

- 14.00-14.20 Jaroslav Hyrsl, Historical use of olivine – the origin of peridots in baroque-period jewellery
- 14.20-14.40 Thanong Leelawathanasuk et al.: Pallasitic peridot : The gemstone from Outer Space

- 14.40-15.00 Loredana Prosperi: Italian gemstones: Peridot from Sardinia, Demantoid garnet from Val Malenco, Omphacite "jade" from the Po Valley, Piedmont, Amber from Sicily
- 15.00-15.20 Tay Thye Sun et al.: Preliminary studies to distinguish omphacite from jadeite
- 15.20-15.40 Edward Boehm: Recent coloured gemstone production & market trends
- 15.40-16.00 Coffee break

Canadian gemstones (Chairman Visut Pisutha-Arnon)

- 16.00-16.20 Willow Wight: Rare gemstones from Mont Saint-Hilaire, Québec, Canada
- 16.20-16.40 Karen Fox: New Canadian occurrences of gem scapolite and demantoid
- 16.40-17.00 Bradley Wilson: Gemstones from southern Baffin Island, Nunavut, Canada
- 17.00 Conference day closes
- 18.30 Apéritif and Dinner at Restaurant Spycher, Congress Centre Interlaken

Sunday 17 July

- 08.00-08.45 EXECO meeting

Testing Techniques (Chairman Emmanuel Fritsch)

- 9.00-9.30 Prof Thomas Pettke: LA-ICP-MS and its applications in gemmology
- 9.30- 9.50 Pornsawat Wathanakul et al.: AFM: an alternative technique for indicating gem treatments
- 9.50-10.10 Manfred Eickhorst: Putting LEDs to work for gemmology
- 10.10-10.30 Michael Hügi: The characteristics of digital photography applied to photomicrography of gemstone inclusions
- 10.30-10.50 Coffee break

Rare stones, Organic materials (Chairlady Margherita Superchi)

- 10.50–11.10 Sutas Singbamroong et al.: Gem characterization of sérandite from Québec, Canada
- 11.10-11.30 Michael Gray: The care and handling of large gemstones
- 11.30-11.50 Stephen Webb et al.: An organic gem material of proposed name “rostellite” derived from the fossilized beaks of whales of the family Ziphiidae
- 11.50-12.10 Stefanos Karamelas: Identification of organic gems from endangered species: An overview
- 12.10-12.15 Announcements
- 12.15-14.00 Lunch
- 14.00-15.00 Conference closing ceremony
- 15.00 Conference ends
- 15.15-15.45 Execo meeting (if needed)

POSTERS

5 min presentation per author

Thursday, 14 July

- 15.05 Wilawan Atichat et al.: Mozambique ruby: Indication of low-temperature heat treatment
- 15.10 Edward Boehm: A photo collage in memory of Dr. Edward J.Gübelin and the many years of his participation in the International Gemmological Conferences and excursions
- 15.15 George Bosshart: Do bi-coloured green and blue beryls exist, which consist of emerald and aquamarine zones ?
- 15.20 Emmanuel Fritsch et al.: Cr³⁺-green common opal from Turnali, North-eastern Turkey
- 15.25 Henry Hänni et al.: A portable Raman system for gemstone identification: The GemExpert Raman probe
- 15.30 Franz Herzog et al.: Colour by Rare Earth elements, as exemplified by a colour changing bastnäsite from Pakistan

Friday, 15 July

- 13.35 Arunas Kleismantas: XVIIth century doublets in liturgical items
- 13.40 Francine Payette et al.: Gem-quality green and blue tourmaline from a Coolgardie pegmatite, Western Australia.
- 13.45 Boontawee Sripasert et al.: Properties of blue spinel from Sri Lanka
- 13.50 Elizabeth Su: Jadeite trading in China
- 13.55 Chakkapan Suthirat et al.: Fancy sapphires from Deniyaya deposit, southern Sri Lanka
- 14.00 Panjawan Thanasuthipitak et al.: Bi-coloured sapphires from basaltic and metamorphic affiliations
- 14.05-14.10 R. Wirz: Bruker FTIR

Gemmology at the interface between mineralogy and crystallography

Thomas Armbruster

Mineralogical Crystallography, Institute of Geological Sciences, University of Bern,
Freiestr. 3, CH-3012 Bern Switzerland, e-mail: armbruster@krist.unibe.ch

Common grounds and differences among crystallography, mineralogy, and gemmology are discussed and highlighted on the basis of few examples. Some simplified definitions of the compared disciplines are as follows: (1) A crystal is a substance in which the constituent atoms, molecules, or ions are packed in a regularly ordered, repeating three-dimensional pattern. (2) A mineral is an element or chemical compound that is normally crystalline and that has been formed as a result of a geological process. (3) Gems are specimens of minerals or organic materials [used for personal adornment] that possess the attributes of beauty, rarity, durability and portability. Thus, according to these definitions, amber is a gem but not a mineral or crystal because it is not crystalline (and hard), and it is formed by a biological rather than a geological process; pearls are crystalline aggregates but they are also of biological origin and do therefore not qualify as minerals. Another interesting case is opal, which has not a periodic crystal structure (on the atomic scale) but is regarded as mineral species for historical reasons.

Nomenclature

Mineral nomenclature is strictly defined by the Commission on New Minerals, Nomenclature and Classification (CNMNC) of the International Mineralogical Association (IMA). A new mineral requires chemical and structural characterization including optical and other physical properties (Nickel and Grice, 1998). CNMNC decides upon application on approval of a new species and its mineral name. More than 70 new minerals were approved in 2010. Minerals are usually organized in groups. As an example, the beryl group in mineralogy comprises beryl $\text{Be}_3\text{Al}_2[\text{Si}_6\text{O}_{18}]$, bazzite $\text{Be}_3\text{Sc}_2[\text{Si}_6\text{O}_{18}]$, stoppaniite $\text{Be}_3\text{Fe}^{3+}_2[\text{Si}_6\text{O}_{18}]$, pezzottaite $\text{Cs}(\text{LiBe}_2)\text{Al}_2[\text{Si}_6\text{O}_{18}]$, and indialite – a high-temperature modification of cordierite – $(\text{Al}_2\text{Si})_3\text{Mg}_2[\text{Si}_4\text{Al}_2\text{O}_{18}]$. Except pezzottaite (rhombohedral) all beryl-group minerals are hexagonal (space group $P6/mcc$).

In gemmology there is the World Jewellery Confederation (CIBJO), which particularly protects consumer confidence in the jewellery industry. However, there are no strict nomenclature guidelines compared to mineralogy. In gemmology the number of trade names is much more versatile and the name refers mainly to colour variation due to incorporation of very minor constituents. Thus so called gem beryls comprise emerald, aquamarine, morganite, heliodor, golden beryl, goshenite, bixbyite, which in mineralogy are all named beryl independent of colour.

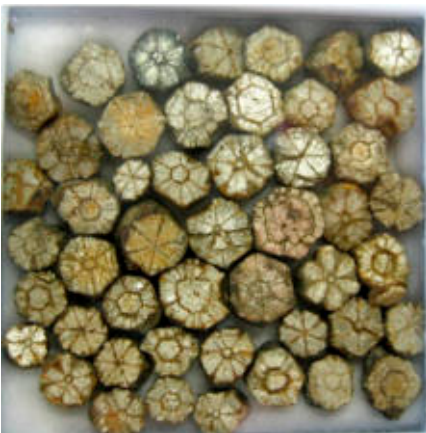
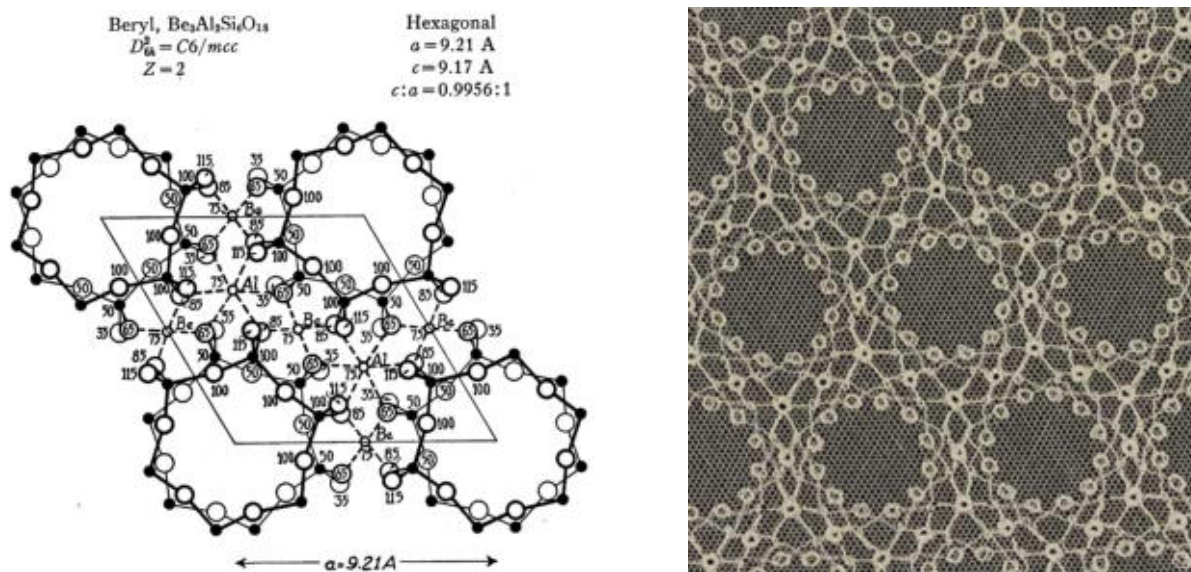


Figure 1. Small mica pseudomorphs (ca. 1 cm in diameter) of complex cordierite-indialite inter-growths (cherry blossoms). Photograph courtesy of John Rakovan.

Closest packing of spheres and diffraction of X-rays and visible light

In crystallography and mineralogy the concept of closest packing allows a simple approach not only to metal structures but also to more complex oxides, sulfides, and chlorides. In case of ionic crystals, a closest packing of anions (e.g., oxygen) produces small voids. Partial occupation of such voids by cations allows deriving the corundum and spinel structure, just to name two examples, which are also of relevance in gemmology. The prominent three-dimensional stacking sequences of close-packed layers are ABAB (hexagonal closest packing) and ABCABC (cubic closest packing).

An ordered arrangement of spheres is usually applied to explain the diffraction of X-rays on a crystal according to reflection by Bragg's law. Only rays which are inphase (addition) after reflection will be amplified whereas antiphase rays will vanish (subtraction). Bragg's law ($n\lambda = 2d \sin \theta$) relates the wavelength λ with the distance d between lattice planes and the reflection angle θ . This simple law is the basis of all structural investigations performed by crystallographers with diffraction methods. The key of the law is that the periodicity of the structure must be of similar magnitude as the applied radiation.



Left: Figure 2. Crystal structure of beryl (Bragg, 1937); Right: Figure 3. The crystal structure of beryl was used as model for a lace for a festive dress of Alice Bragg in 1951.

The same type of closest packing occurs also in opal but the spheres are not atoms but aggregates built by SiO_2 and H_2O , which are about 2000 – 4000 times larger than 1 \AA , the dimension used to scale atoms. As coincidence or virtue of nature the size of the spheres forming opal is in the same order of magnitude as the wavelength of visual light. Thus Bragg's law is also responsible that we observe a colourful diffraction pattern if white light is reflected by opal. The various homogeneous colour domains in opal are produced by light diffraction on coherent arrangements of spheres. If sphere-packing changes orientation, the colour effect (diffraction) will also be influenced. The same diffraction phenomenon as in opal is also observed on the wings of some butterflies or on plumage of birds. In the latter examples diffraction is due to periodic arrangement of scales or the barbs of feathers.

Different aspects of beauty

Only gemmology has beauty mentioned in the definition of the subject. Adoration of beauty in gemmology becomes already evident if cover pages of gemmological journals are compared with those in mineralogy and crystallography. There is no doubt that we all highly appreciate the brilliance of an esthetically cut diamond. Although, as mineralogists we claim that the perfection and shapeliness of some natural crystals cannot be improved by artificial cutting. There is also the charm of natural imperfection as displayed by the cherry blossom stones from Kameoka, Japan. The mica pseudomorphs (ca. 1 cm in diameter) of complex cordierite-indialite intergrowths (Fig. 1) resemble petrified blossoms (Rakovan et al., 2006).

When W.L. Bragg solved and classified the crystal structures of minerals, it was the esthetic aspect of pattern geometry, which fascinated him. The structure model of beryl displayed (Fig. 2) in his book (Bragg, 1937) served as model for a lace (Fig. 3) manufactured to a dress for Lady Alice Bragg, worn 1951 at the Congress of the International Union of Crystallography (IUC) in Stockholm. Her husband Sir Lawrence Bragg was president of IUC. Modern graphic software for the display of crystal structures allows us nowadays to celebrate the beauty of pattern geometry in even better quality (Fig. 4).

References

Bragg, W.L., 1937. Atomic Structure of Minerals, Oxford University press, 292 p.

Nickel, E.H., Grice, J.D., 1998. The IMA Commission on New Minerals and Mineral Names: procedures and guidelines on mineral nomenclature, 1998. Canadian Mineralogist, 36, 1-16.

Rakovan, J., Kitamura, M., Tamada, M., 2006. Sakura Ishi (Cherry Blossom Stones): Mica pseudomorphs of complex cordierite-indialite intergrowths from Kameoka, Kyoto Prefecture, Japan. Rocks and Minerals, 81, July/August, 284-292.

Trapiche tourmaline from Zambia –chemical and structural zoning

Karl Schmetzer¹, Heinz-Jürgen Bernhardt² and Thomas Hainschwang³

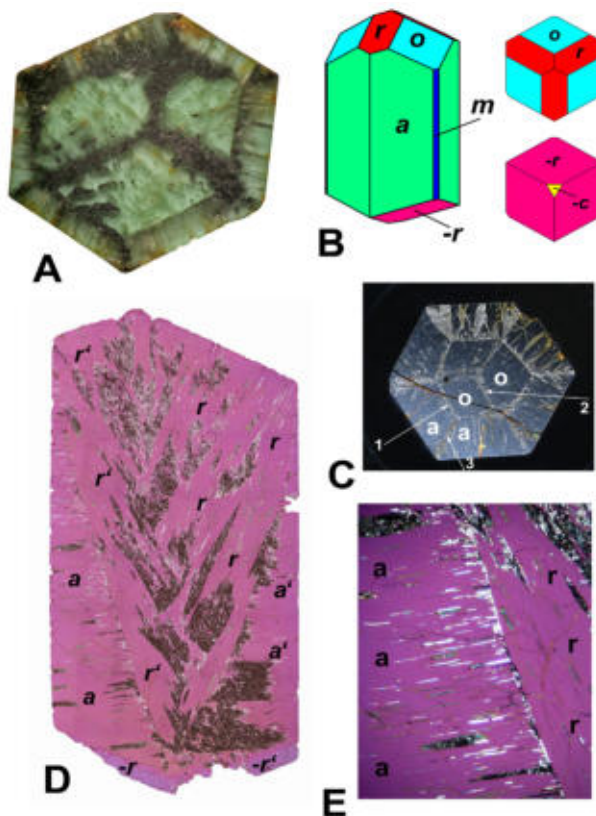
¹ D-85238 Petershausen, Germany email: SchmetzerKarl@hotmail.com

² ZEM, Institut für Geologie, Mineralogie und Geophysik, Ruhr-University, D-44780 Bochum, Germany
email: Heinz-Juergen.Bernhardt@rub.de

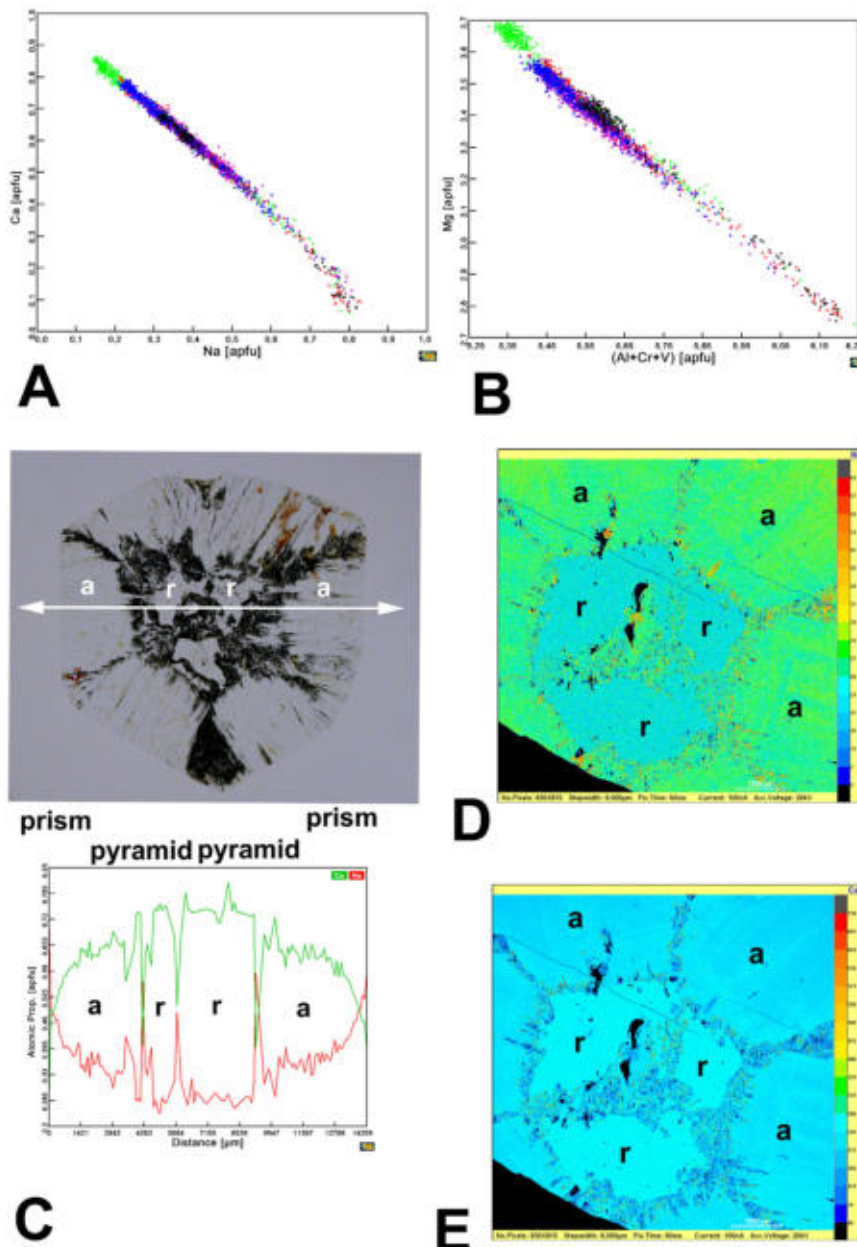
³ GGTL Gemlab-GemTechLab Laboratories, FL 9496 Balzers, Liechtenstein email: thomas.hainschwang@ggtl-lab.org

Trapiche tourmalines from Zambia (Fig. 1A ; see Hainschwang et al., 2007) show the hexagonal prism $a \{11\bar{2}0\}$ as well as the positive pyramids $r \{10\bar{1}1\}$ and $o \{02\bar{2}1\}$ and the negative pyramid $-r \{01\bar{1}\bar{1}\}$ as dominant external crystal forms (Fig. 1B). Numerous slices parallel to the c -axis (Fig. 1C) and perpendicular to the c -axis (Fig. 1D) were examined. The trapiche pattern is formed by liquid and solid inclusions which are trapped at the growth boundaries between pyramidal and prismatic growth sectors (Fig. 1E).

Growth tubes are formed perpendicular to the dominant growth faces. Irregular areas with numerous inclusions are also observed (Fig. 1D). According to microscopic examination, the growth sectors, in which these growth tubes are formed, are inclined at 27° (growth sectors of the pyramids r and $-r$), at 46° (growth sectors of the pyramid o) or at 90° (growth sectors of the prism a) versus the pedion c of the tourmaline hosts.



Electron microprobe analyses show a wide variation of chemical properties. All tourmalines were chemically zoned with an isomorphous substitution of Ca versus Na and Mg versus Al (Fig. 2 A, B; 2101 point analyses of 5 green samples, each colour represents analytical data of one tourmaline). This coupled isomorphous replacement according to the scheme $\text{Na} + \text{Al} \leftrightarrow \text{Ca} + \text{Mg}$ (Fig. 2 A,B) is characteristic for tourmalines of the dravite-uvite solid solution series (dravite $\text{Na}(\text{Mg}^{2+})_3\text{Al}_6[(\text{OH})_4(\text{BO}_3)_3(\text{Si}_6\text{O}_{18})]$, uvite $\text{Ca}(\text{Mg}^{2+})_3\text{Al}_5\text{Mg}[(\text{OH})_4(\text{BO}_3)_3(\text{Si}_6\text{O}_{18})]$). The green colouration of the samples is caused by minor contents of vanadium and chromium. Average vanadium contents were determined for all samples in the range of 0.09-0.31 wt% V_2O_5 , average chromium contents between 0.04 and 0.12 wt% Cr_2O_3 ; only traces of iron were detected (FeO from 0.01 to 0.02 wt%).



Numerous traverses across the tourmaline slices show an increase of Na and a decrease of Ca contents from the core to the rim of all tourmalines (Fig. 2C; scan with 118 analysis points). However, at the boundaries between different growth sectors (forming the geometric trapiche pattern of the samples), we obtained tourmaline analyses with higher Na and lower Ca contents than measured in the adjacent pyramidal and prismatic growth sectors. Element mapping of slices parallel and perpendicular to the c-axis (Fig. 2 D, E; 830 x 815 analysis pixels) confirmed these results.

A proposal for the formation of this complex structural (geometric) pattern and chemical zoning will be discussed.

Reference:

Hainschwang, T., Notari, F., Anckar, B., 2007. Trapiche tourmaline from Zambia. *Gems & Gemology*, 41(1), 36-46

Gem tourmaline from Elba island, Italy

Federico Pezzotta¹, Margherita Superchi², Brendan Laurs³, Elena Gambini⁴

¹ Natural History Museum, Corso Venezia 55, 20121 Milan, Italy. fpezzotta@yahoo.com

² Via dell'Ortensia 17, 20090 Segrate (MI), Italy. margheritasuperchi@alice.it

³ GIA, 5345 Armada Drive, Carlsbad, California 92008 USA. blaurs@gia.edu

⁴ CISGEM, Via Achille Papa 30, Palazzo WJC, 20149 Milan, Italy. gambini.elena@cisgem.it

Introduction

Elba Island in the Tyrrhenian Sea, Tuscany, Italy, is the type-locality of elbaite tourmaline and is among the most classic and famous mineral localities in Europe (Pezzotta, 2005, and references therein). The first important collection of Elba pegmatite minerals, including poly-chrome crystals of tourmaline, was described in 1825 but there is evidence that significant research on the locality dates back to the last decades of the 18th century. Most of the mining activity occurred during the 19th century. Since the beginning of the 20th century, the locality has been considered exhausted. It is noteworthy that in historic times, nearly all the production was devoted to collection purposes; little is known about a gemmological use of the tourmaline from the locality, except for sporadic information concerning the mounting of a few single crystals in jewels. Nevertheless, high quality gem crystals were present in significant quantity, as confirmed by the reports of the time and the magnificent historic collection, including matrix specimens and single crystals, in the Natural History Museum of the University of Florence.

The gem bearing pegmatitic veins occur along the eastern side of the Mt. Capanne monzo-granitic pluton dating from the Pliocene (6.2 Ma), and are hosted inside both the monzo-granitic and the surrounding hornfels rocks. The pegmatites are normally only a few metres long and some decimetres wide; larger veins are rare. Many of them strike in a north-south direction and dip steeply west.

Accessory minerals are typical of lithium-cesium-tantalum (LCT) pegmatites, and include beryl in pale blue and pink varieties, lepidolite, spessartine, petalite, etc.



Fig. 1. A cavity containing pink tourmaline crystals in a pegmatite on Elba island. Photo F. Pezzotta.

Samples, methods, and results

New field research and limited mining activities, performed since 1985 by the first author, resulted in the discovery of a few new pegmatite veins and the recovery of new tourmaline specimens of similar quality to those of the "old" times (e.g., Figures 1 and 2). This study is based on a collection of gemstones cut from tourmaline crystals mostly mined during this recent period. In particular, 29 cut stones were selected and analyzed. Some of these samples are shown in Fig. 3. Chemical analyses were performed by a WDS electron microprobe, detection of chromophore trace elements was made by a UV-Vis-NIR Perkin Elmer 1050 spectrophotometer, a standard gem-

mological refractometer was used for RI and birefringence, a hydrostatic balance for specific gravity, a UV lamp for long- and short-wave fluorescence, a gemmological polarizing binocular microscope for pleochroism and internal features, and a Macbeth Spectralight II Daylight source with Munsell Color Charts was used for colour description (US NBS for colour names).

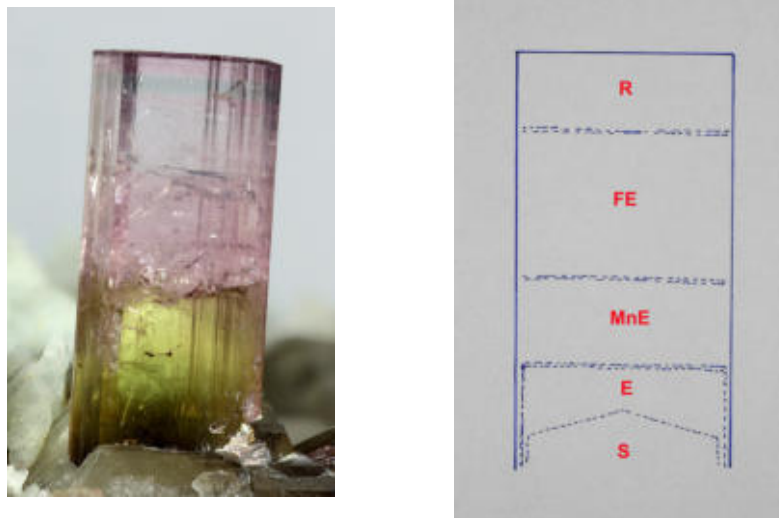


Fig. 2 (left). Typical Elba gem tourmaline. Photo M. Chinellato. (right). Typical compositional evolution of an Elba tourmaline crystal: S - schorl, E - elbaite, MnE - manganese-rich elbaite, FE - fluor-elbaite, R - rossmanite

Microprobe analyses indicated compositions ranging from rossmanite (sample E1), to elbaite and fluor-elbaite (samples E2, E3, E4, E5, E6), to Mn-rich elbaite (remaining samples). Rossmanite, elbaite, and fluor-elbaite had no (or very low) iron, but MnO contents up to 2.4 wt.%. The Mn-rich elbaite had strongly zoned compositions with MnO from 1.8 to 8.2 wt.%, traces of TiO (up to 0.12 wt.%), and traces of FeO (up to 0.26 wt.%). CaO was very low in all samples. UV-Vis-NIR spectra showed the presence of several absorption peaks (e.g., Fig. 4). Investigations of peak assignment are in progress.



Fig. 3. Some of the studied cut tourmaline gemstones, in the range of 0.43 to 4.82 ct. Photos E. Gambini.

Physical data for 10 selected samples are reported in Table 1. These values are consistent with elbaite and rossmanite data from literature. In general, pleochroism ranged from colourless to greenish-yellow, from light green to intense yellow, from colourless to pink, and from very light grayish yellow to intense pink. Observed inclusions were growth tubes parallel to the c-axis, and fluid inclusions including two phases.

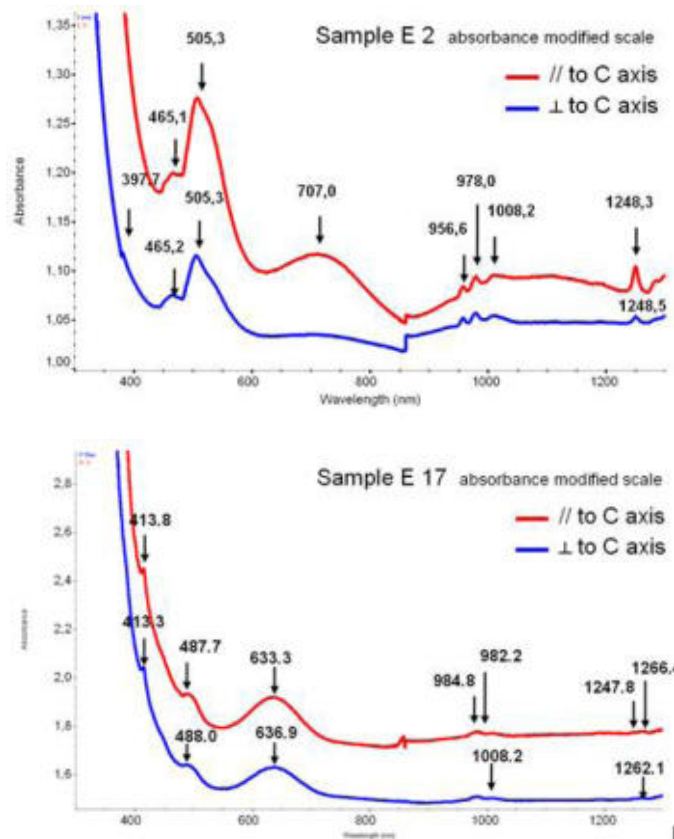


Fig. 4. Polarized Vis-NIR absorption spectra of tourmaline samples E2 (pink, on the left) and E17 (green, on the right). Spectra recorded by Andrea Marzola and Antonello Donini (CISGEM).

Final remarks

Elba pegmatitic deposits have been mined in historic times mostly for tourmaline crystals of collectible interest, without special focus on gem material. This study shows that the locality also has some gemmological interest with the occurrence of gem-quality tourmaline in a variety of colours, including pink and bright yellow-green. Nevertheless, limitations due to local environmental rules make significant further production unlikely. Preliminary data presented in this study reveal two main features of Elba tourmalines: (1) the uncommon yellow fluorescence to short-wave UV radiation (mostly in pink samples), and (2) the high MnO content of the bright yellow-green varieties, similar to the content reported by Laurs et al. (2007) from the Canary mining area in Zambia. Investigations in progress include polarized UV-Vis-NIR spectroscopy of oriented polished slabs of tourmaline crystals of different colours, to be compared with the spectra obtained from the faceted samples, and to allow a correct and complete interpretation of the various spectral features.

n°	Weight in carats	Shape and Cut	Colour	Mussoni indices	Density	n		Birefringence	UV Fluorescence	
						ω	ε		DW (365 nm)	YW (254 nm)
E 2	1.8585	rectangular-octagonal, steps	pale purplish pink	7.5KP 8/3 5KP 8/4	3.07	1.625	1.645	-0.020	inert	Yellow, banded
E 4	3.0490	oval, steps and facets	pale purplish pink	10P 8/3	3.05	1.621	1.642	-0.021	inert	Moderate, yellow
E 6	1.7140	square-octagonal, facets	moderate purplish red	8P 5/10	3.05	1.620	1.640	-0.020	inert	inert
E 7	0.8155	oval, facets	dark to deep yellow - light olive	5Y 5.5/8	3.12	1.625	1.650	-0.025	inert	inert
E 9	0.4010	round, facets	strong greenish yellow	10Y 7.5/9	3.13	1.625	1.650	-0.025	inert	inert
E 10	0.4375	rectangular, steps and facets	grayish greenish yellow - light olive	7.5Y 6.5/5	3.07	1.625	1.645	-0.020	inert	inert
E 14	1.1440	rectangular-octagonal, steps	pale greenish yellow	10Y 9/5	3.09	1.630	1.645	-0.015	inert	Strong, yellow
E 15	0.5015	rectangular-octagonal, steps	brilliant to strong yellow green	2.5GY 7.5/8	3.10	1.625	1.650	-0.025	inert	inert
E 17	0.7275	rectangular-octagonal, steps	light to brilliant yellow green	2.5GY 8/7	3.09	1.625	1.650	-0.025	inert (towards grille) light blue line	inert
E 20	0.8670	oval, facets	(sides) strong greenish yellow (center) strong to brilliant yellow green	(sides) 10Y 7/9 (center) 2.5GY 7.5/9	3.11	1.628	1.650	-0.022	inert	inert

Table 1. Main physical data of 10 selected cut tourmalines.

References

Laurs B.M., Simmons W.B., Rossman G.R., Fritz E.A., Koivula J.I., Ankar B., Falster A.U. (2007) Yellow Mn-rich tourmaline from the Canary mining area, Zambia. *Gems and Gemology* 43/4, 314-331.

Pezzotta F. (2005) The Italian island of Elba, a mineralogical jewel in the Tuscan archipelago. *extraLapis English* 20, 96 pp.

Mn-bearing grossular garnet

Ulrich Henn and Thomas Lind

German Gemmological Association
Idar-Oberstein, Germany
ulihenn@dgemg.com

Two types of manganese-bearing grossular garnet are found in gem quality: 1) raspberry-red grossular from Mexico and 2) brownish-pink to orange-pink hydrogrossular from South Africa.



Fig. 1: Raspberry-red grossular garnet crystals from Mexico. Diameter of the zoned platelet in front: 2 cm.

Raspberry-red grossular is known from Sierra de Cruces Range, Coahuila, Mexico in the form of euhedral rhombo-dodecahedral crystals up to several cm in size (Fig. 1). In some cases the crystals are distinctly zoned. A black core composed of iron-rich grossular garnet is coated by light to medium raspberry-red grossular garnet. Numerous fissures are responsible for the translucent appearance of the raspberry-red material.

The chemical composition determined by electron microprobe analyses is characterized by the major compounds of CaO, Al₂O₃ and SiO₂ as well as minor concentrations of MnO, Fe₂O₃ and MgO. The absorption spectrum (Fig. 2) shows the presence of both Mn²⁺ and Mn³⁺. Mn²⁺ causes absorption bands with maxima at 410 and 430 nm. A broad asymmetric absorption band with a maximum at 512 nm is attributed to octahedrally coordinated Mn³⁺ and responsible for the raspberry-red colour (Geiger et al., 1999). Manganese was analysed to 0.82 to 1.04 wt.% MnO. The refractive index of the raspberry-red grossular garnet from Mexico is 1.737-1.740 and the density 3.56-3.59 g/cm³.

The occurrence of green and brownish-pink to orange-pink hydrogrossular garnet near Pretoria in South Africa is known since 1908. The translucent to opaque material (Fig. 3) forms aggregates which belong to a solid-solution series of grossular Ca₃Al₂(SiO₄)₃ and hibschite Ca₃Al₂(SiO₄)₃-x(OH)_{4x} (with x = 0.2-1.5). Brownish-pink to orange-pink hydro-grossular possesses a relatively low refractive index of 1.680 to 1.705 and a density of 3.24 to 3.35 g/cm³ which is attributed to distinct water contents of 6 to 8 wt.% H₂O (see Henn, 1996). Beside water the chemical composition is characterized by the major components of CaO, Al₂O₃ and SiO₂. Traces of manganese are responsible for the brownish-pink to orange-pink colour. 0.35 to 0.68 wt.% MnO were determined by microprobe analyses. The absorption spectrum is characterized by a broad band in the blue-green spectral range with a maximum at 480 nm which is attributed to octahedral bonded Mn³⁺ (Manning & Owens, 1977).

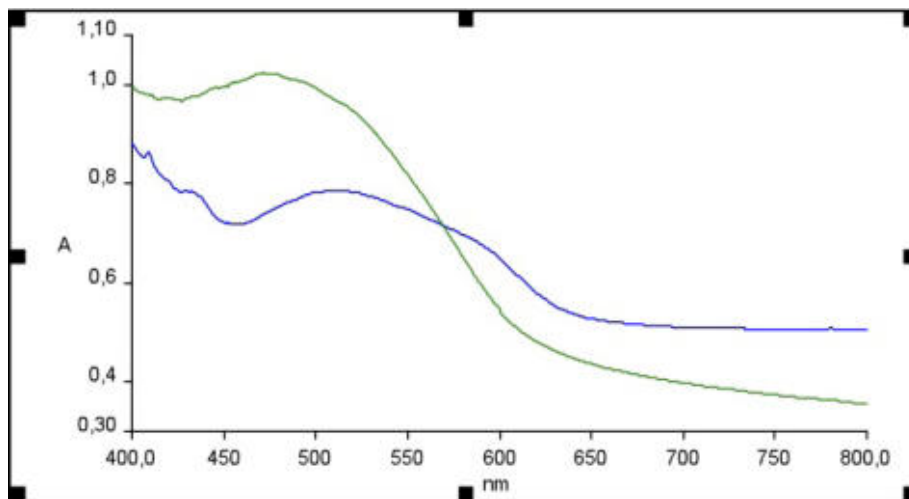


Fig. 2: Absorption spectra of raspberry-red grossular from Mexico (blue curve) and brownish-pink hydrogrossular from South Africa.

The different position of the Mn^{3+} absorption bands of Mexican raspberry-red grossular and South African brownish-pink to orangey-pink hydrogrossular can be explained by structural differences, especially by different deformation of the octahedral sites.



Fig. 3: Orangey-pink hydrogrossular garnet from South Africa. Size of the cushion cut cabochon in front: 3 x 2 cm.

References

- Geiger, C.A., Stahl, A., Rossman, G.R., 1999. Raspberry-red grossular from Sierra de Cruces Range, Coahuila, Mexico. *Eur. J. Mineral.*, 11, 1109-1113.
- Henn, U., 1996. Hydrogrossular aus Südafrika – die sogenannte "Transvaal-Jade". *Z. Dt. Gemmol. Ges.*, 45(4), 189-197.
- Manning, P.G., Owens, D.R., 1977. Electron Microprobe, X-Ray Diffraction, And Spectral Studies Of South African And British Columbian "Jades". *Canadian Mineralogist*, 15, 512-517.

Colorimetric investigation of unstable and stable Spodumene colours

G. Bosshart 1, Tay Y.K. 2, T. Hainschwang 3, M. Krzemnicki 4, R. Dressler 5

1 Horgen-Zürich, Switzerland, george.bosshart@swissonline.ch

2 Parkway Hospital, Singapore

3 GGTL Laboratories, GEMLAB (Liechtenstein)/GemTechLab, Balzers/Geneva.

4 Swiss Gemmological Institute SSEF, Basel, Switzerland

5 Paul Scherrer Institut, Villigen, Switzerland

Colour spectrometry was instrumental in monitoring the continuous colour alterations experienced by five spodumene specimens of diverse hues selected from a batch of mostly bluish-green cut stones, allegedly (γ -ray ?) irradiated in Pakistan (Tay, 2008, and pers. comm.). These alterations expressed themselves as gradually changing optical absorption spectra, rapidly fading colours and modifying hues, observed upon exposure to strong light and to LWUV radiation and after extended relaxation in darkness. The post-irradiation colours of manganiferous specimens #1 to #5 were purple, yellow-green, blue, green and light yellow (Fig. 1a) and, as a result of the exposures, shifted to pale pink and light purple, their precursor kunzite colours (Figures 1b and 3), with the exception of sample #5. The colours observed were caused by two broad absorption bands in the visible range of the electro-magnetic spectrum, the 536 (± 2) nm band increasing and the 637 (± 4) nm band decreasing in intensity during the exposures, most markedly under strong light (Fig. 2). Remarkably, iron-coloured, light yellow sample #5 did not respond to any of the experiments carried out although #5 also showed a 536 nm band and a minor amount of MnO. A second irradiation of the selected samples with ^{60}Co γ -rays generated weaker effects but still permitted to qualitatively reproduce the findings of the first data set. No residual radioactivity was recorded.



Figure 1. Colour representation of irradiated spodumene specimens #1-#5 (from left to right), a) "as received" (upper row) and b) after strong light and UV exposure (lower row). Specimens #2-#4 exhibit clear colour fading and/or a modification of the hue. Approximately natural size. Photos by G. Bosshart.

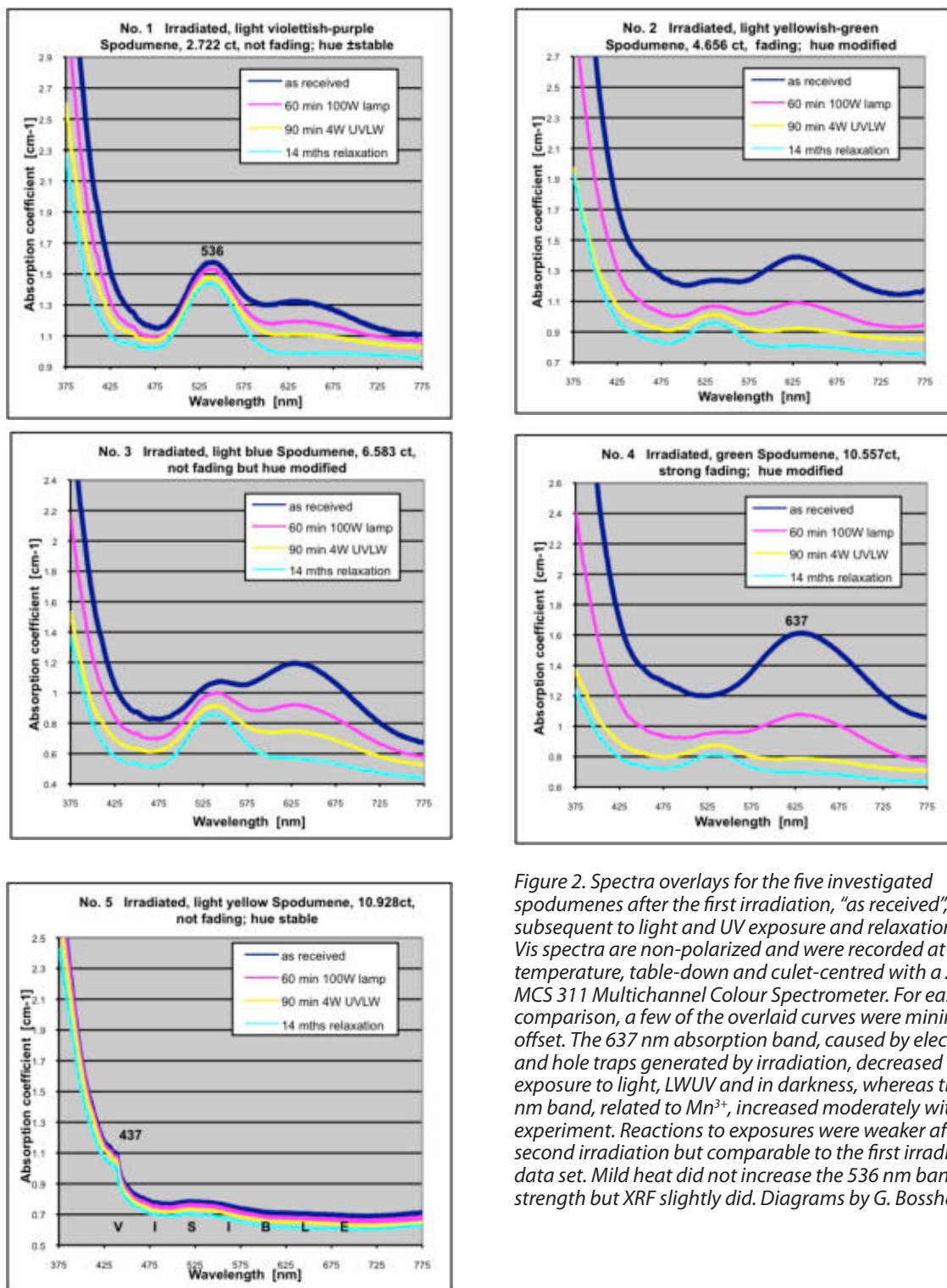


Figure 2. Spectra overlays for the five investigated spodumenes after the first irradiation, "as received", and subsequent to light and UV exposure and relaxation. These Vis spectra are non-polarized and were recorded at room temperature, table-down and culet-centred with a Zeiss MCS 311 Multichannel Colour Spectrometer. For ease of comparison, a few of the overlaid curves were minimally offset. The 637 nm absorption band, caused by electron and hole traps generated by irradiation, decreased with exposure to light, LWUV and in darkness, whereas the 536 nm band, related to Mn³⁺, increased moderately with each experiment. Reactions to exposures were weaker after the second irradiation but comparable to the first irradiation data set. Mild heat did not increase the 536 nm band strength but XRF slightly did. Diagrams by G. Bosshart.

All types of ionizing radiation transform (oxidize) Mn^{2+} to Mn^{3+} and further to rather unstable Mn^{4+} , which reverts to Mn^{3+} (light purple) and Mn^{2+} (near-colourless) when exposed to light, UV or heat. However, the sensitive, radiation-induced 637 nm absorption band did not correlate with the MnO content, the major cation of which, after irradiation, is Mn^{4+} . This very broad band is related to a trap of two electron holes on Mn^{2+} which is linked to the trap of the released electrons on adjacent Fe^{3+} (Hassan & Labib, 1978; hole centre theory disputed by Nassau, 1994). Contrary to the 637 nm band, the area of the 536 nm absorption band correlated well with the sum of MnO and Fe_2O_3 contents (Fig. 4) and can be assigned to the coupled cation substitution of Si^{4+} by Mn^{3+} (purple-pink) and of Al^{3+} by Fe^{3+} before irradiation, respectively to Mn^{4+} and Fe^{2+} (green) after irradiation. Heating to $\geq 200^\circ\text{C}$ will restore and intensify the kunzite colour whereas heating to 500°C will completely bleach all centres in irradiated spodumenes (Hassan & Labib, 1978). Light yellow specimen #5 did not react to γ -ray radiation, strong light or UV as it contained much more Fe_2O_3 than MnO. Its Mn/Fe ratio of 0.40 is markedly opposed to the Mn/Fe ratios of >10 in specimens #1-#4, yet the Fe^{3+} -related Vis-absorption of #5 was not stronger than in specimens #1-#4. Irradiated spodumenes with low Mn and very low Fe contents such as sample #4 appear to develop the strongest absorption band at 637 nm in the red spectral area and, as a consequence, the cleanest green hues of all, whereas those with high Mn levels (e.g. #1) irradiate and fade reluctantly.

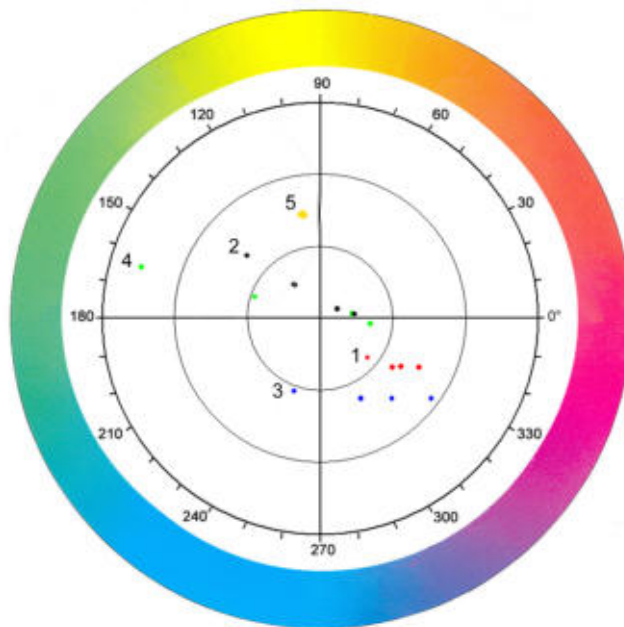


Figure 3. CIE Lab 1976 Chromaticity diagram (Schmetzer et al., 2009) displaying the colour locations of the five investigated spodumenes with labels 1 to 5 indicating their initial, "as received" colours after the first irradiation. The loci of the colours after light and UV exposure line up on the right side of each labelled dot, and the fourth dot in each row marks the colour after 14 months of relaxation in darkness. The rows of specimens #1-#4 run in the direction of the originally faint pink (#2, #4) respectively purple (#1, #3) precursor hues of the spodumenes. Light yellow #5, coloured by Fe^{3+} , did not respond to any of the exposures. Accordingly its colour did not alter even slightly. Standard illuminant D65. Neutral or White point at the origin (or centre) of the a^*b^* coordinate system. Radius of diagram representing a saturation of 15% (a chroma of 0.15). Artwork by A. Bosshart.

Table 1. ED-XRF analysis of the chromophoric trace elements of five irradiated Spodumenes

Trace Element	Spod. # 1 Oxide wt.%	Spod. # 2 Oxide wt.%	Spod. # 3 Oxide wt.%	Spod. # 4 Oxide wt.%	Spod. # 5 Oxide wt.%	Deer 1995 Oxide wt.%
Hue after irr.	l. purple	l. y-green	l. blue	green	l. yellow	<i>purple</i>
MnO	0.231	0.105	0.126	0.055	0.095	<i>0.14</i>
Fe ₂ O ₃	0.012	0.005	0.012	bdl	0.240	<i>0.04</i>
Cr ₂ O ₃	0.011	0.001	0.030	bdl	bdl	<i>n.a.</i>
TiO ₂	bdl	bdl	bdl	bdl	bdl	<i>n.a.</i>
V ₂ O ₃	bdl	bdl	bdl	bdl	bdl	<i>n.a.</i>
Mn/Fe ratio	19.3	21.0	10.5	> 50	0.40	<i>3.5</i>

Data based on composition of pure spodumene (stoichiometric): Li₂O 8.03, Al₂O₃ 27.40, SiO₂ 64.57 wt.%.
bdl : below detection limit, *n.a.*: not analyzed

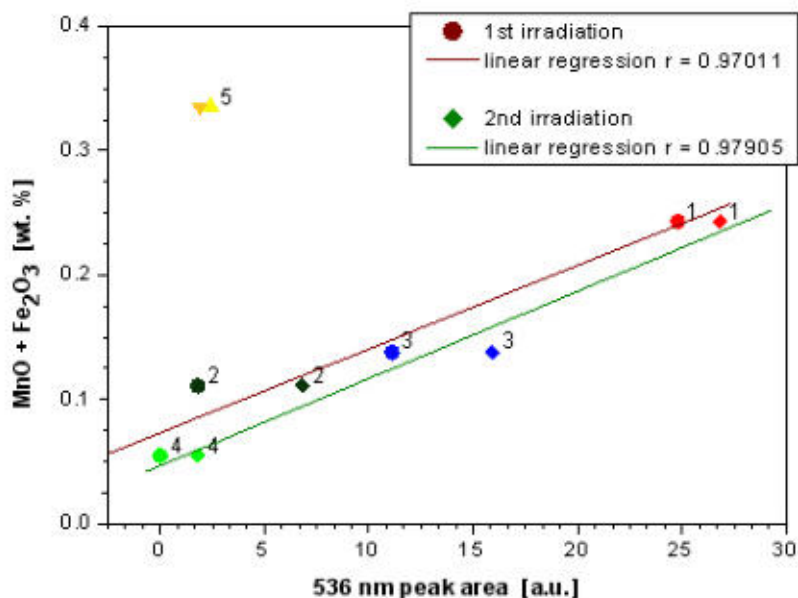


Figure 4. Diagram displaying the linear correlation between the 536 nm peak area (region of interest 470-610 nm) and the sum of the MnO and Fe₂O₃ contents of manganese-bearing spodumene specimens #1-#4 subsequent to the first and second irradiation. Sharply offset is non-reactive, ferriferous sample #5. For comparison refer to Figures 2 and 3 and to Table 1.

Stable colours are encountered in the green to yellow-green spodumene variety hiddenite only. This chromiferous variety may contain fair amounts of iron not only in Brazilian, Sri Lankan and other occurrences, but also in the renowned type-locality specimens from Alexander County, North Carolina, USA. The Cr³⁺ absorption band is located at 621 (± 2) nm and its full width at half maximum fluctuates from approximately 89 to 93 nm, as opposed to the FWHM of 90 to 135 nm of the 637 nm band in irradiated green spodumenes. The Cr doublet at 688/692 nm, if detectable, and the band positions differentiate the two green versions more reliably than the FWHM values. Discrimination of natural pink, purple and green colours from those generated by artificial annealing and irradiation is most challenging.

Acknowledgements

The first author is indebted to Mr. Tay T.S., Far East Gemological Laboratory, Singapore, for the extended loan of the five spodumene samples. Special thanks are also extended to Mr. Y.S. Aw, radiotherapist, at the Parkway Hospital, Singapore, for re-irradiation of the lot and to Dr. F. Herzog, Swiss Gemmological Institute SSEF, Basel, Switzerland, for kunzite and hiddenite analyses by ED-XRF. Prof. Dr. H. Hänni, Basel, Switzerland, E. Boehm, RareSource, Chattanooga, TN, and M. Gray, Coast-to-Coast Rare Stones, Missoula, MN, USA, provided valuable kunzite respectively hiddenite reference samples and documentary material.

References

- HASSAN F., LABIB M. (1978): Induced Color centres in alpha-spodumene called Kunzite. *N.Jb. für Mineralogie, Abh.*, 134, 1, 104-115.
- NASSAU K. (1994): *Gemstone Enhancement*. Butterworth-Heinemann, Oxford, England. ISBN 0-7506-1797-7.
- SCHMETZER K., BERNHARDT H.-J., BOSSHART G., HAINSCHWANG T. (2009): Colour-change garnets from Madagascar – chemical, spectroscopic and colorimetric properties. *J. Gemm.* 31, 5-8, 235-282.
- TAY T.S. (2008): Unusual colour of green spodumene from Pakistan. *Austr. Gemm.* 24, 230.

Colouring Agents and their Spectra in Blue Spinel

Masaki Furuya

Japan Germany Gemmological Laboratory, Kofu, Japan

E-mail: jggl@sapphire.co.jp

Recently spinel seems to become more popular in the market. It may be because spinel comes in beautiful colours, not only red or hot pink, but also bright blue from Vietnam and others. Natural blue spinel is known to be coloured by iron and cobalt (Mitchell, 1977). We examined 41 pieces of blue spinel (eighteen from Tanzania, eleven from Vietnam, nine from Sri Lanka, one from Madagascar, and two synthetic) with UV-visible and EDXRF spectrometry. Additionally 21 of them were analyzed with LA-ICP-MS with the help of GIT to detect their colouring agents.

Spectrum type	Type1-Fe	Type2-Co	Type2'-SynCo	Type3-Fe'&Co	Type4-Fe" & Co
Rep. sample ID	FT7325	FT0562	FT7057	FT7311	FT0563
Fe (ppm)	13283	5791	1	6501	21190
Fe ₂ O ₃ (wt%)	2.355	0.943	0.003	1.027	3.670
Co (ppm)	4.4	96.9	262.5	13.1	11.2
CoO (wt%)	Not detected	0.006	0.050	Not detected	Not detected
Cr (ppm)	1.6	461.7	238.6	2.5	42.8
Cr ₂ O ₃ (wt%)	Not detected	0.094	0.054	Not detected	Not detected
V (ppm)	1.4	182.9	Not detected	2.7	11.8
V ₂ O ₅ (wt%)	Not detected	0.046	Not detected	Not detected	0.004
Photo of representative stone					
Whole samples of each types					
Num of samples	8	8	2	5	18
(ICP tested)	3	5	2	2	9
Fe (ppm)	6696 ~ 13283	5320 ~ 22560	1 ~ 6	5683 ~ 6501	10288 ~ 22189
Fe ₂ O ₃ (wt%)	1.119 ~ 3.994	0.849 ~ 4.150	0.002 ~ 0.003	0.995 ~ 2.006	1.724 ~ 4.040
Co (ppm)	2.6 ~ 4.4	27.8 ~ 96.9	260.0 ~ 262.5	10.8 ~ 13.1	7.8 ~ 20.8
CoO (wt%)	Not detected	nd ~ 0.006	0.047 ~ 0.050	Not detected	Not detected
Cr (ppm)	1.6 ~ 303.6	0.4 ~ 541.7	218.3 ~ 238.6	1.8 ~ 2.5	0.3 ~ 42.8
Cr ₂ O ₃ (wt%)	nd ~ 0.052	nd ~ 0.142	0.049 ~ 0.054	nd ~ 0.003	nd ~ 0.081
V (ppm)	1.4 ~ 44.0	0.7 ~ 203.5	Not detected	2.3 ~ 2.7	3.0 ~ 15.6
V ₂ O ₅ (wt%)	nd ~ 0.010	nd ~ 0.093	Not detected	nd ~ 0.003	nd ~ 0.023

Table1. Chemical composition detected by EDXRF and LA-ICP-MS of each spectrum type

With UV-visible spectrometer tests of 41 samples of blue spinel, the spectra can be categorized into five patterns: Type1-Fe (8 pieces), Type2-Co (8 pieces), Type2'-SynCo (synthetic, 2 pieces), Type3-Fe&Co (5 pieces) and Type4-Fe&Co (18 pieces). Fig. 1 shows the comparison of representative spectra from mainly iron-coloured spinel (Type1-Fe) to mainly cobalt-coloured synthetic spinel (Type2'-SynCo).

In Fig. 1, the Type1-Fe spectrum is featured as an increasing or even absorption around 550-650nm and strong absorption at 457nm. This type has relatively moderate to high iron content but very low cobalt as shown in Table 1. This type shows many iron related absorptions. Weak absorptions at 371 nm and 383 nm, strong absorption at 457 nm and three absorptions in the yellow to red spectral region (556 nm, 587 nm and around 650 nm) are due to iron. In contrast, Type2'-SynCo is featured as a clear summit shape absorption around 540-630nm with three clear peaks. This type is seen in Verneuil synthetic blue spinel with high cobalt and chromium and almost no iron as shown in Table 1. The three absorptions in the yellow to orange-red region seem to correspond to those of iron one seen in Type1-Fe, but their centre positions are different as 543 nm, 580 nm and 622 nm. Type2-Co is featured as a summit shape absorption around 550-630nm with three peaks and high absorption at 457nm. This type is often seen in natural spinel with relatively high cobalt and moderate to high iron content. Its blue and green absorptions are weak to transmit, and its deep red absorption is also weak compared to other types, giving a unique blue body colour to the stone. Also, it causes weak colour change effect (colour shift) from blue to purple sometimes. Type3-Fe&Co is featured as low absorptions in the visible region. This type has a summit shape weak absorption around 550-630nm and its absorption at 475nm is also weak. This type is often seen with mauve spinel from Vietnam. It has moderate cobalt and moderate iron contents as shown in Table 1. Type4-Fe&Co spectrum is featured as a decreasing absorption around 550-650nm and high absorption at 457nm. This type contains moderate cobalt and moderate to high iron contents as shown in Table 1. Under the Chelsea colour filter, most of them show weak red, and some of them show a colour-change effect from blue to violet.

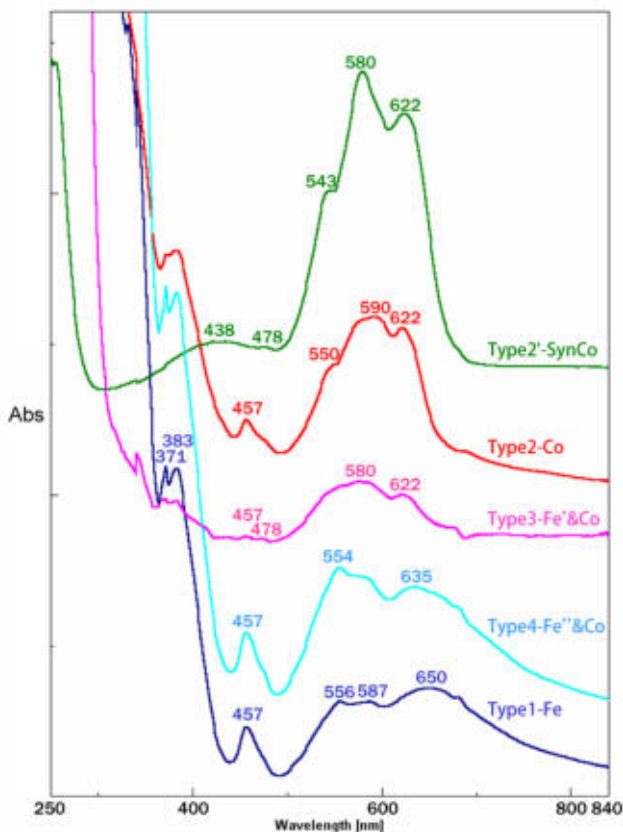


Figure 1. Comparison of spectra (spectrum normalized)

The comparison of these types of spectrum indicates that in natural blue spinels, the increase of cobalt content weakens the red absorption and strengthens the yellow absorption to give a vivid blue appearance to spinel. When we compare the transmission percentage at 680nm in red and the lowest transmission percentage in the yellow area of 550-590nm (characteristic strong absorption in yellow), the rate of increase from the minimum transmission point in yellow 550-590nm to red transmission at 680nm correlates with cobalt content (Correlation coefficient = 0.878 for a sample of 19 pieces, without synthetic stone.)

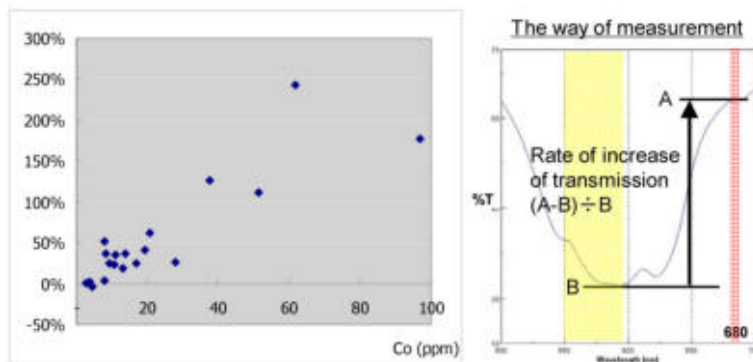


Figure 2. The rate of increase from transmission in the yellow to transmission in the red at 680nm and Co content and the method to determine the correlation.

The spectrum type seems to have a relationship with cobalt and iron contents. Fig. 3 shows cobalt and iron content of each spectrum type. The high cobalt content samples are categorized in Type2-Co, low cobalt content samples are categorized in Type1-Fe. Moderate cobalt content samples are categorized in Type3-Fe'+Co and Type4-Fe''+Co. Type4-Fe''+Co contains higher iron than Type3-Fe'+Co. The difference of iron content can be seen with EDXRF too, as Type4-Fe''+Co samples contain 1.724 ~ 4.040 wt.% of Fe₂O₃, on the other hand Type3-Fe'+Co samples contain 0.995 ~ 2.006 wt.% only.

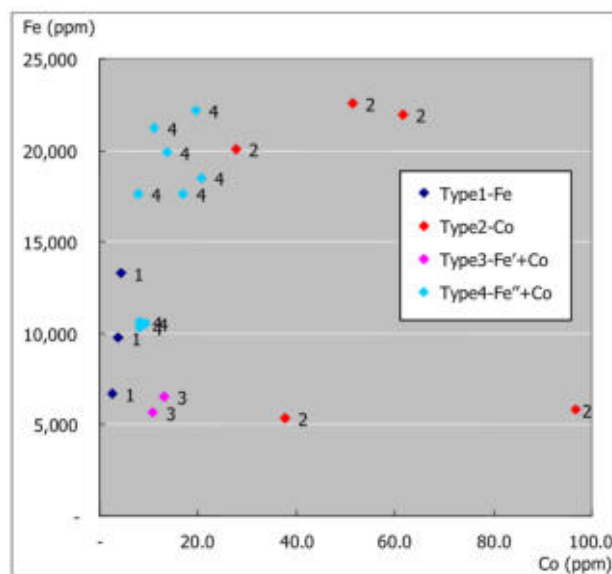


Figure 3. Co and Fe contents of spectrum type

It was introduced in previous researches that the cobalt based absorption is different from iron based one (1990, Andersen, 1997, Kitawaki). Actually absorption at 457nm related to iron is seen in most natural stones with iron. However, in these testing, when we look at the peak points of absorption in yellow to red, such as 550-560nm, 570-590nm and 620-650nm, they vary to some extent. Though some of these absorptions are not detected as a peak such as Type4-Fe" & Co which does not have a clear 580-590nm absorption, the comparison between peak points of absorption and cobalt and iron content does not show clear relations.

Also, chromium and vanadium contents are often detected in spinel and vanadium is also thought as one of the causes of colour change effect in blue spinel (1990, Maddison). Among tested samples, some contain chromium and vanadium as shown in Table 1. However the relationship between colour change and these contents is not clear. As mentioned, cobalt content is related to red transmission and yellow absorbance which causes colour change, too. Thus not only chromium and vanadium but also cobalt content can affect colour change effect in blue spinel.

From these comparisons of spectra and EDXRF and LA-ICP-MS data, cobalt and iron contents are the major colouring agents in natural blue spinel. The content of iron and cobalt is related to the type of spectrum.

Acknowledgement

The author would like to deeply thank the IGC abstract review board, especially Dr. George Bosshart, for their warm support and guidance. Also, LA-ICP-MS testing was completed by courtesy of the Gem and Jewelry Institute of Thailand.

References

Anderson. B.W., 1990 Gem testing 11th ed, London, England, 162-163, 177, 230, 306-307.

Kitawaki, H., 1997 Cobalt coloured natural blue spinel, *Gemmology*, 28(2), 37.

Maddison, P., 1990 Gem trade lab notes. *Gems & Gemology*, 26(3), 226-227.

Mitchell, K., 1977 African grossular garnet; blue topaz; cobalt spinel; and grandidierite. *Journal of Gemmology*, 15(7), 354-357.

Shigley, J.E., Stockton, C.M., 1984 'Cobalt-blue' gem spinels. *Gems & Gemology*, 20(1), 34-41.

EPR of Turquoise and some of its imitations

Jean Marie Dereppe 1 and Claudette Moreaux 2

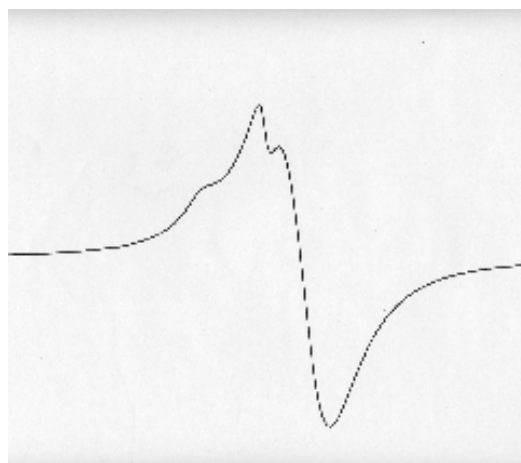
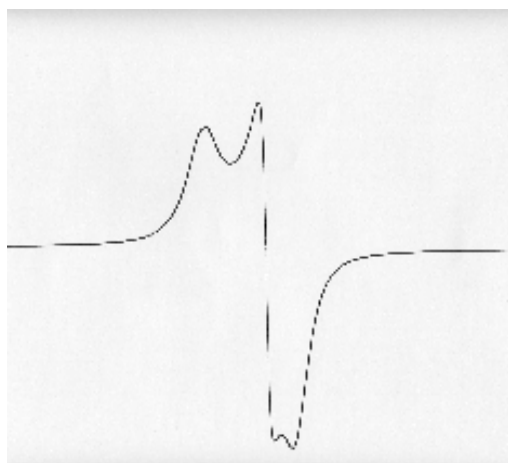
1 University of Louvain. Louvain La Neuve. Belgium. Jean-Marie.Dereppe@uclouvain.be

2 AGB. Court Saint Etienne. Belgium. jefe@skynet.be

Electron Paramagnetic Resonance (EPR) is a spectroscopic technique for studying chemical species that have one or more unpaired electrons such as transition metal ions.

Every electron has a magnetic moment and spin quantum number $s = 1/2$ with magnetic components $m_s = +1/2$ and $m_s = -1/2$. In the presence of an external magnetic field with strength B_0 , the magnetic moments of the electrons align either parallel or antiparallel to the field giving rise to two energy states separated by $\Delta E = g\mu_B B_0$. Where g is the Landé g factor and μ_B is the Bohr magneton. An unpaired electron can move between the two energy levels by absorbing or emitting radiation of energy $\epsilon = h\nu = \Delta E$ which gives the fundamental equation of EPR as $h\nu = g\mu_B B_0$. Many measurements are made at 9-10 GHz in a magnetic field of 0.35 T. Interaction of the electronic spin with the environment and with the other spins gives rise to "fine structures" which displace and broaden the resonance lines.

Turquoise is a hydrated copper aluminium phosphate mineral with copper in the divalent state. Most samples contain small amounts of Fe^{2+} substituted for Cu^{2+} and Fe^{3+} substituted for Al^{3+} .



Figures 1 (left) and 2 (right)

It has been shown by Clark et al. (1979) that the EPR spectrum of turquoise is essentially composed of an asymmetrical line arising from Cu^{2+} in a crystallographic site of C_i symmetry and a symmetrical Lorentzian shaped line attributed to Fe^{3+} . Figure 1 presents the spectrum of a blue turquoise containing essentially Cu and Figure 2 shows the spectrum of a green turquoise containing Cu and a fairly large amount of Fe.

The relative amounts of copper and iron can be obtained by decomposing the EPR spectrum into Cu and Fe components.

Turquoise can be confused with some natural-colour bluish green materials such as Chrysocolla, Variscite, Chrysoprase, Faustite, and others.

Also, as a relatively expensive material, turquoise has been largely imitated by dyed Magnesite, Howlite, Calcite, Dolomite, Plastics, Glass, Ceramics....

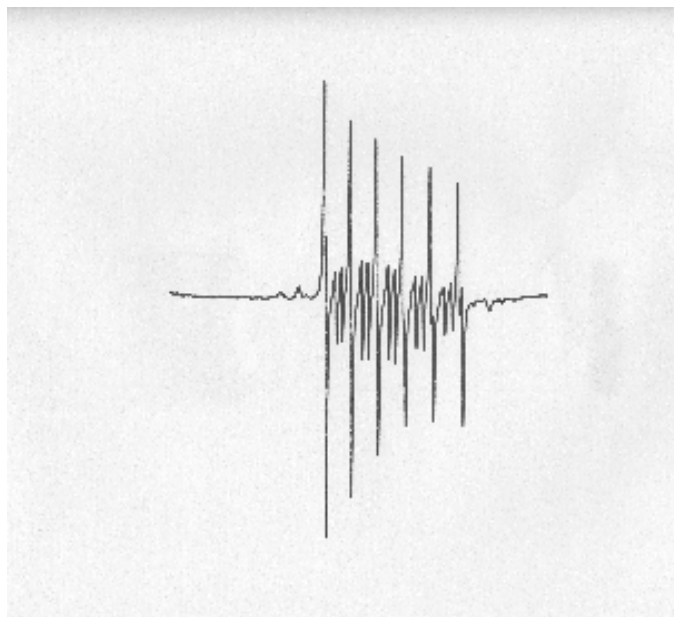


Figure 3

EPR, eventually combined with FTIR spectroscopy or colorimetry, can help to differentiate similar materials and imitations from turquoise. Figure 3 shows the Mn²⁺ EPR spectrum characteristic of magnesite and carbonates.

References

Clark, C.O. et al. (1979). Variable temperature electron spin resonance of turquoise. *American Mineralogist* 64, 449-451.

Quartz cat's eyes with unusual fibre distribution patterns

Jurgen Schnellrath

Centro de Tecnologia Mineral, Rio de Janeiro, Brazil, jurgen@cetem.gov.br

Roberto Salvador Dias Miceli

Centro de Tecnologia Mineral, Rio de Janeiro, Brazil, rmiceli@cetem.gov.br

Hélio Salim de Amorim

Instituto de Física, Universidade Federal do Rio de Janeiro, Rio de Janeiro, Brazil, hsalim@if.ufrj.br

Two quartz cat's eyes submitted for analysis at the gemmological laboratory of the Center for Minerals Technology (CETEM) are described in this work: a brownish-green cat's eye (Fig. 1) of uncertain origin (India?), and a greyish-white cat's eye (Fig. 2) from a new source in Bahia, Brazil.



Figure 1: Brownish green quartz cat's eye (cabochon length: 10.6 mm)



Figure 2: Greyish-white quartz cat's eye (cabochon length 11.3mm)

Both cat's eyes show very unusual distribution patterns of their fibres when observed from the side (Figs. 3 and 4, taken in immersion and using transmitted light).



Figure 3: Distribution pattern of fibres in the brownish-green cat's eye (width 6mm)

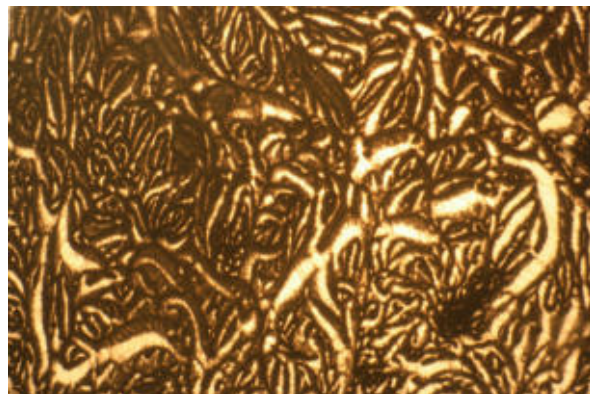


Figure 4: Distribution pattern of fibres in the greyish-white cat's eye (width 12 mm)

This work presents the results of preliminary investigations using scanning electron microscopy (SEM) coupled with an energy dispersive system (EDS) for chemical analysis, X-ray powder diffractometry (XRD), refinement of cell parameters and Laue-grams in order to elucidate the nature of these inclusions and help explaining these patterns.

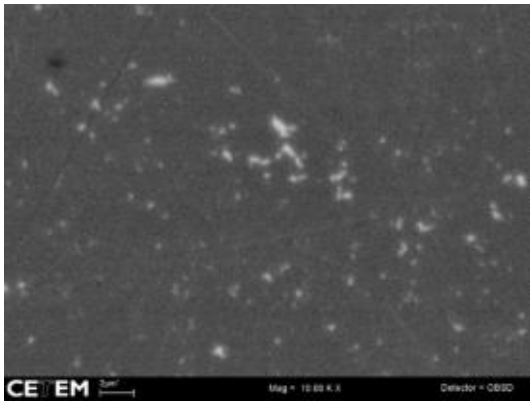


Figure 5. SEM picture of the brownish-white cat's eye. Bright spots represent cross sections of the fibres, tentatively identified as pyroxenes.

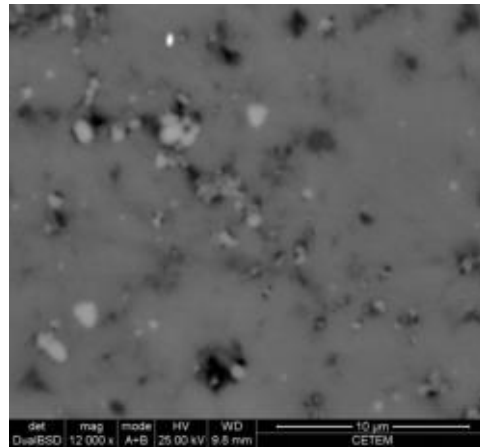


Figure 6. SEM picture of the greyish-white cat's eye. Bright spots represent cross sections of the fibres, tentatively identified as tourmalines.

The vast majority of fibres responsible for the cat's eye effect in the brownish-green quartz possess nanometric diameters (Fig. 5) and could not be detected by XRD. Qualitative SEM/EDS analysis and crystallographic similarities between certain structure units indicate that these fibres are probably members of the diopside - hedenbergite series. Lauegrams showed that these pyroxene fibres are aligned with the a-axis of the quartz host. The pattern could be interpreted as the result of directional eutectic solidification.

Most of the fibres in the greyish-white quartz on the other side have micrometric diameters (Fig. 6) and, based on SEM/EDS analysis and XRD, they belong to the dravite – ferridravite (povondraite) series. The quartz host is not a single crystal, but rather composed of several domains with distinct crystallographic orientations.

Searching for similar patterns in the mineralogical and gemmological literature, we were able to find only a short note showing a very similar pattern to the one observed in the greyish-white cat's eye (Crowningshield, 1963). Indeed, the colour of the quartz cat's eye in the note of this author is also described as greyish-white.

References

Crowningshield, R., 1963. Quartz cat's-eye. *Gems & Gemology*, 11(2), 43.

Irradiated blue common opal from Brazil

Claudio C. Milisenda¹, Jurgen Schnellrath², Jürgen Schütz³

¹ DSEF German Gem Lab, Prof-Schlossmacher-Str. 1, D-55743 Idar-Oberstein, Germany, info@gemcertificate.com

² Laboratório de Gemologia, Centro de Tecnologia Mineral, Av. Pedro Calmon 900, Rio de Janeiro, Brazil, jurgen@cetem.gov.br

³ Emil Weis Opals, Auf dem Hüttenflur 8, D-55743 Kirschweiler, Germany, opals@emilweis.de

Blue opal is considered rare and is known from sources in USA, Mexico, Peru and Brazil. The transparent, faceted, greenish-blue to blue specimens shown in Figure 1 weigh between approx. 1.5 and 7.1 ct and are reportedly from a new find in the Brazilian state of Bahia.



Figure 1: Irradiated blue opals from Brazil

The samples vary in density from 2.00 to 2.03 g/cm³. The refractive index was determined as 1.440. These standard gemmological properties in addition to FTIR spectra classify the samples investigated as opal-CT of volcanic origin (Fig. 2). Published data on blue opals commonly show higher values for both refractive index and density (e.g. Smith, 1988; Caucia et al., 2009) and correspond to opal-C. In addition, the remarkable colour and clarity of the stones raised questions about a possible enhancement. Two of the authors (JS and JS) tried to locate the original source during a field trip to Brazil but no evidence or any record of such a mine in Bahia was found. Instead, we were told that these opals owe their colour to an artificial irradiation using yellowish opal from Rio Grande do Sul as a starting material.

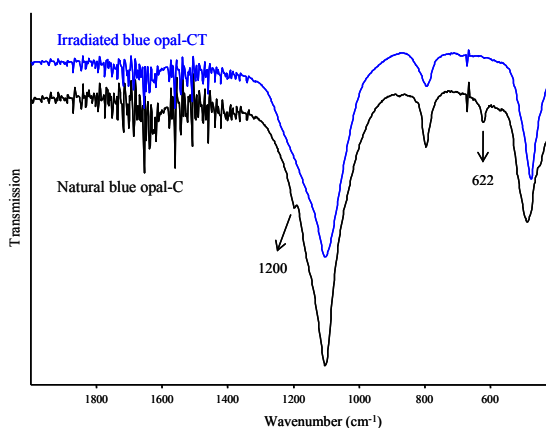


Figure 2: FTIR spectra of an irradiated blue opal-CT sample and a natural blue opal-C sample with characteristic absorptions at around 620 cm⁻¹ and 1200 cm⁻¹.

Recently, we received a series of opals from a volcanic environment in Rio Grande do Sul which purportedly represent samples before and after irradiation treatment. Examples are shown in Figure 3.



Fig. 3: Opals purportedly before (left) and after (right) irradiation

Own experiments indeed show that it is possible to induce a bluish colour in opals by electron radiation, although only a small portion of the stones submitted for irradiation show a distinct colour change (Fig. 4).



Fig. 4: Opals from Brazil before (left) and after (right) they have been irradiated with electrons.

We have just started to investigate the properties of these types of treated opals and natural coloured blue opals with various analytical techniques. Data sampling is in progress and more samples are collected for testing. The physico-chemical characteristics will be presented in detail.

References

- Caucia, F., Ghisoli, C. Adamo, I. 2009. A study on the characteristics of some C- and CT-opals from Brazil. *N.Jb. Miner. Abh.* 185(3), 289-296.
 Smith, K.L., 1988. Opals from Opal Butte, Oregon. *Gems & Gemology*, 24(4), 229-236.

Play-of-colour opal from Wollo, Ethiopia: a new pedogenetic model for gem opal formation

**Benjamin Rondeau¹, Emmanuel Fritsch², Francesco Mazzero³, Bénédicte Cenki-Tok⁴,
Dereje Ayalew⁵, Yves Bodeur¹**

¹University of Nantes, Laboratoire de Planétologie et Géodynamique, UMR-CNRS 6112, 2 rue de la Houssinière, BP 92208, F-44322 Nantes cedex 3, France.

²University of Nantes, Institut des Matériaux Jean Rouxel, UMR-CNRS 6502, 2 rue de la Houssinière, BP 32229, F-44322 Nantes cedex 3, France.

³GEMOA SARL, 59 rue Sainte Anne, F-75002 Paris, France.

⁴Geosciences Montpellier, UMR 5243 - CC 60, Université Montpellier 2, Place E. Bataillon, 34095 Montpellier cedex 5, France.

⁵Addis Ababa University, Department of Earth Sciences, PO box 729/1033, Addis Ababa, Ethiopia.

Abundant play-of-colour opal has been mined in the area around Wegel Tena, Wollo Province, Ethiopia, since the discovery of opal deposits in 2008 (Mazzero et al., 2009; Rondeau et al., 2009, 2010a, 2010b). Highly valuable samples have been cut. Some are very large and display strong play-of-colour with all spectral colours, in particular abundant red (Fig. 1). The most important mining area is close to the village called Tsehay Mewcha. Some other opal-bearing areas have been discovered some kilometres away, and prospection is on going (Fig. 2). All these deposits are found in a single thin stratigraphic level of about one metre inside a 400 m thick volcano-sedimentary unit, an ignimbritic sequence of Oligocene age (30 million years old; Fig. 3).

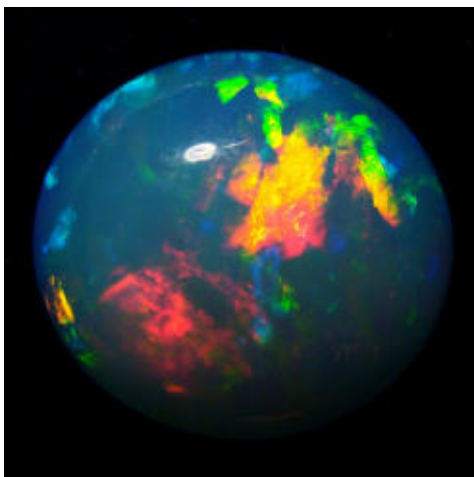


Figure 1: The opal deposits at Wegel Tena, Wollo Province, Ethiopia, have been mined since 2008. Highly valuable play-of-colour samples with milky white body colour and many different diffraction colours, including red such as in this cab, are regularly unearthed in this area. Photo by F. Mazzero.



Figure 2: One of the authors (FM) shows a deposit called "Borena Mickaël". This is one of the numerous places where opal is mined in the area close to Wegel Tena. Photo by B. Rondeau.



Figure 3: All small deposits (in red) are in the same stratigraphic level that corresponds to a weathered layer in a thick volcano-sedimentary series of Oligocene age (30 million years old).



Figure 4: Plant fossils, such as these ramified twigs of millimetric section, are commonly found in opals from Wegel Tena. a) picture width: 2 cm, photo by F. Mazzero. b) picture width: 5mm, photo by B. Rondeau.

The examination of the mother rock layer in the field provided numerous indications that this level has been submitted to a strong weathering episode, with abundant traces of biological activity: root holes, bioturbations, accumulation of clay gravels, and plant fossils inside opal (Fig. 4). The excellent preservation state of these carbon-bearing fossils indicate that opal formed during this weathering episode, at the Oligocene period, when weathering was transforming the rock into a soil (pedogenesis). Moreover, this proves that opal formed at ambient temperature, directly in the wet soil. The exact process of opal precipitation under these conditions is under investigation.

References

- Mazzero, F., Gauthier, J.-P., Rondeau, B., Fritsch, E., Bekele, E., 2009. Nouveau gisement d'opales d'Ethiopie dans la Province du Welo : premières informations. *Revue de Gemmologie a.f.g.*, 167, 4-5.
- Rondeau, B., Mazzero, F., Bekele, E., Gauthier, J.-P., Fritsch, E., 2009. Gem News International: New play-of-color opal from Welo, Ethiopia. *Gems & Gemology*, 45(1), 59-60.
- Rondeau, B., Fritsch, E., Gauthier, J.-P., Mazzero, F., Cenki-Tok, B., Bekele, E., Gaillou, E., 2010a. Play-of-color opal at Wegel Tena, Wollo, Ethiopia. *Gems & Gemology*, 46 (2), 90-102.
- Rondeau, B., Fritsch, E., Cenki-Tok, B., Mazzero, F., 2010b. New opals from Wollo, Ethiopia: geochemical characterization. *Geochimica et Cosmochimica Acta*, 74(12), A880.

Beryl – 30 years later

H.A. Hänni

SSEF, Basel, Switzerland, h.a.haenni@gmail.com

Introduction

The beryl structure is a good example to show developments from a simple mineral with chromophore trace elements to a structure with coupled isomorphous replacements and further to different minerals. The beryls today form a group containing beryl, bazzite, pezzottaite, and stoppaniite. Common and separating features are explained and gemmological relevance is indicated.

In 1980 the author has delivered his doctoral thesis on beryls $\text{Be}_3\text{Al}_2\text{Si}_6\text{O}_{18}$ from Swiss Alpine cleft occurrences (Hänni, 1980). Optical, structural and micro-chemical measurements were performed on a number of tiny crystals usually in the mm to sub-mm order. Microprobe analyses have shown the importance of scandium (Sc), iron (Fe) and magnesium (Mg). Some of the samples had large amounts of Sc and almost no Al, what corresponds to the mineral Bazzite $\text{Be}_3\text{Sc}_2\text{Si}_6\text{O}_{18}$ (Artini, 1916). Those bazzites are blue and opened the view on the effect that Fe had on the colour. Furthermore some samples contained Sc but not as much as needed for bazzite, and the question arose if there was a mixed crystal series from beryl to bazzite.

Months after having finished the thesis, the author started his professional life as a gemmologist at SSEF Swiss Gemmological Institute. With George Bosshart we identified beautiful Colombian emeralds, but also Zambian and synthetic emeralds. And it became clear that the so-called “constants” were not at all constant for a gemstone with the same name-tag. A preliminary research on emerald chemical compositions (in comparison to synthetic emerald) was carried out (Hänni, 1982). From this study it became obvious that various chemical replacement mechanisms affect the physical data of emeralds, too.

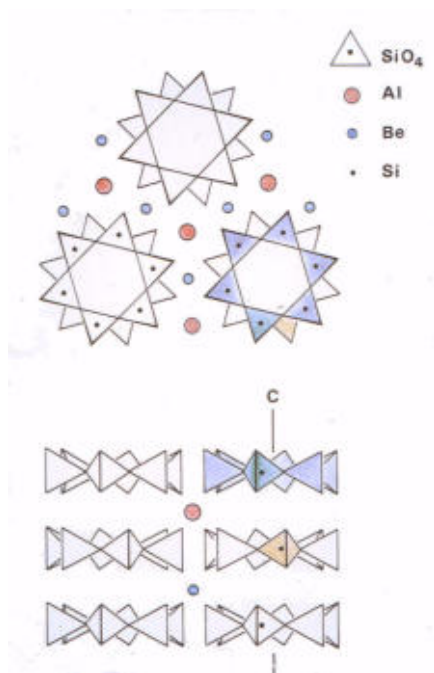


Figure 1. A simplified model of the beryl structure.

A. Basics of beryl

The crystal structure of beryl is determined by rings of 6 SiO₄ tetrahedra, stacked over each other to form a channel in the centre. The channel direction is parallel to the crystallographic c- axis and optical axis. Between the rings and on intermediate horizontal layers Be and Al ions are linking the rings. Al³⁺ ions are surrounded by 6 oxygens, forming an octahedron. The much smaller Be²⁺ ions are packed into 4 oxygens forming a tetrahedron (Fig.1).

Earlier papers have shown that the main formula of beryl can be modified by two major substitutions: the tetrahedral substitution of Be²⁺ by lithium (Li⁺) and the octahedral substitution of aluminium (Al³⁺) by other trivalent ions (Bakakin & Belov, 1962), see Fig.2. These direct substitutions have greatest importance for gem beryl when chromium (Cr³⁺) or vanadium (V³⁺) is taking Al lattice sites. By the introduction of bivalent ions like Fe²⁺ or Mg²⁺ on Al³⁺ positions charge compensation is necessary in order to get the missing positive charge. This balance is usually realised by sodium (Na⁺) that is stored in the channel of the beryl structure. These coupled substitutions (e.g. Al³⁺ against Fe²⁺ plus Na⁺ or Al³⁺ against Mg²⁺ plus Na⁺) are very wide spread and are the main reason for the variation of the physical data RI and SG.

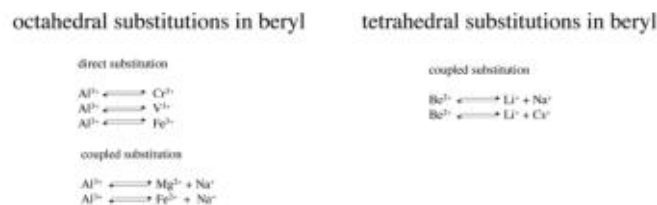


Figure 2. Some of the more relevant substitutions in beryl.

H₂O and CO₂ molecules are also incorporated in channel positions and are further raising the physical data (Cerni & Hawthorne, 1967; Goldman et al., 1978). The beryl structure as described by Bragg & West (1926), has seen a number of refinements (Gibbs et al., 1968; Artioli et al., 1993). Spectroscopic investigations have shown the relationship between chromophore trace elements and absorption spectrum, as well as traces and channel constituents in the infrared spectrum (Wood & Nassau, 1968). Water molecules in alkali-free emeralds have their dipole axis parallel to the channel (Type I water). The rotation of H₂O molecules with their axes perpendicular to the c-axis of the beryl molecules is a consequence of the presence of channel constituents such as Na⁺ or Li⁺ (Type II water). Flux grown synthetic emeralds are water free and contain no alkalis. A rich display of beryl characteristics, origins and individual features has been given by Sinkankas (1981). A modern alternative to the FTIR identification of natural and synthetic emeralds is possible by Raman spectroscopy (Huong et al., 2010).

Chromophore trace element or solid solution admixture

The colour of emeralds has always been attributed to traces of Cr and/or V. A typical Colombian emerald could thus contain 6842 ppm Cr and 4079 ppm V. These contents correspond to concentrations of 1 wt% of Cr₂O₃ and 0.6 wt% V₂O₃ (Cr/V ratios < 1 are known as well).

One could postulate new end-members with beryl structure, such as Be₃Cr₂Si₆O₁₈ or Be₃V₂Si₆O₁₈. The content of 1.0 wt% Cr₂O₃ and 0.6 wt% V₂O₃ correspond to 5.6 Be₃Cr₂Si₆O₁₈ and 4.4 Be₃V₂Si₆O₁₈ molecules, the rest being 90 Be₃Al₂Si₆O₁₈ of 100.

The Colombian emerald cited above could hence be plotted in a triangular concentration diagram, same as mineralogists are doing for other minerals in complex solid solution situations. (Fig.3).

Triangular plot for Al-Beryl, Cr-Beryl and V-Beryl

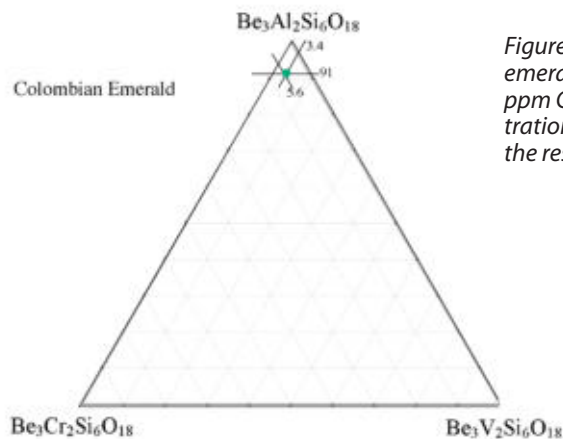


Figure 3. Triangular plot of a typical emerald from Colombia containing 6842 ppm Cr and 4079 ppm V. These concentrations are plotted in molecule units of the respective end members.

B. More recent members of the beryl group

Bazzite $\text{Be}_3\text{Sc}_2\text{Si}_6\text{O}_{18}$ has been found and described in 1916 already, originating from miarolitic occurrences. Hydrothermal formations of bazzite were subsequently found in Alpine clefts (Fig. 4) and other hydrothermal deposits. Further minerals with a beryl structure were identified in the last 30 years. It is interesting to note that beryl research is predominantly done by Italian researchers, as seen by the names and authors of the following minerals.



Figure 4. Bazzite crystal from Fibbia (Gotthard) on adularia. Length 1.5 mm.

Stoppaniite $\text{Be}_3\text{Fe}^{3+}_2(\text{Si}_6\text{O}_{18})\cdot\text{H}_2\text{O}$ was recently found (Ferraris & Rossi, 1996; Della Ventura et al, 2000) and its real composition deviates slightly from the ideal formula by some replacements to $\text{Na}_0.5\text{Be}_3(\text{Fe}^{3+}, \text{Mg}, \text{Al})_2[\text{Si}_6\text{O}_{18}]\cdot\text{H}_2\text{O}$. Originating from volcanic pyroclastic rocks, these crystals are in the lower mm dimensions, as we have seen with bazzite, too.

It may be interesting to note that H.A. Hänni has produced synthetic Fe-Beryl in 1978 in a hydrothermal experiment in the course of his doctoral thesis. As the result was not considered a novelty, it was not published in a publication on its own. The data like chemical composition, refractive indices and powder diffraction values of this new mineral were also published in the English abstract of the thesis, but this material was not remarked by the Italian researchers on beryl who later published on Stoppaniite (Ferraris et al, 1998; Della Ventura et al., 2000).

Pezzottaite $(\text{Be}_2\text{Li})\text{Al}_2\text{Si}_6\text{O}_{18}$ Cs was found in Madagascar in 2002 and first considered as a Cs-rich morganite by some gemmologists, but then identified as a new mineral (Laurs et al, 2003, Hawthorne et al. 2004). In this mineral, the tetrahedral substitution of Be_{2+} by Li^+ is going far beyond what is encountered in morganites (Hänni & Krzemnicki, 2003). That 1/3 of the tetrahedral sites are occupied by Li^+ is reducing the symmetry from hexagonal to trigonal. The charge is balanced by the introduction of Cs^+ in the channel position.

A Cs-beryl from Afghanistan with a content of 9.7 wt% Cs_2O , Pezzottaite has over 14.4 wt%, suggests that a solid solution between Pezzottaite and Morganite could exist (Hänni & Krzemnicki, 2003).

The colour of pezzottaites found so far is pink, due to Mn traces. As the simplified Pezzottaite formula does not necessarily need Mn, other chromophores are imaginable. We are thus looking forward to find blue pezzottaite with traces of Fe!

Discussion

In the last 30 years the beryl group has got at least two new members. The concept of solid solution seems to be a good perspective when relationships between members of the beryl group are discussed. Hypothetic end-members and plotting in triangles and tetrahedra allow a presentation of beryl mineral relationship better than the concept of trace or minor element discussion.

References

- Artini, A. (1916): Due minerali di Baveno contenenti terre rare: Weibeite and Bazzite. *Atti Acca. Lincei Rend.*, 5, 24/1, 313-319
- Artioli, G., Rinaldi, R., Ståhl, K & Zanazzi, P.F. (1993): Structure refinements of beryl by single-crystal neutron and X-ray diffraction. *Am.Mineral.* 78, 762-768
- Bakakin, V., Belov, V. (1962): Crystal chemistry of beryl. *Geochemistry*, 5, 485-500
- Bragg, W.L. & West, J. (1926): The structure of beryl. *Proc. R. Soc. London, A*, 111, 691-714
- Cerni, P., Hawthorne, F.C. (1967): Refractive indices versus alkali contents in beryl: general limitations and applications to some pegmatite types. *Canad. Mineralogist*, 14, 491-497
- Della Ventura, G., Rossi, P., Parodi, G.C., Mottana, H., Raudsepp, M. & Prencipe, M. (2000): Stoppaniite, $(\text{Fe}, \text{Al}, \text{Mg})_4(\text{Be}_6\text{Si}_{12}\text{O}_{36} \cdot n\text{H}_2\text{O})_2\text{Na}_n$, a new mineral of the beryl group from Latium (Ital). *Eur.J.Mineral*, 11, 121-127
- Ferraris, G., Prencipe, M. & Rossi, P. (1998): Stoppaniite, a new member of the beryl group: crystal structure and crystal chemical implications. *Eur.J.Mineral*, 10, 491-496

- Gibbs, G.V., Breck, D.W., Meagher, E.P. (1968): structure refinement of synthetic hydrous and anhydrous beryl. *Lithos*, 1, 275-285
- Goldman, D.S., Rossman, G.R., & Parkin, K.M. (1978): The channel constituents of beryl. *Phys. Chem. Minerals.*, 3, 225-235
- Hänni, H.A. (1980): Mineralogische und mineralchemische Untersuchungen an Beryll aus alpinen Zerrklüften.- Dissertation. Universität Basel. 107pp.
- Hänni, H.A. (1982): A contribution to the separability of natural and synthetic emeralds.- *J.Gemmol.* XVIII, 138-144
- Hänni, H.A., Krzemnicki, M.S. (2003): Cesium-rich morganite from Afghanistan and Madagascar. *J. Gemm.*, Vol. 28, No. 7, 417 - 429
- Hawthorne, F.C., Cooper, M.A., Simmons, W.B., Falster, A.U., Laurs, B.M., Armbruster, T., Rossman, G.R., Peretti, A., Günter, D. & Grobéty, B. (2004): Pezzottaite Cs(Be₂Li) Al₂Si₆O₁₈. A spectacular new beryl mineral from the Sakavalana pegmatite, Fianarantsoa Province, Madagascar. *Mineralogical Record*, Vol. 35, September-October
- Huong, T.T.L., Häger, T., & Hofmeister, W. (2010): Confocal micro-Raman spectroscopy: A powerful tool to identify natural and synthetic emeralds. *Gems & Gemology*, XLVI, Spring, 36-41
- Laurs, B., Simmons, W.B., Rossman, G.R., Quinn, McClure, S.F., Peretti, A., Armbruster, T., Hawthorne, F.C., Cooper, M.A., Falster, A.U., Günter, D., Cooper, M.A. & Grobéty, B. (2003): Pezzottaite from Ambatovita, Madagascar: A new gem mineral. *Gems&Gemology*, Winter, 284-301
- Sinkankas, J. (1981): Emerald and other beryls. Chilton Book Company. Radnor, Pennsylvania. ISBN 0-8010-7114-4. 665pp
- Wood, D.L. & Nassau, K. (1968): The characterization of beryl and emerald by visible and infrared absorption spectroscopy. *Amer. Mineralogist*, 53, 777-800

Acknowledgements

The author thanks Dr. F. Herzog (SSEF Swiss Gemmological Institute) for fruitful discussions of this paper.

A Study of an extraordinary Cs- and Li-rich beryl from Madagascar

Liu Shang-I (gemedward@hotmail.com)^{1,2}, Peng Ming-sheng¹, Li Guo-wu³

¹ Institute of Gems and Minerals Material, Sun Yat-sen University, Guangzhou, China;

² Gemmological Association of Hong Kong, Hong Kong SAR

³ China University of Geosciences (Beijing), Beijing 100083, China

The discovery of pezzottaite raised many questions in gemstone identification. During the study of pezzottaite, the authors discovered that some purplish-red and colourless samples coming from the same pezzottaite mine in Madagascar and which showed similar appearance, physical properties and chemical composition, had been identified as "Cs-, Li-rich beryl" using X-ray single crystal diffraction (Liu et al., 2008, 2009).

Apart from standard gemmological techniques, EMP and LA-ICP-MS, FTIR, Raman and electron paramagnetic resonance (EPR) spectroscopy were used to characterize these materials. All samples showed anomalous properties of very high Li and Cs content (Li₂O up to 2.16 wt.%, Cs₂O up to 13.4 wt.%) and higher values for R.I. (n_e=1.607 and n_o=1.616, DR=0.008-0.009) and S.G.. (2.85-3.00) compared to morganite and bixbite. X-ray single crystal diffraction revealed that they showed the beryl structure (space group= P6/mcc; hexagonal system) with an irregular arrangement of Li⁺ ions in the Be²⁺ site and with Cs⁺ ions in the channel site. The value of the unit-cell parameter (sample LB4) a is similar to that of "normal" beryl, a=9.2127Å. However, the value of c increases dramatically, c=9.2658(8)Å, c/a ratio=1.0057, over the upper limit of the range of "tetrahedron" (substitution of ions in the Be tetrahedral sites) beryl (c/a=0.999-1.003) that has been reported by Aurisicchio et al. (1988). The substitution of Li⁺ for Be²⁺ not only causes an increase in the value of unit-cell parameter c and the c/a ratio of beryl as the tetrahedral cation-oxygen distances increase, but also influences the peak positions of lattice-vibration under IR and Raman.

In contrast to previous findings, a straightforward separation of this Cs-, Li-rich beryl from pezzottaite (Cs(Be₂Li)Al₂Si₆O₁₈) by using chemical analysis or ordinary gemmological tests (e.g. R.I. and S.G) is not possible. Instead of looking at the shifting of some peak positions of the beryl spectrum (Liu et al., 2005), FTIR and Raman spectroscopy studies have to focus on the splitting peaks (doublets) in the superstructure of pezzottaite corresponding to Si-O-(T) bonds (T: tetrahedral site for Li or Be) and Si-O-Si (ring) bonds in the 1200-900cm⁻¹ lattice-vibration domain (Fig. 1). EPR spectra indicated that both pezzottaite and Cs-, Li-rich beryl from Madagascar have the same six hyperfine structure lines corresponding to the nuclear spin of I=5/2 of Mn²⁺ (100% natural abundance), with an identical g-factor (g_⊥=2.0027) (Figs. 2 and 3). However, each of the hyperfine structure lines of pezzottaite is further split into 3 sublines (one stronger line and two weaker lines). This can be ascribed to the distortion of the octahedral (Mn) sites in the structure of pezzottaite.

Although both Li-, Cs-rich beryl and pezzottaite belong to the beryl group (Hawthorne et al., 2004), they show different Laue diffraction images under synchrotron radiation (white beam) x-ray topography (SRXRT) corresponding to different crystal systems with six-fold and three-fold symmetry along the c-axis (//[0001]) respectively (Liu et al., 2007).

The discovery of this extraordinary Cs-, Li-rich beryl reveals the crystal growth environment. This environment changes according to temperature which involves an order-disorder transformation in the beryl structure resulting in Cs-, Li-rich beryl with relatively high temperature and pezzottaite with relatively low temperature. It is probable that the Madagascar sample with an 11.3 wt.% Cs₂O content studied by Evans and Mrose (1966) may be Cs-, Li-rich beryl but not pezzottaite.

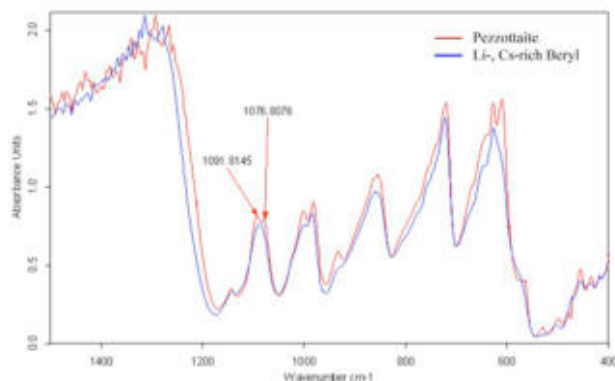


Figure 1. FTIR spectra of Cs-, Li-rich beryl (blue) and Pezzottaite (red) [//C-axis]

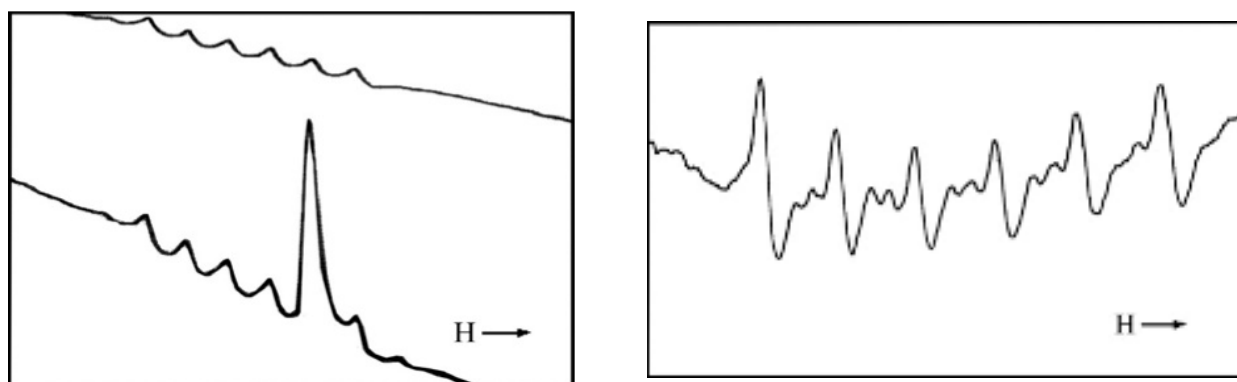


Figure 2 (left) EPR spectra of Mn²⁺ hyperfine structure of Cs-, Li-rich beryl (CB-1) in different orientations [H (Magnetic field): 3350 ± 1000G]

Figure 3 (right). EPR spectra of Mn²⁺ hyperfine structure of pezzottaite (PE-1) from Madagascar [H: 3360 ± 1000G]

References

- Aurischio C. et al. 1988. Reappraisal of the crystal chemistry of beryl. *American Mineralogist*, 73, 826-837
- Evans H.T. and Mrose M.E., 1966. Crystal chemical studies of cesium beryl. Abstracts: Geological Society of America Meeting, 63
- Hawthorne F.C., Cooper M.A., 2004. Pezzottaite Cs(Be,Li)Al₂Si₆O₁₈: A Spectacular New Beryl –Group from the Sakavalana Pegmatite, Fianarantsoa Province. *Mineralogical Record*. No.7, 35(5), 369-378
- Liu S.I., Li Guo-Wu, Peng M.S., 2009. New Investigation of the crystal structure of Pezzottaite. (Proceedings of the 7th Chinese Society for Mineralogy, Petrology and Geochemistry Congress). *Bulletin of Mineralogy, Petrology and Geochemistry*, 28(suppl.), 25 (in Chinese)
- Liu S.I., Li Guo-Wu, Peng M.S., 2008. Crystal Structure Analysis of Pezzottaite and Its Application. *Acta Mineralogica Sinica*, 28(4), 350-356 (in Chinese with English abstract)
- Liu S.I., Peng M.S., Meng Y.F., 2007. Application of synchrotron radiation x-ray diffraction topography to the gemmological field. Proceedings of the Material Science and Technology in Engineering Conference, (Hong Kong SAR), 246-250
- Liu S.I., Peng M.S., 2005. A new gem mineral - The Vibrational Spectroscopic Characterization of Pezzottaite. *Acta Mineral. Sin.*, 25, 60-64 (in Chinese with English abstract). *American Mineralogist*, 2006, 91, 222 (New Minerals: Abstract).

Preliminary report on emeralds from the Fazenda Bonfim region, Rio Grande do Norte, Brazil

J.C. (Hanco) Zwaan¹, J. Kanis²

¹ NCB Naturalis – Netherlands Gemmological Laboratory, Leiden, the Netherlands hancozwaan@gmail.com
² Römerstrasse 4, 55758 Veitsrodt, Germany

Recently emeralds were found in the Fazenda Bonfim region, between the municipalities of São Tome, Caiçara do Rio do Vento and Lajes. This deposit is situated in the Seridó Mobile Belt, located in the Borborema Pegmatitic Province, which previously was particularly known for rare element mineralisation (Be, Li, Ta-Nb), in granitic pegmatites.

Emerald mineralisation occurs associated with ultrabasic rocks within the NNE-SSW running Santa Monica Shear Zone. Small pegmatitic bodies are present in a succession of talc, talc-amphibole and (amphibole-)biotite schists, and emeralds occur in and around those bodies, particularly in biotite schist, at a sharp contact with granitic gneiss, dipping rather steeply at an angle of 40°.

Until now, prospection and exploration have been carried out at a few small open pits along the ultra-basics/granitic gneiss contact, revealing quite a number of emeralds with promising colour and clarity. Future potential of emerald production will depend on the extent of favourable circumstances along the shear zone, both laterally and down the contact. Further drilling programs and starting an underground operation at an early stage will be essential to fully explore and exploit the area.

Usually crystal fragments of emerald with homogeneous colour distribution are found. Very clear fragments typically range between 2 and 5 mm, but larger crystals, reportedly up to 5 cm, have been found.

Polished emeralds typically showed a saturated bluish green with a medium-light to medium tone, and were very slightly to heavily included. Measured refractive indices showed $n_o = 1.587-1.591$ and $n_e = 1.578-1.583$, with a birefringence of 0.008-0.009; the specific gravity varied between 2.72 and 2.74 g/cm³. Most commonly encountered inclusions were partially healed fissures with two-phase (liquid-gas) inclusions, typically square, rectangular or 'comma-like', and fine growth tubes oriented parallel to the c-axis.

Chemistry of the emeralds is characterised by medium Cr₂O₃, and FeO, high MgO, and low Na₂O and V₂O₃ (average wt.% respectively were Cr₂O₃ 0.32, FeO 0.82, MgO 2.27, Na₂O 0.66, V₂O₃ 0.03, (by electron microprobe). Additionally, the emeralds show relatively high K, but low Li values (average 764 and 106 ppm respectively, by LA-ICP-MS).

FTIR measurements reflected spectra of alkali-bearing emeralds with consistently high peaks at 2358 cm⁻¹, indicating the presence of a considerable CO₂ content in the channel of the beryl structure.

An overview of production techniques for Chinese freshwater cultured pearls

Elisabeth Strack

Gemmologisches Institut Hamburg, Hamburg, Germany, info@strack-gih.de

Introduction

The Chinese freshwater pearl industry has so far gone through four stages. Stage 1 lasted from 1962 to 1980 and started at the Zhanjiang Fisheries Institute on Leizhou Peninsula under Professor Xiong Daren who applied the mantle-grown tissue method with the local freshwater mussel *Hyriopsis cumingii*. The pearls were of high quality and were marketed through Japan together with freshwater cultured pearls from Lake Biwa. In 1972 production amounted to 11 tons.

Stage 2 was the period of the 1980s when the mussel *Cristaria plicata* replaced *Hyriopsis cumingii*. The period was characterised by a mass production of white “rice crispies” and flats but also strikingly dyed colours, all still produced with the tissue method. Marketing was through China, production reached 120 tons in 1987 and prices reached bottom level.

Stage 3 covered the 1990s, when farmers used *Hyriopsis cumingii* again. From 1992 onwards, more rounded shapes (at first still off-round and called „potatoes“) appeared on the market and developed into nearly round to fully round shapes. In addition to white, intense natural colours like pink, orange, purple and lilac were seen. Prices were above dumping level again and were even stable and could go into high ranges. From 150 tons in 1991, production reached 900 tons in 1999 and concentrated on the tissue method. A few farmers had trial harvests with mantle-grown pearls that had a round mother-of-pearl bead inserted.

Stage 4 covers the 2000s when production reaches 1.200 to 1.500 tons. *Hyriopsis cumingii* is still nearly exclusively used and all levels of qualities are produced. From 2005 onwards, more and more pearls with a mother-of-pearl bead appeared on international trade fairs, revealing that bead nucleation techniques are by now being used on a regular basis. Bead technologies differed and lead to pearls of different price levels. One could even say that with the passing of the first decade of the 21st century the Chinese cultured pearl industry has already entered stage 5.



Fig. 1: Mantle half of Hyriopsis cumingii with 17 pearl sacks containing pearls produced with the tissue method.

Discussion

The mantle-grown non-beaded method

This method uses a tiny square of mantle tissue from a donor mussel that is implanted into an incision within the mantle of the mussel destined for pearl cultivation. The square is in the range of several millimetres only and will grow into a sack that will eventually secrete pearly substance and produce a pearl. With this method, up to 20 pearls can be produced in each half of a mussel's mantle (Fig. 1).

The gonad-grown bead method Gonad implantation or „in-body“ method

The method resembles the one known for Akoya, South Sea and Tahitian cultured pearls where a round mother-of-pearl bead and a tiny piece of mantle tissue are implanted into the gonad of the destined mollusc. The mantle tissue grows into a pearl sack that surrounds the implanted bead and secretes pearly substance.

With freshwater mussels, the implantation of a rather large bead is a complicated grafting process that resembles surgery. The reason for this is that the gonad is difficult to reach and the grafter risks to injure the intestines and other organs. It is for this reason that only one bead is inserted at a time and that mostly a drilled bead is used that can be inserted with the help of a needle. The mussels are adult *Hyriopsis cumingii* or - as is sometimes reported but not verified - cross-breeds of *Hyriopsis cumingii* with the Japanese *Hyriopsis schlegelii*. The two species are closely related with each other, in fact the Japanese species developed as an island species out of *Hyriopsis cumingii*.



Fig. 2 So-called „Ikecho pearls“, ca. 17x14mm, produced with a round mother-of-pearl bead that was implanted into the gonad.



Fig. 3 So-called „Chinese Kasumigaura“, ca. 12-14mm, produced with a drilled, round mother-of-pearl bead that was implanted into the gonad.

The resulting cultured pearls are large (up to 18mm in length) and have mainly baroque shapes (Fig. 2). The latter is amazing as the inserted mother-of-pearl beads are round and were originally certainly aimed at producing round pearls. The pearls show a wide colour range that equals the most beautiful colours mentioned above for the tissue method. In addition, there is a surprisingly metallic lustre. In Spring 2005, the pearls were first offered in Hong Kong and Basel as „Ikecho pearls“, an unofficial trade name that points to the Japanese name „Ikecho gai“ (used for both *Hyriopsis cumingii* and *Hyriopsis schlegelii*) and might hint at mussel hybrids. Prices for choker lengths were in the range of up to several thousand dollars. The term „Ikecho pearls“ is meanwhile used less frequently, instead the term „in-body“ is preferred.

„Chinese Kasumigaura pearls“

In 2008, „Chinese Kasumigaura pearls“ were offered for the first time in Tucson (Fig. 3). They represent „in-body“ pearls that in their shapes, rippled surfaces and light creamy to yellow, orange and purplish hues resemble cultured pearls from the Japanese Lake Kasu-migaura which are produced with drilled beads in *Hyriopsis schlegelii* or a

cross-breed of *Hyriopsis schlegelii* and *Hyriopsis cumingii* (Fig. 4). The original method of implanting a drilled bead either into the gonad or another inner organ like the stomach of the mussel was in fact transferred from Lake Kasumigaura to China (personal communication, Kazuhisa Yanase and Fuji Voll). While in 2008 prices for Chinese pearls of the Kasumigaura look were nearly equal to those from Lake Kasumigaura, they had dropped to a much lower level of a few hundred dollars in 2011.



Fig. 4: Computer tomogram of a pearl from Lake Kasumigaura in Japan with a drilled mother-of-pearl bead.



Fig. 5: Selection of „fire balls“, produced with a round mother-of-pearl bead inside of the mussel's mantle in a pre-existing pearl sack. The pearls show characteristic tail-like appendices.

Bead implantation into the mantle

Fully round pearls

The method uses also mother-of-pearl beads but they are undrilled and get implanted into already existing pearl sacks within the mussel's mantle. This means that the mussel has already been used for pearl culture with the tissue method and has already produced pearls that were taken out of their pearl sacks at harvest time. The empty pearl sacks remain, situated in rows near to each other; in a next step they will be filled with a mother-of-pearl bead of appropriate size.

Once the beads have been inserted, the mussel goes back into the water for another cultivation period. The resulting pearls are in the same size and colour ranges as the „in-bodies“ and they are also baroque in shape. They tend however to develop a type of tail-like, rather flat appendix to which they owe their trade name „fireballs“ (Fig. 5). Moreover, as pearl sacks are quite near to each other they tend to join so that double-beaded pearls may result. As „fireballs“ can be more easily produced they have a distinct price advantage over the „in-bodies“. The two types can however not always easily be distinguished from each other with the naked eye.

Coin-shaped and bar-shaped pearls

Pearl sacs may be used a third time for producing fancy shapes in the lower price ranges; according to different sources of information this can be done either before or after the pearl sacs have produced beaded full pearls. Disc-shaped beads of either mother-of-pearl or another substance produce coin shaped pearls or fancy shapes like hearts (when the inserted disc had already a heart shape). As the pearls grow in rows they can join and produce double-coins. The joining is always an indication of mantle origin and even coin pearls can develop a „fire ball“ appendix. Instead of flat or domed discs, longish bar-shaped beads can be used that result in bar-shaped pearls. The bars may also join to produce double bars.

„Keshi pearls“

After the third harvest, pearl sacks are often left empty and are left to collapse when the mussels are returned for a last growth period into the water. The result are flat irregular pearls of a petal shape (Fig. 6). Chinese farmers attribute the name „Keshi“ to them. While the name is not correct in the sense of the CIBJO Pearl Book that defines accidentally grown cultured pearls as „Keshis“, it has meanwhile become widely used. The CIBJO commission has more or less allowed for the name in a proposed change from 2009 but has later withdrawn its proposal (Hänni, 2006).



Fig. 6: So-called „Chinese Keshis“ form when the pearl sack is left to collapse after the third harvest and the mussel goes back into the water for a last growth period.

„Soufflé pearls“

In September 2009 baroque pearls of a conspicuously light weight that otherwise resembled „Ikechos“ and „fire balls“ were offered at the Hong Kong fair (Fig. 7). When the pearls were drilled, a black viscous mass was flowing out of the drill hole, accompanied by a strong smell. The smell pointed to a fouling process that had taken place inside of the pearl due to included organic substance. X-radiograms of two pearls revealed large inner cavities (Fig. 7) and by cutting a pearl in half it was seen that it not only contained organic substance but in addition a cement-like matter that started to solidify the moment it came into contact with air. It was revealed (Jack Lynch, personal communication) that the farmers in China used mud from the pond in which their pearl cultivation took place and inserted it into pre-existing pearl sacks. It thus served as a type of nucleus and was later washed out through the drill hole, leaving partially empty pearls that had a low weight. The name „soufflé“ was selected (personal communication by Jack Lynch) in allusion to the French term „soufflure“ that was used in the natural pearl trade for hollow pearls whose shape was blown up by gases in the interior.



*Fig. 7 Left: So-called „Soufflés“, produced by inserting mud into an already existing pearl sack.
Centre: The x-radiograms show a large inner cavity.
Right: Two pearls cut in half revealed the mud-filling.*

Conclusion

For the production of Chinese freshwater cultured pearls both the tissue method and the bead+tissue method are used. While in addition to irregular shapes nearly round to perfectly round pearls can be produced by the tissue method, only baroque pearls are produced with the bead+tissue method. The latter method has two distinctly different modes of application: in-body implantation with one bead and mantle implantation with numerous beads. Distinction between the two types is not always possible by the naked eye unless pearl sacks join and produce double beaded pearls. X-radiography is a method to determine if the mother-of-pearl bead has been drilled, this would indicate an in-body implantation.

References

Hänni, H.A. (2006) A short review of the use of „keshi“ as a term to describe pearls. *J.Gemm.*30, 1/2, 51-58.

Hänni, H.A. (2007) Cultured pearls terminology. Letter to the Editor, *Gems & Gemology*, Summer, 95.

Strack, E., 2006. Pearls. Rühle-Diebener Verlag GmbH, Stuttgart, 696pp.

Acknowledgements

The author would like to thank Boril Dillenburger, Jack Lynch, Fuji Voll and Kazuhisa Yanase for personal communications.

Tokki Pearls: Additional cultured pearls formed during pearl cultivation: External and internal structures

M.S. Krzemnicki¹, A. Mueller², H.A. Hänni³, H-P. Gut⁴, M. Düggelin⁵

¹Swiss Gemmological Institute SSEF, Basel, Switzerland, mkrzemnicki@bluewin.ch

²Hinata Trading Ltd., Kobe, Japan

³GemExpert, Switzerland

⁴Gloor Instruments, Uster, Switzerland

⁵Centre for Microscopy, University Basel, Switzerland

Beaded cultured pearls (e.g. from *Pinctada maxima* or *Pinctada margaritifera*) quite often show imperfections in shape and surface condition. The presence or absence of imperfections is likely coupled at least partially with the grafting procedures (Hänni 2007). Thus the more aseptic and controlled the cutting of the tissue implant (Japanese term „Saibo“) from a donor oyster and the implementation within the recipient oyster, the less such imperfections occur.

The nature of these imperfections varies in a wide range. Quite common are roundish bumps and bulges, which are in fact small additional pearls formed as a by-product on a beaded cultured pearl. These additional cultured pearls may be still attached to the beaded cultured pearl. They may also, however, fall apart when the cultured pearls are harvested. Tradition-ally, these additional cultured pearls are called “tokki” pearls (Japanese).

These additional cultured pearls are quite commonly found during the pearl harvest. They are often found in size of 1 – 5 mm. Larger sizes are more rare. They often show button-shapes, commonly with a more or less flat non-nacreous base, showing a circular structure of nacre layers where the “tokki” was attached to the larger cultured pearl before breaking off.

Radiography pictures show various structures within these tokki pearls. Some show irregular to roundish central cavity structures, similar to those commonly found in non-beaded cultured pearls (Scarratt et al., 2000, Hänni, 2006, Sturman, 2009). Most, however, are characterised by a dark centre with distinct circular structures. Thus, their internal structure may resemble those of a natural pearl. Figure 1 shows a cross section of a pair of such additional cultured pearls (tokki). These tokki pearls show one (left) or two (right) small white central spots of calcium carbonate (Krzemnicki et al. 2010, Krzemnicki 2011), surrounded by a rather loose structure of organic rich dark grey growth rings dominated by conchyn. Finally, they are covered by a nacre layer. The reason for the presence of these white spot(s) is currently not completely understood. Similar features may even be seen in natural pearls (Hainschwang 2010).

As the perfect accumulated circling growth structures suggest, these additional cultured pearls formed in the first stage quite undisturbed from the nacre deposition on the neighbouring large bead. They were “attached” to the larger beaded cultured pearl only at a late stage of nacre deposition.



Figure 1: Cross section through a beaded cultured pearl with two additional cultured pearls ("tokki").

Figure 2 shows a X-ray computed microtomographical section through another "tokki" pearl. It shows a similar internal structure as the specimen in figure 1. However, the darker organic rich center is much smaller in the previous sample, whereas the nacre layer is now dominating. The distinct intersection line between the nacre of the beaded cultured pearl (below) and the "tokki" pearl indicate again, that the "attachment" of this additional cultured pearl happened only at a very late stage of the nacre deposition in the pearl sac.

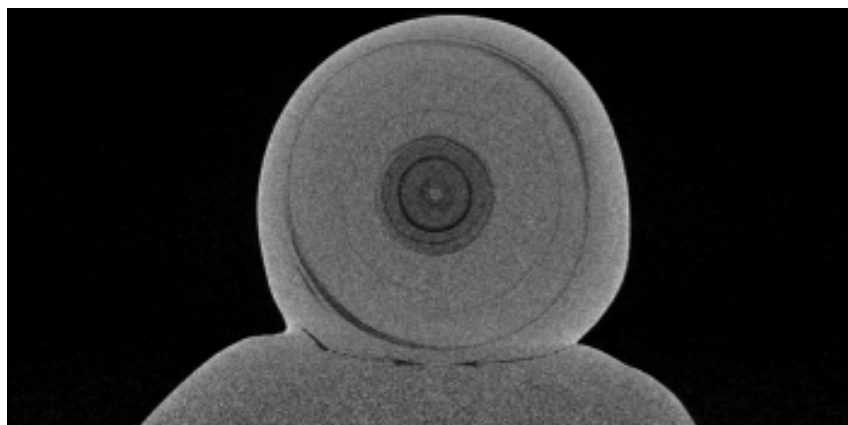


Figure 2: Tomographical section (coronal) through the upper part of a beaded cultured pearl with one additional cultured pearl ("tokki").

Figure 3 shows a scanning electron microscopic (SEM) picture of a section through the central part of another specimen. The picture has been registered in the back-scattered electron mode. Thus the different grey scales represent different chemical composition, i.e. the brighter parts are higher in atomic number (calcium carbonate) than the dark grey parts (rich in organic matter). The picture shows a complex circling structure combined with radial structures, which is far more complex than visually can be observed (dark brown circles with a white calcium carbonate central spot).

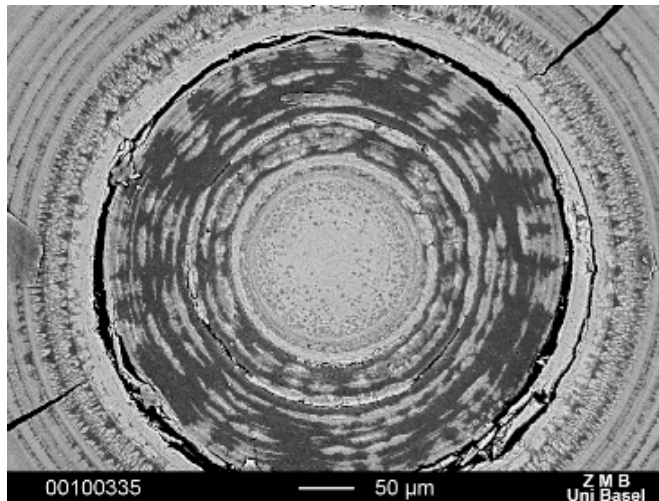


Figure 3: SEM micrograph (Backscattered electron mode) of the central part of another specimen, showing a complex structure of chemically different parts (bright parts: calcium carbonate rich, darker parts: organic rich)

Based on the observed structure of these tokki pearls we assume, that small additional pearl sacs may develop close by the main pearl sac, which forms around the inserted bead as a result of the simultaneous tissue implant. The reason for such additional pearl sacs may be spontaneous tissue transformation (or pearl sac bulging) or due to tiny tissue fragments resulting from a unperfect cutting of the saibo prior to implementation. Usually at a late stage of pearl cultivation, the large pearl sac entraps the small pearl sac(s), thus attaching the “tokki” pearl(s) on the large cultured pearl.

The presentation will focus on the observed structures in such additional cultured pearls (tokki) based on cross sections, radiography, X-ray computed microtomography and scanning electron microscopy (SEM). The structures will be compared and discussed to the ones of natural pearls and cultured pearls, i.e. beaded ones using different bead materials (Hänni et al. 2011) and non beaded ones.

References:

- Hänni H.A. (2006) A short review of the use of ‘keshi’ as a term to describe pearls. *Journal of Gemmology*, Vol. 30, No. 1–2, pp. 52–58.
- Hänni H.A. (2007) A description of pearl farming with *Pinctada maxima* in South East Asia. *Journal of Gemmology*, Vol. 30, No. 7–8, pp. 357–365
- Hänni H.A., Krzemnicki M.S., Cartier L. (2010) Appearance of new bead material in cultured pearls. *Journal of Gemmology*, Vol. 32, No. 1–4.
- Hainschwang T. (2010) A difficult new type of cultured pearl entering the market. *Gemnotes*, Vol. 1, No. 2, pp. 6–11, www.gemlab.net/website/gemlab/fileadmin/user_upload/GEMNOTES/Gemnotes-16-05-10.pdf
- Scarratt K., Moses T.M., Akamatsu S. (2000) Characteristics of nuclei in Chinese freshwater cultured pearls. *Gems & Gemology*, Vol. 36, No. 2, pp. 98–109.
- Sturman N. (2009) The microradiographic structures of nonbead cultured pearls. GIA Thailand, Bangkok, August 20, see: www.giathai.net/pdf/The_Microradiographic_structures_in_NBCP.pdf
- Krzemnicki, S.M., Friess, S.D., Chalus, P., Hänni, H.A. & Karampelas, S. (2010) X-ray computer microtomography: distinguishing natural pearls from beaded and non-beaded cultured pearls. *Gems & Gemology*, Vol. 46, No. 2, pp. 128–134.
- Krzemnicki M.S. (2011) ‘Keshi’ cultured pearls are entering the natural pearl trade. *SSEF Facette*, No. 18, pp. 8–9 and electronic SSEF Trade Alert May 2010, see www.ssef.ch

Cultured Queen conch pearls - A comparison to natural Queen conch pearls

**Nick Sturman¹, Wuyi Wang², Ken Scarratt¹, Akira Hyatt²,
Hector Acosta-Salmon³, Megan Davis³**

¹GIA Laboratory, Bangkok, Thailand, nsturman@gia.edu and kscarrat@gia.edu

² GIA Laboratory, New York, USA wwang@gia.edu and ahyatt@gia.edu

³ Harbor Branch Oceanographic Institute, Florida Atlantic University, hector.acostasalmon@gmail.com and mdavi105@hboi.fau.edu

Introduction

Conch pearls from the *Strombus gigas* or queen conch mollusc are amongst the most beautiful porcelaneous pearls known. The attractive pink colours most prized to connoisseurs have been collected or used to adorn many striking pieces of jewellery throughout history (Fritsch & Misiorovski, 1987), a trend that looks likely to continue so long as the mollusk thrives in its natural environment. This presentation discusses the culturing of conch pearls that was successfully developed in 2006 by Harbor Branch Oceanographic Institute at Florida Atlantic University in the USA and compares selected samples from the 202 cultured samples loaned by the University to the GIA against selected samples from over 300 natural samples obtained by the GIA for examination. Whilst still in the initial stages of development, the production of both bead cultured and non-bead cultured conch pearls could be a way in which conch farming could assist with both the replenishment of this over-fished species and provision of an additional product for the pearl dealer's inventory.

The Culturing

All the samples produced were obtained from hatchery produced *Strombus gigas* (queen conch) molluscs. Conch were relaxed to facilitate seeding, inspection, and harvesting. Allograft (queen conch grafted with tissue from another queen conch), autograft (queen conch grafted with own tissue) and xenograft (McGinty et al., 2010) (grafts between queen conch, milk conch and florida fighting conch) procedures were used to produce the pearls. Conch were seeded with one nucleus and a piece of mantle tissue to produce beaded cultured pearls, or were seeded with two or three pieces of mantle tissue only to produce non-beaded cultured pearls. Pearl samples were obtained after 6 weeks, 12 weeks, 6 months and 12 months of culture. Success rates were as high as 60% for beaded cultured pearls and 80% for non-beaded cultured pearls. After pearl harvesting, the conch were returned to the culture tanks to recover where the existing pearl sacs healed and produced further second generation cultured pearls in the majority of cases.

The Pearls

The bead and non-bead cultured pearls produced are just like the natural pearls externally (colors, shapes and surface structures), as would be expected. Since the same mollusc produces them there should be no obvious differences from their external appearances since nothing about the procedures employed would lead to such differences. The same applies to the spectroscopic results obtained on the samples examined. Nothing in the Raman or UV-Vis-NIR spectra obtained provides anything for gemmologists to use to help differentiate between cultured and natural examples, and this was also true of the chemistry data obtained from EDXRF analysis. The only reliable

way to currently separate cultured pearls from their natural counterparts is via their microradiographic and/or computed micro-tomography structures. In bead cultured pearls the bead nuclei (Fig. 1) are in most cases clearly visible as a circular demarcation between the bead nucleus and overlying growth layers. In the non-bead cultured examples irregular void related structures characteristic of those seen in some nacreous non-bead cultured pearls were often clearly apparent. The colours produced varied from the usual strong and light pink or pink hues characteristic of conch pearls to light orange and orange hues, and a few appeared white, cream or brown. This matches closely with the known natural colors of conch pearls. The sizes ranged from smaller carat weights to the largest cultured example currently reported which weighs 14.41 carats. The latter is an exception rather than the rule though and they generally weigh less than 4.00 carats, however it is clear that the short growth times of 6 to 12 weeks for some of the pearls limit the sizes obtained to date and also the overgrowth thickness measurements that follow. The actual sizes of the pearls produced to date fall between 0.02 and 14.41 carats. Overgrowth thickness measurements on the bead cultured conch pearls varied significantly from 0.05 to 4.00 mm, with the usual range falling between 1.00 to 2.00 mm depending on the size of the specimen. Most of the cultured pearls were in culture for 12 months and appear to have reached an acceptable gem size during that period.

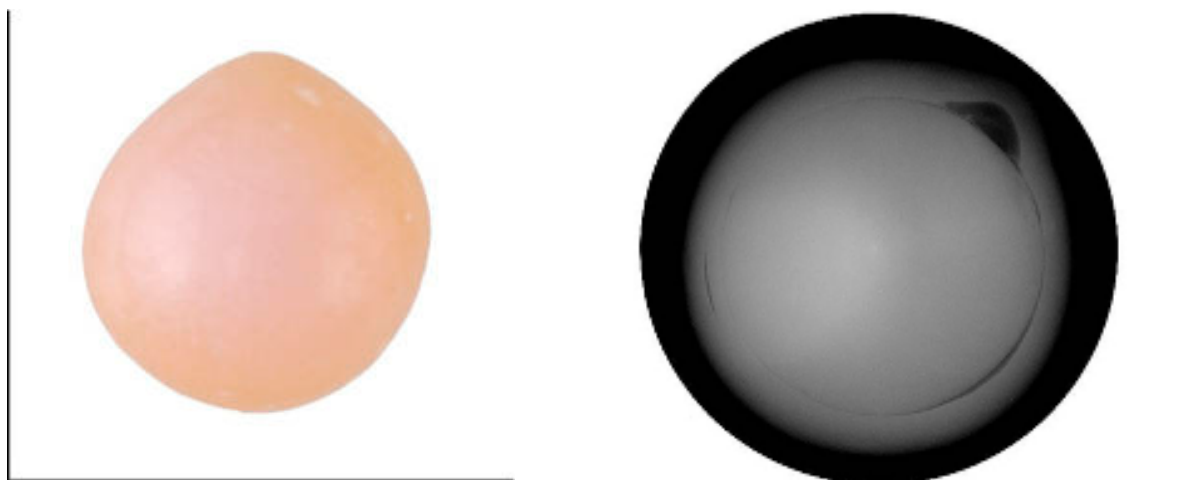


Figure 1. A bead cultured conch pearl (left) and the microradiographic evidence of its bead cultured origin (right)



Figure 2. A non-bead cultured conch pearl (left) and the microradiographic evidence of its cultured origin (right).

Conclusion

Cultured conch pearls are now a reality. The quantity of cultured pearls produced in the future and therefore the commercialization prospects are still to be seen, but the end products are externally very similar to their natural counterparts. Internally the structures either clearly show that the conch pearls are bead cultured or non-bead cultured (see Figures 1 and 2), however some specimens may well cause some identification issues in the same way that some nacreous non-bead cultured pearls cause a degree of concern in the trade at the current time. Further research will be necessary on future production to see just how close the internal structures of non-bead cultured conch pearls from later harvests relate to their natural counterparts. The success of producing numerous specimens of cultured conch pearls also opens-up the possibilities of whole cultured pearls being produced from other gastropods in future.

References

- [1] Fritsch E., Misiorowski E. (1987) The History and Gemology of Queen Conch "Pearls". *Gems & Gemology*, Vol. 23, No. 4, pp. 208-221.
- [2] McGinty E., Evans B., Taylor J., Jerry D., 2010. Xenografts and pearl production in two pearl oyster species, *P. maxima* and *P. margaritifera*: Effect on pearl quality and a key to understanding genetic contribution. *Aquaculture* 302, 175–181.

Natural Melo pearls from the Andaman Sea, Myanmar

Federico Bärlocher

Ambra Greco, Milano, Italy mogok@ticino.com

Introduction

The natural non-nacreous Melo pearls produced by the Melo gastropod (*Melo volute*, Fig. 1) are found in Myanmar in the coastal areas of the Andaman sea. Other marine waters where these non-nacreous pearls grow are in : Vietnam, Cambodia, Thailand, and Indonesia. In Myanmar there are no historical references about Melo pearls. The silky flame-like structure of the Melo pearls, the porcellaneous lustre and the colour vary from a pale yellow to a strong orange. These characteristics make the natural Melo product very attractive for collectors and for top quality jewellery items.

These extremely rare pearls are found in the south of the country, in the Mergui Archipelago (nearly 900 islands) off-shore Tavoy and in the west of the country along the Arakan coast.

The shells are fished at a depth of 20 to 45 metres on sandy and muddy sea floors. The size of the shells varies from 15 to 30 cm.

Normally the pearls are not found in the biggest shells but inside the smallest and thickest ones simply because the pearl represents a disease for the shell hindering it to grow in size like the healthy ones.

The colour of the shells is about the same as the colour of the pearls. The shell also exhibits a silky flame structure like the pearl itself.

Description of Myanmar pearls

Colour : The colour of the pearls varies from light brownish to pale yellow, yellow and finally strong orange that resembles the colour of a ripe papaya fruit.

The most appreciated and valued colour is the "papaya" one.

Shape : The shape of the pearls varies from a frequently baroque shape to oval and rarely round shapes. These are most appreciated by the buyers.

Lustre : The lustre is porcelain-like. When Melo pearls are polished, they become highly attractive and show the flame structure very strongly and beautifully.

Flame structure : The flame structure varies from a tiny flame type (that gives the look of an even colour) to the classic flame type (same effect as the flame of a fire) to the patchy or leopard flame (effect of a spotted pearl).

Normally the most appreciated and expensive flame types are the classic one (Fig. 2) and the leopard one but sometimes customers prefer the tiny flame.

Size : The size of Melo pearls can range from the smallest of 1 ct size to the biggest known in the world of 414 ct (golf ball size).

Hardness, refractive index and composition : The hardness of Melo pearls is about 5 on the Mohs scale; the RI is from 1.51-1.64 and the composition is a mix of calcite and aragonite.

Stability of colour : The Melo pearls are known to slightly fade in colour during long periods of continuous exposure to natural light and to ultraviolet rays.

Durability: Since Melo pearls have a hardness of 5, there are no problems for its long-term durability.

Defects: Cracks on the surface and sand spots inside the Melo pearls are the common problems seen. Most of the Melo pearls on the market have cracks. This is because especially in the past, fishermen were used to boiling all the shell with the animal inside for better cooking the meat of the shell. About the sand spots inside the pearl, this also is a common problem because in the process of growth, the pearl can introduce sand grains that the Melo

animal is collecting. In fact for the market this problem is secondary and most times does not affect the price of the Melo. Sometimes it even increases the beauty and the interest in the pearl.

Marketing and Imitations

Marketing of the Melo pearls in past years has completely moved from Myanmar to Thailand where the important buyers have the possibility to buy the pearls directly from the fishermen who came from Myanmar in Thailand. They pay high prices.

With the strong demand and increasing prices in the last years for these natural pearls (Melo pearls, conch pearls, Tridacna pearls, etc.), the market of fake and imitation "Melo pearls" started with new types and models of pearls that resemble the natural ones (Fig. 3).

Prices

The prices have continuously grown due the short supply in 2010 and the lowest production of Melo shells. This shortage happened because the fishermen are fishing too many shells only looking for the rare and precious Melo pearls and not for the local food market as they did in the past.

Conclusions

Since Myanmar's costal waters offer a perfect environment for the growth of Melo gastro-pods, the importance of their pearls will certainly increase in the future and, uniting special flame structures, intense orange colours, beauty and rarity, they will become attractive additions to the well known rubies, sapphires, spinels, peridots, and jades that historically come from the Mogok and Hparkant mines in upper Burma.



Figure 1. Live Melo gastropod with shell, Myanmar.



Figure 2. Large natural Melo pearl showing an extraordinarily rich flame structure. Mergui Archipelago, Myanmar.



Figure 3. Orange pearl of unidentified origin, imitating a Melo pearl.

Orange diamonds from the Siberian placers: the features of structural defects

Titkov S.V.¹, Zudina N.N.², Sergeev A.M.³, Zudin N.G.⁴, Shiryaev A.A.⁵

¹ Institute of geology of ore deposits, petrography, mineralogy and geochemistry RAS, Moscow, Russia, titkov@igem.ru

² Moscow State Mining University, Moscow, Russia

³ Rony Carob Ltd, Moscow, Russia

⁴ Federal Scientific-Technical Center (L.Ja. Karpov Institute), Moscow, Russia

⁵ Institute of Physical Chemistry and Electrochemistry RAS, Moscow, Russia

In the North-East of the Central Siberian platform, rich diamond placer deposits have been exploited over many years. Despite intensive prospecting, primary sources of the placer diamonds have not been revealed yet. Some researchers suggest nonkimberlitic origin of these sources. The placers contain some rare and unusual types of diamonds, including cubic crystals coloured orange. As known, the orange crystals are among the rarest fancy coloured diamonds (Harris, 1994; Fritsch, 1998; Collins, 2001). In this work we report spectroscopic investigation of orange diamonds from placers of the North-East of the Siberian platform.



Figure 1. An orange cut diamond, 0.46 ct in weight, from a placer in the North-East of the Central Siberian platform.

For the study seven cut diamonds, 0.25-1.07 ct in weight, were selected (Fig. 1). According to GIA colored diamonds color reference charts (2006), the colour of the stones is the following: two - fancy orange, four - fancy yellowish-orange and one - fancy reddish-orange. All the samples were cut of the crystals of cubic habit, which are quite rare in nature. Infra-Red spectra were obtained using the FTIR Perkin Elmer System-2000 spectrometer in transmission and reflectance mode. The photoluminescence spectra were recorded with a HORIBA Jobin Yvon Fluorolog-FL3-221 at liquid nitrogen temperature. Excitation and emission spectra were obtained. The UV-Vis absorption spectra were measured with a Perkin-Elmer double-beam Lambda-9 spectrophotometer at liquid nitrogen temperature.

The IR spectra of the orange diamonds indicated the presence of A centres (two nitrogen atoms in neighbouring substitutional positions next to a vacancy) along with minor amounts of C centres (single substitutional nitrogen) (Fig. 2). Thus, the diamonds studied belong to the type IaA + Ib of the physical classification of diamonds. The majority of the samples contain hydrogen-related defects (IR lines at 1405 cm⁻¹ and 3107 cm⁻¹). All samples show a sharp absorption line of variable strength at the Raman frequency 1332 cm⁻¹.

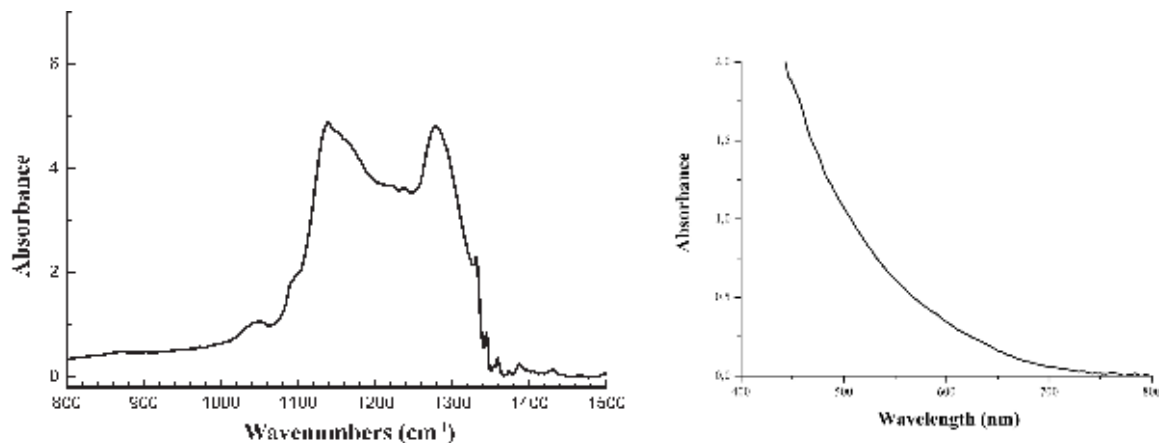


Figure 2 (left). The one-phonon region IR spectrum of an orange type Ia Ib diamond. Figure 3 (right). The visible absorption spectrum of an orange diamond at 300 K.

In addition, a set of weak lines between 1350 cm⁻¹ and at 1390 cm⁻¹ was also observed. These lines were earlier reported for some natural brown and type Ib diamonds (Woods and Collins, 1983), but their nature remains unknown. Platelets (polyatomic segregations in cubic planes of the diamond lattice, which involve carbon and nitrogen atoms) are present in some of the crystals. Such features are quite unusual for natural diamonds of cubic habit.

Absorption spectra showed that the colour of only one of the diamonds studied is due to a broad absorption band peaking near 480 nm. Similar spectra are presented in some reviews as typical of rare natural pure orange diamonds (Harris, 1994, Fritsch, 1998; Collins, 2001). A broad band with maxima at 370-380 nm is also revealed in the spectrum of this crystal. The coloration of all the other crystals is caused by an absorption starting at about 700 nm and increasing toward shorter wavelengths (Fig. 3). In natural crystals, this absorption, commonly attributed to the presence of single substitutional nitrogen impurities (the C-defects), usually is less intense and starts at approximately 500 nm (Collins, 2001), which leads to the appearance of green or yellow colours.

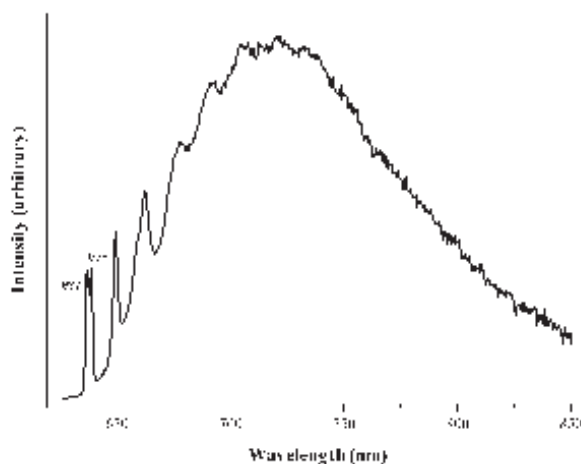


Figure 4. The photoluminescence spectrum of an orange diamond excited at a wavelength of 590 nm and recorded at 77 K.

The photoluminescence spectra of all the orange diamonds exhibited a narrow line at 637 nm, often assigned to phonon transitions of the centre formed by the complex of a nitrogen atom and a vacancy in negative charge state (N-V)- (Fig. 4). However, the phonon replicas observed do not match the phonon replicas of the (N-V)- centre, indicating that we found another defect. Besides a second sharp zero-phonon line at 638 nm was detected. In all the spectra, the system N3 (planar group of three nitrogen atoms and a vacancy) with unusually broadened lines and a narrow line at 575 nm were revealed as well. It should be noted that in our samples the 575 nm line was always less intense than the 637 nm line, which is also typical for HPHT-treated brown diamonds of type II (Collins, 2001). In the spectra of some of crystals studied, weak H3 (503.2 nm) and S1 (503.2 and 510.3 nm) systems and a weak line at 440 nm were also observed.

As known, the orange colour of diamonds can be produced artificially by irradiation and subsequent annealing of type Ia diamonds. In this case, orange coloration is caused by the strong absorption by the H3 and H4 systems (Overton and Shigley, 2008). Hence, the data on structural defects obtained can be used for identification of natural origin of the fancy orange colour in diamonds, and perhaps even for revealing of diamond provenance.

References

- Collins, A.T., 2001. The colour of diamond and how it may be changed. *Journal of Gemmology*. 27(6), 335–339.
- Fritsch, E., 1998. The nature of color in diamonds. In: *The Nature of Diamonds*, ed. by G.E. Harlow. Cambridge University Press, Cambridge, 23–47.
- GIA colored diamonds color reference charts, ed. by King, J.M., 2006. Worzalla Publishing Company, Stevens Point, 16pp.
- Harris H. (1994): *Fancy-Color Diamonds*. Fancoldi Registered Trust, Liechtenstein, 45-46, ISBN 3-952-0643
- Overton, T.W., Shigley, J.E., 2008. A history of diamond treatments. *Gems & Gemology*, 44(1), 32-55.
- Woods, G.S., Collins, A.T., 1983. Infrared-absorption spectra of hydrogen complexes in type-I diamonds. *Journal of Physics and Chemistry of Solids*, 44(5), 471-475.

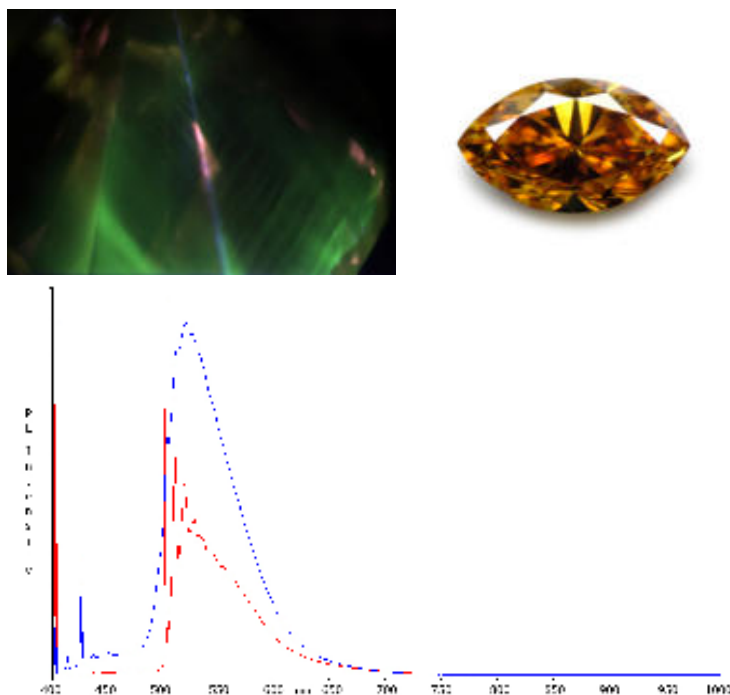
Photoluminescence spectroscopy and imaging of natural type Ib diamonds

T. Hainschwang¹ and E. Fritsch²

¹ GGTL Laboratories, GEMLAB (Liechtenstein)/GemTechLab, Balzers/Geneva. thomas.hainschwang@ggtl-lab.org

² University of Nantes and IMN-CNRS, Nantes, France. emmanuel.fritsch@cnrs-imn.fr

The photoluminescence characteristics of natural type Ib diamonds appear, at first sight, rather unspectacular: even though many type Ib diamonds seem to be near inert under a standard 365 nm UV lamp, green (photo)luminescence can most commonly be observed visually by excitation with a powerful UV source such as filtered xenon light. This green luminescence is easily detected by photoluminescence spectroscopy and has no unusual origin since it is caused by the very common H3 centre with its zero-phonon line (ZPL) at 503.2 nm, manifesting that the diamond contains at least some A aggregates besides single nitrogen. H3 PL is even detected in natural diamonds that were defined as pure type Ib by FTIR spectroscopy, since the H3 defect is a very efficient emitter and since PL spectroscopy can detect extremely low concentrations of this defect.



Figures 1. Green (photo)luminescence in a naturally orange type Ib diamond, as observed under a fluorescence microscope (left). The corresponding photoluminescence spectrum on the right, as excited by a 405 nm laser, shows the traces recorded at room temperature (red) and cryogenic temperature (blue) with the vibronic H3 system and its ZPL at 503.2 nm as the main emission. The emission line at 428 nm is the first-order Raman signal of diamond (for 405 nm laser excitation).

The analysis of a large population of type Ib diamonds and diamonds with a distinct Ib character (i.e. diamonds being dominantly of a different type, but exhibiting features associated with type Ib diamonds) has shown that there is in fact a large variety of responses to excitation with UV and violet light. For this study over 200 diamonds containing single nitrogen were categorized by FTIR spectroscopy. Following this their photoluminescence was

visually analyzed using a custom built UV microscope based on a filtered 200 Watt xenon light source with a Suprasil bulb. Then the defects responsible for the corresponding emission(s) were identified by photoluminescence spectroscopy using 405 nm laser excitation.

This study shows that there are several causes for the green, yellow and orange emissions observed by luminescence microscopy, some of which are known defects and some of which are, to our knowledge, yet undocumented. Photoluminescence spectroscopy has revealed a large variety of emissions in the samples, from classical defects such as N3, H3, NV0 and NV- to highly complex combinations of broad bands and superimposed sharp emissions. To give an example, orange photoluminescence can be caused by dominant NV0 and/or by NV- centres but also by broad bands such as a broad emission centred around 570 nm. At freezing temperature this 570 nm band is superimposed by sharp emissions of which the 692.0 nm centre with associated vibronic bands at 704.5, 718.5 and 722.0 nm is the most noteworthy one (Fig. 2 top row). Other samples show reddish orange photoluminescence caused by a very strong, complicated broad band ranging from 500 to 800 nm, with its maximum at 560 nm. At low temperature these spectra are characterized by a large number of sharp emissions, of which only the NV0 centre can be considered common.

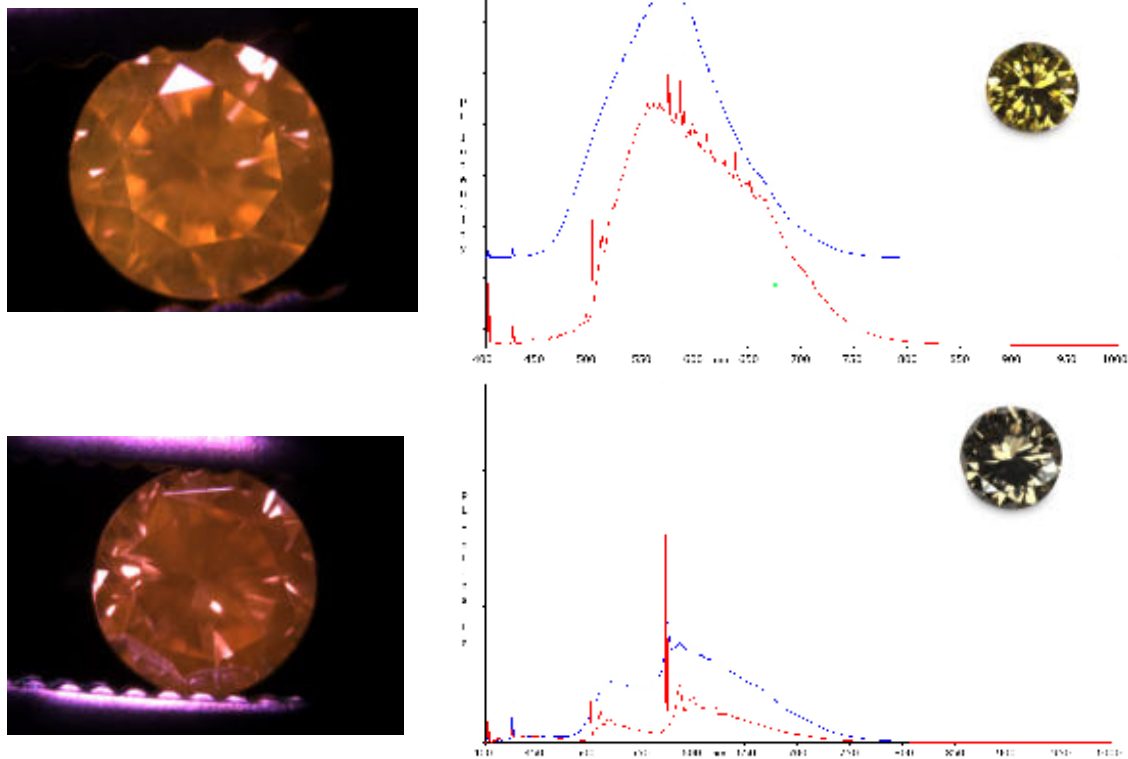


Figure 2. Orange photoluminescence in a naturally yellow (top row) and a naturally brown (bottom row) type Ib diamond, as observed under a fluorescence microscope (left). The corresponding photoluminescence spectra as excited by a 405 nm laser (right), recorded at ambient and cryogenic temperatures (blue respectively red trace), show that the orange PL is caused by a strong NV0 emission system for the brown diamond while broad band emissions are responsible for the orange emission of the yellow diamond.

The same scenario is true for green fluorescence, which is often caused by the H3 centre, but which can also have its origin in more or less complex broad band emissions. Yellow photoluminescence is a particular case since it is only caused by broad band emissions and by no known simple defect centre; nevertheless this case is not easy since there is a large variability from case to case, in spectral shape and position of the maximum of the broad band.

“Birefringence” in diamond : a useful tool to separate natural from synthetic diamond

Emmanuel Fritsch

University of Nantes and IMN-CNRS, Nantes, France. emmanuel.fritsch@cnrs-imn.fr

Thomas Hainschwang

GEMLAB (Liechtenstein), Balzers, Liechtenstein. thomas.hainschwang@gemlab.net

Benjamin Rondeau

University of Nantes and LPGN-CNRS, Nantes, France, benjamin.rondeau@univ-nantes.fr

The separation of natural from synthetic diamonds is again a problem with the advent of small high pressure-high temperature (HPHT) synthetic diamonds in the market, and developments bringing Chemical Vapour Deposition (CVD) syntheses ever closer to that same market. Observation of diamonds in immersion between crossed polarizers can provide useful insight for the distinction of natural and synthetic diamonds.

Natural gem quality diamonds always show a distinct to important anomalous “birefringence”, sometimes called anomalous double refraction (ADR), also called “graining” by gemmologists with a variety of possible patterns (see Kane, 1982). Actually graining is observed in non-polarized light, whereas double refraction is visible between crossed polarizers only.

Minor “birefringence” was seen in early gem-quality synthetic HPHT diamonds, mostly in the form of a cross, or around inclusions (Shigley, 2005 and references therein). Most inclusion-free synthetic HPHT diamonds recently produced will show virtually no “birefringence”, by contrast with the vast majority of natural diamonds of equivalent appearance. This is true independently from their colour or post synthesis treatment. These include diamonds with subtle colour zoning considered to be hard to identify. This is due to their outstanding crystalline quality.



Figure 1: the “brush effect” in CVD synthetic diamonds: dislocation bunches anchored in the seed plate resemble whisker bunches anchored in the handle of a brush. X-ray topograph courtesy Philip Martineau, DTC Maidenhead, England.

Synthetic CVD diamonds exhibit linear, dislocation-related "birefringence", in near parallel bunches, (see again references in Shigley, 2005) with the general appearance of a brush (Figs. 1 & 2). This is unusual in natural diamonds of similar appearance, which generally exhibit the classical planar, non-linear graining.

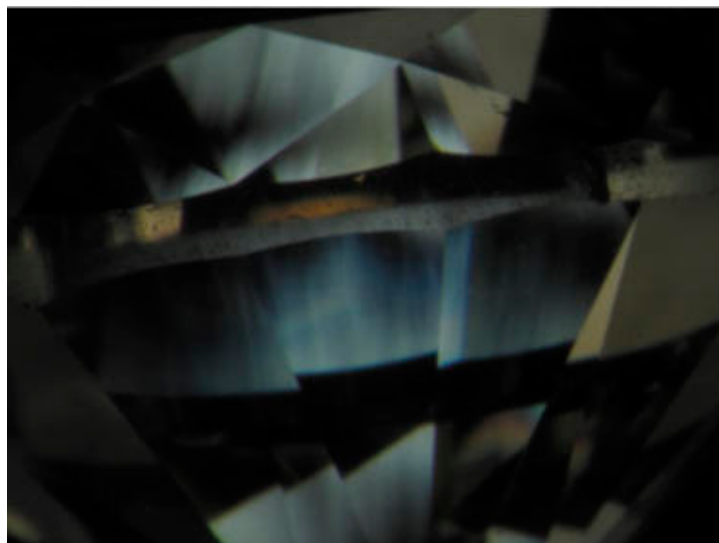


Figure 2: "Birefringence" pattern of a 1.27 ct brown CVD synthetic diamond, exhibiting typical parallel bunches of low birefringence dislocations. Magnification 20x. Micrograph E. Fritsch

As the quality of synthetic diamonds increases, less inclusions and less zoning are present in HPHT diamonds. For CVD stones the density of dislocations also decreases very progressively, so the two categories might converge towards crystals with very little defects. Then, the proposed technique will become all-the-more important as a simple, useful and immediate tool for identification.

References

Kane R.E., 1982. Graining in gem diamond. In D.M. Eash, Ed., International Gemological Symposium proceedings 1982, Gemological Institute of America, Santa Monica, CA. pp.219-235.

Shigley J.E., 2005. Editor, Synthetic diamonds; Gems & Gemology in Review. The Gemological Institute of America, Carlsbad, CA. 294 pages.

Distinction between well and poorly cut diamonds on the basis of dark zone analysis

Yuri Shelementiev and Roman Serov

MSU Gemmological Center, Moscow, Russia. jshelem@geol.msu.ru

In the past decades, many efforts were made by diamond manufacturers in order to establish procedures for the repeatable production of round brilliant cut diamonds with fixed proportions that produce the desired beauty. The diamond industry reproduces millions of copies of the same round cut, but it does not have any method to compare different cuts: princess with emerald, good radiant with bad radiant, good princess with bad round, and so on. Empirical methods of inspecting diamonds one by one do not help much because the appearance of a diamond strongly depends on the lighting environment: one stone looks better in one type of illumination, and the next one in another type of illumination. This situation results in random cut-quality evaluation which is not related to optical performance and beauty. Also, the final purchasers do not have proper guidance for the ranking of different diamonds by beauty, except for a round cut.

There is an understanding that a well-cut diamond reveals high levels of brilliance, fire, and scintillation (Moses et al., 2004). We developed an approach to measure brilliance, fire, and scintillation, for a scanned 3-dimensional diamond model or for a computer-cut diamond model [www.gemology.ru/cut/index.htm]. After analysis of many diamonds, we found that many poorly cut diamonds have more or less the same drawback, namely dark zones. Usually dark zones consist of several neighboring virtual facets (see Fig. 1 for term explanation) or one big virtual facet that looks dark. Some dark zones are visible in one stone position; other dark zones are stable and remain dark when a stone is tilted.

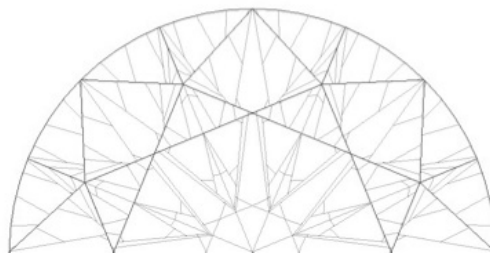


Figure 1. Virtual facet is a polygon that results in crown and pavilion facets overlapping. Here one can see virtual facets as polygons resulting after the second light beam reflection inside a wireframe diamond model.

It is important to study all possible reasons for dark zones in a diamond:

- One reason can be light leakage through the stone's pavilion. These leakage zones are present in virtually all stones, and can be seen in structural lighting devices such as the Idealscope, Hearts&Arrows viewer, etc. (see example at Fig. 2-1).
- The next reason is an obstruction of light from the side where the observer's head and body are located. A classic example is a round diamond with a 45° pavilion angle. The central part of such a stone looks dark because the observer sees the head's reflection there (Fig. 2-2).

- The third reason known as “fish eye” is a leakage through the girdle facets in a diamond with a shallow pavilion, as a result of which the girdle is seen under the table faces (Fig. 2-3)
- The fourth reason is just an absence of light in a sector of space from which diamond redirects light towards the observer’s eyes (Fig. 2-4). These dark zones depend on lighting environment.

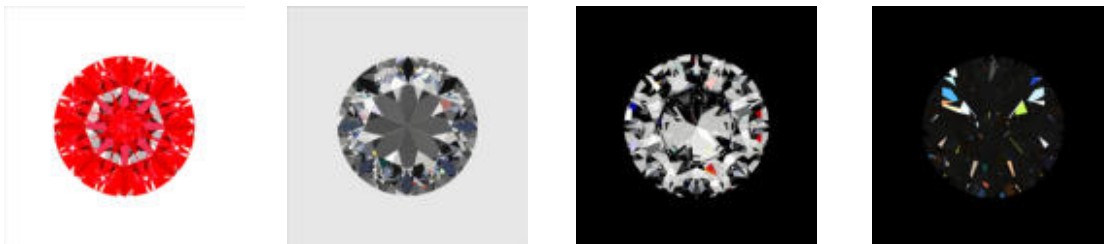


Figure 2. Leakage under the table, visible in Ideal Scope as white areas (1), head obstruction under the table (2), leakage through the girdle facets (3) and many dark zones visible in a room with only few small light sources (4).

In some diamonds dark zones are small and well distributed but in other diamonds dark zones can form big clusters and easily seen by eyes. All reasons mentioned above can work together and dark zones in diamonds can appear bigger because of combination of these reasons.

For the study of dark zones in diamonds, we use a special illumination scheme called “dark zone” in DiamCalc software [<http://www.octonus.com/oct/products/3dcalc/standard/>]. Our dark zone analysis is based on the idea that we need to model light from directions where there is no light in real life. If we put light sources instead of observer’s head, body, and background (lower hemisphere), we can see light in all virtual facets that cannot emit light in any case. The diamond image in Fig. 3, left, shows these zones. Those zones of the diamond looking bright in this type of illumination will be dark in usual illumination. After we know the location of dark zones, we can easily see that the same areas are darker in usual light (Fig. 3, center and right). The area of dark zones in a standard round brilliant cut can be used as a reference for further study.

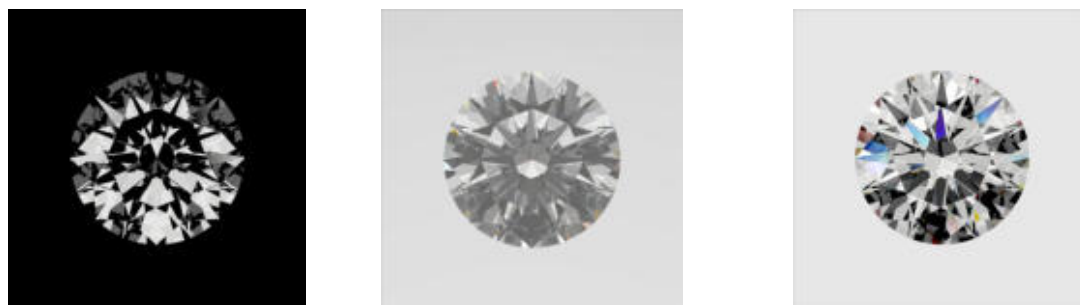


Figure 3. Round brilliant cut in “dark zone” light (left), in diffused light (centre), and office light (right).



Figure 4. The same diamond as on Fig. 3 in the Dark zone light: picture in the left eye (left), in the right eye (centre), and possible resulting picture in human brain (right).

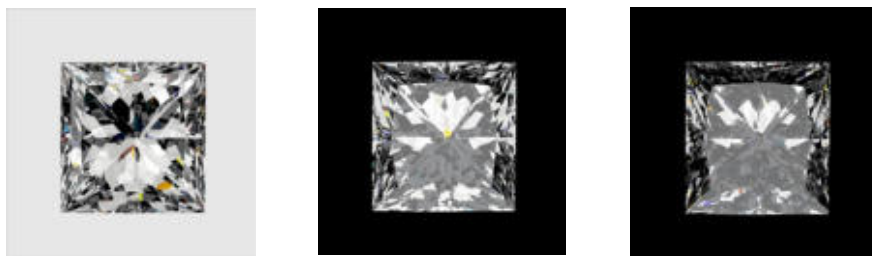


Figure 5. A princess cut has dark area under the table in the Office illumination (left) that is corresponding with white area in the Dark Zone lighting (centre) and with smaller white area in the Stereo Dark Zone lighting (right).

Human vision is stereoscopic. When we look at an object with two eyes, each eye sees its own picture, and these pictures are different from one another (see Fig. 4).

The application of the dark zone concept to the study of the appearance of various diamond cuts will be illustrated here with examples of princess and pear-shaped cuts. Analyses of available princess cuts show that many of them currently have a dark zone under the table (Fig. 5). In Fig. 6, one can see an improved case of the princess cut where dark zones are smaller and better distributed. This type of dark zone is usually perceived as contrast pattern.



Figure 6. This princess cut has less prominent dark area under the table. As in Fig. 5, pictured in the Office illumination (left), in the Dark Zone lighting (centre) and in the Stereo Dark Zone lighting (right).

For the pear shape there is a “bow-tie” effect, which is common on the market and looks like partial darkening resembling a butterfly shape in the central area of a diamond. In the dark zone lighting this area is white (Fig. 7). A change of the facet pattern and proportions of a pear shape results in a considerable decrease of the “bow-tie” effect (Fig. 8). All dark zones in our examples were checked by tilting the stone. They are seen not only in face-up position, but also when a stone is rotated or tilted.



Figure 7. A pear shape diamond with prominent “Bow-Tie” effect. Again, Office illumination (left), Dark Zone lighting (centre) and in the Stereo Dark Zone lighting (right).

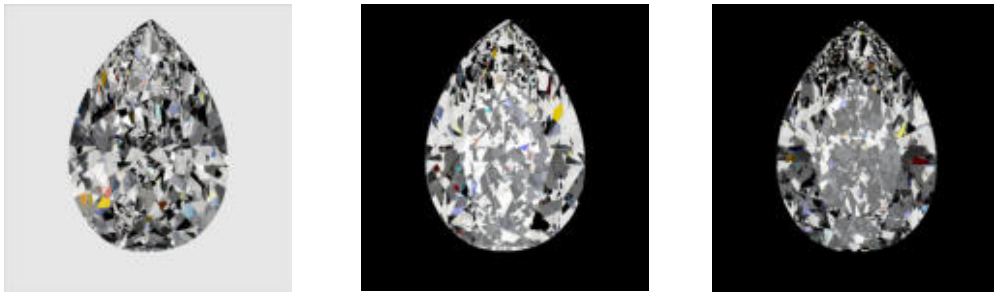


Figure 8. Another pear shape diamond does not reveal the “Bow-Tie” effect. Again, Office illumination (left), Dark Zone lighting (centre) and in the Stereo Dark Zone lighting (right).

Discussion

Dark zones can be much more prominent in real lighting conditions where diamonds are sold and worn. It can happen that some virtual facets neighbouring a dark zone area are not illuminated in the particular lighting environment, and thus the dark area looks bigger because these facets add to the dark zone. In real life, when overall illumination can have different brightness, stereovision can change the resulting picture perceived by the brain and more dark zones can be perceived in the same stone. On the other hand, dark areas that correspond with the observer’s body and head become smaller with increasing distance between diamond and observer.

Conclusion

Understanding diamond optics and methods for diamond-cut analysis helps to distinguish between good and bad cuts. These methods are also useful for improvement of the appearance of fancy cuts. Apart from positive light phenomena such as brilliance, fire, and scintillation, negative phenomena such as dark zones can be useful for diamond performance analysis. Manufacturers of high-performance diamonds should avoid big dark zones and dark zones that remain stable with stone’s tilting. Tools that can reveal dark zones can be useful for rejection of bad looking diamonds.

References

Moses T., Johnson M., Green B., Blodgett T., Cino K., Geurts R., Gilbertson A., Hemphill S., King J., Kornylak L., Reinitz I. & Shigley J. (2004) Foundation for grading the overall cut quality of round brilliant cut diamonds.- *Gems & Gemology*, Fall, 202-228.

Diamond cut study webpage <http://www.gemology.ru/cut/index.htm>

DiamCalc webpage <http://www.octonus.com/oct/products/3dcalc/standard/>

DiamCalc documentation <http://www.octonus.com/oct/download/files/DiamondCalculator3.pdf>

Using synchrotron radiation to analyse diamond crystal structure defects and the relationship of its colour

Joe C.C. Yuan, Ming-sheng Peng, Yu-fei Meng

Solstar diamond Co., Ltd., Zhengzhou, Henan 450016 China, yuanjoechihchun@gmail.com

Abstract

Diamond crystal structure sp³ arrangement is the closest or most dense of crystal structures in the planet. The diamond is generated under high temperature and high pressure of the upper mantle which lies more than two hundred kilometers below the surface. There are hundred millions and even billions of years since volcanic eruption carried the diamonds out of the mantle. While constantly being subjected to sharp changes in temperature and pressure, the diamond crystals had different types of structural defects, such as: dislocation, lattice distortion, plastic deformation, stacking faults etc. These lattice distortions caused the diamond crystals to unequally absorb visible light which made the crystals to display different colours.

The electron beam in the Synchrotron radiation is accelerated to near the speed of light. Then we direct the secondary X-ray beam to impact onto any plane of the crystal, because of the location of the three-dimensional crystal face in different directions resulting diffraction is generated by the reflection refraction. The multiple planes differentiate the X-ray beam into numerous small injection in all directions. The film behind the crystal received the topography of each Laue spot to represent groups of related crystal face shape. According to the condition of the distortion of these spots, we can determine the degree of the diamond crystal structure defects. (Ludwing 2001, Rylov 2001, Yuan 2007)

Keywords: crystal structure defects, synchrotron radiation, white light topography, Laue spots, lattice distortion.

For this paper, we used synchrotron radiation in the X-ray topography of the Beijing synchrotron radiation facility (BSRF) of the Beijing Electron Positron Collider (BEPC) in China, to study a total of 55 natural, artificial and treated diamond samples, to obtain over 200 white light topographies and 1900-2000 of the amplified Laue spots. According to the characteristics of white light amplified topographies, we have classified the distortion of the diamonds into four categories.

Lattice distortion classification based on the following:

- 1, Very strong distortion: every diffraction spot shows strong deformation or radiates from the centre to the edges for edge-like elongated shape and complex texture of their dislocation. It shows the structure of a diamond with strong distortion due to incomplete crystallization. It is observed that the crystal faces are fractured under magnification.
- 2, Strong distortion: slightly elongated shape, deformation, dislocation direction of two to three kinds of cross.
- 3, Moderate distortion: shape does not change, a small number of internal dislocations, light plastic deformation.
- 4, Weak distortion: shape does not change, but a number of crystal dislocations exist internally. The source of the dislocations is the same, while some dislocations show zigzag.

Lattice distortion of various diamonds

A, Natural diamonds:

- 1, Natural brown type Ia diamond: Very strong to moderate distortion
- 2, Natural pink type Ia diamond: Very strong to moderate distortion

- 3, Natural pink type IIa diamond: Strong distortion
- 4, Natural light green type IaA diamond: Very strong distortion (Fig. 1)
- 5, Natural yellowish-green type Ia diamond: Very strong distortion
- 6, Natural greyish white type Ia diamond: Very strong distortion
- 7, Natural grey type Ia diamond: Weak distortion
- 8, Natural light yellow type Ia diamond: Weak distortion
- 9, Natural colourless type Ia diamond: Weak distortion

Natural diamonds are exposed to enormous changes in temperature and pressure underground over million of years which caused structural defects due to highly apparent macro lattice distortion; this causes alterations of the colour to: brown, pink, green, grayish white. In the case of less noticeable macro lattice distortion diamonds, the colours are due to foreign atoms implanted into the lattice as point defects, such as: hydrogen in gray diamonds; nitrogen in yellow diamonds; boron in blue diamonds. Colourless diamond contains almost no other foreign element and only weak lattice distortion.

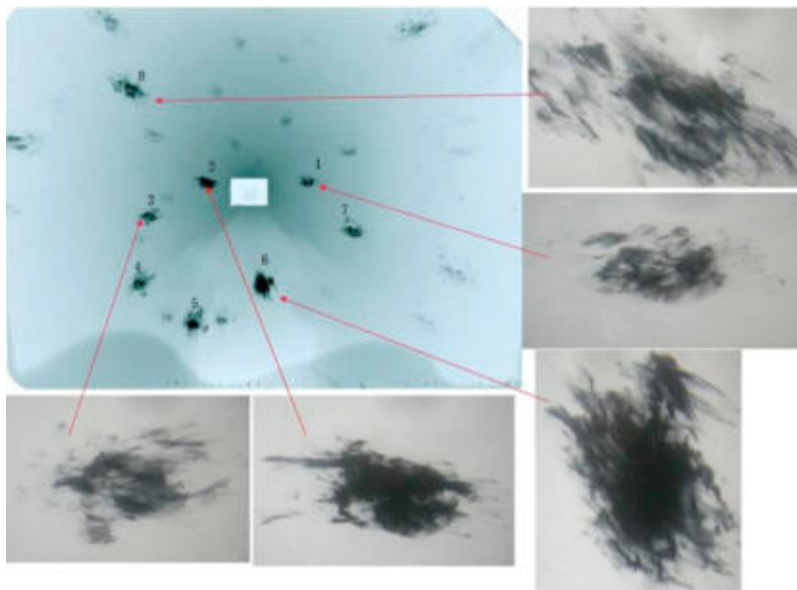


Figure 1. Type IaA natural light green diamond, very strong lattice distortion.

B, Natural diamonds, HPHT treated:

- 1, Natural Type IIa brown diamonds HPHT treated into nearly colourless: Very strong to moderate distortion. (Smith et al. 2000)
 - 2, Natural Type Ia brown diamonds HPHT treated into yellowish-green colour: Strong distortion (Fig. 2).
 - 3, Natural Type IIa near colourless diamonds HPHT, irradiation treated into dark red colour: moderate distortion. Natural brown diamond originally with more obvious macro lattice distortion which has been HPHT treated into nearly colourless or yellow-green colour, still shows obvious lattice distortion. HPHT treatment did not reduce the extent of the lattice distortion.
- Near colourless type IIa diamond with less obvious macro lattice distortion becomes a deep red colour after HPHT, irradiation treatment and annealing, the macro lattice distortion is still less obvious. This illustrates that the HPHT treatment did not affect the diamond lattice structure of the macro state (Collins 2000, Fisher 2000).

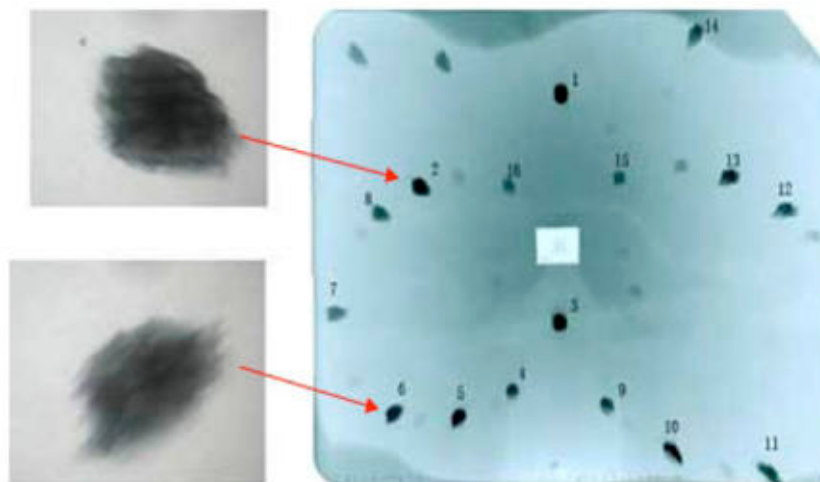


Figure 2. Natural Type Ia brown diamonds HPHT treated into yellowish-green colour, strong lattice distortion.

C, Natural diamonds with irradiation treatment:

- 1, Natural brownish Type IIa diamonds irradiation treated and annealed into deep pink, reddish brown colour: very strong to moderate distortion (Fig. 3).
- 2, Natural brownish Type IIa diamonds irradiation treated and annealed into Purple Pink colour: Moderate distortion
- 3, Natural Type Ia diamonds irradiation treated and annealed into greenish yellow or blue colour: Moderate distortion
- 4, Natural Type Ia diamonds irradiation treated and annealed into greenish yellow, grey, golden yellow or light yellow colour: Weak distortion

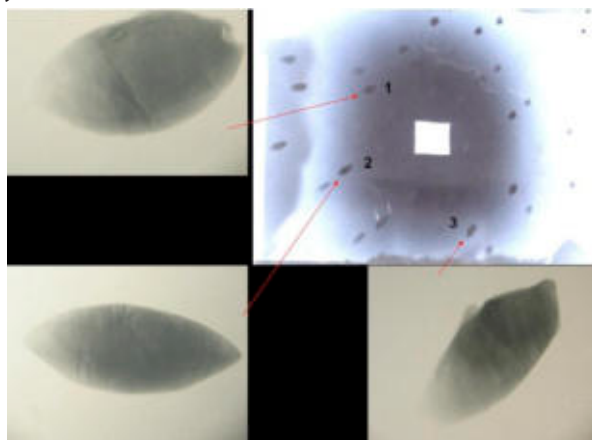


Figure 3. Natural Type IIa diamonds irradiation treated diamonds, weak lattice distortion.

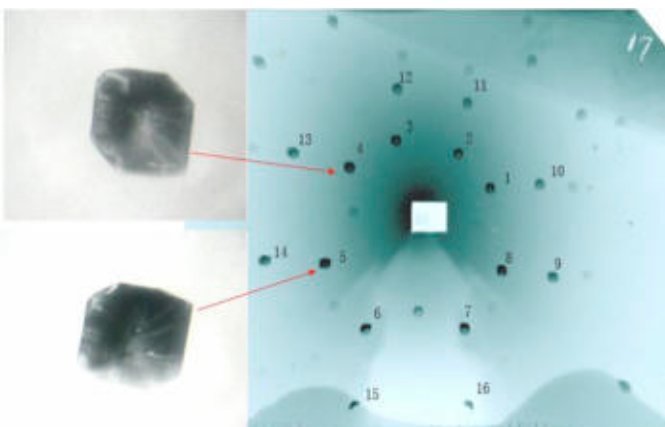


Figure 4 HPHT synthetic colourless into deep pink colour, moderate lattice distortion.

Diamonds are bombarded with modern high-speed electron irradiation which causes only point defects. On the diamond macro lattice distortion of the original state does not change.

D, High pressure and high temperature synthetic diamonds:

- 1, HPHT synthetic yellow colour diamonds: Moderate distortion
- 2, HPHT synthetic Type IIb blue colour diamonds: Weak distortion
- 3, HPHT synthetic colourless diamonds: Weak distortion (Fig. 4).
- 4, HPHT synthetic, irradiation treated and annealed into dark red colour diamonds: Moderate distortion

In the case of HPHT synthetic diamonds, all the macro lattice distortions are moderate or minor. This is due to the growth of the HPHT synthetic diamond in a lab which takes tens to hundreds of hours during which the temperature and pressure are kept stable. The macro lattice structures are more orderly, so the lattice distortions are less obvious.

Conclusion

Efficient X-ray synchrotron radiation white light topography helps us analyse the macro lattice distortion and the resulting relationship with their colour.

Lattice distortion produces brown, pink, green, and greyish-white colours in natural diamonds. This also indirectly confirms that point defects produce the colours grey, yellow, and blue in diamonds. No or only weak lattice distortion and no point defects result in colourless diamonds.

HPHT and irradiation treatment caused only point changes in the diamond; thus causing a colour alteration. Its macro lattice structure is not affected.

HPHT synthetic diamonds are not obvious in macro lattice distortion, because they were grown in a short period of time in a controlled environment, during which the temperature and pressure were kept stable. So their lattice distortion is less obvious.

References

Collins A. T., Kanda Hisao, Kitawaki Hiroshi. Color change produced in natural brown diamonds by high-pressure, high-temperature treatment. *Diamond and Related Materials*, 2000, (9): 113-122

Fisher D, Spits R A. Spectroscopic evidence of GE POL HPHT—treated natural type IIa diamonds. *Gems & Gemology*, 2000, 36(1): 42-49

Ludwing W, Cloetens P, Hrtwing J, et al. Three-dimensional imaging of crystal defects by 'topo-tomography'. *Journal of Applied Crystallography*, 2001 (34):602-607

Rylov G M, Yefimova E S, Sobolev N V, et al. Study of imperfect natural diamonds with the application of the X-ray synchrotron radiation (the "Laue-SR" method). *Nuclear Instruments and Methods in Physics Research (A)*, 2001, (470): 182-188

Smith C.P., Bosshart G., Ponahlo J., Hammer V., Klapper H., Schmetzer K. (2000b): GE POL Diamonds: Before and After. *Gems & Gemology*, 36, 3, 192-215.

Yuan J. C.C., Peng Ming-sheng, Meng Yu-fei. Investigation on Structure Defects of Red Color Diamonds using TEM and Synchrotron Radiation X-ray diffraction topography. 30th International Gemmological Conference 2007 July 16th Oral Session in Moscow, Russia.

Re-assessment of the UV-vis spectra characterization for rubies from marble-hosted deposits

Walter A. Balmer¹ (corresponding author: wb@quicknet.ch), George Bosshart², Chakkaphan Sutthirat^{1,5}, Christoph A. Hauzenberger³, Thomas Pettke⁴

¹Department of Geology, Faculty of Science, Chulalongkorn University, Bangkok, Thailand

²Horgen-Zurich, Switzerland

³Institute of Earth Sciences, Karl-Franzens-Universität, Graz, Austria

⁴Institute of Geological Science, University of Berne, Switzerland

⁵Gem and Jewellery Institute of Thailand (GIT), Bangkok, Thailand

Introduction

UV-vis spectrophotometry is a well-established analytical method which by now had been applied in gemmology for more than 30 years. Especially in coloured gemstones, UV-vis spectrophotometry was a helpful method to investigate the effect and interactions of chromophores present in a given gemstone and responsible for its colour. Besides the study of chromophores, the aim of spectrophotometry in gemmology was also to learn more about the possibility to apply UV-vis absorption spectra for authenticity and origin determination purposes. Bosshart (1982) observed that in rubies, both of natural or synthetic origin, a distinct variation in the shape and depth of the absorption minimum in the UV range can be found. His approach was to numerically describe the shape and position of this absorption minimum by a horizontal profile laid at 0.5 absorbance units above the absolute absorption minimum and by λ and W representing the centre position and the width of the profile respectively (see Fig. 1). The data set consisting of the absolute minimum position λ_0 and the profile coefficient, λ divided by W , were found to vary within wide limits and thus to offer means of separation for natural and synthetic rubies. According to the orientation of the sample, the two examined parameters were then plotted in Cartesian coordinate systems where the values for the absorption minimum λ_0 were represented on the abscissa and the coefficient λ/W mentioned above on the ordinate.

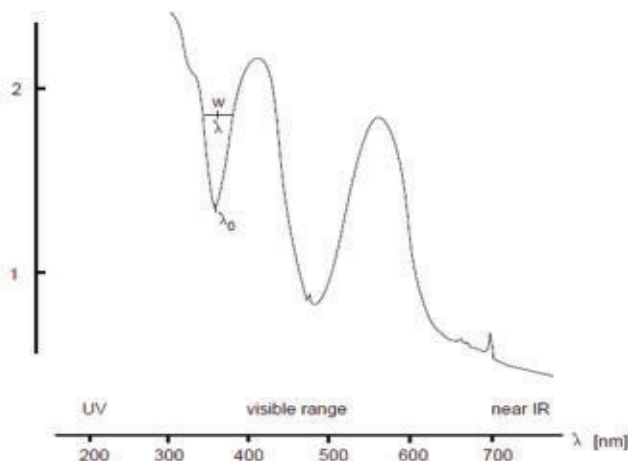


Figure 1: Parameters introduced by Bosshart (1982) in order to numerically evaluate ruby UV-vis spectra.

In retrospective and taking into account that the technical possibilities were limited at the time of publication, the procedure introduced by Bosshart (1982) showed three limitations. The proposed method of recording oriented spectra appeared not to be entirely sufficient in terms of polarization effects. The fact that the measured absorption is dependent on the path length the analysing ray is taking through a sample was not taken into account either. Finally, a given spectrum occasionally could not be characterised by the suggested procedure because the 0.5 absorbance units which were set to be the level where the width W of the absorption minimum was measured, exceeded the top of the Cr absorption band at 410nm and no inter-section with the spectrum could be established. This problematic was encountered especially in the case of less saturated rubies and pink sapphires. Subsequently, it was the goal of this study to modify the approach introduced by Bosshart (1982) in a way that the detected limitations could be eliminated. Further, it was investigated whether there is a potential to widen the focus of UV-vis spectrum analysis from determining authenticity towards a new procedure to allow origin determination on rubies.

New Approach

Starting by analysing the procedure introduced by Bosshart (1982), it was soon confirmed that polarization plays a key role in adequately interpreting a given UV-vis spectrum. Artefacts related to polarization effects are common because extraordinary beam (e-ray) spectra are mostly not pure e-ray spectra but a mixture of ordinary (o-ray) and e-ray characteristics. This phenomenon is related to the fact that sample positioning of cut samples is often difficult. The table of the samples is rarely oriented perfectly perpendicular or parallel to the c-axis which would be necessary in order to obtain undisturbed o- and e-ray spectra. The simplest solution to overcome this problem was to consider o-ray spectra for this study only. o-ray spectra are not disturbed by polarization effects in whatever direction the UV-vis spectrum may have been taken.

The second effect which was investigated to be eliminated was the fact that the measured absorption is dependent on the path length of the beam travelling through a sample. Plots in absorption coefficient do take this fact into account. Accordingly, the collected spectra had to be processed after the following formula in order to convert the collected spectra from absorbance to absorption coefficient or absorptivity.

$$\alpha = \ln 10 * (A / t)$$

α : absorption coefficient [cm⁻¹], A : absorbance, t : optical path length [cm]

As an initial step in this data processing procedure, the thickness of the samples had to be measured. For samples examined in this study, which were present as slabs, this was an easy task. For cut stones, however, an approximation procedure might be to measure the distance between the star facet on the crown of a gemstone and the opposite pavilion surface to estimate the path length if the optical axis of the gemstone is oriented in an oblique direction. The recorded UV-vis spectrum had then to be divided by the measured path length t and multiplied by the logarithmus naturalis of 10 according to the equation mentioned above. Data processing as described can be done by any spectrum calculation software such as Spectrum by Perkin Elmer.

The resulting absorptivity spectra can be understood as being optically normalised. Consequently, this allows direct comparison of the spectra obtained for samples of any thickness. The effect of different path lengths could therefore be ruled out.

Finally, the last obstacle was taken by simply adjusting the profile height to 3 cm⁻¹ absorption units in absorptivity. This corresponds in most cases to a lower height than the formerly suggested 0.5 absorption units in absorbance but still allows the detection of presence or absence of the Fe³⁺ related shoulder at 314nm. Trials with even smaller profile heights failed in this regard. This spectral feature, however, is a major characteristic of the investigated absorption minimum in the UV range and therefore cannot be neglected.

Sample Material and Experiment Conditions

The original ruby spectra (10) from the early work of Bosshart (1982) as well as newly collected ruby spectra (31)

had been incorporated into this study. Besides the spectra of the samples used by Bosshart (1982) a total of 16 samples from the Uluguru and Mahenge Mts in the Morogoro Region, Tanzania, 10 samples from Luc Yen, Vietnam, as well as 5 additional samples from Mogok, Myanmar (Burma) were included in this spectra investigation. To improve the quality of the spectra, parallel windows were polished on each of the oriented samples to allow the analysing beam to travel more readily and to be analysed properly.

In order to be able to clearly differentiate e- from o-ray spectra, well polarized UV-vis spectra were taken with a Perkin Elmer Lambda 950 UV-vis-NIR spectrophotometer using an adapted sample holder for gemstone testing purposes. The measurement parameters were set to 0.5nm data point increments, 2nm slit width, and a data acquisition speed which was accordingly set automatically at 102.6nm/min. Finally, the quartz-halogen/deuterium lamp change was set at 319.2nm and the data collection took place in the range from 860 to 200nm.

Discussion

In general, the ruby spectra from all the investigated marble-hosted localities shared similar spectrum characteristics. The dominant feature was always a strong Cr^{3+} signature which is in accordance to the presence of Cr^{3+} in ruby as its chromophore. For o-ray spectra, broad absorption bands related to Cr^{3+} are found at 410 and 556nm respectively. Typical bands related to Cr^{3+} are also found as sharp peaks at 468, 475/477, 659, 668nm, and 692/694nm (Schmetzer & Bank 1981, Schmetzer et al. 1983). Unlike in ruby from other localities, there was no iron signature found besides an occasional shoulder at 314nm (Bosshart, 1982). This shoulder as well as a deep UV absorption minimum indicate that the iron content is relatively low. This is in good agreement with chemical data for rubies from marble-hosted deposits in general.

Following the spectrum processing procedure as described above, certain changes in the characteristics of a λ_0 versus (λ/W) plot can be recognized. First of all, there are more data points contained in the plot of the modified approach due to the reduced profile height (see Fig. 2). Further, it can be seen that the overlap of rubies from Mogok Myanmar (Burma) and from the Morogoro Region is eliminated almost entirely in the plot of the modified approach. Clusters of the three investigated localities can now clearly be separated. Rubies from Mogok plot at low to intermediate (λ/W) levels between 3.4 and 6.5 and spread laterally from 330 to 350nm. Accordingly, the cluster shape is horizontally elongated. Rubies from Vietnam on the other hand were found to plot at very high (λ/W) levels from 7.3 to 14.3 with a small lateral variation of less than 10nm and centred around 350nm. This population plots more in a vertically elongated pattern. The rubies from the Morogoro Region finally take an intermediate position in the λ_0 versus (λ/W) plot with a tendency towards higher absorption minimum levels from 347 to 357nm. Thus, the cluster has more a triangular-like shape.

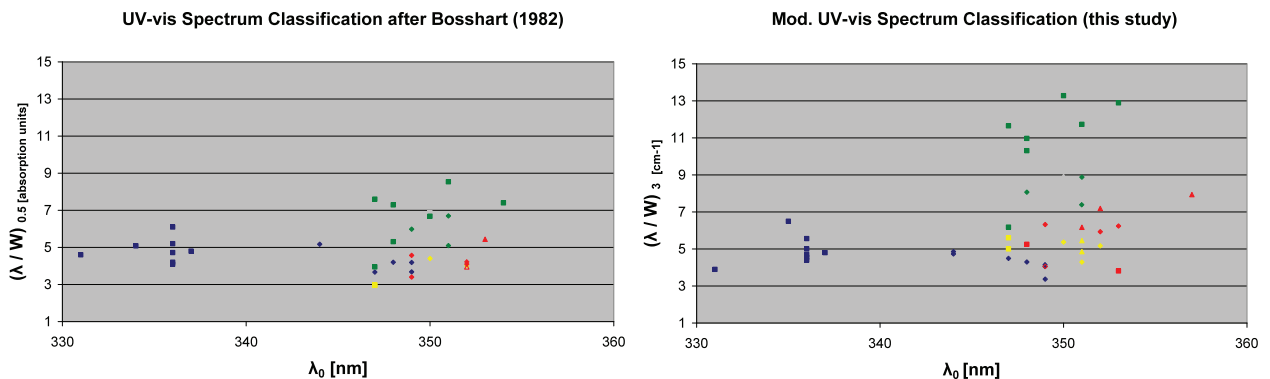


Figure 2: Comparison of a (λ/W) versus λ_0 plot after Bosshart (1982) and the modified approach presented in this study. Rubies from Mogok Myanmar (Burma) are plotted in blue, Luc Yen, Viet-nam in green and the Moro-goro Region in red (Mahenge Mts) and yellow (Uluguru Mts) respectively. The modified approach results in a reduction of the overlap of the populations in the area between 345 and 350nm which allows a clear separation of ruby o-ray spectra collected from samples of the three investigated localities.

During the UV-vis spectra investigation, it was further possible to identify two separate clusters within the Mogok population. The two clusters represent two types of spectra which were observed to be present in this population. The cluster on the right is characterised by spectra containing a shoulder at 314nm whereas the cluster on the left lacks such a spectrum feature. Additionally, it was observed that the tested Vietnamese rubies never showed a Fe³⁺ related shoulder at 314nm whereas rubies from the Morogoro Region, Tanzania seem to represent a population with both spectra types. Distinct differences in the λ_0 versus (λ/W) plot, however, cannot be found for the two types of spectra in the Morogoro Region population.

Conclusion

Through comparative UV-vis spectra analysis of ruby spectra, Bosshart (1982) was able to show that there are differences in the shape of the UV absorption minima. Following a modified procedure it was possible to demonstrate that besides the initial application, the separation of natural from synthetic rubies, there is also a strong potential for ruby UV-vis spectra analysis to be used as a new tool for origin determination of marble-hosted rubies. By converting the collected ruby spectra from absorbance into absorptivity, it was possible to separate the population clusters in a λ_0 versus (λ/W) plot for rubies from three investigated localities Mogok Myanmar (Burma), Luc Yen, Vietnam, and the Morogoro Region, Tanzania (Uluguru Mts and Mahenge Mts) more clearly. Rubies from other deposit types may reveal additional features and are likely to plot in different populations (see Bosshart, 1982). This however had not been covered in this study and is subject to ongoing research. The observations made imply finally to keep a close look on UV-vis spectra features beyond the range which was considered in gemmology traditionally. The presented method of UV-vis spectrum analysis and their interpretations can easily be included in routine testing procedures as an additional and powerful tool for ruby origin determination. The presented method may also help smaller labs with a limited equipment arsenal to still perform origin determination to a certain level when combined with other advanced analytical techniques and the skills of an experienced gemmologist.

References

- Bosshart G., 1982. Distinction of Natural and Synthetic Rubies by Ultraviolet Spectrophotometry, *Journal of Gemmology*, 18(2), p. 145-160.
- Schmetzer K., Bank H., 1981. The colour of natural corundum. *Neues Jahrbuch für Mineralogie, Abhandlungen*, 140, p. 59-68.
- Schmetzer K., Bosshart G., Hänni H.A., 1983. Naturally-coloured and treated yellow and orange-brown sapphires. *Journal of Gemmology*, 18 (7), p. 607-622.

Importance of various “feather type” inclusions for the identification of natural, treated, synthetic and treated-synthetic yellow sapphire

Jayshree Panjekar & Aatish Panjekar

Pangem Testing Laboratory, Pune PANGEMTECH – Panjekar Gem Research & Tech Institute, Pune, India
jayshreepanjekar@gmail.com

Abstract

In India natural yellow sapphire has been one of the most popular gemstones. It is regarded as the gemstone for the planet Jupiter and is generally worn in a ring on the forefinger. It is prized for its yellow colour. The more saturated the yellow colour the higher is its quality. Natural yellow sapphire from Sri Lanka, Myanmar, Thailand, Madagascar and East Africa are continuously in great demand. This high demand for rich yellow colour sapphire has given impetus to treatments on yellow sapphires like heat treatment (Balmer et al, 2006), irradiation, beryllium treatment (Atichat et al, 2004), lead/bismuth glass treatment and their combinations. In recent years, our laboratory has been getting mixed bulk lots of natural, treated and synthetic yellow sapphires. Sometimes treatments are also done on synthetic yellow sapphires to mimic the internal features by inducing feather-like inclusions in them. Material submitted to our laboratory as well as yellow sapphires currently available in the marketplace were investigated by classical gemmological methods, chemical analysis as well as UV-Vis-NIR and mid-IR spectroscopy. These gem materials may be conclusively identified by a combination of these techniques. Not all gem-testing laboratories have sophisticated analytical instruments like LIBS, LA-ICPMS etc to detect Be or EDXRF to detect Pb or Bi glass. In such situations, the standard method of studying the inclusions by microscope would give some evidence to the nature of the yellow sapphire. Besides, high-tech analyses are not economically viable for small sized stones.

This paper presents a full characterization of the various feather-type (fingerprint-type) inclusions, their nature, their structure, their development and the effect heat has on them. These include expanded feathers, disc-shaped feathers, feathers produced due to chemicals, flux feathers, borax feathers, induced feathers in synthetic yellow sapphire as well as feathers observed in yellow sapphires of different origins, by gemmological and modern analytical techniques, in order to determine these features that may be diagnostic for their identification.

Key words: types of finger-print or feather-like inclusions, natural yellow sapphires, treated, synthetic and treated-synthetic yellow sapphires

Materials and methods

Specimens with prominent feather-type or fingerprint inclusions were selected. We examined over 500 natural, treated and synthetic as well as treated synthetic yellow sapphire specimens, of which twenty four faceted known to be of Sri Lankan origin yellow sapphires, six known Myanmar origin yellow sapphires and some 270 treated yellow sapphires from Madagascar, East Africa and Thailand of which some were heat treated, irradiated, beryllium treated and glass filled. Over 200 synthetic yellow sapphires and treated synthetic yellow sapphires were sourced from marketplace. Specimens were examined by standard gemmological methods to determine their optical properties (refractive indices, birefringence and pleochroism), specific gravity, UV fluorescence etc. In depth study of the internal features was done with a gemmological microscope. Qualitative chemical analyses were performed on ten faceted samples (three yellow sapphires from Sri Lanka, one Myanmar four treated yellow sapphires and one synthetic and one-treated synthetic yellow sapphires) using a EDXRF to determine the minor and trace elements. Un-polarized spectroscopic measurements over the near-infrared (9000–4000cm⁻¹) and mid-infrared

(4000–400 cm^{-1}) ranges were carried out using a Nicolet Nexus Fourier transform infrared (FTIR) spectrometer equipped with a diffuse reflectance accessory (DRIFT) and operating with a resolution of 4cm^{-1} . Polarized ultraviolet-visible-near infrared (UV-VIS-NIR) spectroscopic measurements covering the 250–3300 nm range were performed with a Perkin Elmer Lambda 950 spectrometer on all samples. Three known Be-treated yellow sapphires were analysed by LIBS to confirm the Be-treatment (Krzemnicki et al, 2004). All stones were checked with SSEF Diamond Spotter to see whether they transmitted UV light.

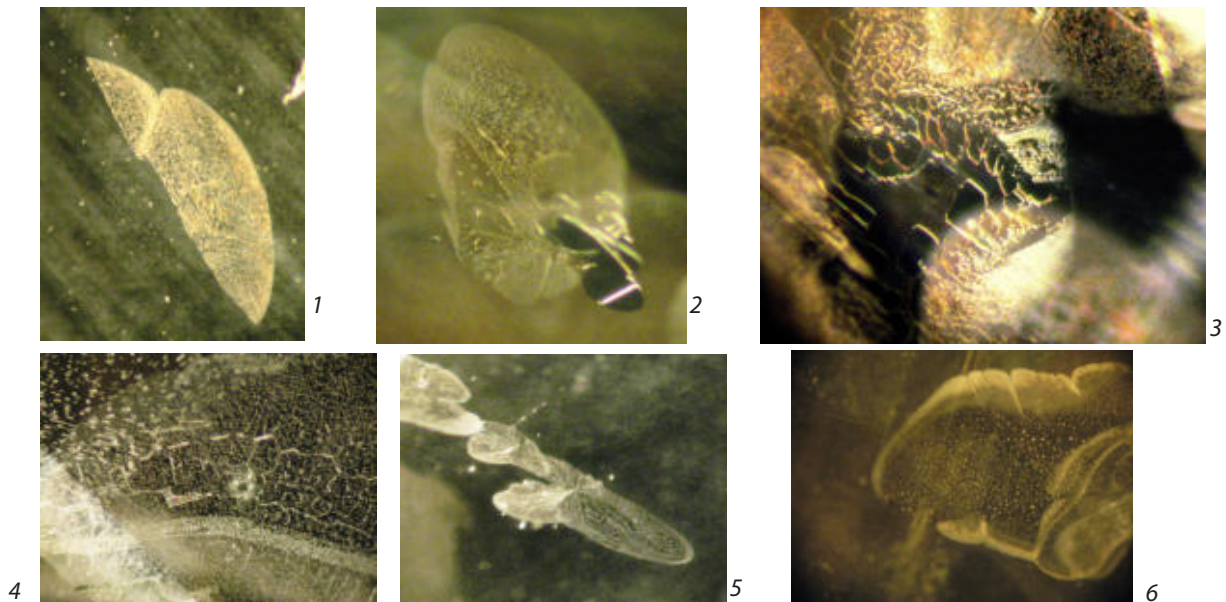
Results

Visual Appearance

Natural yellow sapphire typically ranges from yellow of low-to moderate saturation with a light to medium-dark tone. The natural samples in this study varied in hue, tone, and saturation. The Sri Lankan samples were brighter and more saturated than the Myanmar samples. The colour of the treated yellow sapphires was significantly more intense than that typically associated with natural yellow sapphires. The synthetic and the treated synthetic yellow sapphires were also significantly much darker in tone than most yellow sapphire. All synthetic yellow sapphires and treated synthetic yellow sapphire clearly transmitted the SWUV radiation and gave the fluorescent green or bright blue colour patch with SSEF diamond Spotter.

Microscopic Observation

The natural yellow sapphires in this study had a wide variety of internal features indicative of their natural origin: silk, feathers, various patterns of healed fissures, feathers around crystalline inclusions, feathers made of crystalline inclusions, feathers with liquid films, feathers with two phase inclusions, and growth structures. Treated yellow sapphires revealed several diagnostic internal features (McClure et al 2002; Rankin & Edwards 2003; Schmetzer & Schwarz 2004). Most notably, these consisted of distinctive “expanded feathers” as well as “beaded feathers”. The beryllium treated yellow sapphires contained disc shaped feathers. Some had thick bulbous type flux feathers. Synthetic samples and synthetic treated samples had some very specific inclusions, besides flux feathers, twisted feathers, wispy-feathers, some of the flux feathers contained groups of pinpoint inclusions. Treated synthetic yellow sapphires had remnants of gas bubbles that are indicative of the artificial growth process.



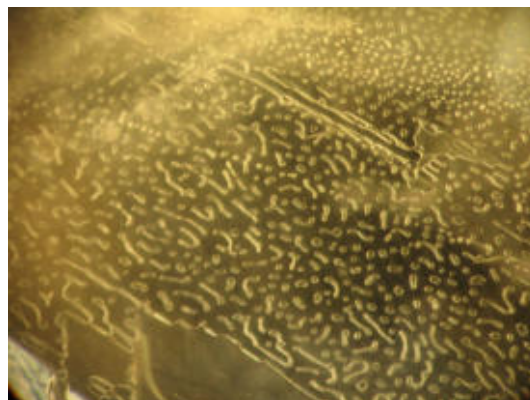
Discussion

Microscopy

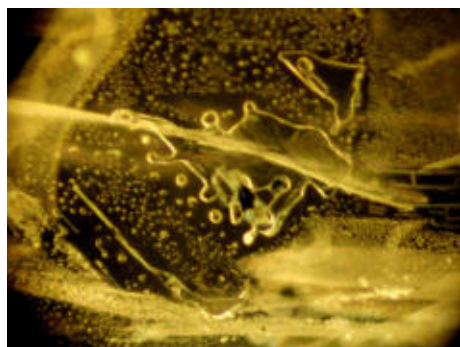
Magnification can provide important information for the separation of natural and synthetic and treated as well as treated synthetic yellow sapphires as most of the inclusions were characteristic (Schmetzer & Schwarz, 2005). We have classified some 18 “feather-type/fingerprint-type” inclusions having diagnostic importance. Among these 7 feather-type inclusions are typical for natural yellow sapphire with no significant treatment, 4 are typical treated yellow sapphires, 2 are characteristic of beryllium treated sapphires and 2 feather type inclusions are seen mostly in the treated-synthetic material whereas there are 3 feather-like inclusions which could be in treated, synthetic as well as synthetic treated yellow sapphires.



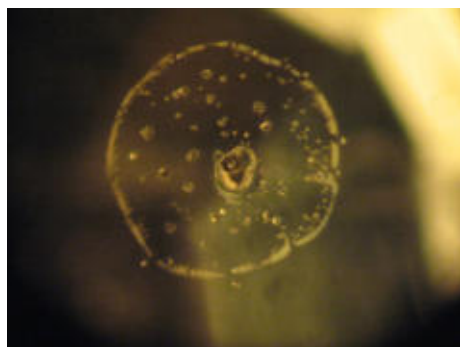
7



8



9



10

Natural yellow sapphires have characteristic feather-like or fingerprint inclusions: (a) feathers made up of very fine acicular liquid droplets (Fig. 1), (b) crystals embedded in feathers (Fig. 2), (c) feathers with liquid film present along side (Fig. 3), (d) feathers that have interconnecting channels (Fig. 4), (e) feathers with negative crystals (f) Multiple feathers with crystal (Fig. 5) and (g) healed feathers with angular expansions. Treated yellow sapphires have (h) expanded feather, (i) typical beaded feathers due to borax (Fig. 6), (j) bulbous type feathers (Fig. 7) and (k) expanded flux feathers (Fig. 8). It was observed that the beryllium treated yellow sapphires often showed due to high temperatures involved (l) disc shaped decrepitation-feathers around central crystal (Fig. 9) and (m) fern shaped re-crystallization of inclusions in feathers. In the treated synthetic yellow sapphires one can notice (n) the twisted feathers and (o) induced flux feathers (Fig. 10). Apart from these there are 3 other types of feathers which are common for treated and synthetic treated yellow sapphires.

Conclusions

Natural yellow sapphires, synthetic- and treated- as well as treated synthetic yellow sapphires have characteristic feather type inclusions. They may be readily distinguished using a combination of gemmological, chemical and spectroscopic features as well as sophisticated techniques such as UV-VIS and FTIR spectroscopy, chemical analysis, can provide clear proof of the identification. Nevertheless, internal features (with magnification) especially the varied feather-type inclusions play an important role as useful diagnostic indicators for gemmologists with basic equipment.

References

- Atichat, W., Sriprasert, B., Wathanakul, P., Pisutha-Arnond, V., Tay, T.S., Puttarat, T., and Leelawatanasuk, T., 2004 : Characteristics of "beryllium" heat treated yellow sapphires. 29th IGC 2004 Abstracts: 207- 214.
- Balmer W., Leelawatanasuk T., Atichat W., Wathanakul P., Somboon C. 2006: Update on FTIR characteristics of heated and unheated yellow sapphire. GIT2006 Conference, Bangkok, December, 6–7, p. 91.
- Krzemnicki, M.S., Haenni, H.A. and Walters, R.A., 2004: A method for detecting Be diffusion-treated sapphires: Laser-induced breakdown spectroscopy (LIBS). *Gems & Gemology*, 40(4), 314-322.
- McClure, S., Moses, T., Wang, W., Hall, M., and Koivula, J.I. 2002: A new corundum treatment from Thailand *Gems & Gemology*, 38(1), 86-90
- Schmetzer, K., and Schwarz, D., 2004: The causes of colour in untreated, heat-treated and diffusion treated orange and pinkish-orange sapphires – a review. *Journal of Gemmology*, 29(3) 149-182.
- Schmetzer, K., and Schwarz, D., 2005: A microscopy-based screening system to identify natural and treated sapphires in yellow to reddish-orange colour range *Journal of Gemmology*, 29(7/8) 407-449.
- Rankin, A.H. and Edwards W., 2003: Some effects of extreme heat treatment on zircon inclusions in corundum. *Journal of Gemmology*, 28(5)257-264.

High temperature fusion of corundum mimics so-called residues in heat treated rubies and sapphires

John I. Koivula

Analytical Microscopist, Gemological Institute of America, johnkoivula@hotmail.com

For more than a decade now some gemmological laboratories have identified certain secondary inclusion features as being the result of flux healing and/or some type of residue being purposefully infused into surface reaching cracks in high temperature heat-treated rubies and sapphires. A visually deployed “scale” of sorts has even been developed and utilized that subjectively estimates through the use of a gemmological microscope the amount or “degree” of filler in these cracks and reports it on gem identification documents.

The widely held belief that intentional flux healing is very commonly used by those doing heat treatment, and some of the resulting “residue estimation systems” do not take into account the high pressure environments that natural rubies and sapphires actually grow in and come from, and that gem corundum incorporates remnants of those growth pressures in both solid and fluid inclusions, releasing that held pressure when the inclusions rupture and the corundum becomes plastic during heat-treatment as it approaches its melting point (+/- 2050°C), but before it reaches that liquefaction temperature. In such a situation it would be obvious that there would be a tremendous outward pressure, and that inclusions without any compensating external pressure on the hosting ruby or sapphire would act as miniature magma chambers, and explosively rupture their host, sometimes resulting in cracks extending all the way to the surface that are lined with re-solidified inclusion debris as well as trapped gases that could very well look like so-called flux healing residues, which is of course the most popular current theory.

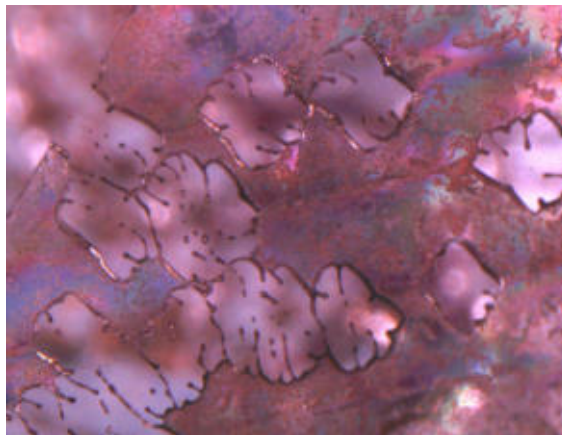


Figure 1. Air bubbles of various shapes trapped in a heat-fused crack in a pink Czocharalski synthetic sapphire. Such patterns look very much like those sometimes referred to as ‘residue’ in high temperature heat-treated natural rubies. 30X

There is plenty of visual evidence to logically show that corundum does in fact turn “plastic” before it melts, as do many solids but, in the case of heat-treated rubies and sapphires this evidence has been largely ignored, and as a result, at least some of the calls stating the presence of residues in surface-reaching cracks in heat-treated rubies and sapphires may have been made in error.

Through experimentation and photomicrographic documentation performed in GIA's advanced microscope laboratory, this lecture shows that monophasic gaseous secondary fingerprint-like "fluid inclusions" (and also lamellar twinning) can be produced in melt grown (Czochralski, Verneuil, etc.) synthetic corundum at only atmospheric pressure, near the melting point of the corundum, with no external matter other than heat-rarified (less dense) air being allowed to enter the surface-reaching cracks.

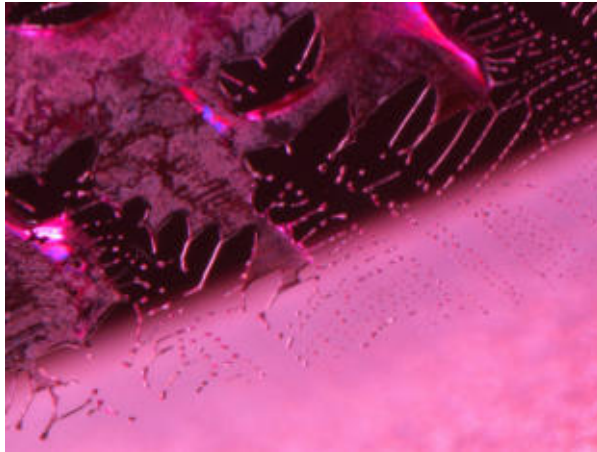


Figure 2. The leading edge of this heat-fused crack in a pink Czochralski synthetic sapphire is composed of air bubbles and interconnected air-filled tubes of various shapes and sizes. 40X

In this presentation, photomicrographs of "fingerprints" in synthetics resulting from simple heating in air will be compared to photomicrographs of so-called residue-lined or infilled cracks or "fingerprints" taken in natural rubies and sapphires that have undergone commercial high-temperature heat-treatment.

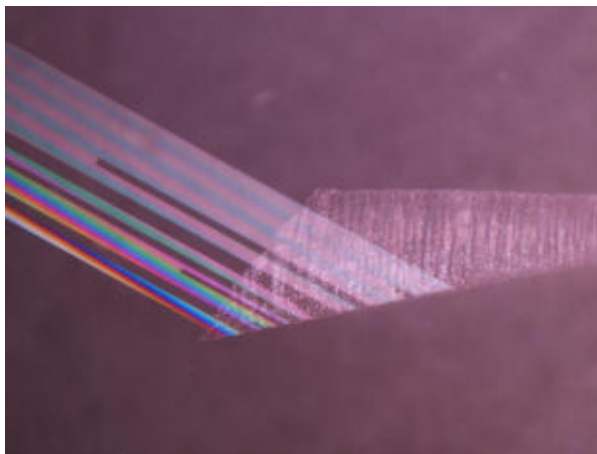


Figure 3. A partially healed crack composed of minute air bubbles has formed through high temperature heat fusion in a pink Czochralski synthetic sapphire. The resulting strain also resulted in the development of a lamellar twin plane that is clearly visible in polarized light. 15X.

Blue coloration of heat-treated zircon

Visut Pisutha-Arnond^{1,2}, Anusara Hentoo², Wilawan Atichat¹, Thanong Leelawatanasuk¹

¹ The Gem and Jewelry Institute of Thailand (Public Organization), Faculty of Science,
Chulalongkorn University, Bangkok 10330, Thailand; e-mail: pvisut@gmail.com

² Department of Geology, Faculty of Science, Chulalongkorn University, Bangkok 10330, Thailand

Abstract

Controversy still exists whether the blue colour of heat-treated zircon caused by a broad absorption band peaking at around 650 nm in the visible range is related to U⁴⁺. Therefore an experiment was carried out to systematically evaluate the relationship between uranium (U) contents and absorption peak or band intensities in the visible and infrared regions on a group of 16 selected rough zircon samples. They were subjected to heat-treatment under reducing conditions consecutively at 800°, 900° and 1000°C and finally at 1000°C under oxidation condition. In Vis-NIR region, reasonably good linear correlations were obtained between total U contents versus 1500 nm (~6700 cm⁻¹) as well as 1100 nm (~9000 cm⁻¹) peak areas (both related to U⁵⁺) after reduction and oxidation heating at those three temperatures. Unlike the above plots, however, there was no correlation between total U content and the areas of the broad 650 nm absorption band when the samples were heat-treated under reduction conditions at those three temperatures. This suggests that the blue coloration of heat-treated zircons is not related to U⁴⁺.

Keyword: heat-treated zircon, blue coloration, uranium content

Introduction

Gem-quality zircon can be found in colours such as blue, colourless, yellow-brown, reddish brown and green. Among those, blue is the most desirable stone colour in the trade (Marlins, 2002). Naturally-occurring reddish brown zircons are routinely heat-treated to blue, yellow to yellowish brown and colourless. Some researchers (Thongnopkun, et al., 2007; Wanthanachai-saeng et al., 2010) suggested that blue coloration of zircon was due to the presence of U⁴⁺ in the structure after reduction heating whereas other researchers (Thongcham et al., 2010) argued such a relationship. Because the direct correlation of the U content with the blue-related absorption intensity has never been carried out systematically, it is therefore the purpose of this study to find out whether there is such relationship.

Samples and procedure

Altogether 16 zircon single crystals were selected based on different shades of colour from colourless to deep reddish brown. Two samples were from from Bo Ploy, 5 samples from Bang Kacha, Thailand and 9 samples from Ratanakiri, Cambodia. All samples were carefully cut and polished into rectangular pieces having the flat surfaces parallel to the c axis at a controlled thickness, then recorded for their specific gravities and sizes. All samples were also measured for important trace element contents by LA-ICP-MS instrument. Each sample was analysed on a five-point traverse across the cut surface. The UV-Vis-NIR and FTIR absorption spectra of all samples were recorded both before and after each heat-treatment. All samples were placed within a graphite crucible in an electric furnace and then heat-treated consecutively at 800°, 900° and 1,000°C in a reducing (pure N₂) atmosphere, and finally at 1,000°C in an oxidizing (pure O₂) atmosphere for about 3 hours at each maximum holding temperature.

Zircon before Treatment

Of those 16 zircon samples, 13 were reddish brown and 3 were colourless, and high and intermediate types

based on their specific gravity values. The UV-Vis-NIR absorption spectra of almost all samples (see Figure 1 as an example) show prominent polarised sharp peaks at 1500 and 1100 nm (or ~ 6700 and ~ 9000 cm^{-1} , respectively), which were assigned to be due to U^{5+} (Vance and Mackey, 1974; Zhang et al., 2003). Moreover, the spectra of the brown samples also show a continuous increase of non-polarised absorption (similarly for both e- and o-rays) from visible towards the UV region with a shoulder or hump at around 490-500 nm (Figures 1 and 2). This absorption feature causes brown to reddish brown colour of those samples.

Zircon after heat-treatment

After reduction heating at 800°, 900° and 1000°C, all samples became clearer, i.e. translucent to transparent. Of those 16 samples, 14 turned blue of which one is deep blue and the others are pale blue, and two samples from Bo Ploy, Thailand are still colourless after heating up to 1000°C. The samples became slightly yellow brown to colourless after oxidation heating at 1000°C again.

The visible spectra of the originally brown samples gave different patterns when measured before and after heating. The non-polarised absorption band from visible to UV region with shoulder at 490-500 nm (causing reddish brown colour) that appeared before heating was eliminated after annealing at high temperatures (Figures 1 and 2). As a result this absorption band was assigned to be due to local structural damages or defect centres resulting from self-irradiation of U and Th (Thongnopkun et al., 2007; Wanthanachaisaeng et al., 2010) rather than due to Nb^{4+} substituting for Zr^{4+} by which the low energy side of the Nb^{4+} band in the UV region extends into the visible range causing the reddish brown colour (Fielding, 1970). Also after reduction heating, the spectra of the blue samples show polarised absorption broad band from 550-850 nm range with maximum at around 650 nm (mainly for o-ray) which causes the blue colour (Fig. 2). This 650 nm broad band was eliminated after annealing in oxidation condition at 1000°C and therefore was suspected to be related to U^{4+} that could have been formed after reduction heating (Thongnopkun et al., 2007; Wanthanachaisaeng et al., 2010). This aspect is the main subject of our investigation below. Also after oxidation heating at 1,000°C, absorption residue similar to those before heating still remains, causing slightly yellowish brown colour (Figures 1 and 2). Hence it is possible that the yellow to yellowish brown colour of heat-treated zircon may represent its incomplete annealing part of structural damage.

After reduction heating at the three temperatures mentioned above, the spectra of all samples in the NIR region still show U^{5+} related peaks at around 1500 and 1100 nm which could be stabilised by charge compensation with trivalent or divalent impurities in the structure (Fig. 1). The plots of total U content versus 1500 and 1100 nm peak areas/cm of those zircon samples after reduction heating at those three temperatures show reasonably good positive linear correlations (Fig. 3). This confirms that the absorption peaks at 1500 nm and 1100 nm is related to the amount of U in the zircon structure and were due to U^{5+} as previously assigned (Vance and Mackey, 1974; Zhang et al., 2003). The plots also confirm that this method can be used for evaluating the relationship of the other absorption peaks with amount of U as well as other trace elements in the samples. A good linear correlation of U contents versus 1500 and 1100 nm peaks was also obtained from a similar plot of those samples when they were heat-treated at 1000°C under oxidation condition.

In order to evaluate the relationship of blue coloration with U, the total U contents were plotted against 650 nm broad band area/cm of all samples reduction-heated at those three temperatures. It appears that there is no correlation of U contents with 650 band area at all three temperature plots (Fig. 4). This suggests that the blue colour of those heat-treated zircons is not related to total U content. This may imply that the blue coloration is not related to U^{4+} as the significant amount of U^{4+} could readily be present in the zircon structure, particularly after reduction heating.

A large number of sharp absorption lines in the visible region measured at 77 and 4.2 Kelvin were observed in U-doped synthetic zircon crystal and were interpreted to be due to U^{4+} (Richman et al. 1967). However all those characteristically prominent sharp peaks in the visible region reported by Richman et al. (1967) are totally different from the 650 nm broad band observed in this study. In fact the 650 nm broad band may overlap with those sharp peaks, one of which is also present near 650 nm (see Fig. 2). Hence the cause of blue colour in those heat-treated samples still could not be resolved as there are also no relationships between 650 broad band area and the total

amounts of other important trace elements such as Th, Hf, Ti, Sc, Nb, Ta, Y, Ce in the zircon structure.

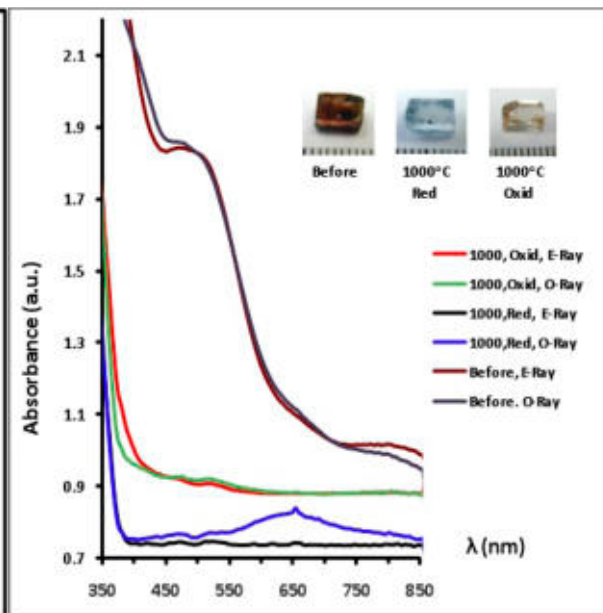
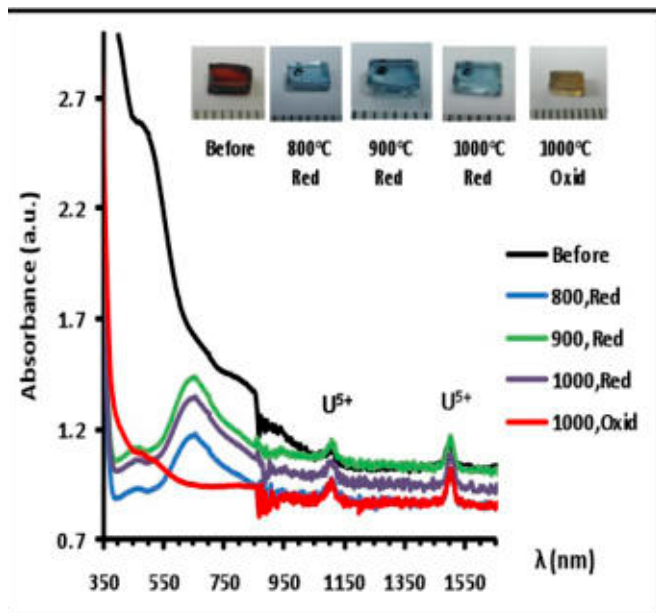


Figure 1: UV-Vis-NIR absorption spectra (o-ray) of a zircon sample (ZRC 1010) recorded before and after reduction heating at 800, 900 and 1,000°C and oxidation heating at 1,000°C. Note the similarity of the visible spectral patterns measured before treatment and after oxidation heating at 1000°C.

Figure 2: Polarized UV-Vis absorption spectra of a zircon sample (ZRC 1007) recorded before treatment and after reduction and oxidation heating at 1,000°C. After the reduction heating, a polarized broad band from 550-850 nm with maximum at around 650 nm appears and may overlap with many small sharp peaks, one of which is also observed near 650 nm.

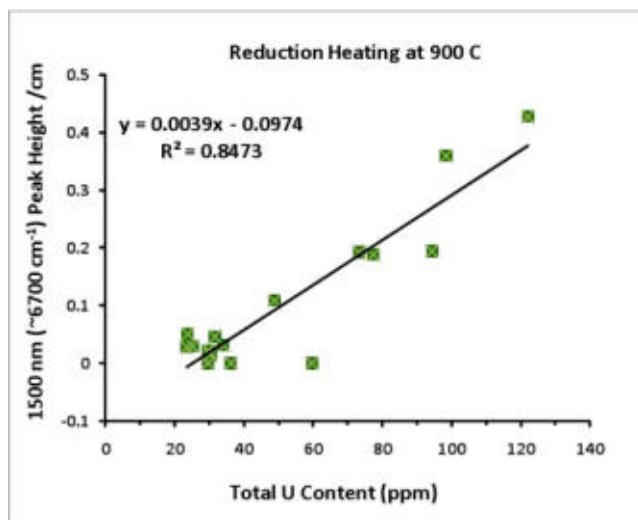


Figure 3: Plot of 1500 nm (~6700 cm⁻¹) peak height [cm] versus total U content of all zircon samples after reduction heating at 900°C.

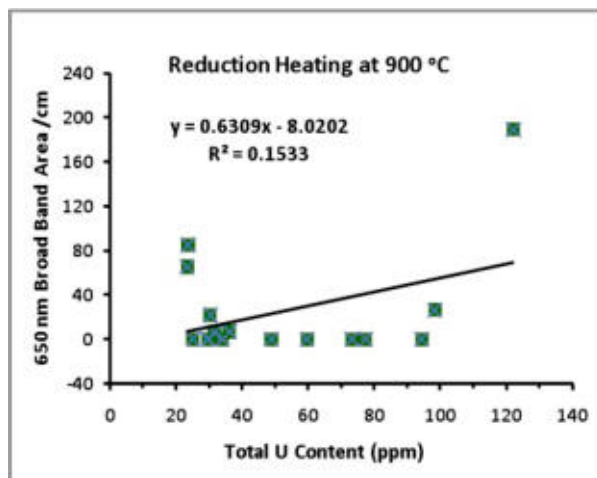


Figure 4: Plot of 650 nm (~9000 cm⁻¹) broad band area [cm] versus total U content of all zircon samples after reduction heating at 900°C.

Conclusion

The non-polarized UV-Vis absorption spectrum of untreated zircon samples with shoulder at 490-500 nm (causing reddish brown colour) is likely to be due to defect centres caused by local structure damages from self-irradiation by U and Th. After annealing at 800°, 900° and 1000°C in both reduction and oxidation conditions, reasonably good linear correlations were found between total U contents versus 1500 nm and versus 1100 nm absorption peak areas (related to U⁵⁺). There is however no correlation between total U content and 650 nm polarized absorption broad band areas (causing blue colour in those samples). Therefore, the blue coloration is not related to U⁴⁺ in the reduction-heated zircon samples as suspected earlier.

Acknowledgements

The experiments and measurements by advanced equipment were carried out at the Geology Department, Chulalongkorn University, and at GIT Lab with kindly help from Ms. Chaniya Rochd.

References

- Fielding, P.E., 1970. The distribution of uranium, rare earths, and color centers in a crystal of natural zircon. *Am. Mineral.* 55:428-44
- Marlins, A., 2002. *Color gemstone: buying guide*, 2nd ed. Gemstone Press: Canada, 79-82
- Richman., I., Kisliuk, P., Wong, E.Y., 1967. Absorption spectrum of U⁴⁺ in zircon (ZrSiO₄). *Phys. Rev.* 155: 262-267
- Thongcham, K., Sahavat, S., Wongkokau, W., 2010. Effects of annealing to colour of zircon. *Proceedings of the 5th International Workshop on Provenance and Properties of Gems and Geo-Materials*, Hanoi, Vietnam, 111-115
- Thongnopkun, P., Chindudsadeegul, P., Therdtteppitak, A., 2007. Color development of zircon by gaseous furnace, 33rd Congress on Science and Technology of Thailand, 1-5
- Vance, E.R., Mackey, D.J., 1974. Optical study of U⁵⁺ in zircon. *J. Phys. C: Solid State Phys.* 7: 1898–1909
- Wanthanachaisaeng, B., Bunnag, N., Sutthirat, C., Ounorn, P., Phattarawarin, P., Pisutha-Arnond, V., 2010. Determination of heat treated zircon by FTIR spectrophotometer. *Proceedings of the 5th International Workshop on Provenance and Properties of Gems and Geo-Materials*, Hanoi, Vietnam, 97-99
- Zhang, M., Salje, E.K.H., Ewing, R.C., 2003. Oxidation state of uranium in metamict and annealed zircon: near-infrared spectroscopic quantitative analysis. *J. Phys.: Condens. Matter* 15: 3445–3470

Emplacement of deposits of coloured gemstones at the intersection of faults with the perimeters of large circular structures

John M. Saul

ORYX, 3 rue Bourdaloue, 75009 Paris, john.saul@wanadoo.fr

In East Africa, major deposits of Crystalline Coloured Gemstones are found on the rim-zones of faint circle scars, commonly in the vicinity of tangential faults (Fig. 1).

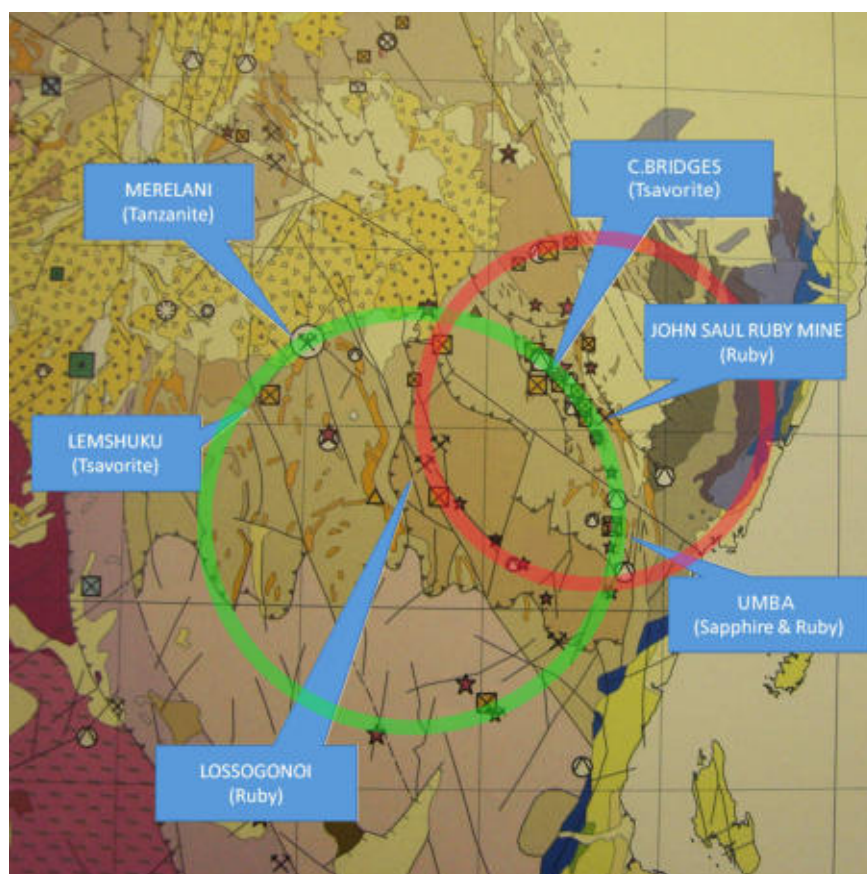


Figure 1: Major deposits of crystalline coloured gemstones and their relation to circular scars, SE Kenya / NE Tanzania.

The John Saul Ruby Mine (Tsavo West, Kenya) is located at the quadruple intersection of the Mwatate River Fault, an unnamed NW-SE trending fault, and the perimeters of two circular structures with diameters 17 and 260 kms (Fig. 2). These structures are discernible on some false-colour satellite images, on topographic maps with an exaggeration of the vertical dimension and on other types of coverage as well.

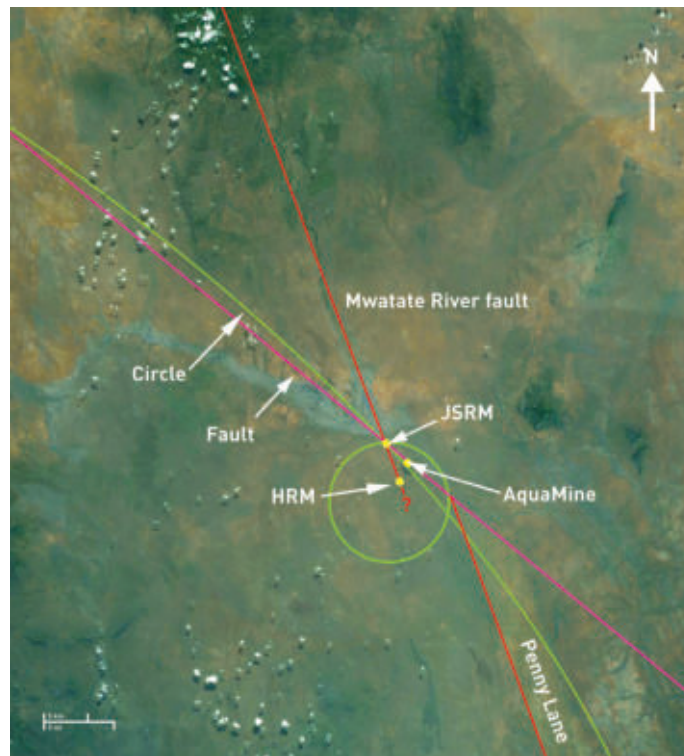


Figure 2: Deposits of crystalline coloured gemstones, associated faults, and circular scars, Tsavo West area, Kenya.

The circular scars are attributed to the Late Heavy Bombardment (LHB), the impact-episode, c. 4000 Ma, that scarred the surface of the Moon and other members of the Solar system (Saul, 1978). Many LHB impacts penetrated the entire thickness of the Earth's crust, leaving 3-D fractures, from less than 15 to more than 5000 km in diameter, that penetrated to the Earth's brittle-ductile boundary. Earth tides, convection, volcanism, earthquakes and other phenomena have prevented these fractures from completely healing and in the course of time they have been episodically available for the movements of fluids and heat. The formation of Crystalline Coloured Gemstones is in part due to the availability of excess heat, allowing gem-forming minerals to crystallize at lower constraining pressures within their permitted P-T stability zones.

References

Saul, John M., 1978. Circular structures of large scale and great age on the Earth's surface. *Nature*, 271 (no.5643) 345-349.

Saul, John M., 2004. Geological Consequences of the Late Heavy Bombardment. *Meteorite*, 10 (no.1) 13-18.

Saul, John M., 2007. The origin of crystalline colored gemstones in Gondwanaland and the greater Himalayan region. *Proceedings 30th International Gemmological Conference, Moscow*.

Acknowledgement:

The author thanks the Richard Lounsbery Foundation for backing this project. A more complete version of this study is scheduled to be linked to: www.swalagemtraders.com

Sapphires from some exotic sources: Azad Kashmir and New Zealand

Lore Kiefert

Gübelin Gem Lab, Maihofstrasse 102, 6006 Luzern, Switzerland, e-mail: l.kiefert@gubelingemlab.ch

When rubies and sapphires are mentioned, people mostly think of the «classic» origins such as Burma (Myanmar), Kashmir, Sri Lanka, Thailand/Cambodia, and more recently East Africa, including the deposits in Madagascar, Tanzania, Kenya and Mozambique. Other commercially more or less important corundum deposits are found in Australia, Vietnam, Cambodia, Laos, China, Montana, Brazil, Colombia, and Afghanistan.

Besides these well documented deposits, there are a number of less well known or new ruby and sapphire occurrences worldwide, such as Baffin Islands in Canada, Greenland, Auvergne in France, Liberia, Sierra Leone, the area around Batakundi in Azad Kashmir (Pakistan), or New Zealand's South Island. This presentation will concentrate on the last two sources.

(1) Violetish blue, purple and pink sapphires from Azad Kashmir in Pakistan

Although not a commercially producing area, sapphires from Azad Kashmir in Pakistan have entered the gemstone market occasionally since the end of the 1990s. While this area is in the Pakistani-controlled part of Kashmir, the gem dealers often sell these goods as Kashmir sapphires, referring to the traditional Kashmir sapphires, which have the legendary reputation of belonging to the most beautiful gemstones in the world. However, these are found near the village of Sumjam in the Jammu and Kashmir area of the Indian part of Kashmir, and show distinctly different features from those of the sapphires from Azad Kashmir.

The area of this gemstone deposit is difficult to access due to its geographic location. So far, there are only few reports on the sapphires from Batakundi (Quinn, 2004; Pardieu et al., 2009; Pardieu, 2010). Pardieu mentions in his 2010 update, that sapphires previously described as coming from Batakundi are probably derived from Basil, according to the look of them. Basil and Batakundi are 30 km apart from each other.

The Basil occurrence was reportedly discovered in 1996 with two deposits located in graphite veins producing pink, purple, and blue sapphires (Fig. 1). A third site, which produces more pink sapphires is located within marbles (Pardieu, 2010). According to Pardieu, the actual Batakundi mine produces rubies rather than sapphires. They are hosted in a marble-type deposit.



Figure 1: Rough sapphire from Batakundi/Basil with a typical crust of fuchsite and graphite around (thickness of rim: approximately 3-4 mm), and three faceted sapphires from this deposit.

The sapphires from this area range from blue to violet to purple and pink in colour, but it is mainly the blue to bluish violet varieties that are reaching the laboratory. The most distinguishing feature of these sapphires is their red lamellae, following growth zones. Besides this, many of them show small black crystal inclusions, which were analysed as graphite. The blue sapphires often show twinning in 3 directions nearly perpendicular (89°) to each other, occasionally with boehmite «needles» at the intersection lines.

(2) Blue, purple, pink and orange sapphire from New Zealand

Finds of sapphires from New Zealand are occasionally mentioned in geological and mineralogical journals (e.g., Grapes & Palmer, 1996), but no commercial sapphire mining is performed in New Zealand. By chance the author came across sapphires from an alluvial deposit on the South Island of New Zealand close to Dunedin. The rough sapphires were recovered during the reworking of an old gold mining area, and ranged in size from 3 mm to 8 mm. Larger sapphires were not found because during the gold mining process the gravel was sieved with a 5 mm sieve and the larger pieces discarded.



Figure 2: Sapphire from New Zealand. The blue rough sapphires in the back are of basaltic origin, the pink and orange samples are from a metamorphic source. The triangular pinkish orange cabochon in the front right corner weighs 1.04 ct.

The colours of the sapphires from New Zealand range from blue to violetish pink to pink and orange (see Fig. 2). Using a combination of spectroscopic and chemical data, there are two types of sapphires: on the one hand blue basaltic ones, which are semi-transparent, but show rutile inclusions and intense blue colours, lacking the bluish green known from other basaltic sources. The second type is purplish pink to pink and orange. These samples are from a meta-morphic source. Some of the pinkish orange sapphires have spectroscopic features similar to natural Padpadscha sapphires from Sri Lanka. The bimodality of these alluvial samples is similar to sapphires found in the Barrington Tops region, New South Wales, sapphires from Pailin, Cambodia (Sutherland et al., 1998) and sapphires from Ban Huai Sai, Laos (Bosshart, 1995; Sutherland et al., 2002).

References

Bosshart, G. 1995. Sapphires and Rubies from Laos. 25th International Gemmological Conference, Rayong, Thailand, 23-26.

Grapes, R., Palmer, K. 1996. (Ruby-Sapphire)-Chromian Mica-Tourmaline Rocks from Westland, New Zealand. *Journal of Petrology*, 37 (2), 293-315

Pardieu, V., Thirangoon, K., Lomthong, P., Saeseaw, S., Thanachakaphad, J. & Du Toit, G. 2009. Sapphires Reportedly from Batakundi/Basil area. A preliminary examination and a comparison with rubies and pink sapphires from other deposits in Central Asia. http://www.giathai.net/pdf/Batakundi_Sapphire.pdf

Pardieu, V. 2010. Update on ruby and sapphire mining in Pakistan and Afghanistan. *Gems & Gemology*, 46 (4), 319-320

Quinn, E., Laurs, B.M. 2004. Sapphires from Afghanistan and Pakistan. *Gems & Gemology*, 40 (4), 343

Sutherland, F.L., Schwarz, D., Jobbins, E.A., Coenraads, R.R. & Webb, G. 1998. Distinctive gem corundum suites from discrete basalt fields: a comparative study of Barrington, Australia, and West Pailin, Cambodia, gemfields. *Journal of Gemmology*, 26 (2), 65-85

Sutherland, F.L., Bosshart, G., Fanning, C.M., Hoskin, P.W.O., Coenraads, R.R. 2002. Sapphire crystallization, age and origin, Ban Huai Sai, Laos: age based on zircon inclusions. *Journal of Asian Earth Sciences* 20, 841-849.

The New England, New South Wales, Australia gem field: geographic typing of a world class giant gem deposit of basaltic placer origin

F. Lin Sutherland¹, Ahmadjan Abduriyim², Gayle B. Webb¹

¹Geoscience, Australian Museum, 6 College Street, Sydney, NSW 2010

²Gemmological Association of All Japan (GAAJ-ZENHOKYO Laboratory), 5-25-11 Ueno Taito-ku, Tokyo, 110-0005 Japan.

New England hosts one of the premier Australian gem fields, although the full extent, quality and complexity of its gem inventory is often overlooked outside Australia. Prospectors discovered the first sapphires and diamonds in the 1850s; diamond mining prevailed initially but lapsed in the 1920s as sapphire mining expanded in stages. Sapphire mining continues at present with a few large and small scale mining and heat treatment ventures (Coldham, 2003; Abduriyim et al., 2010). Estimates suggest well over a million carats of sapphires and diamonds have been extracted from placer deposits. The diamonds have unique features related to their proposed ultra high pressure subduction sources (Barron et al., 2008), while the sapphires are noted for fine blue stones and some of the richest grades reported from sapphire deposits (Sutherland and Webb, 2007). Super-rich volcanoclastic deposits in the Kings Plains area carried sapphire grades > circa 1800 g/ton. (Fig. 1). Other gemstones recovered from the basalt fields here include abundant zircon, sometimes cut into large stones, and rarer ruby, garnet and peridot. The underlying basement granites and folded beds provide a wide range of quartz, topaz, beryl (including emerald) and rarer gemstones (Webb and Sutherland, 1998), but are not considered here.



Figure 1. High grade gem-bearing volcanoclastic 'wash', Kings Plains. Image: T. Coldham. Observed heavy minerals in the sample include sapphire, zircon and spinel.

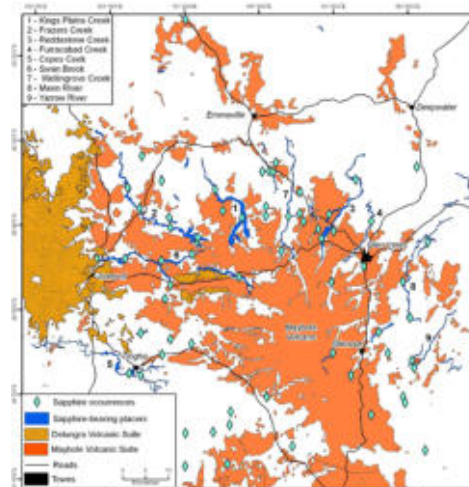


Figure 2. New England basaltic gem field, with distribution of gem-bearing basalts, sapphire sites, placer deposits, and mining/prospecting localities. Compilation: R.E. Brown and F.L. Sutherland.

Previous studies of New England basalts and associated sapphires and zircons (Sutherland 1999; Brown 2006; Vickery et al., 2007) suggest these gemstones formed at depth at several times and were then repeatedly carried to the surface in basaltic eruptions that extended from Late Mesozoic to Late Cenozoic time (81 to 3 myr). A significant sapphire forming and eruptive event dominated the gem field (40-30 myr Maybole volcanism), from which gem-rich volcanoclastic mass flows radiated out through the surrounding drainages (Fig. 2). The New England

gem field is an excellent example of the concept of a 'hydra-headed' eruptive gem field, where earlier eruptive vents cut off by erosion are continually replaced by new vents, recycling gemstones into multi-sourced deposits. Its area (80 X 100 km), rich grades and quality sapphires suggest a world class 'giant' ore deposit status.

Table 1. Initial trace element LA-ICP-MS results (ppm), New England sapphires

Colour	Fe	Ti	V	Cr	Ga	Mg
Blue (n=12)	1940-5729	26-630	1-7	<1-9	55-149	<1-30
Green (n=5)	6787-7435	24-35	9-13	1-5	132-140	10-12
Purple (n=4)	4642-7434	42-73	5-37	290-723	170-210	51-52

Detailed trace element data on cut blue sapphires from an unlocalised NSW source (Abduriyim and Kitawaki, 2006) were used to trace the stones to New England using data from Australian sapphire fields (Sutherland and Abduriyim, 2009). These trace element studies (Table 1) stimulated a project between GAAJ-ZENHOKYO Laboratory, Tokyo, Australian Museum and Gemmological Association of Australia for more detailed studies on the New England gemstones. This project aimed to establish their precise geographic characteristics and increase general outside awareness of their fine gemmological attributes. A preliminary report on current sapphire mining (Abduriyim et al., 2010) and further joint laboratory studies (GEMOC) on the gemstones suggest a more extended, complex origin for the sapphires and zircons (zircon U-Pb ages now range from 38 to 216 myr). The presentation here outlines progress on the New England study and its aims for geographic typing. This will provide geochemical, inclusion, age and other data for a regional gemstone synthesis.

References

- Abduriyim, A., Kitawaki, H., 2006. Determination of the origin of blue sapphire using Laser Ablation Inductively Coupled Plasma Mass Spectrometry (LA-ICP-MS). *Journal of Gemmology*, 30 (1), 23-26.
- Abduriyim, A., Sutherland, F.L. and Coldham, T., 2010. Old Days, present and future of Australian sapphire and ruby; a report from the mining areas in New South Wales, Australia. *The Quarterly Journal of the Gemmological Association of All Japan*, 41 (488-489), 5-10 (in Japanese).
- Barron, L.M., Barron, B.J., Menargh, T.P., Birch, W.D., 2008. Ultrahigh pressure macro diamonds from Copeton (New South Wales, Australia), based on Raman spectroscopy of inclusions. *Ore Geology Reviews* 34 (1-2), 76-86.
- Coldham, T., 2003. The history and importance of heat treatment of Australian sapphire. *Australian Gemmologist* 21 (11), 450-462.
- Brown, R.E., 2006. Inverell Exploration NSW geophysics – new data for exploration and geological investigations in the northern New England area of New South Wales. *Quarterly Notes of the Geological Survey of New South Wales*, 121, 1-38.
- Sutherland, F.L., 1999. Volcanism, geotherms, gemstones and lithosphere since orogenesis. In Flood, P.G. ed. *New England Orogen*, University of New England, Armidale, NSW, 355-364.
- Sutherland, F.L., Abduriyim, A., 2009. Geographic typing of gem corundum: a test case from Australia. *Journal of Gemmology*, 31 (5-8), 203-210.
- Sutherland, F.L., Webb, G.B., 2007. Australian sapphires and rubies. *Rocks & Minerals*, 82, 116-125.
- Vickery, N.M., Dawson, M.W., Sivell, W.J., Mallock, K.R., Dunlap, W.J., 2007. Cainozoic igneous rocks in the Bingera to Inverell area, north eastern New South Wales. *Quarterly Notes of the Geological Survey of New South Wales*, 123, 1-31.
- Webb, G.B., Sutherland, F.L., 1998. Gemstones of New England. *Australian Journal of Mineralogy*, 4 (2), 115-121.

Acknowledgements

Ross Pogson, Australian Museum; T. Coldham, Gemmological Association of Australia; Elena Belousova, GEMOC, Macquarie University; School of Natural Sciences, University of Western Sydney; Merv Walburn, John Wilson, Ken Dawson, Inverell.

Three main types of corundum gem deposits in Vietnam

Nguyen Ngoc Khoi^{1, 2}, Nguyen Thi Minh Thuyet¹, Nguyen Van Nam³, Nguyen Thuy Duong¹

¹Hanoi University of Science, 334 Nguyen Trai str., Thanh Xuan dist., Hanoi, Vietnam

²DOJI Gold & Gems Group, 44 Le Ngoc Han, Hanoi, Vietnam

³Vietnam Institute of Geosciences and Mineral Resources, Chien Thang road, Hanoi, Vietnam. Email: khoinn@vnu.edu.vn

In the past decades, Vietnam has become known as a country with great potential for gem-quality ruby and sapphire. Occurrences of different corundum deposit types have been discovered and mined in several regions. The most important ones are:

1. Marble-hosted deposit type with Luc Yen deposit in Yen Bai province and Quy Chau deposit in Nghe An province as main representatives;
2. Gneiss-hosted deposit type with Tan Huong and Truc Lau deposits in Yen Bai province, and Phuoc Hiep occurrence in Quang Nam province.
3. Basalt-related deposit type with typical representatives Dak Ton deposit in Dak Nong province, Ma Lam, Da Ban deposits in Binh Thuan province, Di Linh deposit in Lam Dong province, etc. (Fig. 1).



Figure 1. This map roughly shows the distribution of the three main corundum deposit types in Vietnam.



Figure 2, a. The corundum crystals embedded in marble typically show a barrel or spindle shape with a length/width ratio from 5:1 - 6:1. This sample was mined from Luc Yen deposit. Photo by Khoi N.N.



Figure 2, b. The typical hues of corundum from the marble-hosted type are "pure" red or pink as shown in this picture. All these cut stones were purchased from Luc Yen mining area. Photo by Khoi N.N.

The characteristics of three main corundum deposit types in Vietnam

Being formed in different tectonic settings and geological environments, these deposits differ in mineralogy, morphology, texture, hosting lithology as well as economic value .

Marble-hosted type

These deposits form along shear zones (Red River shear zone in Luc Yen deposit, and Quy Chau shear zone in Quy Chau deposit), linked to Cenozoic tectonics resulting from continental collision between Indian and Eurasian plates. They form in high-grade, mainly granulite facies, regional metamorphic environments. Corundum is considered to be syn-metamorphic: Luc Yen 30.8-34.0 Ma, Quy Chau 21.0-22.5 Ma (Garnier et al., 2008), whereas the protolith can be Precambrian or younger (Thac Ba Formation). Ruby and sapphire occur as idiomorphic crystals within or at the contact of marble layers with magmatic rocks (pegmatite, syenite) or schists, while fancy sapphire occurs only in pegmatite bodies in association with tourmaline, amazonite, etc. Gem ruby, fancy sapphire and spinel are the main products. Also present are tourmaline, amazonite, humite, pargasite, sodalite... (Khoi, 2004).

Gneiss-hosted type

Corundum in gneisses occurs mostly in fold belt (Con Voi mountain range) of Red River Shear Zone. These deposits form in high-grade, mainly granulite facies, regional metamorphic environments. Metasedimentary belts containing aluminous strata or lenses, in some cases intruded by igneous rocks, are particularly favourable. Corundum is considered to be syn-metamorphic: 22.17-24.52 Ma. The protolith is Precambrian (Con Voi Formation). Rocks that were exposed at the surface during periods of extreme chemical weathering are particularly favourable. Corundum occurs as porphyroblasts or idiomorphic, xenomorphic or skeletal crystals within high grade, regionally metamorphosed belts. It is confined to specific metamorphic layers and concordant lenses of alumina-rich gneisses and schists. Gem corundum and spinel are the main products (Khoi et al., 2010b).



Figure 3, a (left). Short prismatic and sometimes tabular shape with big size are the most prominent morphologies of corundum crystals from gneiss in Vietnam. These stones were collected from Km 23 occurrence, Tan Huong area (Yen Bai province). Photo by Khoi N.N. Figure 3, b (right). Deposits of the gneiss-hosted type are commonly noted for star rubies and pink sapphires like these cut stones from the Truc Lau mine. Courtesy of DOJ Gold & Gems Group. Photo by Binh N.N.

Basalt-related type

Host rocks occur in continental and pericontinental settings related to rifts, deep faults and/or hot-spots. Corundum gems are brought to the surface by alkali basalt eruptions. The highest grades are associated with diatreme and base surge lithologies that erode quickly. Significant corundum can also be present in lava flows and hypabyssal equivalents of these corundum-rich volcanic pulses (Levinson et al, 1994). Typically hosted by Cenozoic or younger rocks: 17.6-1.1 Ma (Garnier et al., 2005). Sapphires are found as xenocrysts in some hypabyssal or eruptive alkalic rocks. The residual soil or regolith (a layer of loose, heterogeneous material) overlying these rocks can

be enriched in sapphires due to intense weathering which liberates the megacrysts from the matrix. Sapphire and zircon are the main products.

Gemmological properties of corundum from three deposit types

Gemmological properties of corundum from three deposit types			
Properties	Marble-hosted type	Gneiss-hosted type	Basalt-related type
Morphology and Appearance	The crystals typically have a barrel or spindle shape with a length/width ratio from 5:1 - 6:1 (Fig. 2, a). Tabular corundum are very rare. The majority of cut stones range from "pure" red or pink to purplish red or pink (Fig. 2, b); other hues such as blue, orangy red, violet, or multicoloured are also found. Stones commonly show strong colour zoning visible with the unaided eye. Diaphaneity usually ranges from transparent to translucent (Kane et al., 1991; Long, 2003; Khoi, 2010a).	Short prismatic and sometimes tabular morphologies (Fig. 3, a); with granular spinel coating. In general, the crystals are much larger than those from the other types. Corundum shows less colour variation, with pink to purplish or brownish pink hues being dominant. Colour zoning is un-common. Asterism (Fig. 3, b) is very common in rubies and pink sapphires. Diaphaneity is semitransparent to translucent or opaque because of fracturing and the abundance of inclusions.	The crystals typically have a hexagonal dipyramidal shape with a length/width ratio of 6:1 (Fig. 4, a). The dominant hues are dark blue, inky blue to dark green, and BGY. Diaphaneity ranges from transparent to translucent (Fig. 4, b).
Internal Features	The most common inclusions are calcite, rutile, apatite, spinel, zircon, corundum, pyrrhotite, graphite, boehmite, hematite, phlogopite, muscovite, hercynite and tourmaline. Straight and angular colour zoning and coloured patches and spots are usually seen, while swirl growth marks are observed in some cases (Kane et al., 1991; Long et al., 2004)	Corundum contains a different diversity of mineral inclusions, such as ilmenite, rutile, apatite, zircon, diaspore, boehmite, magnetite, plagioclase, muscovite, biotite. Although straight and angular growth structures are quite common, colour irregularities are rare or almost absent. Common is pronounced polysynthetic twinning (Khoi et al., 2010b).	The most common inclusions are columbite, pyrochlore, ilmenite, zircon, hercynite, spinel, rutile, corundum and clinozoisite. Colour zoning, colour patches and spots are very common.
Colouring Elements	Corundum contains a high content of Cr (1764ppm) and Mg (105ppm) and a low content of Ga (<75ppm). The Cr ₂ O ₃ /Ga ₂ O ₃ ratio equals or is higher than 10.	Corundum contains a high content of Fe (7653ppm) and Ga (96ppm) and a low to medium content of Cr. The Cr ₂ O ₃ /Ga ₂ O ₃ ratio is mainly < 3.	Corundum contains a high content of Fe (7927ppm), and Ga (177ppm) and low Cr (43ppm) and Mg contents (15ppm). The Cr ₂ O ₃ /Ga ₂ O ₃ ration is mostly < 1.



Figure 4, a (left). The crystals from the basalt-related deposit type commonly have a hexagonal dipyramidal shape with a length/width ratio of 6:1. The stones shown in this figure were selected from the Dak Ton deposit in Dak Nong province, South Vietnam. Photo by Thuyet N.T.M. Figure 4, b (right). The dominant hues of sapphires from the basalt-related deposit type are dark blue, inky blue to dark green, and BGY with diaphaneity ranging from transparent to translucent. These Dak Ton stones were collected and photographed by Khoi N.N.

Different geological environments also determined the difference in gem-quality characteristics of rubies and sapphires, which are reflected in their morphology, colour and clarity. According to these criteria, the quality of

corundums from the three main deposit types of Vietnam changes as follows:

- Corundums in matrix from the gneiss-hosted deposit type are usually of gray to bluish gray, dark red to violetish red and pink colour, and from low to medium transparency due to a high percentage of opaque mineral inclusions (magnetite, ilmenite, biotite)... and high fracturing. The majority of them is not of gem quality. Nevertheless, corundums from placers in Tan Huong and Truc Lau deposits have better coloration and clarity.
- Corundums from both hosting rocks and placers of the marble-hosted deposit type (Luc Yen and Quy Chau deposits) are characterized by dominant red hue with various hints, by the saturation varying from dull to very vivid, and by the tone changing from light to very dark. Inclusions are diversified, but their contents are not high, that is why the transparency of corundums is good. Corundums from this deposit type is of highest quality, some of them are comparable with Mogok stones which are considered as the best in the world.
- Corundums from the basalt-related type are usually of dark blue, green blue or yellow colour, some belong to BGY type. The saturation changes from dull to slightly vivid, the tone from light to dark. Inclusions are plentiful, but their content is low. Corundums from this deposit type are of medium gem quality.

Conclusion

In general, corundums from the marble-hosted deposit type are of the highest quality, corundums from the basalt-related deposit type of intermediate quality, and corundums from the gneiss-hosted type are of the lowest quality, though some pieces can be of high quality.

References

- Garnier V., Ohnenstetter D., Giuliani G., Fallick A.E., Trinh P.T., Vinh H.Q., Long P.V., Schwarz D. (2005) Basalt petrology, zircon ages and sapphire genesis from Dak Nong, southern Vietnam. *Mineralogical Magazine*, Vol. 69 (1), 21-38.
- Garnier V., Giuliani G., Ohnenstetter D., Fallick A.E., Dubessy J., Baks D., Vinh H.Q., Lhomme T., Maluski H., Pêcher A., Bakhsh K.A., Long P.V., Trinh P.T., Schwarz D. (2008) Marble-hosted ruby deposits from Central and Southeast Asia: Towards a new genetic model. *Ore Geology Reviews*, Vol. 34, pp. 169–191.
- Kane R.E., McClure S.F., Kammerling R.C., Khoa N.D., Mora C., Repetto S., Khai N.D., Koivula J.I. (1991) Rubies and fancy sapphires from Vietnam. *G&G*, Vol. 27, No. 3, pp. 136–155.
- Khoi N.N. (2004) Study to establish characteristic attributes of the marble-hosted type of Vietnam ruby and sapphire deposits – the basis for modelling of this type of deposits. *Journal of Earth Sciences*, Vol. 26, pp. 333–342.
- Khoi N.N., Nhung N.T., Thuyet N.T.M. (2010a) Quality characteristics of rubies and sapphires from main deposit types of Vietnam. *Journal of Earth Sciences*, Vol. 32, No. 2, pp. 199–209.
- Khoi N.N., Sutthirat C., Tuan D.A., Nam N.V., Thuyet N.T.M., Nhung N.T. (2010b) Comparative study of rubies and fancy sapphires from two different deposit types in Yen Bai Province, Vietnam. *Proceedings of the 5th International Conference "Provenance and Properties of Gems and Geo – Materials,"* Hanoi, October 17–24, pp. 212–223.
- Levinson A.A., Cook F.A., (1994) Gem corundum in alkali basalt: origin and occurrence. *Gems&Gemology*, 30, 253-262.
- Long P.V., Vinh H.Q., Garnier V., Giuliani G., Ohnenstetter D., Lhomme T., Schwarz D., Fallick A., Dubessy J., Trinh P.T. (2004) Gem corundum deposits in Vietnam. *Journal of Gemmology*, Vol. 29, No. 3, pp. 129–147.
- Simandl G.J., Paradis S. (1999) Corundum in alumina-rich metasediments. In G. J. Simandl Z. D. Hora, and D. V. Lefebvre, Eds., *Selected British Columbia Mineral Deposit Profiles*, Vol. 3, Industrial Minerals. British Columbia Ministry of Energy and Mines, Open File 1999-10.
- Smith C.P., Kammerling R.C., Keller A.S., Peretti R.A., Scarrat K.V., Khoa N.D., Repetto S. (1995) Sapphires from Southern Vietnam. *Gems & Gemology*, 31, 168-186.

Acknowledgements

We are grateful to Teaching and Research Improvement Grants (TRIG) of Hanoi University of Science (Vietnam National University, Hanoi) for financial support to complete this presentation.

Basaltic corundum. A case for the promotion of increased cooperation between gemmological researchers and gemstone producers ?

Terry Coldham

Gemmological Association of Australia, Sydney Australia, terry@sapphex.com

Many articles have been published related to the occurrence of corundum associated with Cenozoic alkali basalt around the globe (e.g. Schwarz et al., 2008). In this presentation such corundum will be referred to as "basaltic corundum". Mostly these articles are quite scientific in their approach (e.g. Khin Zaw, 2006; Limtrakun, 2001) with a lesser number of articles published describing the mineralogical and gemmological characteristics of basaltic corundum. (e.g. Schwarz, 2000; Guo, 1992)

The more scientific publications detail quite complex research relating to, trace element chemistry, petrology, mineralogy and geological processes. They often tabulate the results of analytical work carried out on basaltic corundum and their associated minerals such as zircon (e.g. Garnier, 2005) and then compare results from various locations within the same field and/or those from around the globe (e.g. Sutherland, 2002a & 2002b). These results have been used by several authors to put forward various theories and suggestions as to the genesis of basaltic corundum. (e.g. Guo, 1995; Giuliani, 2006 & 2007)

Little has been published on the visual features of basaltic corundum and their associated minerals. This presentation details and compares the macro features such as colour, growth banding, crystal habit, twinning and inclusions of basaltic corundum and, more especially those of basaltic sapphire from a variety of localities around the world. It will be shown that the mineralogical features of basaltic sapphire, as well as their features as a gemstone are remarkably similar, so similar in fact that it is extremely difficult for even those familiar with the mining and processing of rough basaltic corundum to positively define where a particular piece of rough comes from. The visual similarities of basaltic sapphires found in such widely different geographical locations as China, France, South East Asia, Nigeria and Australia are quite remarkable. The authors of the more scientific gemmological papers are usually not involved in the extraction and processing of the gemstone rough and therefore often do not have the opportunity to make complete and detailed observations of the stone found at a particular locality, let alone compare them with similar material from other localities around the world. Whilst they may be able to do very detailed investigative work on particular rough and cut pieces, they are often restricted by a paucity and/or a limited range of samples typical of a particular deposit. To gain a real feeling for the characteristics of basaltic corundum deposits one really needs to have had the chance of observing large volumes of rough, some-thing that very few geologists, mineralogists or even gemmologists have the chance to do.

In this presentation the features of basaltic corundum, from a diverse range of geographical occurrences will be compared in the endeavor to provide additional clues as to the story of their genesis. Further, it is hoped that the presentation will be the catalyst for the future collection of detailed information on the observations made by miners, dealers, lapidaries and others who have firsthand experience in handling quantities of basaltic corundum, before it is lost or forgotten. This will allow the "linking" of valuable information of observed facts and characteristics from those involved "at ground level" with those involved in academic research. Information gained through further research into the genesis of basaltic corundum may well prove to be of greater significance to our understanding of the geological processes of the earth than that of them as a gemstone.

References

- Garnier V., Ohnenstetter D., Giuliani G., Fallick A.E., Phan Trong T., Hoàng Quang V., Pham Van L. and Schwarz D., 2005. Basalt petrology, zircon ages and sapphire genesis from Dak Nong, southern Vietnam, *Mineralogical Magazine*; February 2005; v. 69; no. 1; p. 21-38
- Giuliani G., Fallick A., Rakotondrazafy M., Ohnenstetter D., Andriamamonjy A., Ralantoarison T., Rakotosamizany S., Razanatsheho M., Offant Y. and Garnier V., et al. 2006, Oxygen isotope systematics of gem corundum deposits in Madagascar: relevance for their geological origin *Mineralium Deposita* Volume 42, Number 3, 251-270,
- Giuliani G., Fallick A., Ohnenstetter D. and Pegere G., 2007, Oxygen isotopes composition of sapphires from the French Massif Central: implications for the origin of gem corundum in basaltic fields *Mineralium Deposita* Volume 44, Number 2, 221-231
- Guo J., Wang F., Yakoumelos G., 1992, Sapphires from Changle In Shandong Province, China, *Gems & Gemology* Volume 28, Number 4 / Winter 1992 255-260
- Guo J., O'Reilly S.Y. and Griffin W.L., 1995 Corundum from basaltic terrains: a mineral inclusion approach to the enigma, *Contributions to Mineralogy and Petrology* Volume 122, Number 4, 368-386
- Khin Zaw, Sutherland F.L., Dellapasqua F., Ryan C.G., Tzen-Fu Yui, Mernagh T.P. and Duncan D., 2006, Contrasts in gem corundum characteristics, eastern Australian basaltic fields: trace elements, fluid/melt inclusions and oxygen isotopes, *Mineralogical Magazine*; December 2006; v. 70; no. 6; p. 669-687
- Limtrakun P., Khin Zaw, Ryan C.G. and Mernagh T.P., 2001. Formation of the Denchai gem sapphires, northern Thailand: evidence from mineral chemistry and fluid/melt inclusion characteristics, *Mineralogical Magazine*; December 2001; v. 65; no. 6; p. 725-735
- Schwarz D., Kanis J., Schmetzer K., 2000, Sapphires from Antsiranana Province, Northern Madagascar. *Gems & Gemology* Volume 36, Number 3 216-233
- Schwarz D., Giuliani G., Ohnenstetter D., Klemm L. and Pardieu V., 2008. Ruby and Sapphire Deposits Related to Basaltic Rocks: A Review/Update. *Proceedings of The 2nd. International Gem and Jewellery Conference*, 178-181
- Sutherland, F.L., Graham I.T., Pogson R.E., Schwarz D., Webb G.B., Coenraads R.R., Fanning C.M., Hollis J.D, Allen T.C., 2002a. The Tumbarumba Basaltic Gem Field, New South Wales: in relation to sapphire-ruby deposits of eastern Australia. *Records of the Australian Museum* 54 (2): 215-248.
- Sutherland F.L., Bosshart G., Fanning C.M., Hoskin P.W.O. and Coenraads R.R., 2002b Sapphire crystallization, age and origin, Ban Huai Sai, Laos: age based on zircon inclusions, *Journal of Asian Earth Sciences* Volume 20, Issue 7 Pages 841-849

Acknowledgements

Special thanks to, Dr. Lin Sutherland, Dr. Robert Coenraads and Richard Hughes for all their assistance..

Historical use of olivine – the origin of peridots in baroque-period jewellery

Jaroslav Hyrsl

Prague, Czech Republic, hyrsl@kuryr.cz

Gemmy olivine has been known from Zeberget Island in the Red Sea for at least 2000 years, but it was always rare. Surprisingly, a lot of large peridots can be seen in baroque jewellery dating from the second half of the 17th century and the first half of the 18th century. Their origin is not certain - they could be also from Kozakov hill in the Czech Republic or from some other source. Fortunately, Zeberget and Kozakov olivines differ significantly in their genesis. The former yielded well-formed crystals, formed from last-stage magmatic fluids after serpentinization of the surrounding peridotites. This type is known only from three localities - Zeberget Is. in Egypt, Mount Kyaukpon near Mogok in Myanmar, and Sapat in Pakistan. All three mentioned localities yielded many cut stones over 100 ct. The second type comes from rounded ultrabasic xenoliths in basalts, typically containing a mixture of olivine, clinopyroxene, orthopyroxene and chromite. Olivine of this genetic type is never crystallized and yields much smaller stones than the first type. It is known from Arizona, Hawaii, Norway, Czech Republic, Ethiopia, Tanzania, China etc.



Figure 1. Box for jewels, St. Vitus cathedral, Prague.



Figure 2. The largest peridot on the box for jewels.

Several baroque objects in European treasuries were studied by the author. The peridots are often very large, up to almost 3 cm across. They are very clean, with veils of small inclusion found in just a few. The most interesting inclusions were found in the Box for jewels from St. Vitus cathedral in Prague, which was made in Augsburg around 1670. It contains abundant tiny, sharp, transparent crystals. They are oriented in a few layers and form a group of crystallographically oriented „phantoms“ inside. Phantoms can be formed in crystals only during growth in several stages from hydrothermal or magmatic fluids, and therefore the origin from Zeberget Island is confirmed with a very high probability. If Zabargad source is correct, it means it was exploited intensively in the middle of 17th century and the stones were sold to central Europe. The mining was probably short-living, because after the middle of 18th century large peridots have been very rare again.

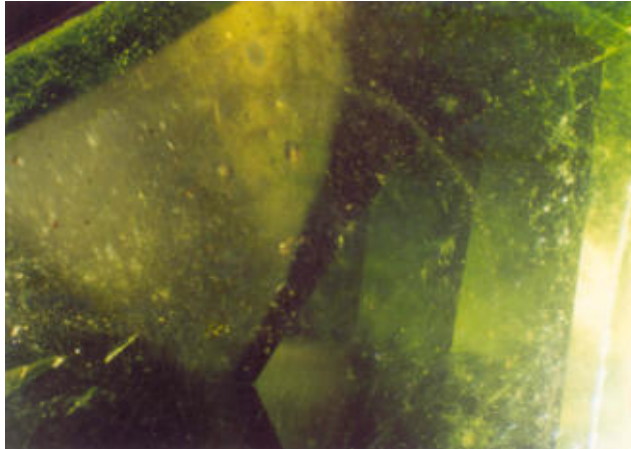


Figure 3. Phantoms in peridot on the box of jewels.

Table 1. Some examples of objects with peridot (both identified and supposed)

- Basel - Dorothy monstrance, Basel, ca. 1440 (verified by H.Hänni et al.)
- Dresden - Drachenkante (rock-crystal cup), Augsburg (?), 17th century
 - Table clock with St.Hubertus, J.H.Köhler, Dresden, after 1720
 - Apis altar, Dresden, probably 1724 - 1738
- Istanbul - Festival throne, Ottoman, middle 18th c. (contains 954 large peridots according to a catalogue)
- Köln - Monstrance, Ch.Schweling, Köln, 1657
- Limburg - Monstrance, Ch.Schweling, Köln, 1667
 - Procession cross, J.D.Treudel, Frankfurt, 1673
- Marienstern - Reliquary of St.Eustachius, Prague, 1st third of 14th c. (verified by J.Hyrsli)
- Milan - Altar of Volvinio in St.Ambrosio, Milan, 824 - 859 (verified by M.Superchi)
- Prague - Box for jewellery, Augsburg, around 1670 (verified by J.Hyrsli)
 - Cross, 18th c. (verified by J.Hyrsli)
- Trier - Ring of Archbishop Arnold II, Trier, 1242 - 1259
- Wien - Monstrance of the Star Cross Order, Augsburg, ca.1668 (verified by J.Hyrsli)
 - Column of the Virgen Mary, Augsburg, 1670 - 1680
 - Reliquary of Christ's crib, Prague, after 1368 (verified by J.Hyrsli)
 - Gemstone flower, Wien, ca. 1760 (verified by W.Mican)

Pallasitic peridot : The gemstone from outer space

**Thanong Leelawathanasuk¹ , Wilawan Atichat¹, Chakkaphan Suthirat^{1,2}, Pornsawat Wathanakul^{1,3},
Boontawee Sriprasert^{1,4}, Nalin Narueedeesombat¹, Pimpicha Srithunayothin¹ and Scott Davies⁵**

¹ Gem and Jewelry Institute of Thailand (GIT), Faculty of Science, Chulalongkorn University, Bangkok10330, Thailand; Email: lthanong@git.or.th

² Department of Geology, Faculty of Science, Chulalongkorn University, Bangkok10330, Thailand

³ Department of Earth Sciences, Faculty of Science, Kasetsart University, Bangkok 10900, Thailand

⁴ Department of Mineral Resources, Rama 6 Rd., Bangkok10400, Thailand

⁵ American-Thai Trading Company, Bangkok, Thailand

“Pallasite” is a meteorite group which is named after the German naturalist Peter Simon Pallas. The term «pallasite» is to describe a class of stony iron meteorites that contains silicate mineral inclusions in a nickel-iron matrix. Commonly, the silicates are olivine (peridot) inclusions. The abundance of peridot in this meteorite makes pallasite one of the most attractive meteorites for meteorologists, geologists and meteorite collectors. Relatively rare, there have been approximately 60 finds of pallasite meteorite, representing less than 1% of all known meteorites. Based on trace element and oxygen isotope analysis, the majority of pallasites have been categorized in a ‘main group’ (MG). It is generally accepted that all MG pallasites originated in the asteroid belt between Mars and Jupiter, either from the core-mantle boundary of a single parent body, or as the result of a collision event between two parent bodies. The minority of pallasites are classified as Eagle Station group (ES): Olivine is rich in iron and the metal matrix is rich in nickel and Pyroxene group (PX) which takes its name from the high orthopyroxene content.

Pallasites and pallasitic peridots have also been used in jewellery which makes them the only genuine gemstones from outer space on Earth. The pallasites are regarded as representatives of core/mantle boundary materials that are closely related to the iron meteorites. This study aims at finding out the characteristic of these extraordinary gemstones and revealing how to distinguish this gem peridot from its terrestrial counterpart.

In this study, twelve pallasitic peridot samples claimed to originate from four different localities (five from Fukang area, Xinjiang Province in China, one from Brahin area, Gomel region in Belarus, three from Esquel area, Chubut in Argentina and three from Brenham area, Kansas State in the United States). All samples were provided by co-author SD, a geologist and gem dealer (see Fig. 1).

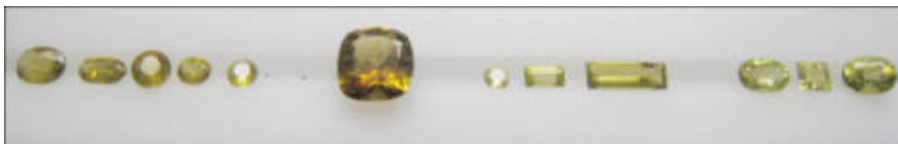


Figure 1: Twelve pallasitic peridot samples used in this study originating (from left to right) from Fukang, Brahin, Esquel and Brenham.

Table1: Summary of gemmological properties of 12 pallasitic peridots.

Sample no.	Wt.	RI	SG	LW/SW
Fukang05	0.21ct	1.660-1.690	3.37	Inert/inert
Fukang04	0.14ct	1.660-1.690	3.37	Inert/inert
Fukang01	0.12ct	1.665-1.692	3.36	Inert/inert
Fukang02	0.10ct	1.668-1.695	3.38	Inert/inert
Fukang03	0.06ct	1.660-1.692	3.40	Inert/inert
Brahin01	0.79ct	1.672-1.688	3.39	Inert/inert
Esquel01	0.03ct	1.670-1.685	3.38	Inert/inert
Esquel02	0.06ct	1.670-1.685	3.41	Inert/inert
Esquel03	0.19ct	1.665-1.690	3.37	Inert/inert
Brenham02	0.16ct	1.670-1.685	3.38	Inert/inert
Brenham03	0.09ct	1.665-1.685	3.36	Inert/inert
Brenham01	0.22ct	1.670-1.688	3.40	Inert/inert

Microscopic examination reveals prominent needle-like inclusions oriented in two directions in peridot from Fukang and Brenham and brown platelet inclusions in peridot from Brahin.(see Fig. 2)



Figure 2: Needle-like and brown platelet inclusions in pallasitic peridots

Semi-quantitative EDXRF analyses revealed that chemical compositions of pallasitic peridot samples from different localities are very close to each other and cannot be used for distinguishing one from the others. They roughly contain 40.70-38.49 wt% MgO, 43.24-44.74 wt% SiO₂ and 15.24-16.75 wt% Fe₂O₃ with trace amounts of chromium (0.05–0.12 wt% Cr₂O₃), manganese (0.32–0.42 wt% MnO) and nickel (0.02-0.09 wt% NiO₂).

The UV-Vis absorption spectra typically show iron absorption peaks at around 400, 450, 470 and 495 nm and an increasing background toward the UV region (see Fig. 3). The Mid-IR spectrum shows H₂O absorption bands at 1500-2000 cm⁻¹ (see Fig. 4).

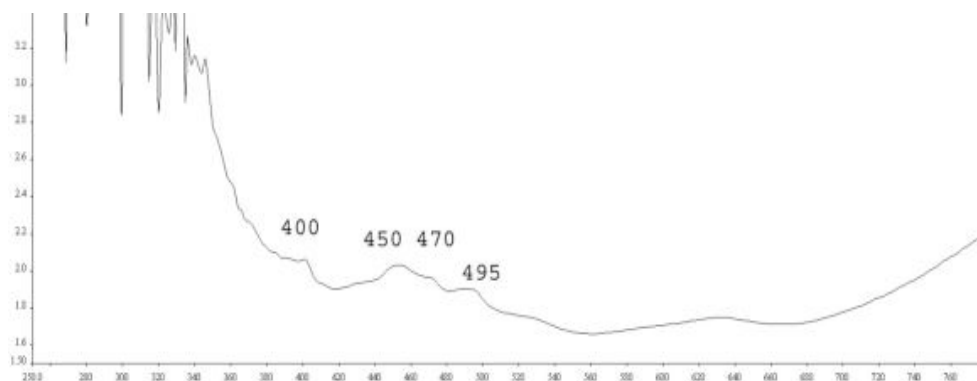


Figure 3. Representative unpolarized UV-Vis absorption spectrum of a pallasitic peridot.

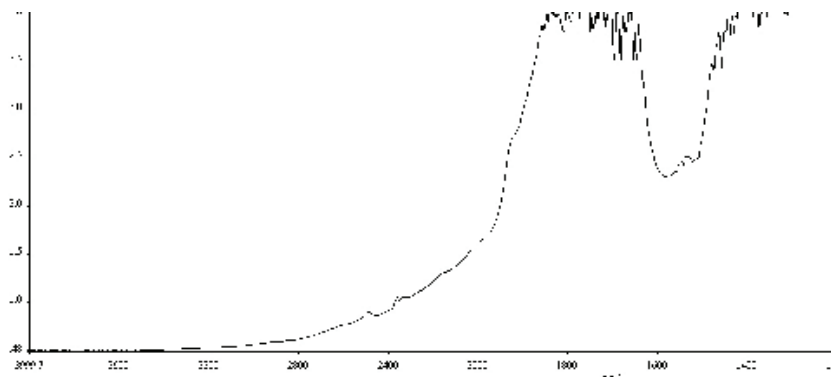


Figure 4. Representative Mid-IR spectrum of a pallasitic peridot.

In an attempt to separate pallasitic peridot from its terrestrial counterparts, we compared the above results with the data obtained for ten terrestrial peridot samples of undisclosed origins from the GIT reference collection. We discovered that the basic gemmological properties such as RI, SG and fluorescence were not sufficient to differentiate these extra-terrestrial gem-stones from their terrestrial counterparts. The UV-Vis and Mid-IR spectra are also very similar to one another. However, some trace element data seem to show differences for these two peridot origins. For example, nickel contents of pallasitic peridots are significantly lower than those of the terrestrial peridots and they are also slightly different in Ni vs Mn + Cr ratio. Therefore, the correlation diagram of Ni_2O_3 versus $\text{Ni}_2\text{O}_3/\text{Cr}_2\text{O}_3+\text{MnO}$ shows clearly the separation of these two groups of peridot (see Fig. 5).

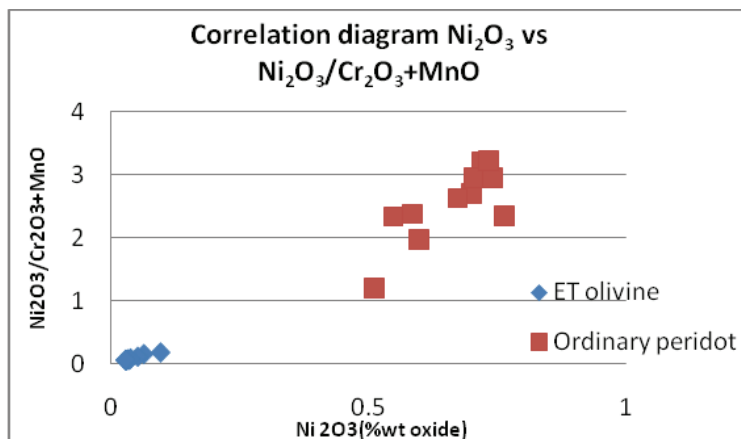


Figure 5. The correlation diagram between Ni_2O_3 versus $\text{Ni}_2\text{O}_3/\text{Cr}_2\text{O}_3+\text{MnO}$ shows clearly the separation of extra-terrestrial peridots (ET olivine) from terrestrial peridots.

In summary, pallasitic peridot samples from different localities seem to have very similar characteristics. Also the pallasitic peridots possess basic gemmological properties that are very similar to those of the terrestrial counterparts. It seems, therefore, almost impossible to distinguish these two types of material based on gemmological determinations. However, inclusion features such as needles and brown platelets seem to be typical for these extra-terrestrial gem materials which are consistent with the inclusions of pallasitic peridots reported earlier (Sinkankas et al., 1992). Nonetheless, we also found that many of them are inclusion free. Advanced spectroscopic techniques such as UV-Vis and FTIR also revealed very similar characteristics of these two types of olivines.

As inclusions are not present in all pallasitic peridot, this feature alone cannot be used to differentiate pallasitic gems from their terrestrial counterparts. Based on this study, the trace element data seem to be the only positive clue to differentiate these two types of gem material, i.e., Ni_2O_3 versus $\text{Ni}_2\text{O}_3/\text{Cr}_2\text{O}_3+\text{MnO}$ plot. This difference can be explained by the fact that the pallasitic peridot is extra-terrestrial material which may have its chemical composition similar to those found in the core/mantle zone while ordinary gem peridot originated from the earth's mantle/crust zone which are totally different in the geological environment that may reflect the difference of certain trace element contents.

Acknowledgements

Technical support by G. Bosshart was much appreciated.

References

Deer W.A., Howie R.A., Zussman J. (1995) : An Introduction to the Rock-forming Minerals. Longman, England, 2nd ed., 3-13. ISBN 0-582-30094-0.

Sinkankas, J., Koivula, J. and Becker, G. 1992. Peridot as an Interplanetary Gemstone. *Gems and Gemology*, vol.28, no.1, p. 43-51

Key words: Pallasite, Peridot, Chemical composition, UV-Vis spectrum, MIR spectrum

Italian gemstones: peridot from Sardinia, demantoid garnet from Val Malenco, omphacite “jade” from the Po Valley, Piedmont, amber from Sicily

Loredana Prosperi¹, Iaria Adamo², Rosangela Bocchio², Valeria Diella³, Alessandro Pavese²

¹Instituto Gemmologico Italiano, Milano, Italy, l.prosperi@igi.it

² Earth Sciences Department, University of Milan

³ Institute for the Study of the Dynamics of Environmental Processes,
National Research Council (CNR), Milan

Peridot from Sardinia

The gem variety of olivine is today known by gemmologists as peridot. Compositionally, it belongs to the solid-solution series between forsterite [Fo: Mg₂(SiO₄)] and fayalite [Fa: Fe₂(SiO₄)], but most material falls within the range of 80-90% forsterite. Peridot has been reported from a number of sources worldwide. Some deposits of gem-quality olivine are found in Italy. One of the most important sources is located near Pozzomaggiore, Sassari Province, in the north-west of Sardinia where olivine occurs in mantle xenoliths included in the Pliocene-Quaternary alkali basalts. These nodules have dimensions varying from 1 to 25 cm and contain a typical four-phase assemblage of olivine, ortho- and clinopyroxene and spinel. 10 faceted gems from 0.14 to 2.53 ct and 2 rough samples of about 0.5-1 cm have been analysed. The samples have been characterized by standard gemmological testing, combined with advanced analytical techniques (X-ray powder diffraction, mid-IR and UV-Vis-NIR spectroscopy, EMPA-WDS and LA-ICP-MS measurements) in order to determine their optical, physical and chemical properties.

The gemmological properties of peridot from Sardinia are :

Colour Yellowish green

Transparency Transparent

Refractive indices n_α 1.650 - 1.652

n_γ 1.688 - 1.690

Birefringence 0.038-0.039

Specific gravity 3.32-3.36

UV fluorescence Short and Long wave: inert

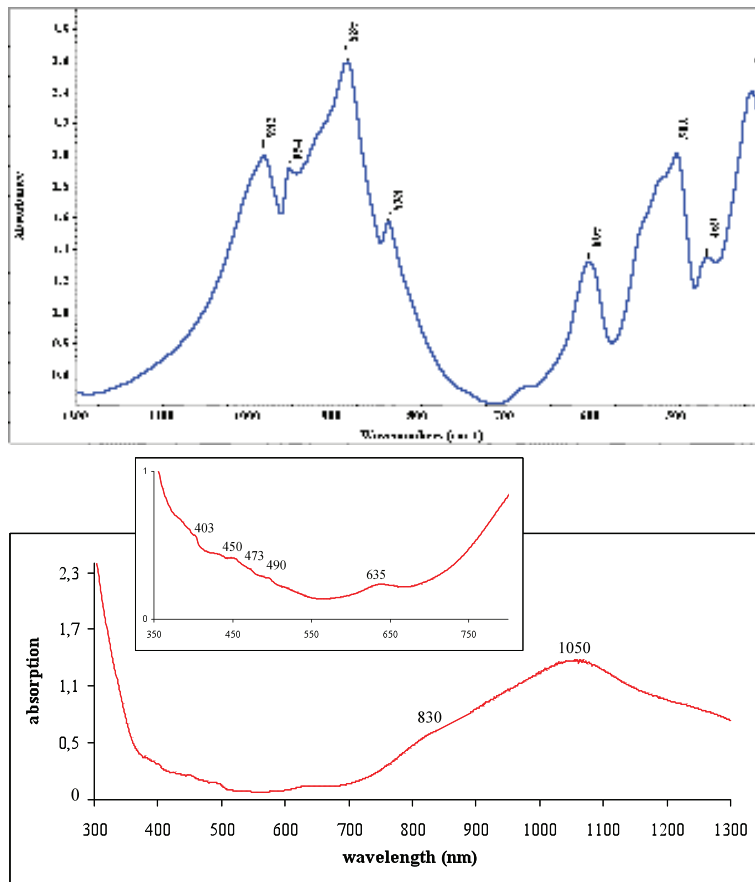
Microscopic features The most common inclusions are partially-healed fissures. Some samples also contain roughly circular to oval-shaped decrepitation “halo” fissures, also known as “lily pad” inclusions. Rarely, minute dark crystals, probably chromite spinel, fluid inclusions, growth planes and traces of polysynthetic twinning are observable.

Chemical analyses of two samples indicate a composition of Fo91Fa9, typical of most peridot. MnO is low (0.11-0.15 wt.%) whereas the content of NiO is slightly higher (0.38-0.39 wt.%) and close to the rather constant value of 0.40 wt.% reported in literature for mantle olivine at Fo≈90.

The KBr pellets mid-infrared spectrum of the material on study exhibits several absorption bands, located at about 982, 954, 885, 838, 605, 503, 469, and 415 cm⁻¹.

Their positions, well known to be related to composition, agree with the iron content of our samples.

The UV-Vis-NIR pattern of peridot from Sardinia is characterised by a broad band at 1050 nm, with a shoulder at about 830 nm, in the near-infrared range, and by an increasing absorption toward the ultraviolet region. Weak bands at 403, 450, 473, 490, and 635 nm are also present. All these spectral features, previously observed in peridot from other occurrences, are due to the Fe²⁺ ion, confirming that iron is mainly responsible for the coloration.



Demantoid garnet from Val Malenco

Val Malenco, one of the classic Italian mineral districts, has been known to mineralogists and collectors the world over for almost one century. Its reputation is due mainly to the superb crystals of demantoid garnet, an andradite variety. They add beauty and interest to many collections.

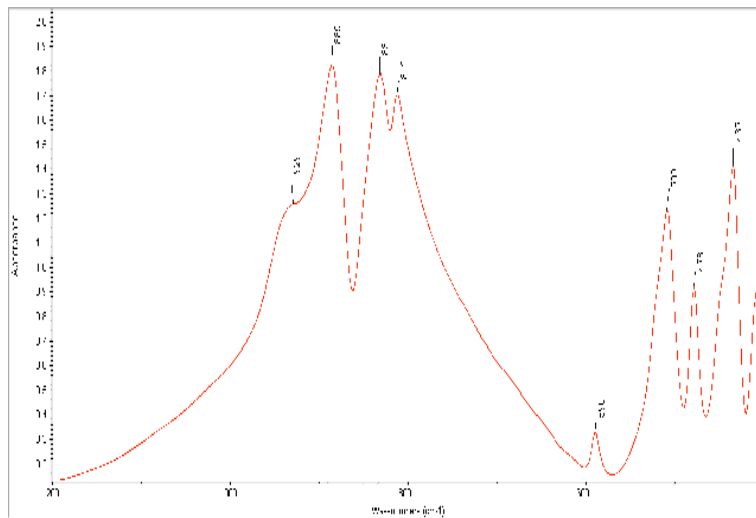
Val Malenco (130 km north of Milan, in the Province of Sondrio) is a valley which cuts deeply into the southern slope of the Bernina Massif, the highest of the Rhaetian Alps.

The main rock formations in the central area of Val Malenco are serpentinites and serpentine schists (antigorite schists), which often include minor formations of talc schists and chlorite schists. Demantoid is found sometimes as beautiful crystals in the asbestos-filled lithoclasts of the serpentinite outcrops (in the central part of Val Malenco). 12 faceted gems from 0.25 to 3.14 ct and 4 rough samples have been analysed.

The gemmological properties of demantoid from Val Malenco are :

Colour	Brownish and yellowish green to green, medium to dark
Transparency	Transparent
Refractive index*	greater than 1.79
Optic character	Singly refractive with moderate to strong anomalous double refraction
Specific gravity	3.79-3.88
UV fluorescence	Short and Long wave: inert
Microscopic features	Horse-tail inclusions, mineral inclusions, fractures, some healed fissures, straight growth lines (zoning)

The KBr pellet mid-infrared spectrum of the material on study exhibits several absorption bands, located at about 929, 885, 831, 812, 590, 509, 478 and 435 cm^{-1} .



Omphacite “jade” from the Po Valley, Piedmont

A dark-green jade has been discovered by mineralogists Franco Manavella and Franco Salusso in secondary alluvial deposits in the Po Valley (Piedmont, northern Italy).

The interest for the dark-green jade in question is also stimulated by paleo-ethnological implications, due to this material having been mined, used and traded in prehistoric times by the local population to manufacture a variety of articles like stone blades for axes.

The alluvial pebbles are suitable to be cut as small cabochons, but owing to their dark green colour, the cabochons are being cut with a hollow base to improve transparency.

10 faceted have been analysed.

The gemmological properties of Po Valley “jade” are :

Colour	dark green
Transparency	Translucent
Refractive index	1.67-1.68
Specific gravity	3.35-3.36
UV fluorescence	Short and Long wave: inert
Microscopy features	microcrystalline texture, black and green veins and spots, fractures, and embedded prismatic, transparent, colourless crystals.

The results of gemmological testing of the jade-like material from the Po Valley suggest an omphacite-like composition. The results of chemical analyses too indicate an omphacitic composition.

The chromium content occurring in the omphacite “jade” is responsible for the dark-green precious colour as supported by optical spectroscopy. The IR transmission pattern is featured by a broad band at about 3430 cm^{-1} , due to OH incorporated in the pyroxene structure.

The non-polarized spectrum over the visible energy range (350-800 nm range) of omphacite “jade” from the Po valley confirms that the dark-green hue is due primarily to Cr^{3+} .

Amber from Sicily

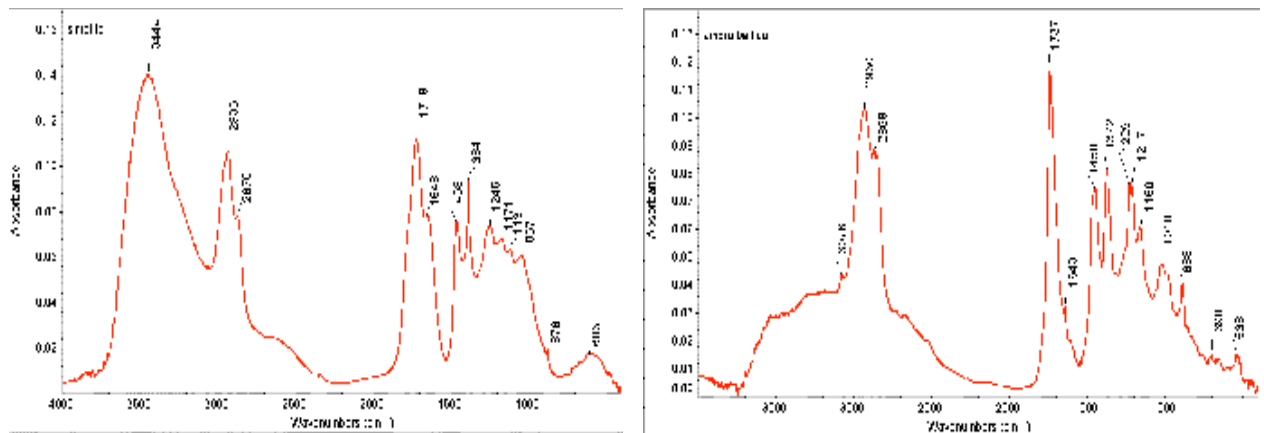
Amber is a hard fossilized plant resins which derived from the protective exudates of several species of ancient conifers and flowering trees.

Significant commercial deposits of amber occur in Europe around the Baltic sea, in the Dominican Republic and in Mexico. In Europe amber occurs also in Romania (called rumanite and in Sicily called Simeite. The age of Sicilian Amber: Simeite dates from around 25 – 35 millions years. The name derived from Simeto river, in fact primary amber deposits should be localized in the area where the Simeto, Salso and Dittaino rivers originate. Actually the most remarkable specimens of simeite were found chiefly on beaches near Catania but also near Porto Empedocle.

Gemmological features of Sicilian amber are :

Colour	Brownish orange, yellowish orange, brown, brownish red
Transparency	Transparent to opaque
Refractive index	1.54 (distant vision)
Fracture:	conchoidal
Optic character	Amorphous
Specific gravity	1.05-1.10
UV fluorescence	bluish white- yellow green
Melting point	300-380° C
Microscopic features	insect (flies, midges, ants, spiders, butterflies),, organic inclusions (leaves), crystals (calcium sulphates, rare quartz, salt), bubble

A way to recognize this amber is through FTIR spectroscopy, It show a particular spectrum, different for example from Baltic amber. Baltic amber shows a characteristic shoulder followed by a peak at 1150 cm⁻¹. Simeite has two peak more before 1250 e 1110 cm⁻¹ and not before 800 cm⁻¹ band.



The price of this amber is high: more or less 250 euros / gram.

References

- Adamo I., Bocchio R., Diella V., Pavese A., Vignola P., Prosperi L., Palanza V. (2009) "Demantoid From Val Malenco, Italy; Review and update G&G, Vol45, No, pp 280-287.
- Bianchi Potenza B., De Michele V., Liborio G., Nana G.P. (1989) Olivine from Val Malenco (Sondrio), Italy: a material of gemmological interest. *La Gemmologia*, Vol. XIV, No. 3-4, pp. 23-33.
- Bianchi Potenza B., De Michele V., Liborio G., Rizzo R. (1991) Olivines from Sardinia (Italy): a material of gemmological interest. *La Gemmologia*, Vol. XVI, pp. 17-28.

Preliminary Studies to Distinguish Omphacite from Jadeite

**Panjawan Thanasuthipitak¹, Tay Thye Sun², Wilawan Atichat³, Henry A. Hänni⁴,
and Theerapongs Thanasuthipitak¹**

¹ Dept Geol Sci, Chiang Mai University, Chiangmai, Thailand;

² Far East Gem Lab, 360, Orchard Road #09-04, International Building, Singapore 238869;

³ GIT, Gemmological Research and Testing Building, Faculty of Science,
Chulalongkorn University, Phayathai Road, Bangkok 10330, Thailand;

⁴GemExpert GmbH, Postfach 921, CH4001, Basel, Switzerland.

Introduction

Since 1990, there is a boom in the jadeite-jade business due to the prosperity of the Mainland Chinese and their purchasing power. Nearly all jadeite-jade sold in the trade are from Myanmar and some from Russia. For this research, samples were purchased from Yangon, Myanmar and Hong Kong (Fig. 1).

In 2004, the word Fei Cui was officially declared to mean jadeite-jade by the Chinese in China and Hong Kong. In order to strengthen the confidence of consumers, the Gemmological Association of Hong Kong together with the Hong Kong Accreditation Service (GAHK, 2006) decided to set up a standard for jadeite nomenclature and testing methods. This is in line with many other gemstone nomenclatures like those for diamonds or pearls which already are established as international guidelines.

As there is great interest in jadeite, other look-alike jadeite material has appeared in the jewellery trade e.g. omphacite (black inky jade) (OuYang et al., 2003, Okano et al., 2009), icy jade (pure colourless jade) (OuYang, 1999; Hänni, 2007; Shi et al, 2009), black jadeite (jadeite coloured by hydrocarbon) (OuYang, 1999), Hte Long Sein (dark green opaque jadeite) (OuYang et al, 2001) and of course Maw Sit Sit or Kosmochlor (Chhibber 1934; Gübelin 1965; Harlow et al 1987; OuYang 1984; Mevel et al 1986; Win Htein and Aye Myo Naing, 1994; Hänni et al 1997). Therefore, there is a need to fortify what is considered as jadeite or omphacite for that matter.



Figure 1. Selection of jadeite samples (left) showing the range of colours from brown to green, greyish-green and colourless, whereas omphacite (right) is showing dark green to black.

Objective, material and method

Jadeite jade and kosmochlor have been studied in detail by various authors (Damour, 1863; Chhibber 1934; Gubelin 1965; OuYang 1984; Mevel et al 1986; Win Htein and Aye Myo Naing, 1994; Hänni et al, 1997). In this study, the focus is on jadeite and omphacite. A total of 84 rough jade samples bought from Myanmar and Hong Kong were studied using basic gemmological methods such as visual observation, R.I., S.G., microscopic method, and also petrographic study through thin sections together with XRD, UV-vis-NIR and FTIR spectrophotometry methods. Results: Our basic gemmological finding could identify jadeite-jade and kosmochlor. The R.I. of omphacite (1.66 – 1.72) distinguishes it from jadeite, while visual observation, microscopic method and S.G. seem to yield rather inconclusive results, most likely due to the association of both pyroxene (jadeite, omphacite and diopside) and other minerals such as amphibole, pumpellyite and piemontite. Using the FTIR-DRIFT method, it was possible to identify jadeite-jade. Bulk XRD allows to distinguish the different pyroxene minerals from others. Petrographic study of thin sections is destructive and not suitable for distinguishing between the different pyroxene minerals because most of the stones encountered in the trade, like our samples, are of fine-grained texture.

Discussion: Ideally, the composition of jadeite should not depart greatly from $\text{NaAlSi}_2\text{O}_6$. In most natural jadeite at least 80% of the pyroxene M1 site is occupied by Al, and at least 80% of the M2 site is taken by Na (Deer et al., 1992). Omphacite, on the other hand, is chemically much more complex. It is essentially a solid solution of jadeite and diopside with some amount of aegirine. Theoretically, omphacite should have a composition of $\text{Na}_{0.5}\text{Ca}_{0.5}\text{Al}_{0.5}(\text{Mg,Fe})_{0.5}\text{Si}_2\text{O}_6$, or mineralogically 50% jadeite and 50% augite ($\text{Jd}_{50}\text{Di}_{50}$), but actual compositions range at least from $\text{Jd}_{40}\text{Di}_{60}$ to $\text{Jd}_{55}\text{Di}_{45}$.

The composition ranges (Fig. 2) of the (Ca-Mg-Fe) diopsidic pyroxene, Na-Al pyroxene (jadeite), and Na-Fe³⁺ pyroxene (aegirine), show that omphacite lies between the boundary plane $0.2 \leq \text{Na}/(\text{Na}+\text{Ca}) \leq 0.8$, and $\text{Al}/(\text{Al}+\text{Fe}) \geq 0.5$, while jadeite lies between $\text{Na}/(\text{Na}+\text{Ca}) \geq 0.8$ and $\text{Al}/(\text{Al}+\text{Fe}) \geq 0.5$. If we are to adopt this mineralogical classification strictly, any jade sample containing less than 80% Al as compared to Mg+Fe²⁺, less than 50% Al as compared to Fe³⁺, and less than 80% Na as compared to Ca, should not be called jadeite.

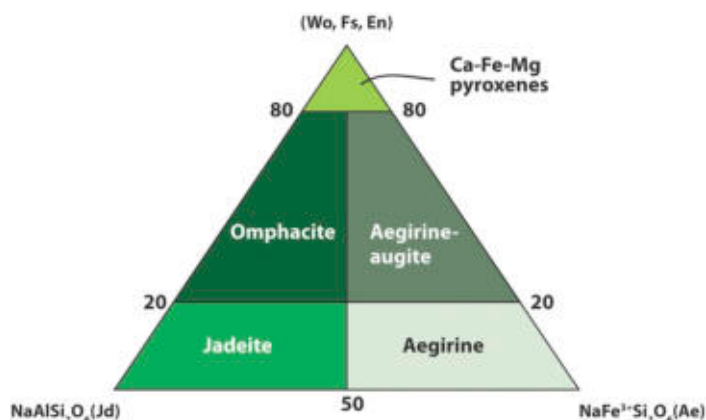


Figure 2. End member component of omphacitic pyroxene (after Clark and Papike, 1968).

Apart from the chemical, hence mineralogical, differences between omphacite and jadeite, there are also differences in symmetry of the crystals of the two minerals. Although both minerals are clinopyroxenes crystallized in a monoclinic system, jadeite has only one space group: C2/c, while omphacite has three polymorphs with symmetry: C2/c, P2/n and P2 (Gaines et al., 1997) due to the differences in temperature of their formation. This is enough reason to separate omphacite from jadeite, or from the term 'jade' as generally perceived by the public.

Conclusion

The preliminary conclusion is: in order to distinguish jadeite from omphacite one could use visual observation: omphacite is dark to very dark green to opaque whereas jadeite can be colourless to pale or bright green; RI: omphacite is 1.68 to 1.72 whereas jadeite is 1.65 to 1.67; SG: omphacite is 3.35 to 3.40 whereas jadeite is 3.33 to 3.36; and EDAX: jadeite should contain more than 80% Na compared to Ca, and more than 80% or 50% Al compared to Mg+Fe²⁺ or to Fe³⁺ respectively. Any chemical compositions departing from this should not be called jadeite.

References

- Standard Methods of Testing Fei Cui (Jadeite Jade) for Hong Kong, issued by The Gemmological Association of Hong Kong Limited 2006.
- Chhibber, 1934, *The Mineral Resources of Burma*, Macmillan, London, p 320.
- Clark and Papike, 1968, Crystal-chemical characterization of omphacites. *Am. Min.* 53, 840-867.
- Damour, 1863, Notice et analyse sur le jade vert: réunion de cette matière minérale à la famille des wernerites. *Comptes Rendus des Séances de l'Académie des Sciences*, Vol.56, pp. 861-865.
- Deer, Howie, and Zussman, 1992, *An Introduction to the rock-forming minerals*. ELBS with Longman, 696 pp.
- Gaines, Skinner, Foord, Mason, and Rosenzweig, 1997, *Dana's new mineralogy*, 8th ed., John Wiley & Sons, 1819 pp.
- Gübelin, 1965, Maw-sit-sit – A new decorative gemstone from Burma, *Journal of Gemmology*, 9, No.10, pp 329-344.
- Harlow and Olds 1987, Observation on terrestrial ureyite and ureyitic pyroxene. *American Mineralogist*, 72, pp 126-136.
- Hänni and Meyer, 1997, Maw-sit-sit (kosmochlore jade): A metamorphic rock with a complex composition from Myanmar (Burma). *Proceedings of the 26th International Gemmological Conference*, Idar-Oberstein, Germany, pp 22-24.
- Hänni, 2007, A European Gemmologist's Thoughts on Jadeite jade. *The Journal of the Gemmological Association of Hong Kong*, Vol.XXVIII, pp. 25-29.
- Okano, Kitawaki, Abduriyim, and Kawano, 2009, Natural omphacite. GAAJ- ZENHOKYO Lab Report, 6 pp.
- Ou Yang, Li, Li, and Kwok, 2003, Recent studies on inky black omphacite jade, a new variety of pyroxene jade. *J. Gemm.* 28(6), pp. 337-344.
- Ou Yang, 1999, How to make an appraisal of jadeite, *The Australian Gemmologist*, Vol.20, No.5, January-March, pp 188-192.
- OuYang, 1984, A terrestrial source of ureyite, *American Mineralogist*, 69, pp. 1180-1183.
- OuYang, and Li, 1999, Review of recent studies on black jadeite jade, *The Journal of Gemmology*, Vol.26, No.7, pp. 417-424.
- OuYang, and Qi, 2001, Hte Long Sein – a new variety of chrome jadeite jade, *The Journal of Gemmology*, Vol.27, No.6, pp. 321-327.
- Shi, Xia, Chu, and Cui, 2009, Jadeite jade from Myanmar: its texture and gemmological implications, *The Journal of Gemmology*, Vol.31, Nos.5-8. pp. 185-195.

Recent coloured gemstone production & market trends

E. Boehm, Geologist, G.G., C.G.

Chattanooga, TN Edward@RareSource.com

Overall coloured gemstone production from classic gemstone sources has decreased over the past five years while gemstones simultaneously increased in popularity in many traditional and emerging markets. This has created a complex supply and demand situation that has forced miners and jewellery designers alike to seek alternative sources for their gems. Several factors have attributed to these trends. Decreasing production is largely due to increasing costs of production stemming from higher fuel prices and lower availability of water needed to process gem bearing soils. Socio-political, fair trade, and environmental regulation initiatives have also contributed to lower colored gemstone production from traditional sources. Another is the “gold factor” as record demand and prices have revived gold mining from traditional sources as well as areas that were previously uneconomical to exploit.

Over the past decade, designers and manufacturers have gradually been shifting their focus from diamonds to colored gems, often featuring color as the center pieces in their creations. In recent years, the worldwide economic crisis forced many wholesalers and retailers to move even faster into the colored stone arena. They are experimenting with all types of fine quality, commercial, and ornamental gem materials as they seek to reduce overall production costs and improve profit margins. Miners have responded with a plethora of new ornamental gem materials as well as new sources for the traditional big three to make up for reduced production from the classic sources. However, increased demand over the past two years from Brazil, Russia, India, and China, otherwise referred to as the BRIC countries, has resulted in more diminished supply despite the global economic crisis.



The author in front of the Banque Suisse Mine at Ilakaka, Madagascar.

Source countries have experienced wild fluctuations in supply and demand over the past five years. Burma has suffered from decreasing ruby production in Mogok and Mong Hsu while Madagascar, Tanzania, and Mozambique have enjoyed consistent increases in ruby production and demand. Glass filled corundum from Madagascar entered the market before the economic crisis with little initial acceptance from western markets, however, the need for lower priced material in recent years, has driven many retailers to this questionable product, which in turn will likely further diminish consumer confidence in our industry. Spinel from Vietnam, Tajikistan, and Tanzania has enjoyed strong demand due to the high quality of available material and popularity amongst designers seeking an untreated alternative to ruby and sapphire. Sapphires from Sri Lanka, Madagascar, and Burma experienced significant price resistance during the crisis, but recent demand from India and China, record auction prices for

fine Kashmir sapphires, as well as the publicity surrounding the recent Royal Wedding, have driven prices for all blue sapphires to new highs. Sapphires of all colors have benefited as many designers are again choosing to incorporate spectral colored sapphires in their designs. Pink sapphire prices fell after large quantities were discovered in Madagascar in the early 2000's, but since their popularity continues to grow, despite significant production decreases in recent years, pink sapphire prices from all localities have increased steadily in the past two years. Emeralds are enjoying renewed demand as more source dealers have begun to embrace treatment disclosure practices. Colombian emerald production has decreased in the classic mines of Muzo and Cosquez but increased in the newer mines around La Pita and small amounts of fine material also continues to be found in Peñas Blancas near the village of Borbur. Brazil and Zambia still report strong production from their respective sources. The Belmont mine in Brazil has developed one of the most advanced sustainable mining and ethical trading initiatives in the industry today. Also, large scale mining conglomerate, Gemfields, has entered into a partnership with the Democratic Republic of Zambia implementing strategic Fair & Ethical trade initiatives. Though they sell only rough through auctions to a select group of sight holders, Gemfields plans to invest significant resources into advertising promoting Fair Trade faceted Zambian emeralds in jewellery.



*20.66 ct
Untreated blue
Sapphire from Sri
Lanka*

*Spinel octagon
& Spinel rough
from Tanzania*

The theme of ICA's recent Congress in Brazil was "Ethical Mining & Fair Trade", which brought many leaders of the colored gemstone community together to discuss issues related to this important and increasingly relevant topic. Many ideas and initiatives were presented by the Government of Brazil, numerous industry leaders, and gemmological laboratory representatives. It seems quite clear that colored gemstones and jewelry will soon have similar Fair & Ethical Trade / Sustainability initiatives in place as is seen in the diamond, coffee and banana industries. Young consumers are particularly concerned with the impact that gemstone production has on human and environmental sustainability, as well as socio-political concerns. This new and important consumer will help drive the industry toward stronger initiatives while also providing an outlet for less common colored gems from smaller artisanal operations. As a result, ornamental gemstones have also gained market share in the last five years as suppliers and designers seek to introduce lower cost but equally enchanting and sustainable gems geared toward the rapidly growing younger and product-conscious consumer market.

References

- Focus On Brazil (2010): InColor, Fall/Winter, pp. 1-43.
 Gemfields Co. UK (2011): Emerald Buyers Guide. pp. 1-14.
 Jewelry News Asia (2011) April: Hong Kong & China Jewelry Retail Sales See Strong Growth, p. 17, p. 22. pp. 37-38.
 Michelou J.C. (2010): Nigeria's Artisanal Miners Moving Forward. InColor, Fall/Winter, p. 64.
 Ribeiro M., Director of The Belmont Group (2011): Sustainable Mining Investments – Challenges & Opportunities. ICA Congress Brazil.
 Rongsiyuan Z., Liuyanhong R., Liuruimei L., & China Gold News (2009): White Book about Chinese Color Stone Market. pp. 1-49.
 Shor R.& Weldon R. (2010): An Era of Sweeping Change in Diamond and Colored Stone Production and Markets. Gems & Gemology, Vol. 46, No. 3, pp. 166-187.

Rare Gemstones from Mont Saint-Hilaire, Québec, Canada

Willow Wight

Canadian Museum of Nature, Ottawa, Canada wwight@mus-nature.ca

Introduction

Mont Saint-Hilaire, Quebec, about 40 km east of Montreal, has become a world-class mineral locality, beginning in the mid-nineteen sixties. The small, alkaline complex intruded the Paleozoic rocks of the St. Lawrence Lowlands during the Cretaceous period. The roughly circular pluton rises abruptly some 350 m above the surrounding flat lowlands. The number of minerals found there now stands at over 400. It is the type locality for 58 minerals, and new minerals are still being described. These numbers are remarkable considering the relatively small size of the quarried area (<0.5 km²). Historical and geological information is given in Horvath and Gault, 1990, and Wight, 1996, with many references.

Identification of gems from Mont Saint-Hilaire (MSH) is often difficult because many of the stones are small, and it can be hard to get reliable RI readings. Few of the rarer gems are available, and their identification is difficult if the investigator has no knowledge of their existence. Table 1 gives a description of some MSH gemstones with properties that may be helpful in identification.

Sérandite

The discovery of sérandite in 1965 made MSH a famous locality. MSH is the only important source of sérandite, and splendid large specimens up to 20 x 7 cm are now in museums around the world. Sérandite was first faceted in 1974, and this began a continuing fascination for gemstones from this locality for collectors of the rare and unusual. Although too soft for use in jewellery, sérandite's colour is distinctive and beautiful. Sizes are usually less than 1.5 ct, although larger cabochons exist.

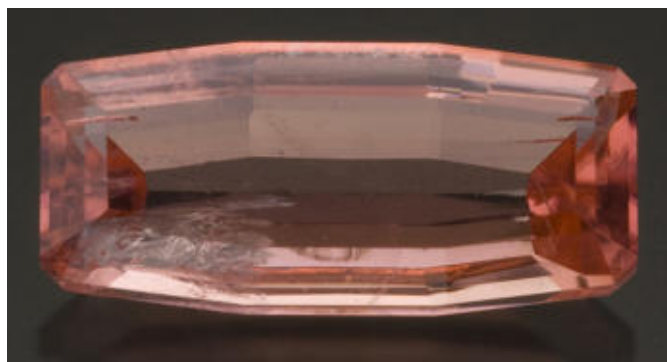


Figure 1. Serandite on albite and microcline, 9.0 x 5.0 x 4.0 cm (CMNMC 56673) and gem 1.33 ct (CMNGE 21709)

Carletonite

Carletonite was first described from MSH, which remains its only known locality. Rare finds of cornflower-blue crystals up to 5 cm; single crystals, zoned in shades of light to dark blue, pink to colourless to white, up to 6 cm, and a few transparent, deep blue terminated crystals up to 1.5 cm make carletonite one of the top three most coveted MSH minerals. The few gems are very small.



Fig. 2. Carletonite crystal, 7.0 x 5.5 x 5.0 cm (CMNMC 83877) and gem, 1.48 ct (CMNGE 21669). This is the largest carletonite gem known.

Catapleiite

Catapleiite is relatively common at MSH, with colourless, beige, or pale grey crystals from mm size to superb groups of tabular to platy crystals up to 5 cm and rosettes to 15 cm in diameter. The best and largest specimens in the world are from this locality. Colourless catapleiite has been faceted for collectors. Perhaps 30 stones exist (up to 2.48 ct).



Fig. 3. Catapleiite. Colourless, tabular crystals, 4 x 3 x 3 cm (CMNMC 37369) and gem 1.86 ct (CMNGE 21680)

Leifite

Colourless to white, light yellow or light violet leifite is relatively rare at MSH, but superb mineral specimens in a variety of habits have been found. About 25 leifite gems are known (up to 2.82 ct).

Natrolite

Natrolite is common at MSH in elongated prisms up to 10 cm. The first gem of 8.70 ct was faceted in 1976, using a special cut to bring out brilliance in a material with such a low refractive index. The largest known natrolite gem from MSH weighs 19.37 ct; others range from 3 to 10 carats.

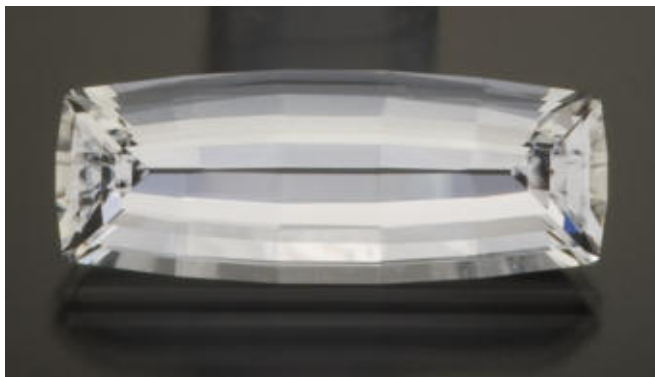


Fig. 4. Natrolite gem, 19.37 ct (CMNGE 21696)

Remondite-(Ce)

In 1991, fragments of transparent orange crystals were first identified as burbankite, but subsequent analyses proved them to be remondite-(Ce). There are about 30 faceted stones (1.72 to 7.75 ct). The most interesting feature is the strong colour change: orange or yellowish orange in incandescent light to greenish yellow in fluorescent or daylight. The colour and the colour change are caused by the presence of rare-earth elements cerium and neodymium.



Fig. 5. Remondite-(Ce) gem, 6.62 ct (CMNGE 21699) showing colour change. Left: green in fluorescent light; right: orange in incandescent light.

Rhodochrosite

Rhodochrosite at MSH has been found in a range of shades from lighter pink to dark red, in a variety of habits. Stones are generally less than 6 ct, but the largest in the CMN collection is 18.14 ct.

Shortite

Shortite is a rare carbonate mineral; it is often overlooked because of its strong resemblance to calcite, which occurs in the same environments. Transparent to translucent, lemon-yellow shortite has been faceted (0.35 to 3.52 ct). It decomposes in water— an additional challenge to the lapidary.

Sodalite var. hackmanite

Both blue sodalite and its variety hackmanite, which can be yellow to pink to reddish-purple, are common at MSH. Hackmanite is distinguished in being photochromic. Transparent, light yellow hackmanite has been faceted into amazing gems. They become raspberry pink after about 15 minute's exposure to ultraviolet light. The colour fades gradually to the original light yellow, but the process is repeatable. Notable hackmanite gems weigh 15.33, 9.77, 3.25, 3.23 carats. One rare pink hackmanite (2.41 ct) becomes more saturated when exposed to UV light.



Fig. 6. Sodalite variety hackmanite. Crystals coated with analcime, 5.5 x 4.5 x 3.0 cm (CMNMC 86129); gems: light yellow, 3.23 ct (CMNGE 21721); rare, pink, 2.41 ct (CMNGE 21722). Left: normal lighting. Right: showing tenebrescence after fluorescence.

Sphalerite

Sphalerite gems from MSH occur in a range of colours, and are similar to those from other localities. Notable examples are colourless (11.48 ct), yellow (25.45 ct), light green (11.91, 24.74, 42.16 ct), dark green (55.62 ct), and red (6.5, 13.94 ct).

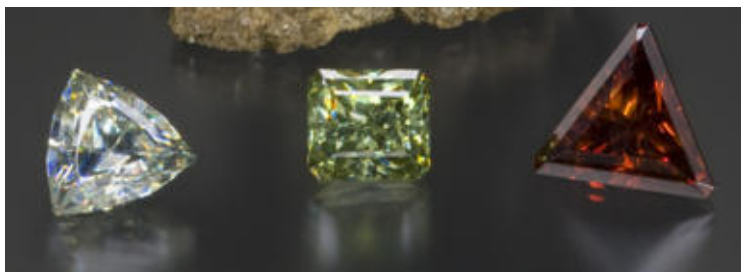


Fig. 7. Sphalerite gems: colourless, 11.48 ct (CMNGE 21724); light green, 11.91 ct (CMNGE 21725); dark red, 13.94 ct (CMNGE 21726)

Villiaumite

Villiaumite from MSH is considered the world's best, with the discovery of masses up to 10 cm and rare, sharp crystals 2–10 mm across. Colours range from dark red, pink, orange, to colourless; some is bi- or tricoloured. Faceted examples range from 0.27–12.10 ct; larger stones are very dark red. Although its colour can be attractive, villiaumite is very soft, cleaves easily, and is somewhat water soluble.



Fig. 8. Villiaumite. Subhedral crystal, 5.0 x 5.5 x 2.5 cm (CMNMC 54040) and gems: colourless, 3.59 ct (CMNGE 21741); dark red, 7.50 ct (CMNGE 21740)

References

- Horvath, L. and Gault, R.A., 1990. The mineralogy of Mont Saint-Hilaire, Québec, *Mineralogical Record*, 21(4), 285–352. Comprehensive article with many references.
- Wight, W., 1996. The gems of Mont Saint-Hilaire, Québec, Canada. *J. Gemmology*, 25(1), p. 24–44. (history and locality information with comprehensive references, and check-lists for most MSH gems)
- Wight, W., 2001. Check-list for rare gemstones—leifite, *Canadian Gemmologist*, 22(4), 125–127.
- Wight, W., 2002. Check-list for Rare Gemstones—remondite-(Ce), *Canadian Gemmologist*, 23(2), 53–55.

Acknowledgements

The author is grateful to Bradley Wilson, and to her colleagues at the Canadian Museum of Nature, especially R.A. Gault, M. Picard, and Dr. J.D. Grice for a critical reading of the manuscript. All photos except that of remondite-(Ce) were taken by Michael Bainbridge for the CMN, and are of specimens now on display in the Vale Earth Gallery at the Canadian Museum of Nature, Ottawa. The gems are those acquired in 2007 from long-time collector at MSH, Gilles Haineault.

Table 1: Properties of some rare gemstones from Mont Saint-Hilaire, Québec, Canada (updated and modified from Wight, 1996).

Mineral	Description	Properties	Identification
Carletonite (Figure 2) KNa ₄ Ca ₄ Si ₈ O ₁₈ (CO ₃) ₄ (OH,F)•H ₂ O Tetragonal	intense blue (pink, colourless; colour zoning common) H: 4 to 4.5 Cleavage: perfect	U(-) ω=1.521 ε=1.517 Pleochroism: weak, o, v. pale B, ε, v. pale pinkish brown	Very few gems are available. The low RI is significant. Intense blue colour is similar to that of sodalite, which is common at MSH, but usually opaque. Haüyne, blue apatite, and sapphirine might be confused.
Catapleiite (Figure 3) Na ₂ ZrSi ₃ O ₉ •2H ₂ O Monoclinic (pseudohexagonal)	colourless, greyish (light brown) H: 5.5 Cleavage: perfect	B(+) α=1.588 β=1.591 γ=1.624	There are a few rare colourless, birefringent minerals with similar RI that might cause confusion. May fluoresce green LW&SW UV
Leifite Na ₇ Be ₂ (Si,Al) ₁₈ O ₃₉ F ₂ Trigonal	light violet to colourless H: 6	U(+) ω=1.515 ε=1.519	Low RI is significant. Petalite, dolomite, magnesite and stichtite could be confused May fluoresce green SW UV
Natrolite (Figure 4) Na ₂ Al ₂ Si ₃ O ₁₀ •2H ₂ O Orthorhombic	colourless H: 5 Cleavage: perfect	B(+) α=1.479 β=1.485 γ=1.491	Easily by low RI. There are very few rare, colourless, birefringent gemstones with low RIs. May fluoresce white LW&SW UV
Remondite-(Ce) (Figure 5) Na ₃ (Ce,La,Ca,Na,Sr) ₃ (CO ₃) ₅ Monoclinic	orange (colour- change); greenish Y in fluorescent light to yellowish O in incandescent light H: 3 to 3.5	B(+) α=1.632 β=1.633 γ=1.638 gem 1.630-1.632 (0.002)	Distinctive colour-change. Birefringence notably low for a carbonate. If no colour change, orange garnet, zircon, sphalerite and scheelite might be confused. May fluoresce wk pink LW&SW UV
Rhodochrosite MnCO ₃ Trigonal	pinkish red H: 3.5 to 4	U(-) ω=1.810 ε=1.598	RIs and large birefringence are useful. Cleavage: perfect rhombohedral
Sérandite (Figure 1) Na(Mn,Ca) ₂ Si ₃ O ₈ (OH); isomorphous series with pectolite Triclinic	orange, pinkish- orange, pink Pleochroism: mod. pink/O	B(+) α=1.668 β=1.671 γ=1.703	RI gems 1.674-1.708 (0.035). A few gems of similar colour (e.g. calcite, beryl, tourmaline, topaz, grossular) might be confused. Cleavage: perfect
Shortite Na ₂ Ca ₂ (CO ₃) ₃ Orthorhombic	intense yellow, greenish yellow Pleochroism: mod. Y/G/grey H: 3 Cleavage: distinct	B(-) α=1.531 β=1.555 γ=1.570	Lemon yellow colour is distinctive, as are softness and large birefringence. Calcite, dolomite or barite might appear similar. Decomposed by water
Sodalite (Figure 6) Na ₄ Al ₃ Si ₃ O ₁₂ Cl Cubic Sodalite var. hackmanite	blue (white, grey) H: 5.5 to 6 light yellow, pink after exposure to UV; pink	I η=1.483 Transparent to opaque Transparent Strongly photosensitive	Light yellow hackmanite should not be confused if photochromic properties are obvious. Very low single RI is helpful. Some fluoresces bright O LW&SW UV; phosph. Y-W
Sphalerite (Figure 7) ZnS Cubic	yellow, green, brownish green, green, dark red	I η=2.37 to 2.40 Dispersion very high	Single RI >1.81, high dispersion, and adamantine lustre are distinctive.
Villiaumite (Figure 8) NaF Cubic	colourless to pink to dark red; some bi- or tricoloured	I η=1.326 H: 2 to 2.5 Cleavage: perfect	Single RI is significant—no other isotropic gem has such a low RI. Soluble in water

New Canadian occurrences of gem scapolite and demantoid

Karen E. Fox

Canadian Gemmological Association Waterloo, Canada k_e_fox@yahoo.com

Canada, although not known as a prolific producer of gemstones other than diamond, does from time to time yield interesting deposits of gem-quality material. The cut stones from these finds make their way into jewellery and collections, and thus it behooves the gemmologist and appraiser to be aware of their existence. Two recent discoveries of note are UV-fluorescent scapolite from Baffin Island, and a striking green andradite garnet, variety demantoid, from Asbestos, Québec.

Scapolite

The six scapolite gemstones shown in Figure 1 range in weight from 0.91 ct to 3.51 ct and were cut from material found in 2008 in the vicinity of Kimmirut, a hamlet on the south end of Baffin Island in the territory of Nunavut, Canada. This region has received media attention because it is also the site of the “Beluga Sapphire Occurrence” discovered in 2002 (Gertzbein, 2005).

The stones vary in colour from a light, moderately strongly saturated, yellow to a medium, greyish yellow (GIA colour description system – tone, saturation, hue). All specimens are weakly dichroic, displaying a very light yellow o-ray and a colourless e-ray.

Refractive index readings from the three faceted stones indicate uniaxial negative optic character, with $n_e=1.542-1.543$, $n_o=1.556-1.558$, and birefringence about 0.015. Preliminary specific gravity measurements range from 2.65 to 2.68. These physical properties place the material at an intermediate position along the solid solution series for the scapolite group with end members marialite and meionite (Henn & Bank, 1990; Deer et al., 1995; Superchi et al., 2010).

Diaphaneity for the stones under discussion is transparent to semitransparent. In general, a greyer cast and reduced diaphaneity are associated with an increasing density of long, very fine to coarse, parallel needle-like inclusions aligned along the c-axis, and some stones display a distinct cat’s-eye effect. Thicker needles appear black to the naked eye or under a hand lens, while very fine short needles impart a slight sheen and produce a hazy appearance (Fig. 1, top centre).



Figure 1. Light yellow to greyish yellow scapolite gemstones from Baffin Island, Nunavut, Canada (0.91 ct to 2.51 ct).

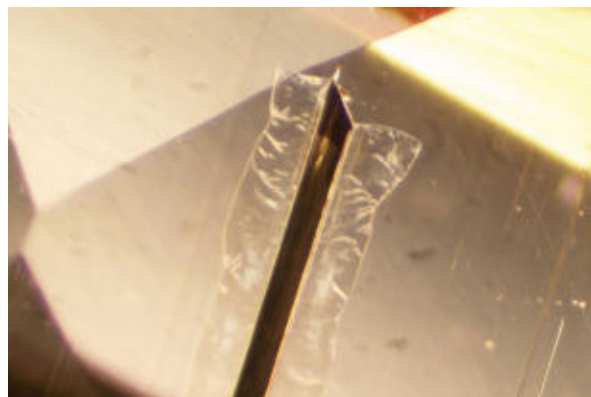


Figure 2. Fissure planes arc away from the edges of long, dark, ribbon-like inclusions in scapolite.

Magnification reveals that some thicker needles actually take the form of long flat ribbons. In many cases, arced fissures are seen to extend for great lengths along the inclusions, originating along opposite edges of the ribbons (Fig. 2), while narrower needles may be decorated by strings of flat disc-like fractures. In general, these elongated inclusions are not hollow, but rather filled by a dark material that can be drawn from the stone during polishing and left in short needle-like fragments upon the surface. Blockier crystal forms and partially healed fissures decorated by droplet-like features are also observed (Fig. 3).

A striking property of these specimens is their very strong yellow fluorescence under long- and short-wave ultraviolet illumination, somewhat masked in stones with dense needle inclusions. Additionally, some stones also show a slight tenebrescence characterized by a shift in body colour to a stronger blue/grey upon exposure to short-wave UV radiation, fading within seconds of removal of the excitation.

Andradite, variety Demantoid

The Jeffrey mine, located near Asbestos, Québec, is one of Canada's last-remaining asbestos mines. It was once one of the world's largest producers of chrysotile. Although it has been mostly dormant for years, limited collecting expeditions have yielded many interesting mineral specimens, including various colours of grossular garnet. In the 2007 to 2009 timeframe, the rough material for the faceted stones depicted in Figure 4 was gathered.

These six demantoid garnets range in weight from 0.19 ct to 0.50 ct and are typical of the sizes produced by this site. The colours can be characterized as medium light to medium in tone, with moderately strong to vivid saturation in yellowish-green to green hues. Colour is often irregularly distributed throughout the stones. High dispersion produces significant "fire" in the lighter toned, less included gems. No appreciable colour shift between daylight and incandescent illumination was observed for the two vivid green specimens, although incandescent light does slightly accentuate the yellow component in the remaining stones. This is in contrast to demantoid from the nearby Black Lake mine, Québec, which has been reported to show significant colour shift (Wilson & Wight, 1999).

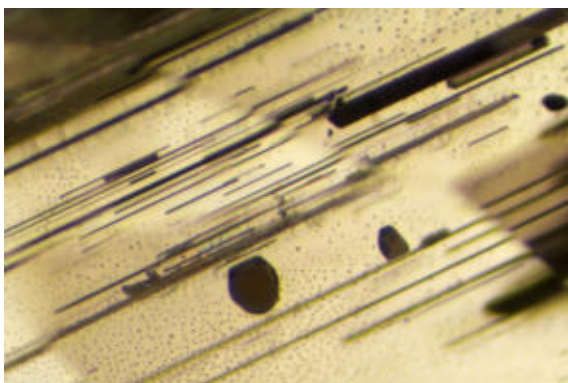


Figure 3. Blocky crystals and terminated blades are visible on the background of a partially-healed fissure in scapolite.



Figure 4. Yellow-green to intense green demantoid garnets from Asbestos, Québec (0.19 ct to 0.50 ct).

The refractive index of these specimens is beyond that of the index-matching fluid available at the time of testing (1.79). Between crossed polarizers, the stones exhibited bright interference colours and variable dark extinction patches, the so-called anomalous double refraction which is an expression of the typical internal strain inside garnets.

All stones displayed a distinct pink glow when viewed through the Chelsea filter, but no obvious spectrum could be identified using an OPL grating spectroscope. They were also inert to long- and short-wave ultraviolet radiation.

Inclusions are common in these stones, including fractures and healed fissures, and particularly radiating fibrous bundles and “horsetails” (Fig. 5). Often the fibres emanate from a dark, irregularly shaped core with which an enhanced green coloration is associated (Fig. 6). Although the locality’s reputation as a major chrysotile producer suggests that the fibrous bundles will also be chrysotile, as has been reported for material from Russia (Phillips & Talantsev, 1996), detailed analytical work has yet to be performed.

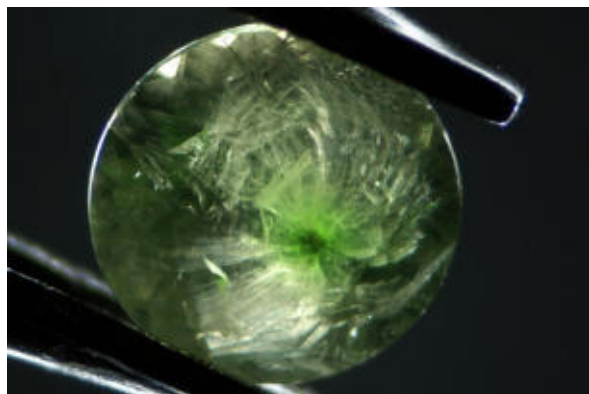


Fig. 5. A luxuriant radiating fibrous bundle, or “horsetail” inclusion, is featured in this 0.32 ct demantoid from Asbestos, Québec.

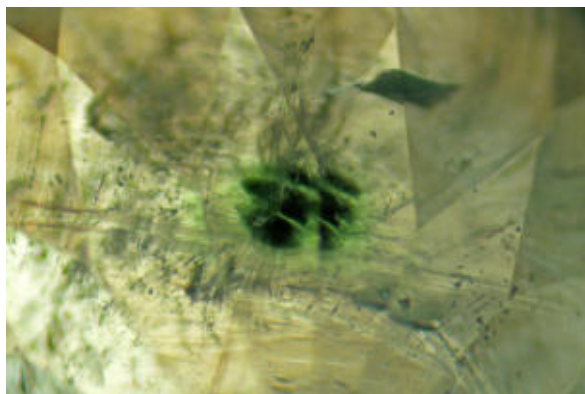


Fig. 6. Fibres often radiate from a darker core with which enhanced green coloration is associated.

Recent news reports suggest that the Jeffrey mine may soon be reopened and expanded, extending its lifetime an additional 25 years and thus improving the possibility that further material of this type will become available to gem cutters.

References

- Deer W.A., Howie R.A., Zussman J., 1995. *An Introduction to the Rock-forming Minerals*. Longman, England, 2nd ed., 3-13. ISBN 0-582-30094-0.
- Gertzbein, P., 2005. Geology surrounding the Beluga Sapphire Occurrence, Kimmirut, Nunavut, A preliminary examination. *Canadian Gemmologist*, 26(2), 50-56.
- Henn, U., Bank, H., 1990. Violet gem scapolite crystal said to be from Afghanistan. *Canadian Gemmologist*, 11(4), 106-109.
- Phillips, W.R., Talantsev, A.S., 1996. Russian demantoid, czar of the garnet family. *Gems & Gemology*, 32(2), 100-111.
- Superchi, M., Pezzotta, F., Gambini, E., Castaman, E., 2010. Yellow scapolite from Ihosy, Madagascar. *Gems & Gemology*, 46(4), 274-279.
- Wilson, B.S., Wight, W., 1999. Gem andradite garnet from Black Lake, Quebec. *Canadian Gemmologist*, 20(1), 19-20.

Acknowledgements

Sincere thanks are offered to Bradley Wilson of Alpine Gems, gem cutter and explorer extraordinaire, who kindly loaned the gemstones which served as the focus for this work.

Gemstones from southern Baffin Island, Nunavut, Canada

Bradley S. Wilson

Alpine Gems, Kingston, Ontario, Canada brad@alpinegems.ca

Within the last decade, sapphire, cobalt spinel, moonstone and a suite of other gemstones including tourmaline, garnet, zircon, sphene, diopside and scapolite have been discovered in the Canadian Arctic on the southern-most part of Baffin Island, Nunavut. Although gemstone occurrences have been known in the region for nearly a century, it was the discovery of sapphire in 2002, and the subsequent exploration activity, that attracted media attention and brought knowledge of these gemstones to the gemmological and geological communities. Walker (1915) described some of the earliest known occurrences of gemstones in the area, including garnet and cordierite (iolite) from a mysterious locality named "Garnet Island". In addition, lapis lazuli from Soper River has been known since 1950, and probably earlier (Davidson, 1959; Hogarth, 1971).

Southern Baffin Island is underlain by a complex series of Paleoproterozoic metamorphic rocks. Most of the gem deposits in the region are hosted in clastic and carbonate metasedimentary rocks with metamorphic grades ranging from upper-amphibolite to granulite facies. Metamorphism has been dated at 1.82-1.86 Ga (St-Onge et al., 1998). The geologic setting of southern Baffin Island is analogous to that of gem-producing regions from Afghanistan to Vietnam (LeCheminant et al., 2004).

Sapphire

The discovery of gem-quality sapphire in 2002 is certainly the region's most significant coloured gemstone find. Prior to this, transparent sapphire had never been found in Canada. In November of 2003, True North Gems Inc., a Canadian junior mining company, acquired the mining rights and in 2004 commenced exploration for sapphire in the region (Wilson, 2007). Exploration included bulk sampling, prospecting, core-sample drilling, geologic mapping and geophysics. The initial discovery site, located approximately 2.5 km southwest of the hamlet of Kimmirut, is called the "Beluga Sapphire Occurrence" (Gertzbein, 2005). While their efforts lead to the discovery of additional sapphire-bearing sites, Beluga remains the most significant occurrence.

Sapphire occurs primarily in calc-silicate lenses within a marble unit. At the Beluga Sapphire Occurrence, corundum occurs primarily as blue, colour-zoned, euhedral crystals up to 7.7 x 2.1 cm in size. Larger crystals are known from the nearby Aqqik occurrence. Faceted sapphire ranges from colourless to various shades of blue and yellow. The largest gem cut to date is light blue and weighs 7.81 carats.

Spinel

As early as 1915, crystals of lilac-coloured spinel were described from southern Baffin Island (Walker, 1915). Over the past three decades, numerous spinel discoveries in this region have produced some spectacular crystal specimens (Grice et al., 1982; Grice and Gault, 1983; Wilson, 1997, 2007). Most of these spinels are black, violet, blue or pinkish-violet, and faceted gems are small (less than half a carat).

In 2005, True North Gems announced a find of cobalt blue spinel on their Beluga sapphire property (True North Gems, 2005). Their press release states that the intense blue colour is due to the presence of cobalt. A spectral study by Williams (2009) confirms this claim. This occurrence is now referred to as "Qila". Most of the spinel at the Qila occurrence consists of irregularly shaped, opaque to translucent fragments as large as one centimetre. Seve-

ral small cabochons have been cut from Qila spinel.

A second locality a few kilometres away from Qila has produced several euhedral spinel crystals as large as 2.7 cm, along with a few tiny transparent fragments. Three gems weighing up to 0.16 carat have been faceted. Their colour is also caused by cobalt (pers. comm., B. Williams, 2010).

Garnet

Although garnet is a common rock-forming mineral in the region, only a few localities have produced faceted gems. Garnet of a fine deep red colour, along with cordierite (iolite), was found prior to 1915 on “Garnet Island”, located somewhere along the southern coast of Baffin Island between Kimmirut and Cape Dorset (Walker, 1915). Despite attempts to find and verify the existence of this occurrence, “Garnet Island” remains a lost locality. Analytical work has shown this garnet to be almandine-pyropite with a corresponding ratio of approximately 2:1 (pers. comm., A. Locock, 2008). Faceted gems as large as 7.60 ct have been cut from this material (Wight, 1986). A very small amount of gem-quality, medium-dark pinkish-red garnet was found in 2008 in the Beaumont Harbour area, located 50 km west of Kimmirut. The only gem cut to date weighs 2.44 carats.

Cordierite (Iolite)

Several occurrences of iolite are known in the general Markham Bay area, about 120 km northwest of Kimmirut (Wilson, 2007). One of these iolite occurrences was found in 1992 while searching for the “Garnet Island” locality described by Walker (1915).

Tourmaline

Dark brown to medium-dark orange-brown gemmy tourmaline crystals have been found in the marble in the Kimmirut area. Analysis of samples from an occurrence discovered by the late Paul Gertzbein in 2003 reveal that these are the calcium magnesium tourmaline mineral uvite (pers. comm., K. Day, 2011). This locality has yielded orange-brown gemstones as large as 0.61 carat. A second occurrence south of Kimmirut has produced transparent rough weighing over 20 grams that is so dark when viewed parallel to the c-axis that stones look virtually black.

Moonstone

Three localities along the southern coast of Baffin Island have produced attractive moonstone cabochons: the Kimmirut area, the Crooks Inlet area, and Glencoe Island. Kimmirut area moonstone occurs within coarse-grained pegmatite, ranges from opaque to translucent, and tends to be an orange-brown to very attractive orange colour with a good display of adularescence (Wilson, 2005). Crooks Inlet moonstone occurs as isolated anhedral crystals within marble, is mostly opaque, and is white with silvery-white adularescence. The moonstone from Glencoe Island is translucent to transparent, and is tan in colour.

Lapis lazuli

Two occurrences of lapis lazuli occur within marble on the west bank of the Soper River approximately 14 km NNE of Kimmirut. The main occurrence has been known to local people since at least 1950 and its location is indicated as “lazurite” on a geologic map of the area (Davis, 1959). The author has heard anecdotal evidence placing local knowledge of the locality back at least several decades earlier. The main occurrence was mapped out and shown to extend for almost 170 metres (Hogarth, 1971). Hogarth and Griffin (1978) believe the lapis lazuli originated during the metamorphism of a sequence of evaporitic sedimentary rocks. Lapis lazuli from the surface of the main occurrence is crumbly and highly fractured (probably due to frost action), and has an overall blue to slightly grayish-blue colour dispersed with centimetre-sized patches of tan and grey. The second occurrence, located about 1.5 km to the northeast, is considerably smaller. It contains material possessing a distinctly green to bluish-

green colour.

Other gems

Other gems found in the region include zircon (largest faceted stone weighs 0.31 ct), scapolite (as large as 9.87 ct), diopside (< 2 ct), pargasite (> 4 ct), oligoclase (as large as 6.90 ct), sphene (< 0.5 ct) and apatite (< 1 ct). Of these gems, scapolite deserves special mention for some of its unusual properties. Some of the gem-quality scapolite occurrences between Glencoe Island and Kimmirut have produced rough that is highly fluorescent under long-wave ultraviolet light, a property that is retained after the gems are cut. Rough from one of these localities is fluorescent, tenebrescent, and has numerous parallel inclusions that yield cat's-eye gems when properly cut.

References

- Davidson, W. L., 1959. Geology, Lake Harbour, Baffin Island, District of Franklin, Northwest Territories. Geological Survey Canada, Map 29-1958.
- Gertzbein, P., 2005. Geology surrounding the Beluga Sapphire Occurrence, Kimmirut, Nunavut: a preliminary examination. *Canadian Gemmologist*, 26(2), 50–56.
- Grice, J.D., Gault, R.A. and Waller, R., 1982. Spinel from Glencoe Island, Northwest Territories, Canada. *Rocks & Minerals*, 57(4), 155–157.
- Grice, J.D. and Gault, R.A., 1983. Lapis lazuli from Lake Harbour, Baffin Island, Canada. *Rocks & Minerals*, 58(1), 13–19.
- Hogarth, D.D., 1971. Lapis lazuli near Lake Harbour, southern Baffin Island, Canada. *Canadian Journal of Earth Sciences*, 8, 1210–1217.
- Hogarth, D.D. and Griffin, W.L., 1978. Lapis lazuli from Baffin Island—a Precambrian meta-evaporite. *Lithos*, 11, 37–60.
- LeCheminant, A. N., Groat, L. A., Dipple, G. M., Mortensen, J. K., Gertzbein, P. and Rohtert, W., 2004. Gem News International: Sapphires from Baffin Island, Canada. *Gems & Gemology*, 40(4), 344–45.
- St-Onge, M.R., Scott, D.J., Wodicka, N. and Lucas, B.S., 1998. Geology of the McKellar Bay-Wight Inlet-Frobisher Bay area, southern Baffin Island, Northwest Territories; in *Current Research 1998-C*; Geological Survey of Canada, 43–53.
- True North Gems, 2005. True North Gems discovers rare gemstone on Baffin Island property. Press Release, November 17, 2005.
- Walker, T. L., 1915. Minerals from Baffin Land. *Ottawa Naturalist*, 29, 63–66.
- Williams B., 2009. What's new with cobalt? *Gem Market News*, 28, Issue 3, p. 9, 15.
- Wight, W., 1986. Canadian gems in the national museum of Canada. *Canadian Gemmologist*, 7(2), 34–45, 50–55.
- Wilson, B. S., 1997. A new occurrence of spinel from Arctic Canada. *Rocks & Minerals*, 72, 191.
- Wilson, B.S., 2005. Recent exploration for coloured gemstones in Canada. *Canadian Gemmologist*, 26(2), 57–63.
- Wilson, B.S., 2007. Coloured gemstones from Canada. Chapter 10 in "The Geology of Gem Deposits", Mineralogical Association of Canada Short Course 37, Yellowknife, Northwest Territories, 255–270.

Laser ablation ICP-MS: technical aspects and capabilities of a versatile trace element microprobe

Thomas Pettke¹, Michael S. Krzemnicki²

¹Institute of Geological Sciences, University of Bern, Baltzerstrasse 1+3, CH-3012 Bern, Switzerland (pettke@geo.unibe.ch)
(www.geo.unibe.ch/people/Pettke)

²Swiss Gemmological Institute SSEF (gemlab@ssef.ch)

Laser ablation inductively coupled plasma mass spectrometry (LA-ICP-MS) has become a prime tool for the in-situ analysis of major to trace element concentrations in solid materials, and can successfully be used for in-situ isotope ratio analysis (see e.g., Sylvester, P., 2008. Laser ablation ICP-MS in the Earth Sciences: Current practices and outstanding issues. Mineralogical Association of Canada Short Course Series Volume 40, pp. 348). Applications range from minerals including their solid and liquid inclusions to organic compounds to frozen liquids, with limits of detection down to the sub-ng per g range for certain trace elements.

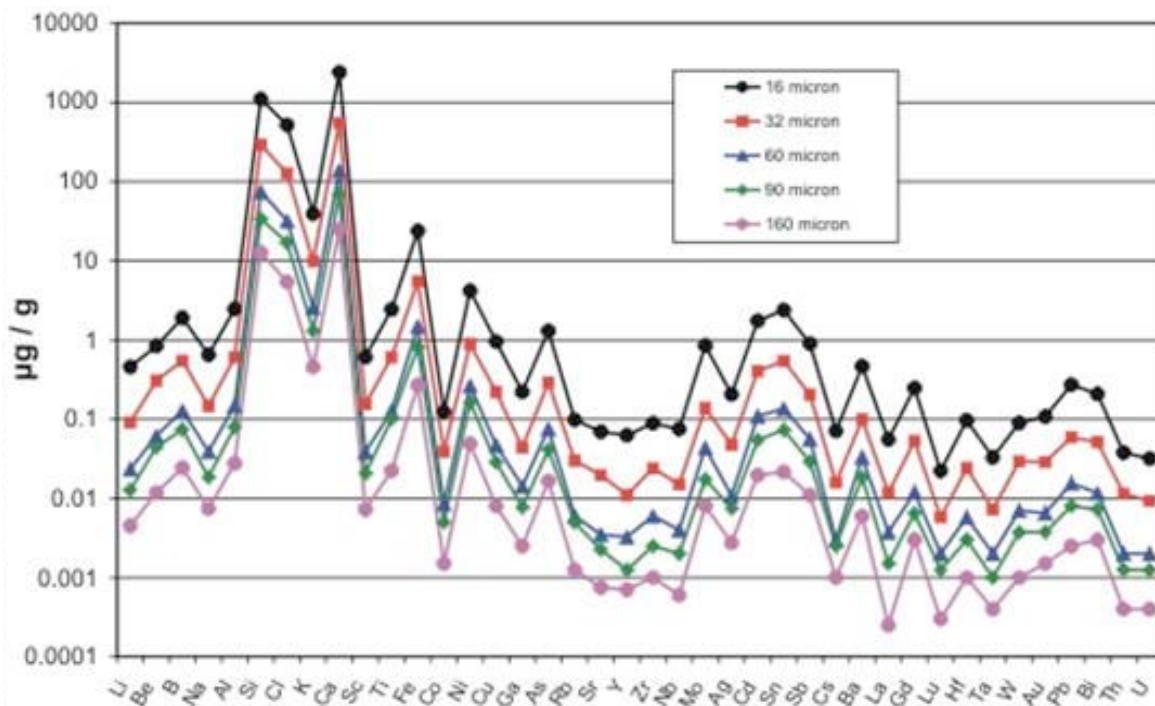


Figure 1: LA-ICP-MS limits of detection achieved for laser beam sizes of 16 to 160 μm diameter as defined in the inset (10 Hz, 8 J/cm²; SRM 612 from NIST).

To date, this technology has found only limited applications in gemmology, partly because it is a very sophisticated and costly tool, but also because it is not completely non-destructive. The laser ablates a minute part of the sample, leaving tiny laser spots on the surface, preferably the girdle of a gemstone. This contribution introduces some of the characteristic features of LA-ICP-MS, emphasizes critical aspects of the technique and documents its capabilities and potential using selected examples, including quasi non-destructive applications.

Laser ablation ICP-MS consists of two instrumental parts, the laser ablation system and the mass spectrometer for analyte detection. This setup allows for one of the fundamental advantages over other trace element microprobes, namely that the sample liberation process (i.e., laser ablation) and the measurement of ion signals in the ICP-MS can be optimized independently, thus significantly reducing matrix dependence of analytical results. In other words, commonly available and well-characterized standard reference materials (SRM) can be employed to quantify analytical signals from samples of different matrices. For example the silicate glass SRM from NIST (National Institute of Standards and Technology) can successfully be used to quantify measurements of e.g., silicates, oxides, carbonates, sulfates, phosphates or other rare minerals that are often important in gemmology. Problems commonly referred to as «elemental fractionation» can thus be minimized. This is only possible, however, when using a well optimized LA-ICP-MS analytical strategy, and critical aspects to this will be illustrated. These include:

- 1) Optimization of the laser ablation conditions for different matrices and analytical aims to be achieved, including quasi non-destructive analysis
- 2) Procedures to minimizing problems commonly referred to as «elemental fractionation»
- 3) Optimization of the mass spectrometer measurement conditions to minimizing matrix dependence of signal quantification
- 4) Problems related to interferences that may become important notably for uncommon chemical compositions as often encountered in gemmology

Another near-unique capability of LA-ICP-MS is the fact that major to trace element concentration data can be obtained from one analytical spot, thus allowing to directly relate the trace element inventory to the major element composition of the samples.

Figures of merit (internal and external analytical precision, analytical accuracy) will be addressed in detail to illustrate which analytical strategies are most important in producing accurate data at good external precision. The external precision (i.e., the precision of repetitive spot analysis of a homogeneous sample) has about 1-2 % uncertainty at the 2 standard deviation level for most elements. Consequently, the accuracy of trace element concentration data may be sometimes limited by the knowledge of the external standard material (SRM) required for data quantification. Clearly, great efforts are needed to produce accurately quantified reference materials that can be made available to the entire analytical community.

The application of LAICPMS has greatly contributed to the understanding of trace element concentration and distribution in gemstones and pearls. As it is a microanalytical technique, it is however mandatory to choose the points for analyses carefully not only to avoid that the laser spots are too visible on the sample, but mostly to avoid effects of chemical zoning. The versatility and capabilities of LA-ICP-MS are demonstrably great. Future applications will reveal the usefulness of this instrumentation for chemical and isotopic source fingerprinting in gemmology.

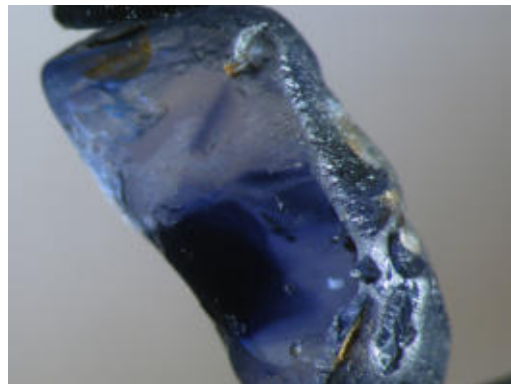
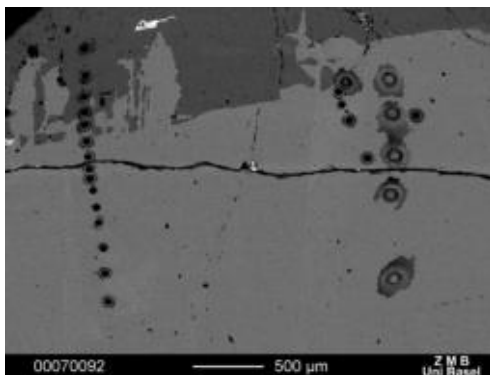


Figure 2 (right): Sapphire from Madagascar with strong colour zoning and a few tiny laser spots on the surface. Fig 3 (left): SEM backscattered electrons micrograph on a sapphire/chrysoberyl intergrowth (different grey shades) with umerous laser spots surrounded by a deposition rim due to the ablation process.

AFM: an alternative technique for indicating gem treatments

Pornsawat Wathanakul^{1,2}, Somruedee Satitkune², Thanapong Lhuaamporn², Wilawan Atichat¹, Thanong Leelawatanasuk¹ and Monruedee Thawornmongkonij¹

¹The Gem and Jewelry Institute of Thailand (GIT)

²The Gem and Mineral Sciences Special Research Unit, Department of Earth Sciences, Faculty of Science, Kasetsart University, Bangkok 10900, Thailand; pwathanakul2@gmail.com

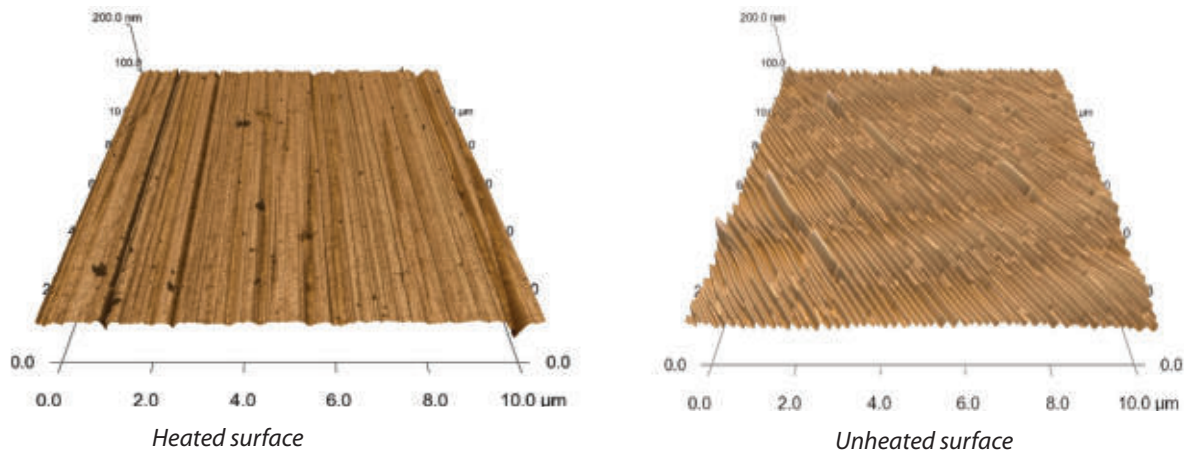
The atomic force microscope (AFM) is actually a mechanical based device for determining the surfaces of materials on a micro- to nanometre scale; a sharp tip on a movable beam. This so-called 'cantilever' is used for sweeping or sensing back and forth over a tiny surface area on either a tapping or a contact mode, resulting in nanometre-scaled morphological images of sample surfaces. Evidences or surface features that have normally been hidden from human eyes, not visible with an efficient microscope, or even an electron microscope, can be disclosed by AFM. Materials scientists are especially familiar using it in their research (e.g., Heffelfinger et al., 1997; Curiotto and Chatain 2009; Cuccureddu et al., 2010), whereas its application in mineral sciences has gradually increased. In gemmology, however, it has been known only in pearl surface research so far. A gem research group supported by the GIT has applied AFM techniques on gem surfaces, to alternatively determine the heat treatment, its possible extent experienced by gem corundum, and other on-going experiments in order to open a new forum in a finer scale of gemmological research to our community.

The problem in evidencing the heat treatment extent of gem corundum, specifically ruby, is one of the examples. Gemmologists normally use their experiences in inspecting of mineral inclusion alteration features under the microscope and by UV-Vis as well as infrared absorption spectra (e.g., Smith, 1995; Beran and Rossman, 2006; Paretto, 2008) to prove whether or not that gem corundum had undergone a heat treatment. Besides, some specific instrumentation such as laser tomography and luminescence might also be employed to clearly determine such treatment. Arguments among gem laboratories still exist, how one could correctly say this stone had undergone either low or high temperature heating.

Ruby samples from Mong Hsu, Myanmar, and Mozambique (said to be from Montepuez) were collected for experiments, especially because their properties are known to gemmologists. The apparent c-plane surface of flat samples was cut and polished. Heating experiments at 800, 1200, 1650°C in an electric furnace were conducted for 1, and 2 hours. Beforehand, FTIR spectra were also used for comparative heating determination of those samples. The samples were well cleaned, and kept from dust and moisture in a desiccator before measuring by the AFM. Either a tapping or a contact mode can be employed; the radius of a silicon probe tip is around 7 nm. The micro-nanometre scaled topographic surface images of ruby samples were then recorded. Besides, calculation of the root mean square (RMS) average roughness was processed to reflect the surface roughness of each sample; the surface topographic images and RMS roughness features of samples from each batch were compared.

The micro-nanometre scaled surface features of ruby samples undergone heating at 800, 1200, and 1650°C revealed the obvious increase of step edge sharpness, and trends of gradually rougher surfaces with the increased atomic step thickness, with respect to those increasing temperatures. In general, the heated stones tend to have sharper atomic step edges, and rougher atomic step surfaces than those of the unheated ones. An example of AFM images showing distinct differences in surface roughness of two specimens cut from a Mozambique ruby

sample is shown below; the surface heated to 1200°C displays sharper and rougher atomic steps of the unheated one.



Heating of more sample batches with longer soaking times revealed consistent results. It is, therefore, suggested here that AFM is another promising tool in gemmology for identifying corundum, heat treatment, and possibly indicating its extent. However, more AFM images of different crystallographic sample orientations need to be produced. Besides, the data base on average values of AFM measuring parameters such as the RMS roughness and the atomic step height should be collected for comparison because factors such as structural defects and/or trace element content and inclusion dissolution after heating could have influenced atomic structures of gemstones due to their different geological occurrences.

Furthermore, some examples of AFM applications on gem surfaces which had been exposed to various kinds of treatment, e.g., heating with beryllium, glass-filling, as well as diamond surfaces have also been conducted, and intended to be contributed to the 32nd IGC, Interlaken, Switzerland.

References

- Beran, A. and Rossman, G.R. 2006. OH in naturally occurring corundum. *European Journal of Mineralogy*; July, August 2006; v. 18; no. 4, 441-447. DOI: 10.1127/0935-1221/2006/0018-0
- Cuccureddu, F., Murphy, S., Shvets, I.V., Porcu, M. and Sidorov, S.I. 2010. Surface Morphology of c-plane sapphire produced by high temperature annealing. *Surface Science* 604:1294-1299
- Curiotto, S. and Chatain, D. 2009. Surface morphology and composition of c-, a- and m-sapphire surfaces in O₂ environment. *Surface Science* 603: 2688-2697
- Heffelfinger, J.R., Bench, M.W. and Carter, C.B. 1997. Steps and the structure of the (0001) alumina surface. *Surface Science* 370: L168-L172
- Smith, C. 1995. A contribution to understanding the infrared spectra of rubies from Mong Hsu, Myanmar, *J. Gemm.*, 1995, 24, 5
- Peretti, A. 2008. New Important Gem Discovery in Tanzania: The Tanzanian "Winza" (Dodoma) Rubies. *Contributions to Gemmology* No. 7, April 2008.

Acknowledgements

The research on micro to nano surface features of gem corundum has been granted by the GIT. The Science Equipment Centre, Faculty of Science, Kasetsart University is thanked for access to the AFM facility. Appreciations are also extended to staff at the GIT, Department of Earth Sciences, KU, and the Gem and Mineral Sciences SRU for their generous support and assistance.

Putting LEDs to work for gemmology

Manfred Eickhorst

System Eickhorst, Hamburg, Germany meickhorst@eickhorst.com

LEDs, the future illumination for gemmology, are a very special story of faith, hope but also performance. I have been eyewitness of this development over decades and also engaged myself as designer of various gemmological instruments and luminaries.

Microscopy and Spot illumination

The fibre-optic cold-light illumination was the first illumination workhorse. It entered gemmology in the 1970's and replaced the incandescent bulbs which produced much heat and yellow light. Today the first 1 Watt LED spot-light on a goose-neck guide is available.

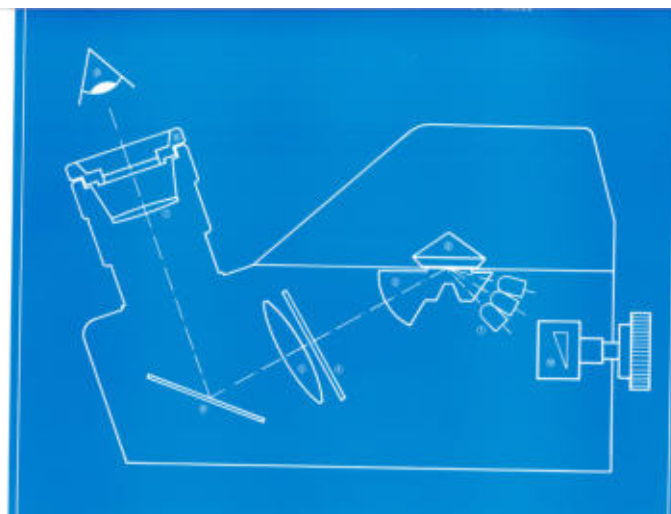
Spectroscopy

The problem in spectroscopy was to get fairly bright and well focussed light into the gemstone examined. Fibre-optic cold-light has greatly advanced lighting for spectrometers and LEDs may become a valid alternative for the future.

Refractometry

In 1980 the author filed a patent for the application of LEDs in refractometers. LEDs were the perfect substitution of the historic sodium vapour lamp, the standard for monochromatic 589 nm refractometer illumination. The direct arrangement of three LEDs bundled next to the refractive hemicylinder provided sufficient light intensity and brought LEDs the final breakthrough (Fig. 1). The first patent, granted in the United Kingdom, attested the basic idea of this configuration: the use of punctual mono-chromatic LED light of 589nm for compact illumination INSIDE the refractometer.

Figure 1. Longitudinal section through a dimmable long-scale refractometer fitted with three internal LEDs in front of the hemicylinder, developed and patented by System Eickhorst, Hamburg.



The low development of heat as well as the option of battery operation were luring details for me as an innovator. The end of the production of sodium vapour lamps – with Phillips as the last manufacturer – accelerated the application of this new light source, a product from the solid state world of semi-conductors and transistors. Due to the low power of 0.01 Watt each, no one ever thought of using LEDs as universal illumination 30 years ago – but that is exactly what has happened in the meantime.

Microscopy and General lighting

In the past decades, the luminous efficiency of LEDs has been boosted, starting with 10 lumen per Watt. The state of the art today is 50 lm/W and up to 80 lm/W.

The actual success story began in the last years with the availability of 1-5 Watt LEDs for gemmological purposes as well as for common illumination.

Again due to the low lighting intensity, the application for the close-up-range was the beginning of a new illumination for gemmologists.

For example, pin-pointers with 1W LEDs instead of fibre optics became an interesting solution for designers of gem microscopes. In addition they were more economic and less faulty than fibre-optic illuminators during their lifetime. Then came coaxial incident lighting for microscopes in replacement of the former fluorescent ring lights.

Now we stand at a crossroad in microscopy: Should the illuminance be diffuse for colour grading or should diamonds be made to sparkle to impress the end consumer ?

The decision for either plain diffuse illumination or punctual illumination is imposed on the designer of instruments or luminaries. Indeed LEDs are also able to illuminate plainly but only in combination with a diffusor. But the diffusor is swallowing a lot of light intensity – which is exactly what LEDs inherently do not produce!

This can optimally be described with the example of darkfield illumination for gemmological microscopes. A circular ring of 10-20 LEDs will make a highly refractive precious stone to sparkle – but does not ease the examination of the gemstone. This is documented by various microscope types.

The first LEDs comparable in lighting power to that of a 25 Watt quartz halogen light source became available very recently in the new GEMMASTER LED microscope, ideal for indirect illumination. An additional attractive aspect for the gemmologist, apart from the good intensity and choice of lighting colours, is the minimal production of heat. No more hot microscope stages after ten minutes of working, only.

It is remarkable that this is also the moment of truth for the fibre optic coldlight sources. An extremely powerful LED source can be presented now for this important gemmological tool. The lighting power of a 150W coldlight source by means of LEDs has been reached. The charm of LEDs is the lighting colour which, for the first time, can produce daylight character without the disadvantage of using filters. The life-time of LEDs is almost limitless compared to that of conventional quartz halogen bulb light sources.

Diamond colour grading will present a new application for LEDs, avoiding the problem of overgrading because LEDs possess a daylight spectrum and do not contain longwave UV components - which stimulate unwanted diamond fluorescence. In the early days of diamond grading, incandescent yellow light was transformed with a blue filter into "daylight". Today there is the possibility of grading natural body colours of diamond in authentic "day"light.

The characteristics of digital photography applied to photomicrography of gemstone inclusions

Michael F. Hügi, M.Sc. FGA

Head of the Scientific Commission, Swiss Gemmological Society, Bern, Switzerland michael.huegi@gemmologie.ch

This presentation covers some new technical possibilities of digital photomicrography of inclusions in gemstones and the subsequent image processing. The overwhelming success of the digital photography technique in the last decade gives rise to new possibilities to overcome the system-related constraints of conventional photomicrography, e.g. the small range of contrast sensitivity of photographic films or the limited depth of field. Thus, digital imaging leads to results, which are close to the real visual impression of microscopic observations.

(1) Development of analogue photomicrography

First attempts of photographic documentation of microscopic features in minerals have been made in the late 19th century. Photomicrography became an indispensable tool to gemmology, although some scientists as F. Zirkel (1873) criticised its restricted focal depth and the lacking possibilities to omit irrelevant details compared to hand drawing (Fig. 1).

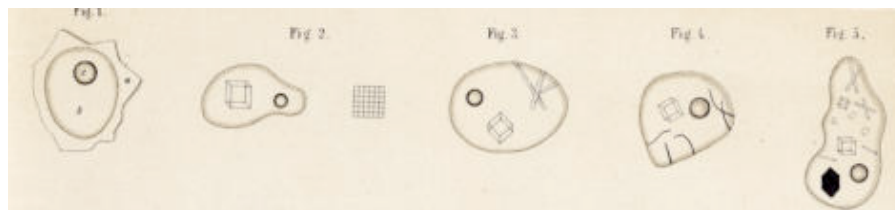


Figure 1: Drawing of multiphase inclusions by F. Zirkel in his work «Die mikroskopische Beschaffenheit der Mineralien und Gesteine», 1873.

Early applications of gemmological photomicrography were published in the works by H. Michel (1914, Fig. 2) and by E. Gübelin (1953), who showed the usefulness of inclusions for origin determination of gemstones. J. Koivula (1981 and 2003) published important contributions to photomicrographic methods. Many of these techniques are still valid in the digital era. The probably most comprehensive work on internal characteristics of gems are the three tomes of the «Photoatlas of Inclusions in Gemstones» by E. Gübelin and J. Koivula (1986, 2005, 2008), which sets standards of analogue photomicrographic techniques.

The improved lens speed of modern gemmological microscope optics as well as the availability of stronger light sources (halogen bulbs or LED illumination) allow nowadays the use of polarised light as standard method of gemmological microscopy. With a polarizing filter mounted on the microscope, blurring of the image due to birefringence can be suppressed. Furthermore, working with crossed polarisers enables the examination of inner characteristics of a stone, e.g. as anisotropic mineral inclusions, twinning planes and anomalous double refraction.

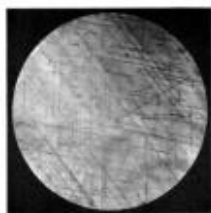


Figure 2: One of the earliest photomicrographs of inclusions in gemstones: Rutile in Burmese ruby, published by H. Michel in 1914.

(2) Digital photomicrography

A principal advantage of digital photography is that it is possible to process a series of images taken with different settings to a compound picture, which corresponds more to the real visual impression of the microscopic observation than a one-shot photo. This method can be applied in order to extend the contrast range of a photo (HDRI) as well to increase the focal depth of a scene.

(a) Extension of the range of contrast sensitivity (High Dynamic Range Imaging, HDRI)

The luminance range in natural environment, i.e. the contrast ratio of light and dark areas, has typical values of about 1:10'000. When taking photographs of inclusions in gemstones, light spots, e.g. reflecting facets or inclusions with metallic lustre, can considerably increase this value. While the human visual perception is able to cope with such strong contrasts, the dynamic range of photo sensors even of modern digital cameras or photographic films has values of only about 1:1000 and is therefore too limited to represent the entire contrast range of a scene in one exposure.

High Dynamic Range Imaging (HDRI) represents a new method of processing digital images, which allows the reproduction of luminance ranges far beyond those available previously. In a first step, a series of photos with different exposures are taken (exposure bracketing), so that the entire luminance range of the scene is covered (Fig. 3). As a second step, these source photos are combined by specific software (such as Photomatrix Pro, Photosphere, Photoshop) to one HDR-image with a 32-bit colour depth. As it is not possible to reproduce these HDR-images by conventional media as computer monitors, beamers or by printing techniques, it is necessary to compress the HDR-image to a reproducible 8-bit photo by a third step called «tonemapping». If this process is applied correctly, the result will be a well-balanced photo mimicking the impression of the human visual perception.

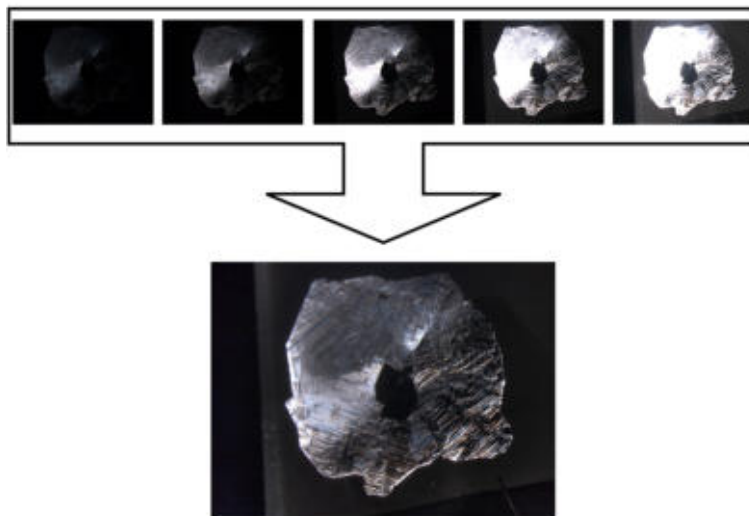
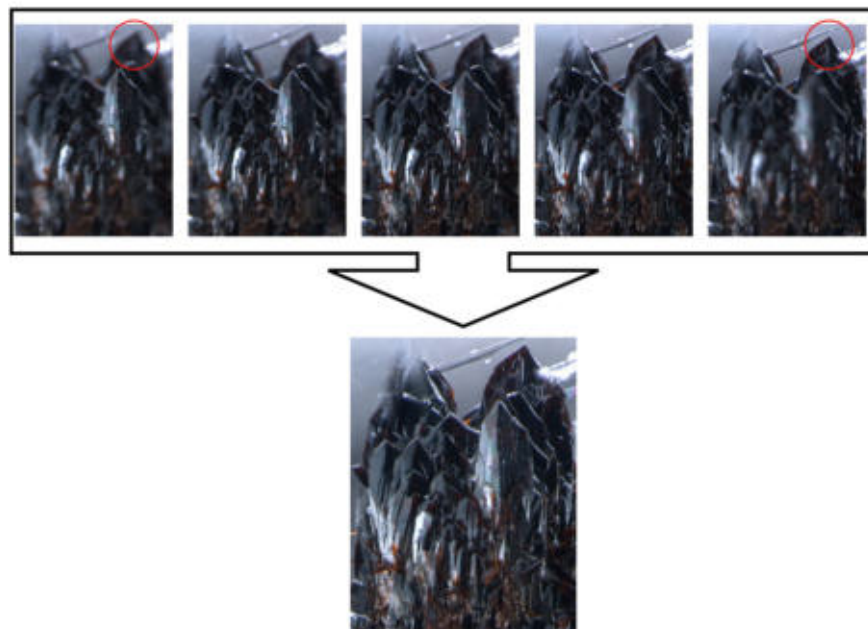


Figure 3: Hematite in quartz from Minas Gerais, Brazil. Width of field approx. 12 mm. Top row: 5 source images, exposure bracketing with -4 EV, -2 EV, 0 EV, +2 EV and +4 EV (exposure value). Bottom: HDR-Image after tonemapping. Within both the light and shadow areas of the hematite crystal details are well recognizable.

(b) Extension of focal depth

During the visual microscopic examination, the observers brain records the spatial distribution of the inner characteristic of gemstones by the continuous adjustment of the focus on different levels. However, when taking a photomicrograph, the focal depth is reduced to the fixed focal plane of the exposure. With increasing magnification, the focal depth even decreases, so that a three-dimensional object is only partially in focus. Digital imaging and subsequent specific computer processing allow a controlled extension of the focal depth in order to produce im-ages of even relatively big objects entirely within focus. After taking a series of several shots of an object at

different levels of the focal plane (focal bracketing), the processing with specific software (e.g. Syncroscopy Auto-Montage) produces an image with the desired focal depth (Fig. 4). This method allows not only the extension of the focal depth; it may also serve as a first step of more extensive 3D-modelling or spatial analysis of internal characteristics of gemstones.



*Figure 4: Columbite-tantalite in aquamarine from Shigar Valley, Northern Pakistan. Height of field approx. 2.3 mm
Top row: 5 source images, focal bracketing with incremental lowering of the focal plane from left to right. Circles: the same object, in resp. out of focus. Bottom: Processed image with Syncroscopy Auto-Montage: the focal depth is extended throughout the whole field of view.*

Digital photomicrography in combination with adequate image processing provides a great opportunity for gemmologists to reproduce his or her visual observation closer to reality than ever. But as these methods also bear the danger of fraudulent manipulation, they impose the responsibility on the gemmologist to reproduce the objects how they are, and not how they should be.

References

- Gübelin, E., 1953. Inclusions as a Means of Gemstone Identification. Gemological Institute of America, 220 pp.
- Gübelin, E., Koivula J., 1986. Photoatlas of Inclusions in Gemstones, Vol. 1. ABC Edition, Zürich, 532 pp.
- Gübelin, E., Koivula J., 2005. Photoatlas of Inclusions in Gemstones, Vol. 2. Opinio Publishers, Basel, 829 pp.
- Gübelin, E., Koivula J., 2008. Photoatlas of Inclusions in Gemstones. Vol. 3. Opinio Publishers, Basel, 672 pp.
- Koivula, J., 1981. Photographing inclusions. *Gems & Gemology*, Vol. 17, No. 3, pp. 132 – 142.
- Koivula, J., 2003. Photomicrography for Gemmologists. *Gems & Gemology*, Vol. 29, No.1, pp. 4 – 23.
- Michel, H., 1914. Die künstlichen Edelsteine. Wilhelm Diebener, Leipzig, 109 pp.
- Zirkel, F., 1873. Die mikroskopische Beschaffenheit der Mineralien und Gesteine. Wilhelm Engelmann, Leipzig, 500 pp.

Gem characterization of sérandite from Québec, Canada

Sutas Singbamroong and Nazar Ahmed

Gemstone and Precious Metal Laboratory, Dubai Central Laboratory Department, Dubai Municipality, Dubai, United Arab Emirates, sssutas@dm.gov.ae

Sérandite, $\text{Na}(\text{Mn}^{2+}, \text{Ca})_2\text{Si}_3\text{O}_8(\text{OH})$, is a unique mineral found at Mont Saint Hilaire, Québec, Canada. It has very distinctive colour of slightly pinkish orange or “salmon” with silky luster and usually occurs in tabular or prismatic crystals. Nevertheless, gem quality of the crystals is rare, therefore, mostly very small faceted or translucent-to-opaque sérandite have been seen. Limited gemmological and spectroscopic data are available. This study presents a more complete characterization of these samples showing unusual size and gem-quality.

9 faceted slightly pinkish orange gem-quality sérandite samples ranging from 0.70 to 2.86 ct (Fig. 1) were studied using standard gemmological and spectroscopic methods including UV-Vis and IR absorption spectroscopy, Raman scattering, and EDXRF chemical analysis. The refractive indices were $n\alpha = 1.675\text{-}1.676$, $n\beta = 1.680\text{-}1.681$, $n\gamma = 1.710\text{-}1.711$; birefringence $+0.036$; pleochroism-strong yellow and pink; hydrostatic SG 3.37 and 3.45; UV fluorescence-all nine samples were inert to both long- and short-wave UV radiation; Chelsea filter reaction-none; and absorption band at about 500-550 nm with desk-model spectroscope. Microscopic observation revealed as main internal characteristics “fingerprints” composed of fluid remnants and two-phase fluid-gas inclusions and clusters of small transparent pyrochlore crystals and brown acicular and prismatic aegirine crystals both identified by Raman spectroscopy.



Figure 1. Nine faceted slightly pinkish orange gem-quality sérandite samples ranging from 0.70 to 2.86 ct.

UV-Vis absorption spectra were characterized by a broad band centred at 520 nm, with a shoulder at approximately 420 nm and sharp peaks at 342, 357, 408 nm with increasing absorption toward the UV region (Fig. 2). These features are typical of Mn^{2+} absorptions and cause the colour of sérandite.

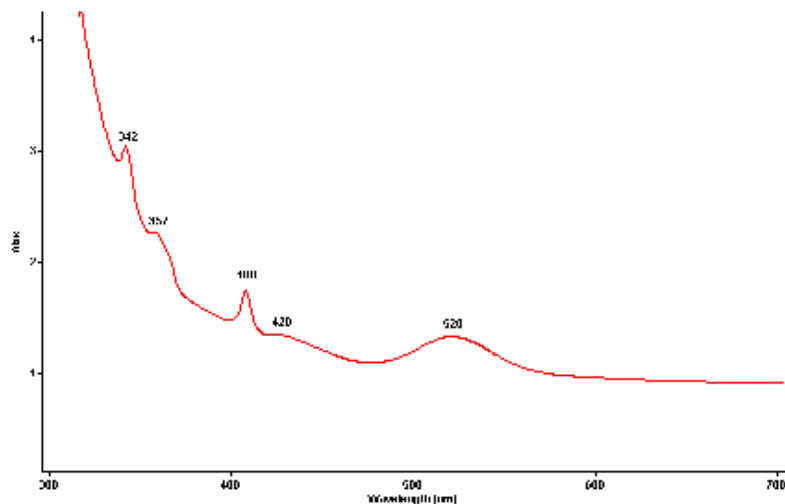


Figure 2. UV-Vis spectrum revealed typical Mn^{2+} absorptions which cause the colour of sérandite from Québec, Canada.

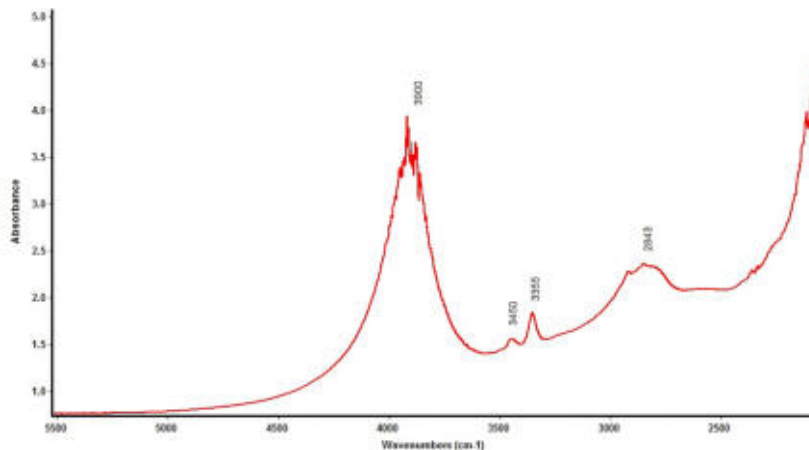


Figure 3. The strong Mid-IR spectrum band at 3900 cm^{-1} is due to structural OH, a major component of sérandite.

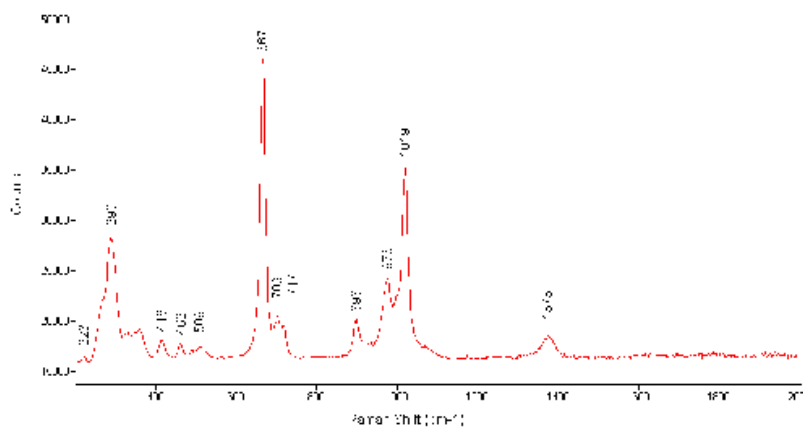


Figure 4. Raman spectrum of sérandite from Québec, Canada.

The Mid-IR spectra exhibited complete absorption below 2100 cm^{-1} and prominent absorption band at 3900 cm^{-1} . Less prominent bands were also present at 3450, 3355 cm^{-1} with broad absorption band centre at about 2843 cm^{-1} (Fig. 3). The strong band at 3900 cm^{-1} is due to structural OH, a major component of sérandite.

Raman shift spectra showed several sharp peaks at 1019, 976, 898, 703, 667, and 290 cm^{-1} and smaller peaks at 1373, 509, 462, 416 and 223 cm^{-1} (Fig. 4). The spectral pattern is similar to those reported for sérandite in the RRUFF project database.

EDXRF analyses showed major amounts of Si and Mn, and traces of Ca and Fe. Na cannot be detected by EDXRF. The predominant concentration of Mn over Ca is characteristic of sérandite from Québec.

Reference

Kammerling R.C. et al., 1995. Faceted sphalerite and other collector stones from Canada, Gem News, Gems&Gemology, Vol. 31, No. 1, pp. 65-67.

The care and handling of large gemstones

Michael Gray

Coast-to-Coast Rare Stones P.O. Box 1328 Fort Bragg, California 95437 gemst1@gmail.com

Every laboratory eventually will be called upon to identify a large gemstone in the course of business. But what makes a gemstone large? It depends on the species, the origin, or even the colour. Most people in this conference know what the largest diamonds are, possibly the largest rubies and sapphires, spinels, and emeralds. But what about other species that might come through the laboratory, such as quartz, topaz, spodumene, or peridot? And what about the lesser known materials, such as calcite, fluorite, or benitoite?

How are they cut? Large gemstones present their own set of problems during fashioning that may cost many times more than “normal” stones.

There are several factors to consider when taking in large gems. First might be transportation. Many stones that are large for their species are easily packaged for transport, but what about stones that weigh thousands of carats? The stone may arrive safely, but how does one ensure that it makes it back to the client in the same condition?

Then there is the valuation of the large gemstones. Because of their provenance, they may be worth more per carat than their small counterparts. But that may not always be true.

What happens if a large stone is damaged in your care? Costs for repairs are much higher than on smaller stones, because of the larger amount of time for preparation, along with the cutting and polishing and the more substantial loss of weight. Then there is the expense of transportation and insurance above that of shipping smaller stones.

The talk will be highlighted with examples of large gemstones, how they are cut and polished, and peppered with personal experiences of problems and solutions in handling these behemoths of our industry.



While only weighing 10.01 carats, this Hiddenite, the Cr-green variety of spodumene, from North Carolina, USA, is considered the largest and finest specimen to come from the type locality of hiddenite. Collection of Elvis Gray and Bernadine Johnston.

An organic gem material of proposed name “rostellite” derived from the fossilized beaks of whales of the family Ziphiidae

Stephen Webb

19 Wastney Terrace, Nelson 7010, New Zealand skwebb@xtra.co.nz

Ian Longley

Concepts in Stone, Founders Park, 87 Atawhai Drive, Nelson 7010, New Zealand longley@xtra.co.nz

Spencer Currie

Grace Jewellers, PO Box 72566, Papakura 2244, New Zealand spencer_currie@vodafone.co.nz

A novel ornamental material derived from the unusually dense fossilized upper jawbone of beaked whales is described. Although the material is prehistoric, beaked whales (Family Ziphiidae) are still extant and some 20 species are known. Living whales have a dolphin-like appearance, range in length from 4 to 12 metres (Bianucci et al. 2008) and are reported worldwide (McLeod et al. 2006).

These fossils date from between 2.5 million to about 20 million years ago (Miocene / Plio-cene). The material occurs on sea beds world wide: it has been recovered during commercial and research fishing operations from the North Sea, North Atlantic, the coasts of Florida, California, the Clarion-Clipperton fracture zone of the Pacific, Peruvian coast, south of Tasmania, Japan, South Africa (Bianucci et al. 2007, 2008) and New Zealand.

This material is attractive (Figures 1 and 2) not only because of its gemmological properties but also because it makes available a cetacean-derived product that poses no threat to living whales. Moreover, this resource is a by-product and not a cause of current marine harvesting activities.

Description

The material is cream-coloured and mottled with green and brown patches. Under magnification it appears as a very dense crystalline aggregate containing black dendritic areas, whorl patterns (Fig. 3) and small branching stick-like inclusions (Fig. 4). Bianucci et al. (2007) describe the material as phosphatised and glauconised bone. Indeed, the material shows presence of minerals in the bone voids (Fig. 4) and the patches of green (Figures 1 and 6) are suggestive of glauconisation. The material is similar, but not identical, to odontolite as described by Liddicoat (1993).

Reaction to acid

The material reacted readily to concentrated hydrochloric acid evolving small bubbles suggesting the presence of carbonate. Effervescence also occurred with dilute HCl. At a concentration of 0.25M (0.9%), rostellite evolved bubbles, but far fewer than that exhibited by calcite in a comparison test.

Luminescence under ultra violet

Twenty pieces were examined giving creamy fluorescence in paler areas and none in darker areas. Fluorescence was brighter under long wave than short wave. No residual phosphorescence was noted.

Spectra

Two pieces were examined by transmitted visible light and ten pieces by reflected visible light: no bands or patterns were seen. FTIR spectrum is shown in Fig. 7.



Figure 1. Partially finished cuts of rostellite showing patterns on longitudinal (lower) and transverse sections with voids in the material (upper). The small scale graduations are mm.

Figure 3. Transverse section showing Haversian systems as whorls.

Figure 5. Use of fibre optic light to demonstrate translucency. The piece is $\approx 45\text{mm} \times 35\text{mm} \times 7\text{mm}$.

Figure 2. Finished rostellite items. The square cut is side 14mm.

Figure 4. Longitudinal section showing mineralised blood vessel cavities.

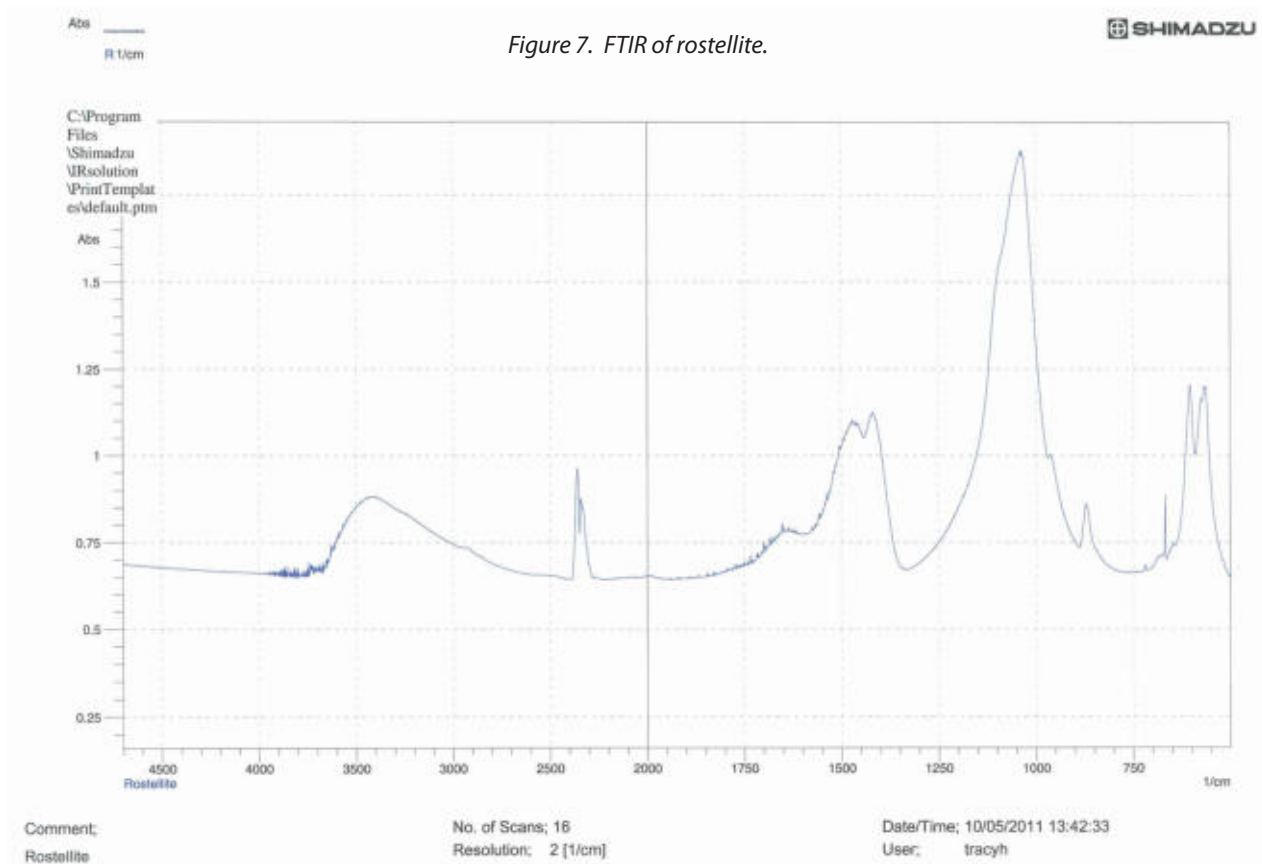
Figure 6. Cabochons of rostellite, left (25mm x 15mm) longitudinal cut showing grain effect, right transverse cut showing block-like distribution of colour.

Light transmission

Darker areas are opaque. Lighter areas can be translucent or opaque – a 7mm thickness was translucent (Fig. 5) and a 6mm thickness was opaque.

Fracture

Uneven, evidence of grain similar to wood in some longitudinal fractures.



Refractive index

Minimum 1.590, maximum 1.601. Ten samples were examined. One gave one shadow edge at 1.595 regardless of rotation. On rotation the others gave maximum and minimum readings that could be estimated after resolution with a polarising filter. Birefringence varied from 0.000 to 0.100 with a mean value of 0.050. The shadow edges were more diffuse than those seen in typical single crystal specimens such as quartz. This is probably due to the polycrystalline nature of rostellite. The poor definition of the shadow edges prevented observation of their range of movement, hence the optic sign could not be ascertained.

Although carbon dioxide was evolved from the material with acid, the refractive properties are far from those of carbonates. It is tentatively suggested that a CO₂ rich apatite such as francolite, reported in some fossil bones (Elorza et al., 1999), might be responsible. Here the CO₂ is thought to be incorporated into the apatite molecular structure (Deer et al., 1992). This, in addition to the polycrystalline nature, might help account for the smaller birefringence which is closer to francolite (0.013) than calcite (0.172) (Deer et al., 1992).

Hardness

Just under 5. All hardness tests were performed under a x20 binocular microscope to assess which surface was scratched. The material scratches fluorite but is not scratched by fluorite which indicates its hardness above 4. It is scratched by but does not scratch apatite which suggests that it is slightly softer than apatite.

Lustre

vitreous when polished.

Specific gravity (hydrostatic)

Ten samples (approximately 5 to 9 g) were assessed using a Tanita model 1210N balance. Mean = 2.79, maximum = 2.83, minimum = 2.70. The distribution of voids in the material probably accounts for the variability of these data.

Working and polishing

Although it is fairly soft, diamond tools are necessary for satisfactory working of this material. It is then easy to cut, shape and polish to a glassy finish. Since it is somewhat brittle and easily fractured during working, it is more suited to cabochons and mounted items rather than finely detailed pieces and ring stones. The material exhibits a wide range of pattern and colour that lends itself to producing items with a strong visual impact. This is influenced by cutting orientation, variation in infiltration of minerals and possibly by the species. Working qualities also vary with orientation: pieces cut lengthways have an open fibrous texture - similar to whale skeletal bone. Transverse cuts appear denser and can allow a more brilliant polish.

Standard working procedure

- Diamond trim saw with water coolant to cut.
- 220 grit diamond wheels and discs with water coolant for initial shaping.
- 220, 400, 600 grit carborundum sandpaper (wet) sanding process.
- 600 grit carborundum sandpaper (dry); avoid overheating the stone.
- Tin oxide paste on leather wheel to polish. Avoid excessive pressure or overheating.

Nomenclature

Any gem/ornamental material benefits from a suitable name that is descriptive, easy to spell, concise and euphonious. The name *rostellite* is proposed as it meets these requirements; *rostellum* being the diminutive of the Latin word *rostrum* beak.

Compliance issues

Although ziphiids are on Appendix II of CITES (Convention on International Trade in Endangered Species), fossils are exempt. Nevertheless, local jurisdictions may limit inter-national movement under legislation such as heritage and antiquities Acts.

References

- Bianucci, G., Lambert, O., Post, K., 2007. A high diversity in fossil beaked whales (Mammalia, Odontoceti, Ziphiidae) recovered by trawling from the sea floor off South Africa *Geodiversitas* 29(4): 561-618.
- Bianucci, G., Post, K., Lambert, O., 2008. Beaked whale mysteries revealed by seafloor fossils trawled off South Africa. *South African Journal of Science* 104, March/April 2008.
- Deer, W.A., Howie, R.A., Zussman J., 1992. *An Introduction to Rock Forming Minerals* 2nd edition. Longman, 696pp.
- Elorza, J., Astibia, H., Murelaga, X., Pereda-Suberbiola, X., 1999. Francolite as a diagenetic mineral in dinosaur bones (Laño Iberian Peninsula): microstructural, petrological and geochemical features. *Cretaceous Research* 20, 169-187.
- Liddicoat, R.T., 1993. *Handbook of gem identification* 12th Ed, 4th printing. Gemological Institute of America, 364pp.
- MacLeod, C.D., Perrin, W.F., Pitman, R., Barlow, J., Balance, L., D'Amico, A., Gerrodette, T., Joyce, G., Mullin, K.D., Palka, D.L. and Waring, G.T., 2006. Known and inferred distributions of beaked whale species (Cetacea: Ziphiidae). *Journal of Cetacean Restoration and Management* 7(3): 271-286.

Identification of organic gems from endangered species: An Overview

Stefanos Karamelas

Gübelin Gem Lab, Maihofstrasse 102, Lucerne 6006, Switzerland e-mail: s.karamelas@gubelingemlab.ch

Organic (actually organogenic) gems are directly formed through biological processes; i.e., materials of animal and plant origin used in jewellery. Several of the organic gems' host animals and plants belong to endangered species and their trade is controlled to avoid use that would threaten their survival. CITES (Convention on International Trade in Endangered Species of Wild Fauna and Flora) is the most widely accepted convention which governs the trade of endangered species.

There are three appendices in the CITES regulations which describe the type of the protection of the endangered species. Appendix I covers species threatened with extinction (trade in these species is permitted only in exceptional circumstances, e.g. old material –before the inclusion of this species in CITES-; or purely scientific research). Appendix II covers species that are not necessarily threatened with extinction but whose trade must be controlled to avoid use that would threaten their survival (a certificate issued by the management authority of the country -or state- of export/import -re-export- is required for any new material released). Appendix III covers species that are protected in at least one country. Even though the CITES is respected (almost) worldwide, some legal issues are still open, e.g. international ivory trade remains one of the most controversial wildlife trade issues (Reifenstein et al., 2008). Some countries (or states) apply the agreement in slightly different ways (Pedersen, 2010). More information on the exact legalization as well as a full list of protected species can be seen on the CITES website, www.cites.org.



*Figure 1a: Beautiful pearls with spectacular flame structures could be found inside the *Strombus gigas* gastropod. These are mainly pink coloured, however pearls of other colours can also found. This shell is about 15 cm long and the white pearl is 10 mm long.*



*Figure 1b: Beautiful pearls flame structures could be found inside the *Cassis spp* gastropod. These are mainly light brown coloured, however pearls of other colours can also found. This shell is about 12 cm long and the pearls are 10 mm.*

In this abstract, a brief overview of some of the most common organic gems submitted to gemmological laboratories for reports and means to identify them are given. Natural pearls are by far the most common organic gems submitted. Several molluscs (mainly bivalves and gastropods) are protected by CITES; the best known to gemmologists are the gastropods *Strombus gigas* («queen conch») which is listed in the Appendix II of CITES (see Fig. 1a). These animals are fished principally in the Caribbean region for their meat (Federman et al., 2007). Beautiful natural pearls with spectacular flame structures may be found inside (Fritsch & Misiorowski, 1987; Federman et al., 2007; Hänni, 2010); attractive pottery and cameos are done with their shell. It is rare that «queen conch» pearls (and shells) are accompanied with the needed CITES certificates. Moreover, there are other molluscs containing similarly flame structured pearls, e.g. *Cassia* spp., the «emperor helmet» mollusc (see Fig. 1b). In most cases, separation of coloured pearls and cameos from the two gastropods cited above cannot be done only using «classical» gemmology (i.e., microscope, UV lamps etc.), but separation is usually possible by means of UV-Vis spectroscopy. This is because even if two pearls from the two molluscs present the same surface patterns and colours, they give slightly different spectra in the ultraviolet region (Karamelas et al., unpublished data). Successful cultivation of *Strombus gigas* gastropods (Wang et al., 2009) as well as close surveillance of the *Strombus gigas* quotas, would probably change the actual situation.

Tridacnidae spp. bivalves («giant clams») are also fished for their meat. They are also used as holy water stoup in catholic churches (a.k.a. «bénitier»). Pearls are occasionally found in the shells which are mainly white and sometimes show flame structures. Tridacnidae spp. animals as well as their by-products fall under Appendix II of CITES regulations. Other molluscs may also have natural white pearls with similar structures. These are sometimes very hard to separate from «giant clam pearls». Only big sized white pearls (above 20 mm) can be identified using classical gemmology as «giant clam pearls» by their sheer size. «Non-nacreous» white pearls with «flame structures» of this size are rarely found in other molluscs. Sometimes material from the inner part of the «giant clam shell» is used to make beads for pearl culturing (Superchi et al., 2008), which is hard to identify. In some cases, these beads can be identified using LA-ICP-MS (when the pearl is drilled and its geometry permits it; Abduriyim and Kitawaki, 2006) and OCT (optical coherence tomography; Ju et al., 2010).



Figure 2a: Pink coloured *Corallium secundum* from Sandwich islands. From this material can be made highly priced coral beads. Courtesy of MNHN, Paris, image width 10 cm.

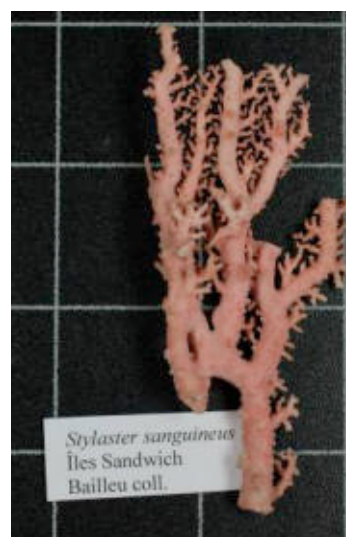


Figure 2b: Reddish pink coloured *Stylaster sanguineus* Sandwich islands. From this material can be made highly priced coral beads. Courtesy of MNHN, Paris, image width 10 cm.

Corals are other organic gems used in jewellery (Fig. 2). The highest priced coral is the pink-to-red coloured variety of *Corallium* spp. Stylaster corals can have these colours too, but they are protected by Appendix II (*Corallium* corals from waters around China are listed in Appendix III). Stylaster corals can usually be identified under the microscope by observing their growth structures, which are different from *Corallium* corals. Sometimes however, no structures are observed on some coral beads under the microscope. In these cases, Raman spectroscopy is a useful tool to separate *Corallium* from Stylaster pink-to-red corals (Figure 3; Karampelas et al., 2009). The identification of the *Corallium* species in China protected by Appendix III is much more difficult. Other protected corals of gemmological interest from the Appendix II are from Tubiporidae spp. ("organ pipe corals"), *Antipatharia* spp. (a category of "black coral"), and *Heliopora* sp. ("blue coral"). Most of them can be identified using "classical gemmology".

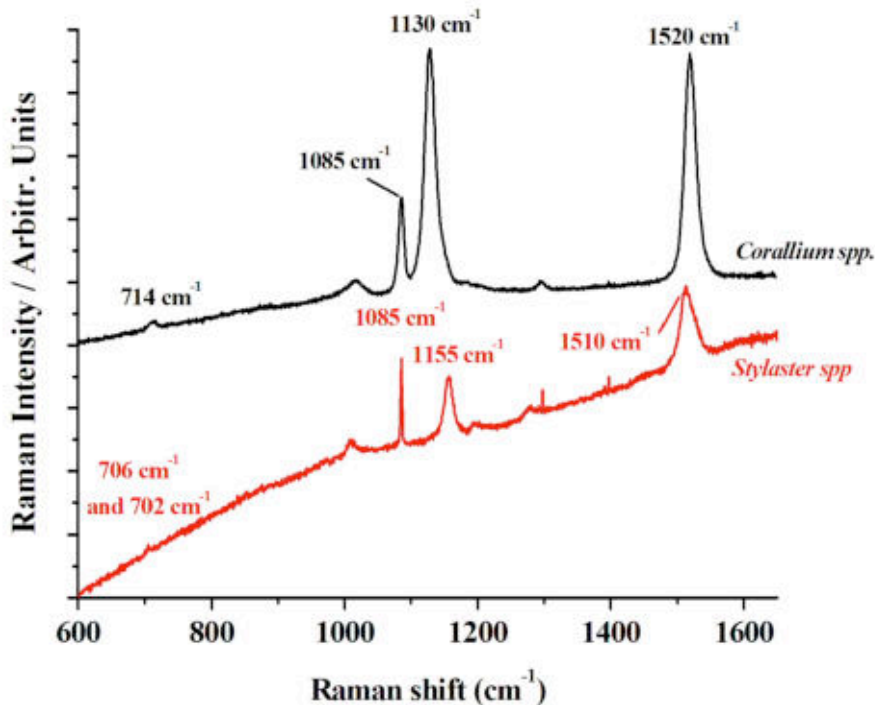


Figure 3: The Raman spectra were acquired using green excitation (acquisition time: 180 sec.). In the spectrum of *Corallium* spp. coral (black line), bands due to calcite are observed at about 714 and 1085 cm^{-1} . The two bands at about 1130 and 1520 cm^{-1} are due to ("unmethylated") polyenic pigments. In the spectrum of *Stylaster* spp. coral (red line), bands due to aragonite at about 702, 706 and 1085 cm^{-1} are observed. The two bands at about 1155 and 1510 cm^{-1} are due to carotenoids ("methylated" polyenic pigments). The spectra have been stacked and shifted vertically for clarity.

Rarely, ivory is submitted to gemmological labs to check if it is protected by CITES; thus its origin must be identified. Sometimes, certification under a microscope can be done easily, noting the presence or absence of Schreger lines. Schreger lines occur in ivory from elephants and mammoths but not in other types of ivory, such as from walrus and hippopotamus. If the Schreger lines are present, the angle where the lines cross can be used to see if it is an elephant or a mammoth ivory. Some of the elephant ivories are protected by CITES while the latter are not. The problem is that growth lines are not always observed on the surface of the ivory under a microscope. In these cases, sophisticated instruments, such as micro-computing tomographs, are used to identify them (Schwarz et al., unpublished data). If it is an elephant ivory, studies of spectroscopic features, chemical (and isotopic) composition, and sometimes slightly destructive DNA analysis should be used in order to identify the possible geographi-

cal origin of the specimen (Banerjee et al, 2008; Jacob et al, 2008; Cutler & Götherström, 2008).

In the future, more gems may be listed in the CITES Appendices (e.g. pearls from *Melo* sp. gastropods) and some others could be excluded (e.g. *Strombus gigas* gastropods). Moreover, there are some organic gems protected by CITES that still cannot be identified properly (e.g., there are some freshwater molluscs, mainly from Unionidae family, protected by CITES -Appendix I and II- such as *Unio* sp., *Quadrula* sp., *Potamilus* sp.). Gem labs may face more problems in identifying some CITES protected organic gems, requiring a compilation of highly sophisticated non- (or micro-) destructive methods. Among these are radiography and X-ray micro-computed tomography for inspection of their internal structures, XRF and LA-ICP-MS for their chemical analysis, and Raman, FTIR, and UV-Vis-NIR spectroscopy. Thus, gemmological laboratories should be constantly aware of the CITES updates and continue to do research on them (updated appendices could be found in the following link: <http://www.cites.org/eng/app/index.shtml>).

Acknowledgements

The author thanks Muséum National d'Histoire Naturelle in Paris, Dr. Benjamin Rondeau (University of Nantes, France), Pr. Emmanuel Fritsch (University of Nantes, France), Mr. Thomas Hainschwang (GGTL, Gemlab-Gemtechlab located in Balzers, Liechtenstein, and Geneva, Switzerland), Dr. Jens-Oliver Schwarz (Institute of Geosciences at Johannes Gutenberg University of Mainz, Germany), as well as the International Centre of Ivory Studies (INCENTIVS; Johannes Gutenberg University of Mainz, Germany) for the samples of this study and the fruitful discussions.

References

- Abduriyim, A., Kitawaki, H., 2006. Applications of LA-ICP-MS (Laser Ablation-Inductively Coupled Plasma-Mass Spectrometry) to the gemmological field. *Gems&Gemology*, 42 (3), 87-88.
- Banerjee, A., Bortolaso, G., Dindorf, W., 2008. Distinction between African and Asian Ivory. *Ivory and Species Conservation Proceedings of INCENTIVS Meetings 2004-2007*, 37-49
- Cutler, A., Götherström, A., 2008. African or Asian? DNA Analysis of Byzantine and Western Medieval Ivories. *Ivory and Species Conservation Proceedings of INCENTIVS Meetings 2004-2007*, 73-79
- Federman, D., Bari, H., Lam, D., Hendrickson, S., Chin, E., 2007. The pink pearl: A natural treasure of the Caribbean. SKIRA Eds, Milano, Italy, 173 pp
- Fritsch, E., Misiorowski, E., 1987. The History and Gemology of Queen Conch "Pearls." *Gems & Gemology*, 23 (4), 208-221
- Jacob, D. E., Stracke, A., Wiegand, B., Dindorf, W., 2008. Tracing ivory by its chemical and isotopic composition. *Ivory and Species Conservation Proceedings of INCENTIVS Meetings 2004-2007*, 93-99
- Hänni, H.A. (2010) Explaining the flame structure of non-nacreous pearls. *Australian Gemmologist*, 24, 4, 85-88.
- Ju, M.J., Lee, S. J., Min, E. J., Kim, Y., Kim, H. Y., Lee B. H., 2010. Evaluating and identifying pearls and their nuclei by using optical coherence tomography. *Optics Express*, 18 (13), 13468-13477
- Karampelas, S., Fritsch, E., Rondeau, B., Andouce, A., Métivier, A., 2009. Identification of the endangered pink-to-red *Stylaster* genus coral by Raman spectroscopy. *Gems&Gemology*, 45 (1), 48-52
- Pedersen, M., 2010. It's so pretty, but is it legal? A look at the jewellery and animal products that we cannot bring back from holiday. <http://www.maggipec.co.uk/Freearticles2.html>
- Reifenstein, V., Kitschke, C., Ziegler S., 2008. Elephant conservation and the ivory trade. *Ivory and Species Conservation Proceedings of INCENTIVS Meetings 2004-2007*, 13-25
- Superchi, M., Castaman, E., Donini, A., Gambini, E., Marzola A., 2008. Nucleated cultured pearls: What is there inside. *Zeitschrift der Deutschen Gemmologischen Gesellschaft*, 59 (1-2), 33-40
- Wang, W., Scarratt, K., Acosta-Salmon, H., Davis, M., 2009. Queen conch cultured pearls: A new gem. *Gems&Gemology eBrief*, (1) 2, Nov. 4, 2009

GemExplorer

*A guide to the world's major sources of
coloured gemstones, diamonds and pearls*

A free app available in iTunes, for more details see www.ssef.ch



SSEF 
SCHWEIZERISCHES GEMMOLOGISCHES INSTITUT
SWISS GEMMOLOGICAL INSTITUTE
INSTITUT SUISSE DE GEMMOLOGIE

Experts in Origin Determination of Gemstones

Mozambique ruby : Indication of low-temperature heat treatment

**Wilawan Atichat¹, Thanong Leelawathanasuk¹, Boontawee Sriprasert^{1,2},
Visut Pisutha-Arnond^{1,3}, Pornsawat Wathanakul^{1,4}, and Chakkaphan Suthirat^{1,3}**

1. The Gem and Jewelry Institute of Thailand (GIT), Faculty of Science, Chulalongkorn University, Bangkok 10330, Thailand; e-mail: wilawan@cholopui.com; awilawan@git.or.th

2. Department of Mineral Resources, Rama 6 Rd., Bangkok 10400, Thailand

3. Department of Geology, Faculty of Science, Chulalongkorn University, Bangkok 10330, Thailand

4. Department of Earth Sciences, Faculty of Science, Kasetsart University, Bangkok 10900, Thailand

Mozambique has become one of the most important sources of ruby in the past few years. Rubies from Mozambique range in colour from purplish red to red and look very similar to stones from Myanmar. The Mozambique stones sold in the market vary from unheated high gem-quality materials to heat-treated ones (including those undergone flux-assisted heat-treatment), and to the most common glass-filled materials. However based on information from many dealers, a number of stones being sold as unheated ruby had actually undergone heat treatment at relatively low temperature (between 500-1000°C) to improve their colour. This issue, therefore, causes concern to our lab because such low-temperature-heated stones are quite difficult to differentiate from the unheated ones.

Being motivated by such concern, GIT has conducted an experiment on a set of rubies from Mozambique (Fig. 1). The samples were heat-treated by an undisclosed burner at 800°C, and then at 1000°C in an electric furnace under oxidation condition to get rid of purple hue. However, the treatment times could not be disclosed.

Microscopic examination of the stones before heating reveals prominent boehmite tubes, various crystal inclusions, cloud and needle-like inclusions. Mineral inclusions found in these samples are mica and amphibole (Fig. 2).

Stones heated at 800 °C still appear to have no significant change of inclusion features, such as undisturbed mineral inclusions and well formed needle like inclusions (Fig. 3). Stones heated at 1000 °C, however, show prominent change of their inclusion features such as melted mica inclusions and typical tension-discoid inclusions, twinning planes with broken tube-like needles. Certain samples show rounded cracks around the melted crystals (discoids) (Fig. 4).



Figure 1. A set of unheated rubies from Mozambique.

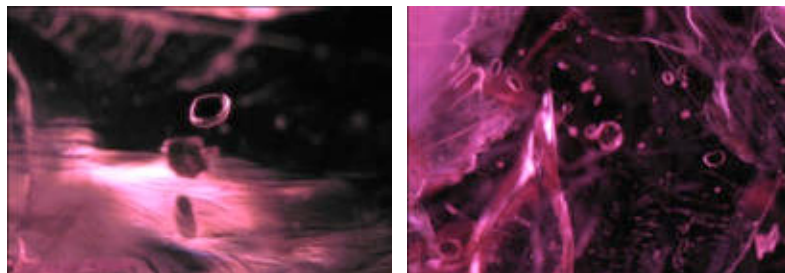


Figure 2. Undisturbed mineral inclusions in unheated rubies.

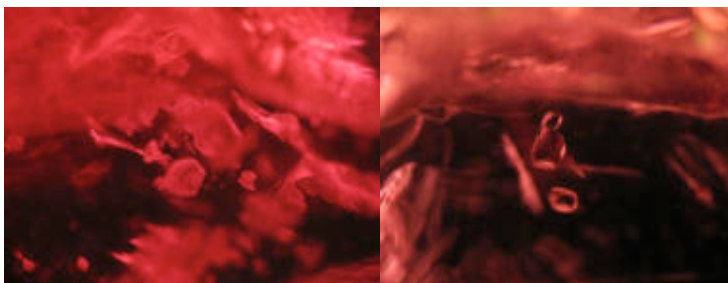


Figure 3. Apparently undisturbed mineral inclusions in rubies after heating at 800°C.

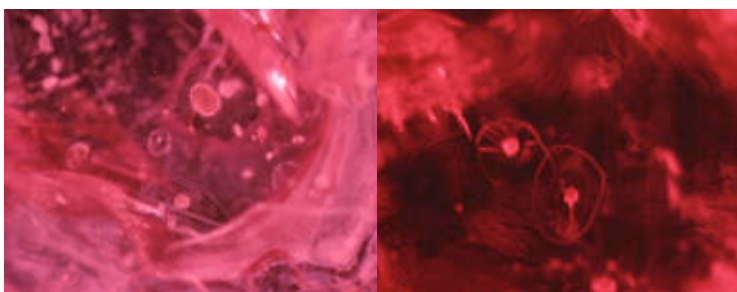


Figure 4. Altered inclusions (mostly mica) in heated rubies at 1000 °C.

Microscopic examination of heated stones reveals no conclusive indication of heating, especially at 800°C but evidences of heating become clearer when stones were heated at 1,000°C. The presence of boehmite which is a heat sensitive and FTIR active mineral inclusion in a number of untreated stones may be helpful to differentiate such heating. For some unheated stones, FTIR spectra show strong IR active bands over the 1250-800 cm^{-1} range with peaks at around 3079 and 3309 cm^{-1} of -OH stretching (Fig. 5), whereas those of heated rubies at 800° and 1,000°C show rather weak or without absorption bands related to hydroxyl mineral (Fig. 6). Hence the presence of strong IR active bands of boehmite is a good indication of unheated stone. Furthermore stones having undergone low temperature heat treatment tend to show the FTIR absorption bands at 3230 and 3309 cm^{-1} . Especially the presence of 3230 cm^{-1} can be used as a good evidence for heating (Fig. 7).

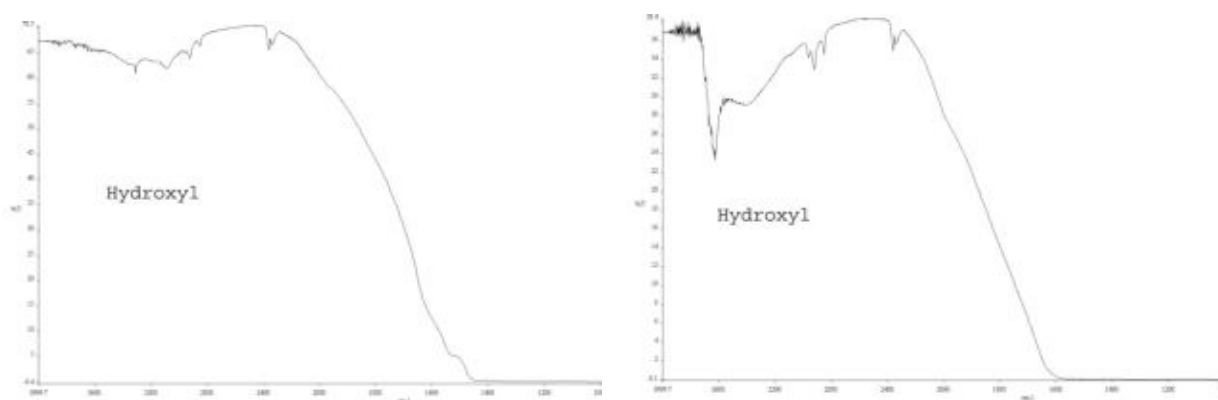


Figure 5: FTIR spectra of unheated rubies from Mozambique showing boehmite absorption peaks.

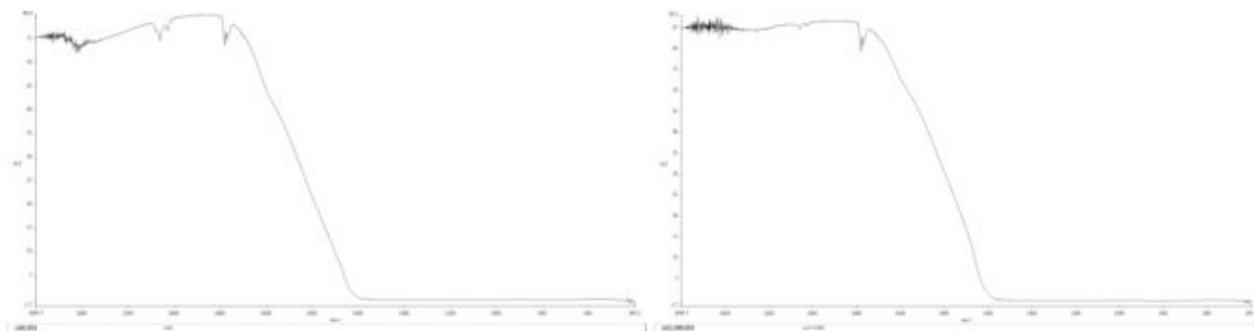


Figure 6: FTIR spectra of Mozambique rubies heated at 800°C (left) and 1000°C (right)

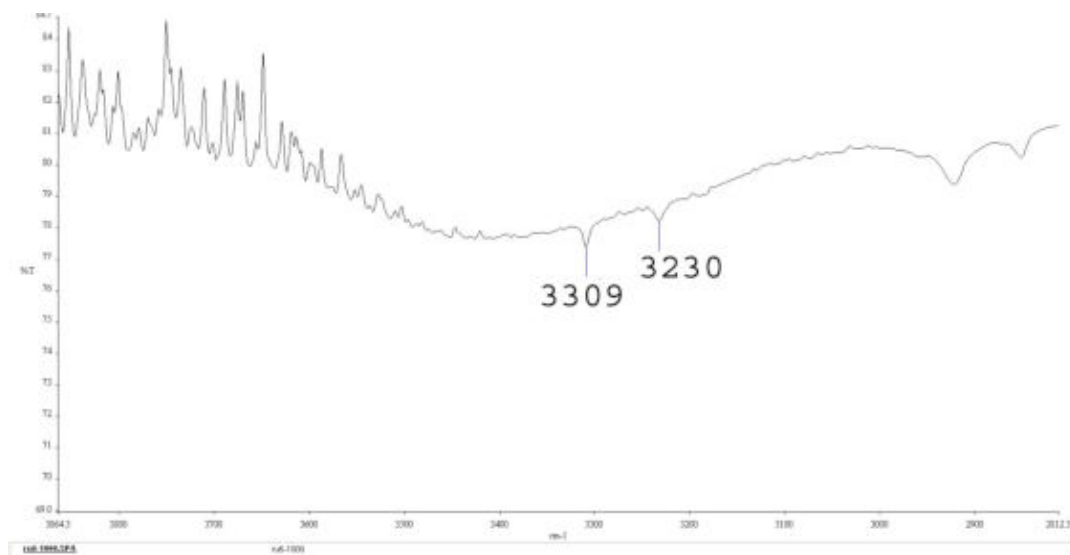


Figure 7: The presence of peaks 3309 cm^{-1} together with 3230 cm^{-1} in heat treated ruby.

In summary, ruby showing disturbed inclusions and the absorption bands at 3230 and 3309 cm^{-1} on the FTIR spectrum strongly implies that the stone was heat-treated, whereas the presence of only strong IR active bands of boehmite appears to be a good indication of unheated stone.

References

- GIT (The Gem and Jewelry Institute of Thailand) Gem testing Laboratory, 2010. "Mozambique" RUBY: AN UPDATE, GIT Lab Review, Issue 2010, 1–6.
- Hänni, H.A., 2008. New rubies from Tanzania. SSEF Swiss Gemmological Institute Newsletter, May 3, 2008.
- Laboratory Manual Harmonisation Committee (LMHC) <http://www.lmhc-gemology.org/>
- Pardieu, V., Thanachakaphad, J., Jacquat, S., Senoble, J.B., Bryl, L.P., 2009. Rubies from the Niassa and Cabo Delgado regions of Northern Mozambique: A preliminary examination with an updated Field Report Annex. http://www.giathai.net/pdf/Niassa_Mozambique_Ruby_September13_2009.pdf

Keywords

Mozambique ruby, low temperature heat-treatment, FTIR spectrum

A photo collage in memory of Dr. Edward J. Gübelin and the many years of his participation in the International Gemmological Conferences and excursions

E. Boehm Geologist, G.G., C.G.
Chattanooga, TN Edward@RareSource.com

The first International Gemmological Conference, took place in 1952 in Locarno, Switzerland, and was organized by Professor K. Schlossmacher and Dr. Edward Gübelin. Others present at the inaugural IGC meeting were B.W. Anderson, A. Bonebakker, O. Dragstead, G. Gobel, K. Siess, and H. Tillander. The original idea for this meeting was due to the restructuring of the Inter-national Jewelry and Gemstone Federation (BIBOA) in which the Gemmological Associations were replaced by National Federal Committees. The federation evolved over the years to become the present day CIBJO.

This year's 32nd IGC in Interlaken brings it back to Switzerland for the third time in its 59 year history, qualifying it as the longest running conference in the field of gemmology to remain in its original format.

This first IGC in Locarno (1952) has been followed by conferences in Amsterdam (1953), Copenhagen (1954), London (1955), Munich (1956), Oslo (1957), Paris (1958), Milano (1960), Helsinki (1962), Vienna (1964), Barcelona (1966), Stockholm (1968), Brussels (1970), Vitznau (1972), Washington D.C. (1975), The Hague (1977), Idar-Oberstein (1979), Kashiko-Jima (1981), Beruwela (1983), Sydney (1985), Rio de Janeiro (1987), Tremezzo (1989), Stellenbosch (1991), Paris (1993), Bangkok (1995), Idar-Oberstein (1997), Bombay (1999), Madrid (2001), Wuhan (2004), Moscow (2007), Arusha (2009)

This photo collage in memory of Dr. Gübelin is intended to give homage to his devotion to the ideals of the IGC and his commitment to attending numerous conferences and excursions throughout the years. This poster is also in honour of his friends and colleagues that shared his passion and helped to inspire his lifelong contributions to gemmology.



IGC Madrid, Spain 2001

Do bi-coloured, green and blue beryls exist, which are composed of emerald and aquamarine zones ?

G. Bosshart

Horgen / Switzerland, george.bosshart@swissonline.ch

Since numerous colour-zoned minerals occur in nature, like strikingly multi-coloured tourmalines (Fig. 1: red/dark green/pink/yellow), spodumenes with pyramidal colour zoning (Fig. 2: purple/light green) and emeralds with sharply defined basal zoning, e.g. from Torrington, New England, Australia (Fig.3, Cr-green/colourless/Cr-green) and from Colombia (Cr-green/ yellow-green/Cr-green), the question came up: Do bi-coloured, emerald-aquamarine beryls also exist ? Going by the information from numerous leading mineral and gem dealers in Europe, the United States, and Brazil and by the outcome of extensive literature searches, the answer was : No. But a very few beryl occurrences world-wide might prove them wrong.



Figure 1 Red/dark green/yellow/purple tourmaline from Madagascar, exhibiting a pronounced sequence of sharp colour zones.



Figure 2 Purple kunzite crystal with a pyramidal zone of light green colour.



Figure 3 Torrington (NSW) emerald crystal with typically sharp, colourless and green colour zoning.

The Binn Valley (Binntal) in the southwestern Swiss Alps is one of the best known mineral eldorados in the Alps thanks to an overwhelmingly rich variety of mineral species. Typically most of these minerals are of small size and come in limited quantities but many are extremely rare and a number of them even endemic, especially some of the sulfosalts. The find of emerald crystals in the Feldbach valley, Binntal, by Swiss rockhounds T. Mumenthaler and A. Frey in the early 1980s, kept secret for two decades, came as a surprise when published in 2003 (in French and German).. The occurrence is located at the contact of a steeply dipping mica schist band and a white dolomite lens. It is exposed to harsh atmospheric conditions so that emerald crystals mostly were found in the weathered debris wash. In 18 short summer campaigns, approximately 250 emerald specimens were recovered by (double-) straining extraction (Fig. 4).

The emeralds themselves were not remarkable for their size (mm to cm) but for their transparency and especially for the quality of their colour, duplicating that of Colombian emeralds, as a result of similar chemical compositions with the V^{3+} chromophore dominating over Cr^{3+} (Krzemnicki & Bosshart, 2003). Freely grown crystals were intact and transparent. However, elongated beryl prisms in full contact with the quartz matrix, were multiply broken in basal directions, encrusted with rusty-brown ferrous oxide and accordingly brown-green in appearance. Mumenthaler and Frey also observed a few specimens of emerald crystals on matrix accompanied by a single aquama-

rine-blue beryl crystal. Such associations had also been reported from the Habachtal emerald deposits in the Austrian Alps (Fig. 5).

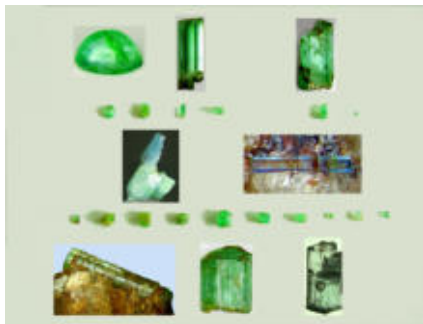


Figure 4 Selection of emerald crystals from the Binn Valley, Valais, Switzerland.



Figure 5 Rock specimen from Habachtal, Austrian Alps, carrying separate emerald and aquamarine crystals. Courtesy NHM Vienna.

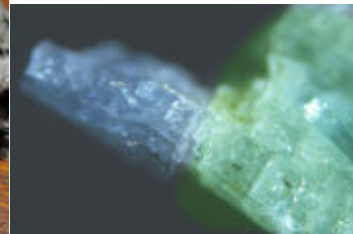


Figure 6 The most outstanding of all green and blue beryl crystals from the Binn Valley finds. Emerald plus aquamarine ?

More spectacularly, however, a Binntal beryl crystal with a green base was noticed to possess a blue top (Fig. 6). This unique specimen triggered the present question and study. The only other occurrence of bi-coloured beryls known at the time was Habachtal. One example is the bi-coloured beryl in Fig. 7a showing a green top and a bluish-white milky base, another shows a blue-green top and a blue base (Fig. 7b) and a third is a blue to green crystal chip (Fig. 7c) seen at the Munich Mineral show 2010. Several specimens from other sources were rejected from this investigation due to a lack of obvious blue and green colour. The only other bi-coloured beryl single crystal, originating from the Skardu Province in Northern Pakistan, shows green to light blue colour zoning (Fig. 8). No other emerald occurrence currently is known to produce the bi-coloured beryl material in question.



Figure 7a Bi-coloured Habachtal beryl specimen, consisting of an emerald top and a milky base (due to inclusions) separated by a talc band. Donation G. Grundmann.



Figure 7b Bi-coloured Habachtal beryl crystal on mica schist matrix. Courtesy NHM Vienna.



Figure 7c A blue to blue-green Habachtal crystal chip (the nicest one was sold). Property A. Steiner.



Figure 8 Frosty bi-coloured beryl crystal of 96.57 ct from the Skardu Province, Pakistan. Photo courtesy K. Scarratt.

Chromophore contents

In the course of analytical work, the very delicate Binntal specimen regrettably broke into many tiny pieces. Although separately saved as blue and green mineral fragments, they provided chemical data which were not trustworthy. The green part, for instance, did not show any Cr. This is incompatible with the former Binntal emerald analyses (Krzemnicki and Bosshart, 2003).

Both the Habachtal and Skardu specimens contain Cr in their green parts, the first one even vanadium. However, the Skardu sample was low in Cr and Fe, data which do not explain its saturated green colour at the crystal top and the pronounced Cr absorption spectrum. The blue part of the Habachtal specimen was lower in Fe than the green part, but still contained substantial vanadium. The blue part of the Skardu sample is also free of chromium. EDXRF analyses will have to be rerun.

Absorption characteristics

In its green part, the Sardu beryl boasts a strong Cr spectrum. Cr absorption is also present in the Habachtal sample and possibly in the Binntal specimen. The latter two are underlain by a non-specific absorption, most likely caused by iron. The blue to light blue parts of the beryls differ from each and require further analysis. The Skardu sample shows a weak aquamarine spectrum and therefore approximates an emerald-aquamarine beryl. However, the aqua part is not overly saturated blue.

Conclusion

Bi-coloured blue to green beryls occur in two versions : (1) as intergrowths, representing two distinct growth phases which differed in their chemical nutrients and other parameters. They are separated by a sharp demarcation plane or a thin mineral layer other than beryl, and (2) as beryl single crystals grading from a light blue to a green zone, without either zone purely consisting of emerald and aquamarine. Perfectly coloured Cr,V-green and true aquamarine-blue crystals which are zoned or grade from emerald to aquamarine (or vice versa), however, appear to occur extremely rarely at best. This is a consequence of the two beryl varieties normally growing under markedly different conditions. However, given two growth phases providing the conditions for emerald and aquamarine crystallisation, the "emeraqua" miracle is definitely conceivable. Yet they have to be found.

References

- Mumenthaler T., Frey A. (2003): L'éméraude de la vallée de Binn. *Cristallier Suisse*, 13 (4), 4-11. Smaragd aus dem Binntal. *Schweizer Strahler*, 13 (4), 24-30.
- Krzemnicki M.S., Bosshart G. (2003): Der Binntal-Smaragd als Juwel. *Schweizer Strahler*, 13 (4), 31-33. L'éméraude du Binntal en tant que bijou. *Cristallier Suisse*, 13 (4), 12-14. ISSN 0370-9213.
- Parker R.L. (1973): *Die Mineralfunde der Schweiz (The mineral finds of Switzerland)*. Wepf & Co, Basel. Re-edited by Stalder H.A., de Quervain F., Niggli E., Graeser St.. ISBN 3-85977-002-0.
- Stalder H.A., Embrey P., Graeser St., Nowacki W. (1978): *Die Mineralien des Binntales (The minerals of the Binn Valley)*. Naturhistorisches Museum der Stadt Bern.

Acknowledgements

Thanks are due to Dr. T. Mumenthaler, Zurich, for donating a number of small Binntal specimens including the bicoloured crystal pictured in Fig. 4 and to Dr. E. Gerber, Natural History Museum, University of Fribourg, Switzerland (with the interaction of A. Frey, Estavayer-le-Lac), for the loan of two beryl on quartz specimens. Dr. Günter Grundmann, Technical University of Munich, Germany, donated his Habachtal crystal (Fig. 7a) and K. Scarratt, GIA, Bangkok, Thailand, loaned the Pakistani bicoloured crystal (Fig. 8). A. Steiner, Bramberg, Austria, provided a few Habachtal crystals for photography. Dr. S. Karampelas kindly determined EDXRF data.

From rough to report – Use of technology

Israel (Eli) Eliezri

Coldiam Ltd Ramat Gan, Israel Colgem@netvision.net.il

Step by step, we are moving forward to where more and more gemmological data is measured by advanced technology, and where we rely less on human expertise.

In the IGC Symposium in Tanzania (2009), Mr. Yuri Shelementiev et al. presented the tendency of moving from subjective to objective measurements of the 4C's of polished diamonds.

In this paper, we would like to present the evolution of the technology and the practical usage from rough diamonds through the cutting process up to polished diamonds.

The real goal is to maximize the utilization of the rough diamond by maximizing the value of polished diamonds to be cut from it and to get the best price in the market.

When diamonds are cut from the rough, the goal is to maximize the value of the potential diamonds. The value is determined based on the 4C's. In most cases, when one of the 4C's is increased, the other parameters tend to decrease (increase in Carat weight reduces clarity). Full detailed and useful information on the rough is the key factor for increasing the value of the polished diamond. Information includes the exact 3D modeling of the rough, exact 3D modeling of the inclusions and the colour of the diamond. For each potential diamond to be cut, the forecasted 4C's is crucial.

The same technologies are used when the diamond is fully cut and determination of the 4C's is required.

Demonstrations of the technologies specially designed for this purpose will be presented

References

1. Yuri Shelementiev et al. 2009, Proceedings of the 31st IGC, Arusha, Tanzania
2. Product pipe line <http://www.sarin.com/>
3. Galaxy 1000 <http://www.sarin.com/g1000.asp>

Cr³⁺-green common opal from Turnali, North-eastern Turkey

Emmanuel Fritsch¹, Benjamin Rondeau², Hasan Kolayli³

¹University of Nantes, Institut des Matériaux Jean Rouxel, UMR-CNRS 6502, 2 rue de la Houssinière, BP 32229, F-44322 Nantes cedex 3, France.

²University of Nantes, Laboratoire de Planétologie et Géodynamique, UMR-CNRS 6112, 2 rue de la Houssinière, BP 92208, F-44322 Nantes cedex 3, France.

³ Department of Geology, Karadeniz Technical University, Trabzon, Turkey.

A new deposit of “emerald”-green common opal has been discovered at Turnali, a small village 40 km ENE of Oltu by car, in the Erzurum Province, NE Turkey. This locality provides opal of such quality that it has already been mounted locally in rings and pendants (Fig. 1). All this jewellery activity is located in Oltu.

The deposit consists of small diggings in a serpentinized peridotite massif. Opal occurs as pods or lenses in faults cutting these peridotites. Opal probably formed thanks to the serpentinization of olivine in peridotites because of water circulations along the faults. This mineralogical reaction is known to free some silica, which then precipitates, in the present case in the form of opal. Such opalization has already been documented in numerous serpentinized peridotite massifs, for example in New Caledonia or Poland (Silesia).

Fourier-Transform Raman spectrometry of this opal revealed a main Raman band at about 338 cm⁻¹, which is typical for opal-CT (Ostroumov et al., 1999). Chemical analysis by Energy Dispersive Spectrometry (EDS) on a Scanning Electron Microscope (SEM) showed that these opals are made unsurprisingly of silica, with aluminum and calcium as minor elements, plus significant traces of chromium (1000 to 1500 atomic ppm). Chromium concentration was much higher in fibrous inclusions observed using the SEM (Fig. 2) than in the volume of opal immediately nearby. EDS analysis of these fibre areas revealed the additional presence of iron and magnesium. UV-visible absorption spectra of the green opal showed chromium-related absorption bands (Cr³⁺), including the weak tell-tale forbidden transitions around 680 nm, with two major broad absorptions around 420 and 610 nm, defining the transmission window in the green (Fig. 3).



Figure 1: Dark green common opal from Turnali, Erzurum Province, NE Turkey, mounted in jewels such as earrings and pendants. Photo by H. Kolayli.

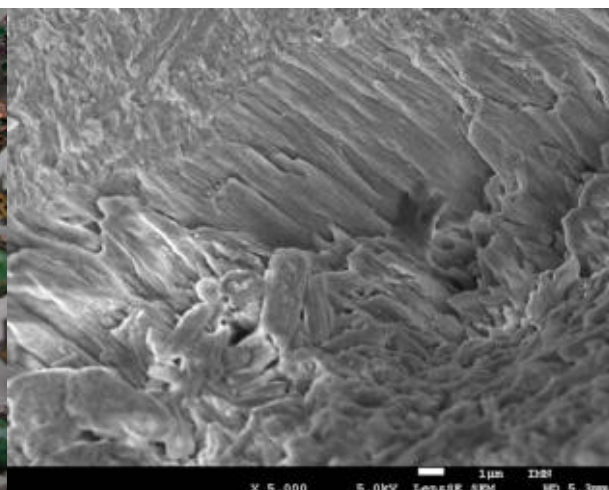


Figure 2: SEM observation of these green opals revealed the presence of fibrous inclusions with high Cr content, which are likely the cause of colour. Micrograph E. Fritsch.

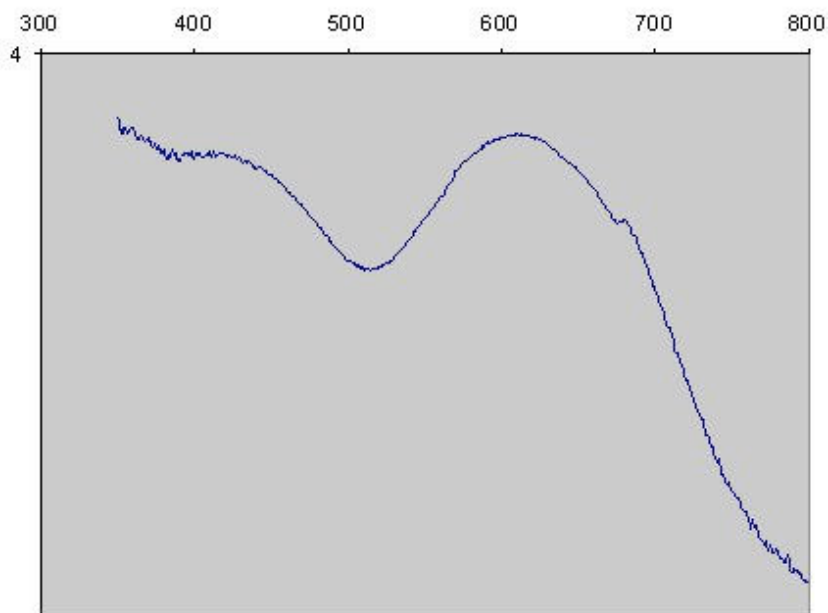


Figure 3: UV-Visible absorption spectrum of a chard of green opal from Turkey, exhibiting the two broad bands typical of Cr^{3+} absorption at about 420 and 610 nm, defining a transmission window in the green, with the tell-tale forbidden transitions at about 680 nm.

We suggest that the green colour of these opals is therefore due to the presence of minute green, Cr-containing fibrous inclusions. The geological settings and their composition is consistent with a serpentine, but we did not get confirmation of this yet. This new type of opal found amazingly rapidly its way to the local market. Also, several geologists have noticed other kinds of emerald-green silica in the general area, including chalcedony. Hence, some additional find of green gem opal is likely, and systematic exploration is underway.

References

Ostrooumov, M., Fritsch, E., Lasnier, B., Lefrant, S., 1999 Spectres Raman des opales: aspect diagnostique et aide à la classification [Raman spectra of opals : diagnostic aspect and help for classification; in French]. *European Journal of Mineralogy*, 11, 899-908.

A portable Raman System for gemstone identification: The GemExpert Raman probe

H.A. Hänni

SSEF, Basel, Switzerland, info@gemexpert.ch

J. C. Hunziker

Herrenschwanden, Switzerland, johannes_hunziker@yahoo.com

Introduction

Raman spectroscopy has been introduced in gemmology about 30 years ago, e.g. by Dharmelincourt et al., 1977, Delé-Dubois et al., 1986. The same authors have given a small collection of comparison spectra for identification. Hänni et al. (1996, 1997) have published reports on gemmological applications of Raman spectroscopy. The Raman systems used so far were working with a microscope to analyse the surface or sub-surface of materials in the confocal mode. The analytical method thus analysed the host gemstone, mineral inclusions or organic fillers for hiding fissures. Databases with Raman spectra of gemstones have been published by Maestrati (1989), Ostertag (1996) and RRUFF on the internet. Conventional Raman systems are bulky and costly and need a solid bench to be calibrated. Experiences with a portable Raman system were reported before by Häberli (2010).



Fig. 1 The GemExpert Raman probe with sample stage, PC with the identification programme is not shown.

The GemExpert portable Raman probe

The present GemExpert Raman produced by BWTek is an up-to-date instrument of the i-Raman series that is in the true sense portable and affordable. It has a reference database of gemstone spectra that allows an instant identification of gemstones. Equipped with a stabilized laser emitting at 785 nm (lasting for thousands of spectra recordings) and a measuring head at the end of an optical fibre, it is extremely practical to use in gemstone identification. The data base of 300 reference spectra includes common and rare gemstones from Amblygonite to

Zoisite. The advantage of a large gemstone database included into the system is evident because a confirmation with external spectra (e.g. from RRUFF library on Internet) does not necessarily have the same excitation and spectral window. The GemExpert Raman is using the gemstone surface to identify the sample. Gemstones of about 4mm and larger can be analysed. Identification takes typically a few seconds up to a minute. The recorded sample spectrum is displayed on a PC in comparison with the best fitting reference spectrum. A report can be printed out for testifying the result and later reference. The application of GemExpert Raman is possible in a wide field, such as in gemmological laboratories, in museums, at gemstone dealers offices, and in gem mines. While a polished surface is still the best condition for identification, also crystals and uncut stones can be identified. However, there are a few small limitations to its use: With a Raman spectrum it is not possible to differentiate between natural and synthetic stones. Inclusions in gemstones are usually too small to identify, as no microscope is attached to the GemExpert Raman in the basic equipment. Chromium-bearing gems like ruby, emerald, green jade show another restriction of the application since these stones produce a strong fluorescence that masks the characteristic Raman peaks of the sample. This problem could be overcome with a different laser source.

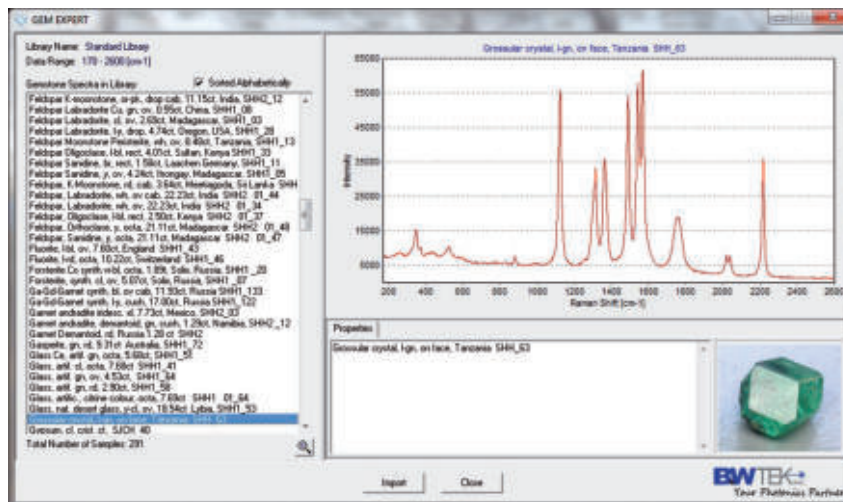


Fig. 2 A screen shot of sample spectrum for grossular garnet, as produced with the portable GemExpert Raman probe.

References

- Dhamelincourt, P. & Schubnel, H.-J. (1977): La microsonde moléculaire à laser et son application dans la minéralogie et la gemmologie. - Revue de Gemmologie, Association Française de Gemmologie, No. 52.
- Delé-Dubois, M. L., Dhamelincourt, P., J. P. Poirot and H. J. Schubnel, (1986): Differentiation between gems and synthetic minerals by laser Raman microspectroscopy), Journal of Molecular Structure Volume 143, March 1986, Pages 135-138)
- Häberli, S. (2010): Edelsteine, gut und bö: Edelsteine, Gläser und Perlen an oberrheinischen Goldschmiedwerken des 13. bis 16. Jahrhunderts., 2010, Dissertation, Universität Bern.
- Hänni, H.A., Kiefert, L., Chalain, J-P. & I.C. Wilcock (1996): Ein Renishaw Raman Mikroskop im gemmologischen Labor: Erste Erfahrungen bei der Anwendung.
- Z.Dt.Gemmol.Ges. 45/2, 55 -70. Hänni, H.A., Kiefert, L., Chalain, J-P. & Wilcock, I.C. (1997): A Raman microscope in the gemmological laboratory: first experiences of application.- J. Gemmol.25,6,394-40
- Maestrati, R. (1989): Contribution à l'édification du catalogue Raman des gemmes. - Diplôme d'Université de Gemmologie, Université de Nantes.
- Ostertag T. (1996): Spezielle Anwendung der Raman-Spektroskopie in den Gebieten der Mineralogie, Petrologie und Gemmologie. Diplomarbeit Albert-Ludwigs Universität, Freiburg im Breisgau (Germany).
- RRUFF <http://rruff.info/> RRUFF Project , Department of Geosciences University of Arizona 1040 E 4th, Tucson, AZ, USA. 85721-0077

Bastnäsite from Pakistan coloured by Rare Earth Elements (REE), exhibiting a colour-change

F. Herzog & M.S. Krzemnicki

SSEF Swiss Gemmological Institute, Basel gemlab@ssef.ch

It is well known that traces of Rare Earth elements (REE), very much like the transition elements, can play the role of chromophores for minerals (Nassau, 2001). Chemically, Bastnäsite is a fluorcarbonate of Rare Earth elements (REE) and hence may reveal insight into the colour-mechanism, caused by these elements. In this study the analyses of three different Bastnäsites will be presented. The two first samples (A: 8.82 ct, and B: 3.65 ct) show a moderate (A) to weak (B) colour-change from greenish-yellow in daylight to a brownish red in incandescent light. Based on the information of our suppliers, sample A originates from Zagi Mountain, Northwestern Pakistan, whereas the stone with a weaker colour-change (B) was found in the Pamir range in Tajikistan. The third stone (C: 1.17 ct), also from Zagi Mountain, does show this effect only weakly as its colour at daylight is already brownish red.



Figure 1: Colour-change from yellowish-green (daylight, left) to brownish-red (incandescent light, right) of a Bastnäsite (sample A: 8.82ct) from Zagi Mountain, Pakistan.

Bastnäsite ($(\text{Ce},\text{La},\text{Y})\text{CO}_3\text{F}$) is well known to mineralogists as one of the most important ores for Rare Earth elements (REE), which are widely used in industrial products. It is mostly found in fine-grained masses, mixed with other REE-minerals. The gemmologist is very rarely (if at all) confronted with this usually brownish yellow mineral. Although it is relatively soft (Mohs-hardness 4.5), brittle, and shows an imperfect cleavage (rhombohedral/basal), bastnäsite may - as a rare cut stone - be considered a gemstone, especially, if the mineral shows a colour-change behaviour when viewed under different lighting conditions (daylight versus incandescent light).

Bastnäsite - (REE), where the REE in its structure can be predominantly Lanthanum (La) or Cerium (Ce), belongs to the hexagonal crystal system, ditrigonal-dipyramidal class $D3h$, and its main crystal habit is a tabular hexagonal prism, eventually combined with forms of the dipyramidal class.

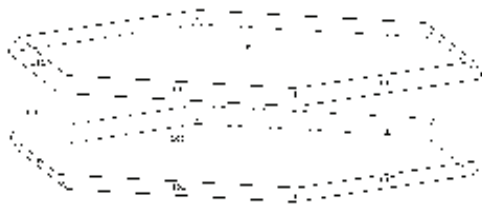


Fig.2 : Typical crystal habit of Bastnäsité
(SHAPE 7.2.3)

Faceted colour-changing Bastnäsité is not new and has already been described by Massi (2007). The general cause of its colour-change is similar to other minerals (Schmetzer et al. 1980, Bernstein 1982), namely an absorption band in the area of 575 nm with two distinct transmission windows on either side of this band. The agent (chromophore) for this absorption band may vary, depending on crystal chemistry and site coordination.

The UV-Vis spectroscopy of the REE is very complex (Dieke et al. 1963) as many electron transitions are possible and very close to each other. The electron-configuration for triply ionized REE-elements, as is the case within bastnäsité, is somewhat simpler (see also Bernstein 1982). Some bands - among others the important 575 nm band - were attributed to neodymium (Nd), which was also detected as traces by qualitative EDXRF-analysis in our samples.

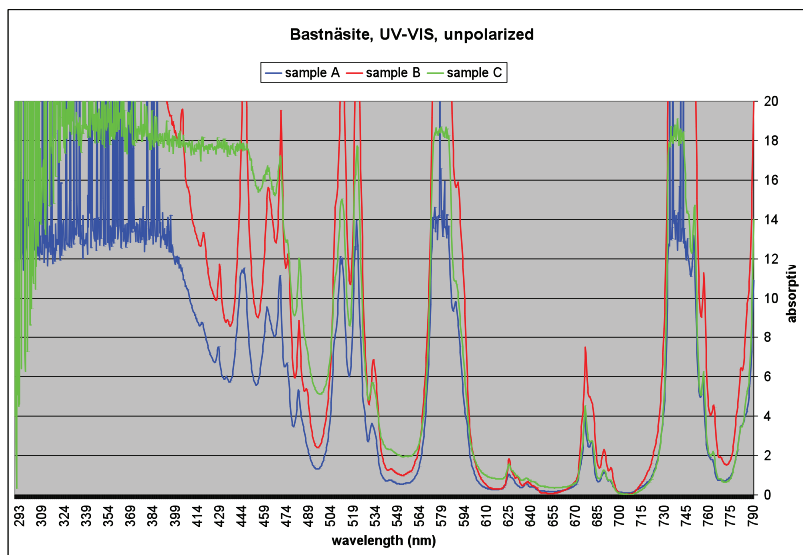


Fig. 3: UV-Vis absorption spectra (unpolarized) of the three studied bastnäsités (A, B, C) showing distinct absorption bands due to REE, predominantly Nd.

To understand first the colour, and then also the colour-change in our samples, the visual observations have to be related to colorimetric data, UV-Vis spectra and chemical analyses. The results will be compared with UV-Vis spectra taken for a colour-changing glass, doped with samarium (Sm) and neodymium (Nd) – those absorption spectra show a striking similarity with the colour-changing bastnäsités analysed.

To conclude, for understanding a colour or even a colour-change effect, not only the position and width of the absorption bands, but also the depth of the transmission windows, the colour distribution of the light sources and the colour-sensitivity of the different cones of the human eye have to be taken into account.

More detailed information on the colour behaviour and the quantification of the colour-change will be presented at the conference.

Acknowledgments

Thanks go to G. Bosshart and to Prof. Dr. H.A.Hänni, who both provided samples for the present study.

References

Nassau K.: *The Physics and Chemistry of Color*, 2nd Edition, 2001, Wiley Interscience, ISBN-10: 0471391069

Massi, L. (2007): Color-change bastnäsite-(Ce) from Pakistan, *Gems & Gemology*, Vol. 43, No. 2, pp. 165-166.

Schmetzer, K., Bank, H., Gübelin, E. (1980): The alexandrite effect in minerals: chrysoberyl, garnet, corundum, fluorite, *Neues Jahrbuch für Mineralogie*, Vol. 138, pp. 147-164.

Bernstein, L.R. (1982): Monazite from North Carolina having the alexandrite effect, *American Mineralogist*, Vol. 67, pp 356-359.

Dieke, G.H. and Crosswhite, H.M. (1963): The spectra of the doubly and triply ionized Rare Earths, *Applied Optics*, Vol. 2, No.7, pp 675-686

Shape: Software by Shape Software, 521 Hidden Valley Road, Kingsport, TN 37663, USA

XVIIth century doublets in liturgical items

Arunas KLEISMANTAS

Department of Geology and Mineralogy, Faculty of Natural Sciences, Vilnius University,
M.K. Ciurlionio 21/27, LT-03101, Vilnius, Lithuania, E-mail: arunas.kleismantas@gf.vu.lt

Introduction

Gems are glowing in liturgical items. To the present day it has been believed that gems in God temples are named correctly. For centuries very big rubies in crowns of rulers, kings and czars were listed in various sourcebooks and inventories. Even today this information has not been amended in many museums. Those red coloured, shiny large gemstones decorating crowns are not rubies. They were correctly identified when museums let in gemmologists for examinations. Such examples have recently been mentioned (Pardieu & Hughes, 2008), e.g. the Black Prince's Ruby and other gemstones of red colour and similar exterior. Many museum collaborators and art critics still think that crowns are decorated by big rubies.

What kind of gems were used in churches in Europe of the XVIIth century, are they rubies or other precious minerals? The author faced this complicated task while researching the chasing of the picture "Mother of God and Infant Christ" kept on the altar at the Basilica Minor of the Visitation Zemaiciu Kalvarija in the Lithuanian Art Museum. In the crowns of the altar picture "Mother of God and Infant Christ", there are fifty gemstones. They were identified as: five diamonds, one smoky quartz and twelve rock crystals. The upper part of four rock crystals are artificially covered by half transparent brownish yellow material, seven are artificially assembled gems composed of: rock crystal - rock crystal, one rock crystal – glass, four of them consist of glass – rock crystal and the upper part of one composite gem consists of glass and the lower part, as it is presumed, consists of quartz (rock crystal) and twenty-five colourless artificial gems are made of glass. Composite gems which are of minor interest consist of two parts which are glued together by transparent colourful dyes. All these composite gems are called doublets.

Material and methods of research

50 gemstones were identified in a liturgical object. Among them, 7 doublets were studied and described in detail. Microscopic, physical and optical tests were used for gemstone identification. The following equipment was used for these analyses: Gemoscope, thermal conductivity duo-tester, refractometer, loupe, analytical scales, for calculating the weights from measurements.

Complex analyses were performed in order to determine the gluing resin of one dark red colour doublet and of one yellowish green colour doublet. During the research micro-schematic, thin-layered spectral chromatography and IR analysis research methods were applied. Analyses of coloured materials were performed by Jurga Bagdzeviciene.

Results of doublet analyses

There are seven crown doublets of the altar picture "Mother of God and Infant Christ", five of which are assembled with red colour dyes, two are with green colour dyes. After performing micro-schematic, thin-layered chromatographic and IR analyses of the red colour material used for gluing chases of doublet casings, it was identified as cochineal colorant of organic nature. Cochineal is made of insect females of *Dactylopius coccus*, parasitizing on cactus. They accumulate from 94% to 98% of carmine acid in their gonads which is a highly important dyeing material (Kleismantas, 2011). This very intense red colour material is inert to environmental influences: it is

resistant to high temperature and sunlight – it does not change its colour. The altar picture of the “Mother of God and Infant Christ” at the Basilica Minor of the Visition Zemaiciu Kalvariija has survived four fires. The picture was restored - several times and the dyeing material in doublets apparently has not changed its colour.

Five red coloured composite gems (weighing 8.41 ct, 7.37 ct, 2.16 ct, around 8.5 ct, 7.5 ct) in the casing of the picture “Mother of God and Infant Christ” are glued with natural materials. The upper part of four gems is a transparent faceted plate of glass, the lower is rock crystal. The shapes of these cut gems are not traditional – rectangles with rounded corners, a faceted crown and a pavilion with dimpled edges. The crown of the gemstones is not high with big table which is surrounded by 4 facets (Fig. 1). The pavilion of these gems is convex and edge-dimpled which are concave by unequal forms. The pavilion reminds the blossom of an unexpanded flower (Fig. 2).

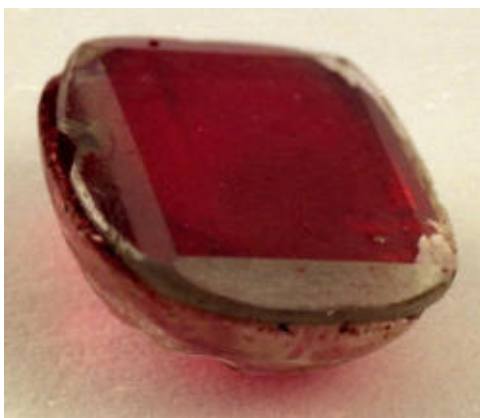


Figure 1. Glass – rock crystal doublet glued by cochineal dyeing. Photograph by the Lithuanian Art Museum.



Figure 2. Glass – rock crystal doublet the pavilion reminds the blossom of an unexpanded flower. Photograph by the Lithuanian Art Museum.

One composite gem of red colour of the picture casing imitating ruby is a different doublet than described above. The crown of the doublet is made of a natural mineral – rock crystal and the pavilion is made of artificial material – glass (Fig. 3). The crown of doublet is cut in the form of a rose with 28 facets. The pavilion was step cut with 21 facets and a diagonal cut culet. This doublet is different from the other described doublets by different shape as well as differently located composite parts of doublet. This doublet may have been cut in another workshop.



Figure 3. Rock crystal – glass doublet glued by cochineal colorant. Photograph by the Lithuanian Art Museum.

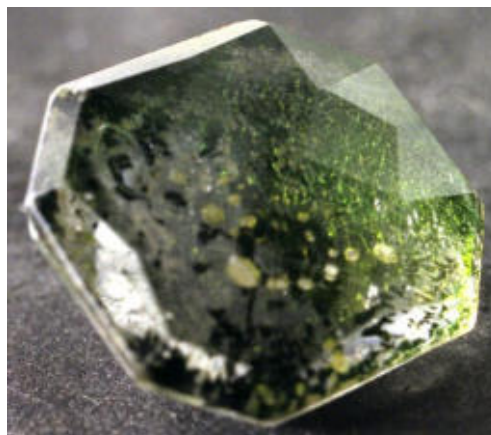


Figure 4. Rock crystal – glass doublet glued by copper resinate dyeing. Photograph by the Lithuanian Art Museum.

Two green coloured doublets imitating emeralds on the infant's crown of the picture „Mother of God and Infant Christ“ are of different shape and are made of different composite parts: rock crystal – rock crystal, glass – rock crystal. Crystal of one doublet (11.42 ct) glued by light permeable glue of yellowish green colour – resin. After performing micro-chemical analysis of glued surface of doublet it was concluded that for doublet gluing copper resinate was used. The crown of the doublet was cut by the form of octagonal Rose with 30 facets, the culet included (Fig. 4). The shape of the cut is mixed but quite proportional. The pavilion is step cut with 28 facets together with culet. Glass – rock crystal doublet (about 1.2 ct) glued by intensely green colour dyeing. The crown of the doublet is not high with not very big table which is surrounded by 4 facets. Pavilion is with 8 facets of which 4 are concave.

Discussion

During a visit of the cathedral of Tarragon city in Spain in 2008, the author found a religious object which, he is certain, contains the same doublets as in the picture of “Mother of God and Infant Christ” at the Basilica Minor of the Visitation Zemaiciu Kalvarija. The liturgical item of Tarragon cathedral was created by silversmith Kaspara Randers in 1682. The picture of “Mother of God and Infant Christ” in Zemaiciu Kalvarija was created in XVIIth century (Bieliniene, 2003). After comparing the cuts and colours of the doublets of Zemaiciu Kalvarija and the red and green coloured gems of religious works of art in Tarragon it can be stated that the same doublets were used in the religious object in Tarragon because the colours of the doublet dyes match. It is coloured by cochineal and it matches the green pigment and the cuts which are typical just of this period. The author is sure that the description of the two religious liturgical items was used for the same doublets. According to the analytical results, masters of XVIIth century created liturgical items using the same doublets with cochineal imitating rubies and doublets glued with green colour imitating emeralds. After comparing doublets of XVIIth century used for two different liturgical items it was determined that only during this period special material was used for gluing doublets and they were cut in shapes typical just of this period.

Conclusions

After studying crown gemstones of the altar picture “Mother of God and Infant Christ” (Lithuania) at the Basilica Minor of the Visitation Zemaiciu Kalvarija it was concluded that red and green colour gems are doublets which are glued by coloured dyes. After studying the glue surface of red coloured doublets it was decided that the dyeing material is cochineal and after analyzing gluing material of green colour it was concluded that the resin was coloured by an organic copper salt. After studying doublets of XVII century in liturgical works of art, it can be stated that according to components of doublets, their gluing colorants and their shape of cut, the production period of gems can be defined.

References

- Bieliniene J. 2003. Recalled Experience, Envisaged Life of Tradition. (in Lithuanian). *Literatura ir Menas*. 2003.09.26. (2969).
- Kleismantas A. 2011. Ruby in Monarchs' Crowns and Ecclesiastical Liturgical Appliances. *Baltic Jewellery News*. March 2011 (21). 66-67 pp.
- Pardieu V, Hughes R.W. 2008. Spinel: resurrection of a classic. In *Colour. International coloured gemstone association*. Summer 2008. 10-14, 16–18pp.

Gem-quality green and blue tourmaline from a Coolgardie pegmatite, Western Australia

Francine Payette

Geologist, gemmologist, Perth, Western Australia francinepayette@netscape.net

Dr Leo Klemm

Analyst, Gübelin Gem Lab, Lucerne, Switzerland

In Western Australia, the Coolgardie pegmatite field is best known for its world-class specimens of ferrocolumbite that have been mined for many decades from the Giles beryl-columbite pegmatite at Spargoville. The pegmatites are part of the Eastern Goldfields Terranes and were injected into metamorphic country rocks of the Yilgarn Craton (Figure 1), one of the oldest landscape preserved anywhere on Earth (4404 ± 8 Ma). The pegmatites have not been dated, but are interpreted to span the age range of 2550-2840 Ma (Jacobson et al., 2007). By 1915, major pegmatite areas of Coolgardie had been found looking for elements with special properties (lithium, tantalum, beryllium). Recently, gemmy green and blue tourmalines have been recovered from a pegmatite south of the beryl-columbite pegmatite (Figures 2 and 3).



Figure 1. Location map. Coolgardie is located about 600 km east of Perth.



Figure 2. The tourmaline workings consist of a pit about 1.6 metre deep and up to 12 metres across.

The chemical composition of five faceted stones and one rough piece was determined by LA-ICP-MS. The evaluation of the analyses (Klemm & Hardy, 2009) indicates that the tourmalines are predominantly elbaite (60 – 73%) with subordinate foitite (17 – 23%) and some minor olenite (0 – 14%) and schorl (0 – 10%) components. The gemmological and spectroscopic properties of tourmaline from this locality are consistent with properties of

tourmaline from other localities worldwide (see, e.g., Webster, 1983).



Figure 3. Tourmalines in matrix from the Coolgardie pegmatite. Size of specimen, about 8.5 cm; length of tourmaline crystal in the centre, about 9 mm.

The tourmalines are primarily green to bluish green and blue (Figure 4). Some specimens are bicoloured green/blue in a direction perpendicular to the c-axis and concentric colour zoning in different shades of blue is sometimes noted. A few specimens recovered close to the surface exhibit closely spaced specks of brilliant colour, and local collectors name these brilliant specimens pin fire tourmalines.



Figure 4. A representative selection of Coolgardie tourmaline colours.

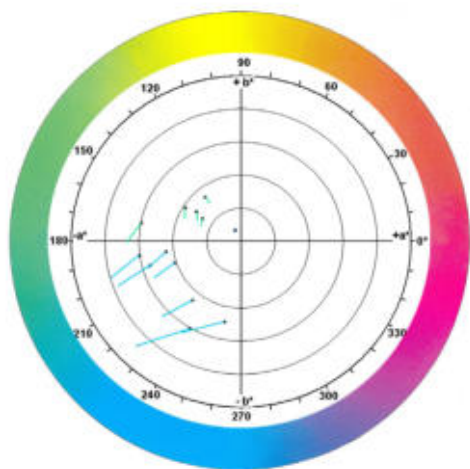


Figure 5. A separate location of the blue and the green colour groups of tourmaline from Coolgardie, Western Australia, can be recognized in the CIE Lab chromaticity diagram. The radius of the diagram corresponds to 25 % saturation. The length of the lines starting at the black dots (D_{65} locus, daylight equivalent) and ending at the A locus (incandescent illuminant) indicates the strength of the colour change. The green specimen near the $-a^*$ axis indicates the transition from the green to the blue colour group (intermediate length of the colour change line, intermediate colour position). The three specimens in the 220° to 270° sector show an inverse colour change (the locus D_{65} is at a higher hue value than locus A). The black dot near the centre represents the colour of a greenish-grey sample. Diagram courtesy G. Bosshart.

Colorimetric parameters of a number of samples are presented in both the CIE Lab chromaticity diagram (Figure 5) as well as in the absorption spectra overlays (Figures 6a and 6b). The blue group shows stronger saturation and higher absorption than the green group. The two colour versions are clearly separated from each other. In addition, the blue group shows a stronger colour variation, indicated by the length of the line starting at the black dot, the locus for daylight equivalent light D65, and ending where the locus of the illuminant A (incandescent light) is situated. One sample was greyish green. According to its low saturation, colour locus of this sample is close to the origin (the centre) of the CIE Lab system.

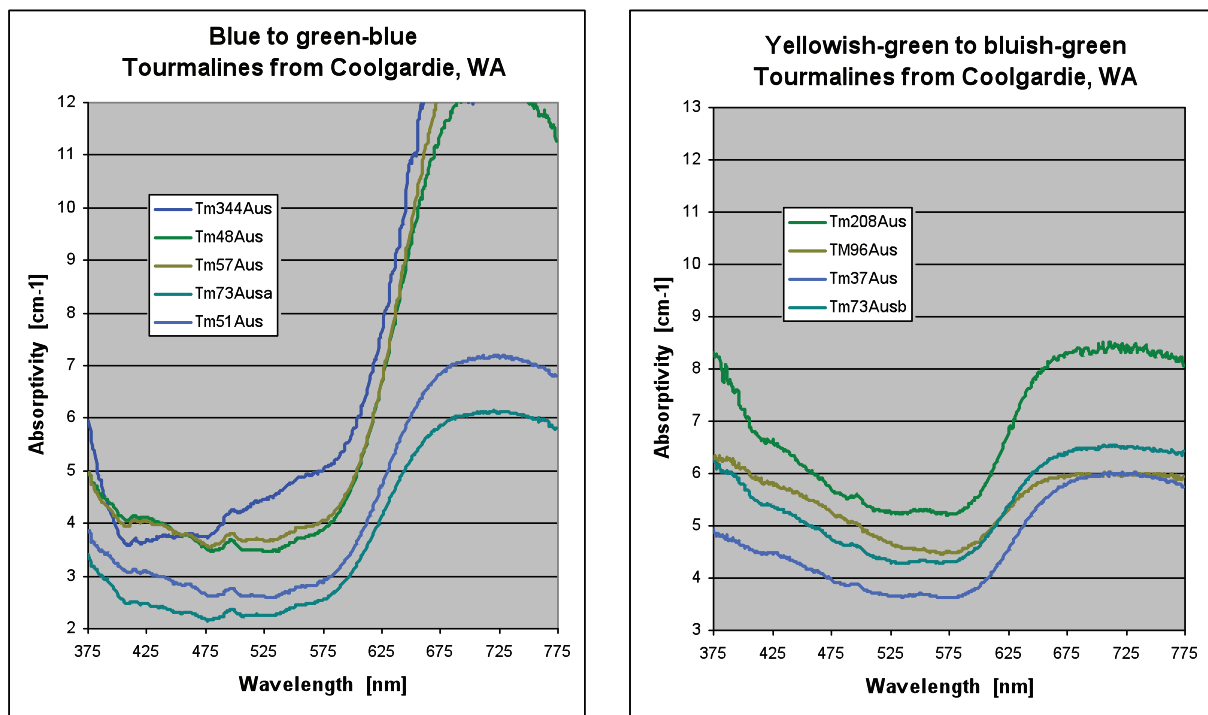


Figure 6a (left) and Figure 6b (right) basically consist of the same spectral components but in different relative strengths. The 720 nm band of the blue group, strongly absorbing the red and orange portions of the spectrum, is responsible for the blue colour transmission of tourmalines from Coolgardie, WA. Spectral overlays courtesy G. Bosshart.

Conclusion

The results of this study confirm that the tourmalines from Coolgardie are worthy of attention as gem material. Thus far, most of the finds has remained in Australian collections.

Acknowledgements

Warm thanks to George Bosshart, Horgen-Zurich, Switzerland, who measured some of the tourmaline specimens with a Zeiss MCS 311 colour spectrometer.

References

- Jacobson M.I., Calderwood M.A., Grguric B.A. (2007) Guidebook to the Pegmatites of Western Australia. Hesperian Press, Western Australia, 356 p.
- Klemm L., Hardy P. (2009) Determination of tourmaline species by advanced chemical analysis. Poster session, 3rd European Gemmological Symposium, Bern, Switzerland.
- Webster R. (1983) Gems, 4th ed., revised by B.W. Anderson, Butterworths, London, pp. 146-152.

Properties of blue spinel from Sri Lanka

Boontawe Sripasert^{1,2}, Wilawan Atichat², Chakkaphan Sutthirat^{2,4}, Gamini Zoysa³, Thanong Lee-lawattanasuk², Nalin Naruedeesombat², Pimpicha Sritunayothin², Chanida Makakum^{1,2}, and Warangrat Pttharapanich²

¹Department of Mineral Resources, Bangkok, 10400, Thailand: e-mail:boontawe@gmail.com

²The Gem and Jewelry Institute of Thailand (Public Organization), Bangkok, 10330, Thailand

³Mincraft Company, Colombo, Sri Lanka

⁴Department of Geology, Faculty of Science, Chulalongkorn University, Bangkok, 10330, Thailand

Spinel belongs to the gemstones found in various shades of colour. A gem-quality red spinel is usually considered a highly priced gemstone whereas the blue variety is somewhat rarer and lower in value compared to the red one. In this short communication, we report preliminary results of our on-going investigation on the gemmological characteristics of naturally coloured blue spinels, from a new deposit in the South East of Sri Lanka. Based on both standard and advanced testing techniques, these blue spinels have similar properties to those from Myanmar and Vietnam.

Key words; Sri Lanka, Blue spinel, Gemmological Properties

Introduction

Generally, gem-quality red spinel is considered a highly priced variety whereas other varieties of spinel are not well known and considerably lower in value compared to the red one. However, one spinel variety that might increase in price is the blue one due to its rarity and beauty. Based on geological and gemmological points of view, blue spinel is not a common gem and gem quality is hard to find in the market. Nevertheless, it became more familiar in local gem markets in Sri Lanka and Vietnam. In Sri Lanka, some cut blue spinel from a new source is now available in the Ratnapura market (Fig. 1).

The new spinel source is in an area called Okkampitiya in the Ella area which is located in the south-east of Sri Lanka. Small scale open pit mining is carried out along the colluvial deposits in the small valley near the Maligawilla Village. In this gem deposit, many gemstones such as corundum and spinel had been found associated with zircon, quartz and other minerals. For this short communication, some gem quality spinel samples from the new mining site were studied.

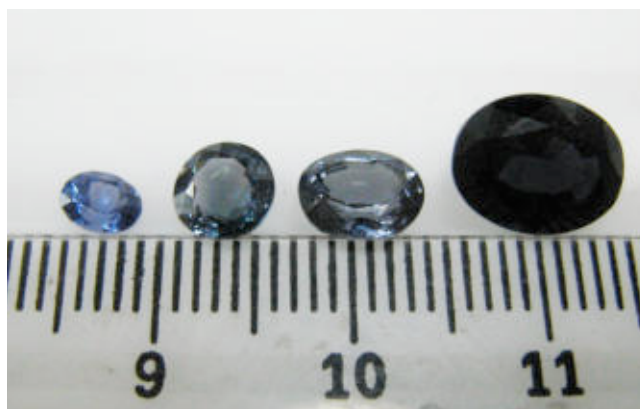


Figure 1. Cut blue spinel samples from Sri Lanka. (scale is in mm).

Materials and methods

Twenty three rough blue spinel crystals, provided by one of the co-authors (GZ), were care-fully cut, polished on both sides to reveal colour and internal characteristics and studied by using both standard gemmological instruments and advanced spectroscopic techniques (EDXRF, UV-Vis-NIR, FTIR and PL spectroscopy) at the GIT-Gem Testing Laboratory (GIT-GTL). The EDXRF spectrophotometer is EDAX model Eagle III probe operated at 35 KeV with 80 mA and 100 seconds live time. The UV-Vis-NIR spectrophotometer used in this study was a Perkin Elmer Model Lambda 950, recording in absorbance mode at wavelengths between 200-1500 nm. The FTIR analysis was carried out with a Nicolet Fourier Transform Infrared (FTIR) spectrometer, Model 670, with He-Ne Laser as the reference source. The measured spectra were recorded in absorbance mode at wave-numbers between 400 and 5000 cm^{-1} and 0.5 cm^{-1} resolution with a scanning time of 128 seconds. The Raman and photoluminescence (PL) study was carried out with a Laser Raman spectroscope, a Renishaw Raman system Model 1000 with Ar laser source emitting at 514 nm, in Raman shift at wavenumbers from 200 to 2000 cm^{-1} and in wavelengths from 500 to 1,000 nm, respectively.

Gemmological properties

All the greenish to violettish blue spinel crystals are fairly transparent and clean. They have even colour distribution and a few fractures which make them suitable for shaping into high quality stones. Refractive indices range from 1.718 to 1.721 and the specific gravities vary from 3.55 to 3.62 which fit the characteristics of spinel minerals (Klein and Hurlbut, 1999). All samples are inert to both LWUV and SWUV radiation. Microscopic characteristics of all samples comprise needle-like inclusions, fingerprint-like inclusions, and healed fissures (Fig. 2).

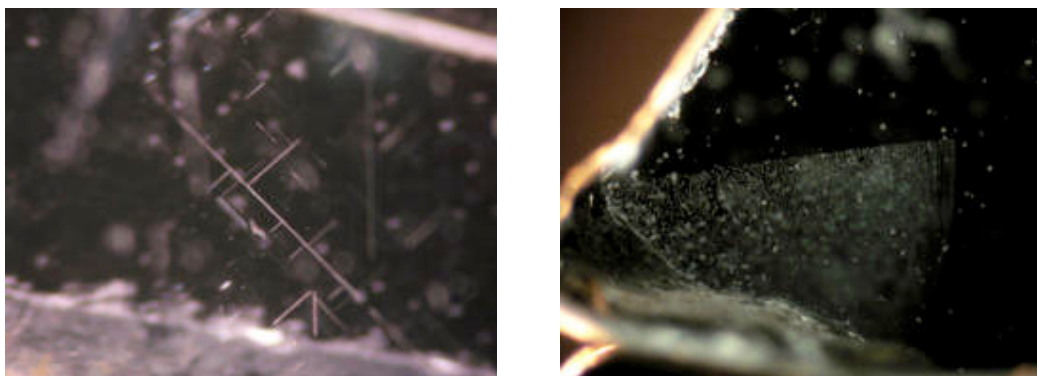


Figure 2. (a) Needle-like and (b) fingerprint-like (b) inclusions in the spinel samples.

Chemical and Spectroscopic properties

Chemical compositions of those spinel samples analysed by EDXRF give rather high iron content (1.565-4.755 wt.% Fe_2O_3 for purplish blue and 1.021-4.903 wt.% Fe_2O_3 for greenish blue) and low to very low contents of V, Cr, Mn, Ni, Co, and Ga. The Zn content is a little bit higher in purplish blue than in greenish blue spinels (0.063-5.676 wt.% to 0.139-0.813 wt.%). The UV-Vis-NIR spectra of a representative blue spinel sample (Fig. 3) reveal absorption peaks at about 371, 385, 457 nm (related to Fe^{2+}) and broad bands at around 575-590 and 625-627 nm (related to $\text{Fe}^{2+}/\text{Fe}^{3+}$ charge transfer or Co^{2+}) similar to those documented by a number of investigators (Shigley and Sloclzton, 1984; Fritsch and Rossman, 1987; Muhlmeister, S., et al., 1993; Bunnag and Thanasuithipitak, 2003; Smith, C.P., et al., 2008) The FTIR spectra of representative samples (Fig. 4) show absorption peaks at approximately 1426-1431 cm^{-1} and broad absorption from 3000 to 7000 cm^{-1} . The PL spectra of representative samples related to Cr^{3+} (Gaft, et al., 2005) are displayed in Figure 5.

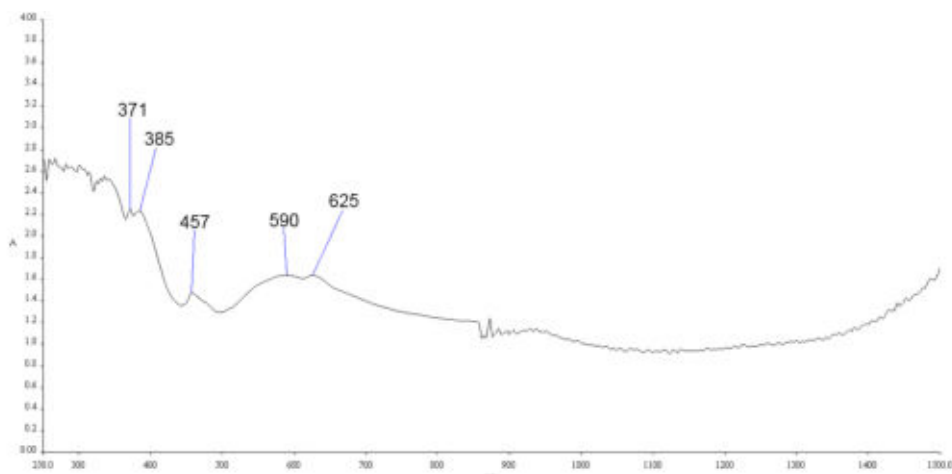


Figure 3. Representative UV-Vis-NIR spectrum of greenish blue to violetish blue spinel samples. Peaks at 371, 385, 457 nm are related to Fe^{2+} and broad bands at around 590 and 625 nm are related to $\text{Fe}^{2+}/\text{Fe}^{3+}$ charge transfer or Co^{2+} (Shigley and Sloczton, 1984; Fritsch and Rossman, 1987; Muhlmeister, S., et al., 1993; Bunnag and Thanasuithipitak, 2003; Smith, C.P., et al., 2008)

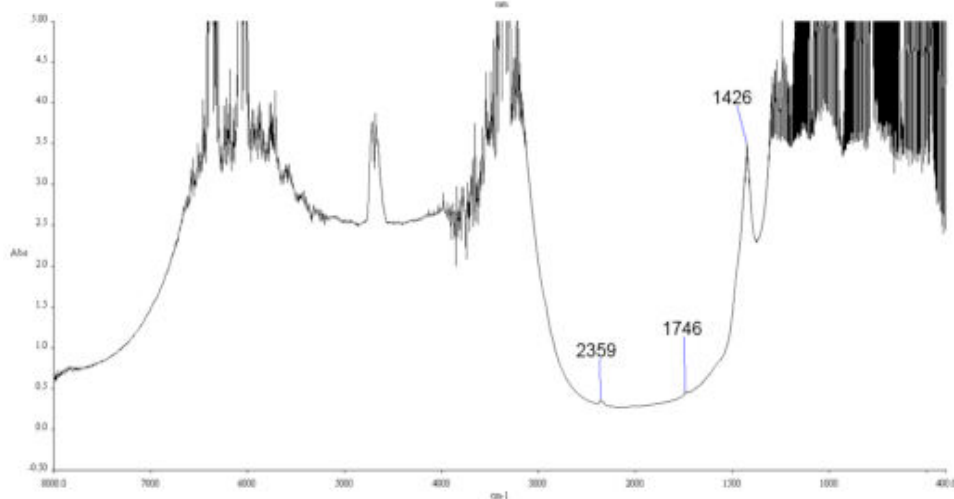


Figure 4. Representative FTIR spectrum of greenish blue to violetish blue spinel samples. Peak at 1426 cm^{-1} may be due to vibration of C-O (from air?) (Smith, B.C., 1999)

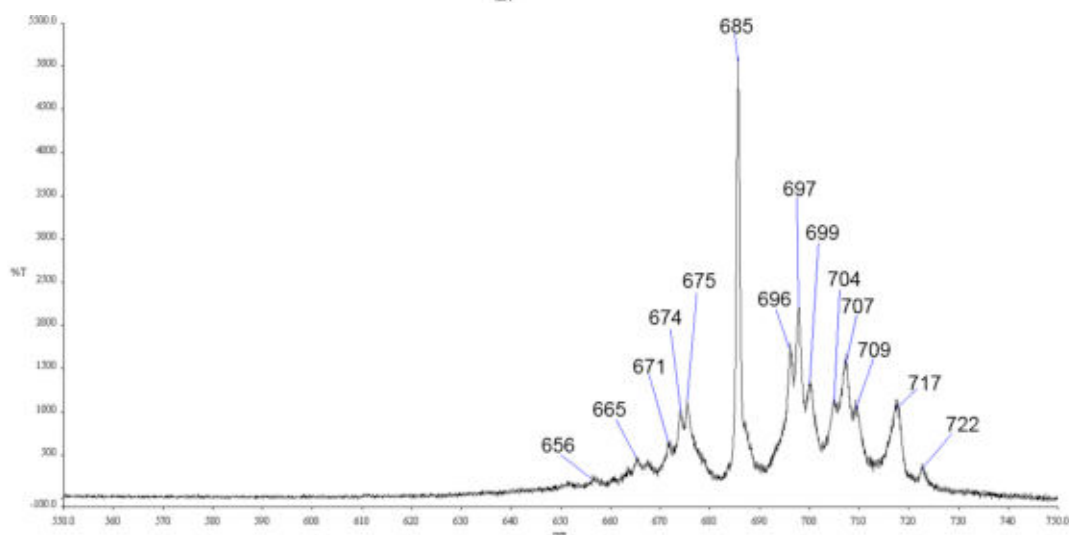


Figure 5. Representative PL spectrum of greenish blue to purplish blue spinel samples. peaks at 675 685 697 707 717 nm due to Cr^{3+} (Gaft, et al., 2005)

Discussion and Conclusions

Based on our preliminary study, it appears that the physical and gemmological properties of the naturally coloured blue spinel (not cobalt-blue spinel) from a new source in Sri Lanka are similar to those from other localities in Sri Lanka, Myanmar and Vietnam. However, these blue spinels are comparable in terms of colour appearance and could compete with other blue gemstones such as sapphire, tanzanite or blue zircon if they become available in large quantities.

Acknowledgements

The authors are deeply thankful to the GIT for providing the financial support and equipment for this research project.

References

- Bunnag N. and Thanasuithipitak, P., 2003, Mogok spinel : optical (UV-Vis-NIR) absorption spectroscopic study, *Chiang Mai J. Sci.*,30(2), 69-79.
- Fritsch, E. and Rossman, G.R., 1987, An update on color in gems. Part I. Introduction and colors caused by dispersed metal ions, *Gems & Gemology*, 23(3), 126-139.
- Gaft, M., Reisfeld, R., and Panczer, G.,2005, *Luminescence spectroscopy of minerals and materials*, Germany. 356pp.
- Klein, C., and Hurlbut, C. S.,1999, *Manual of Mineralogy*. 21st Ed., New York, 681 pp.
- Muhlmeister, S., Koivula, J.I., Kammerling, R.C.,Smith, C.P., Fritsch, E. and Shigley, J.E., 1993, Flux-grown synthetic red and blue spinels from Russia, *Gems & Gemology*, 29(2), 81-98.
- Shigley, J.E. and Sloczton, C.M., 1984 ,Cobalt-blue Gem Spinel, *Gems & Gemology*, 20(1), 34-41.
- Smith,,C.P., Beesley, C.R., Darenius, E.Q, and Mayerson, W.M., 2008, A closer look at Vietnamese spinel, *In Color, Spring*, 31-34.

Jadeite trading in China

Elizabeth Su

DuaSun Collection, Shanghai, China esu_gems@yahoo.com

As a young jadeite dealer and gemmologist working with affluent clients mostly in mainland China and Hong Kong, I have experienced many different situations in jadeite trading and gained important insights into the market.

During the reign of Emperor Qianlong in the 18th century, the jadeite occurrences in Upper Burma (today Kachin State, Myanmar) were detected by his troops. The material was transported to the Emperor's palace via Tengchong and Kunming on the old Jade road which was part of the ancient Silk road and Tea-horse road (Anon., 2004), Nowadays the rough jadeite trade uses a new and less rugged road to China, from Myitkyina via Ruili to Kunming (Bosschart, 2006). As soon as the deposits in Upper Burma were detected, jadeite became known as a unique and miraculous jade material, superior to the other forms of jade. Slowly jadeite became available and affordable to buyers outside the court. To this day, jadeite is highly coveted in China and other Asian countries (Hughes et al. 2000)

In this article I will open the latest map of rough jadeite trading in China (Fig.1), which shows the most important centers and the new market-places. Jadeite rough is exported (1) by air plane and boat from Yangon to the leading import and auction centre of Pingzhou in the city of Foshan and on to Guangzhou, Jieyang and Sihui in Guangdong Province and (2) by truck from Myitkyina to Ruili (Fig. 2) and on to Tengchong (Fig. 3) and Yingjiang, respectively to Kunming in Yunnan Province. All-quality jadeite rough auctions are held twice a month in Pingzhou, Foshan. The bidders and buyers are from everywhere in China. Finished jadeite goods auctions are held in Beijing, Shanghai and other important cities and places.



Figure 1. Map showing the location of Pingzhou in Guangdong Province and of the other important rough jade centres. Market-places for finished goods are numerous and spread out over most of China.

Jadeite dealers from Yangmei village in the city of Jieyang, Guangdong province, are the biggest buyers of jadeite rough. They are born in the same village or town and among them, most are friends or relatives. When they detect



Figure 2. Specialty jade market scene in Jiegao, Yunnan province. Photo by George Bosshart.

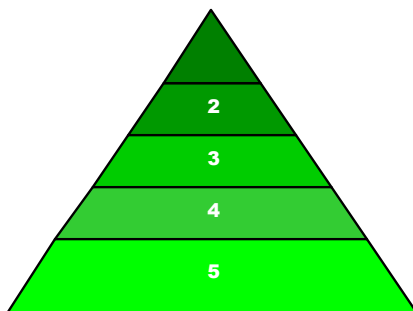


Figure 3. Boulder cut in two with a pure white jadeite band bordered on opposite sides by a dark-green iron-coloured jade band and a paler Cr-green jadeite band. Tengchong rough jade market. Photo by George Bosshart.

a jadeite boulder of outstanding quality, they can raise funds very quickly from their family or village. This explains why they are able to offer higher prices than other bidders and win the top jadeite boulders. Auctions for rough and cut jadeite were held four times per year in Yangon. The sales figures for Spring 2011 auction climbed to over 3 billion US dollars. As of now, auctions will be held every two months.(www.mmtimes.com). To Westerners it may be an eye-opening fact that Yangon ruby and sapphire auctions are of entirely secondary importance.

The total Chinese sales of jewellery in 2010 amounted to 245 billion RMB (equaling 37.7 billion US \$ approximately). The total rough jadeite sales volume of about 40 billion RMB was only slightly lower than that of gold and diamond (www.sina.com). The recent half year has been the craziest and most risky period in jadeite trading history. The price of top quality jadeite is shooting up into the sky, not changing every month but every day. The composition of jadeite buyers has also changed a lot: from wealthier people to less rich people, from individual buyers to company buyers, from coastal city buyers to continental buyers, even in Inner Mongolia.

All kinds of jadeite goods appear in the market, and spread to all levels of buyers, which is shown in the jadeite trading pyramid resulting from my market research (Fig. 4). As a result of the high degree of popularity of jade and the elevated prices, all sorts of treated jade are being offered and sold. Treated and imitation jade is not covered in this survey.



	Client Levels	Goods Levels	Price Range (RMB)
1	Top Clients	Top Jadeite Goods	500,000~ 300 million
2	Rich Clients	Superb Jadeite Goods	200,000 ~ 2 million
3	Medium Clients	Good Jadeite Goods	30,000 ~ 500,000
4	Normal Clients	Normal Goods	5,000 ~ 50,000
5	Basic Clients	Poor Quality Goods	20 ~ 5000

Figure 4. Pyramid of Chinese buyers of finished jadeite goods and today's prices (100 RMB equal 15.38 US \$ approximately, exchange rate of 6 June 2011). It should be noted that the price ranges indicate the prices for single items or single sets of items.

Customers who are willing to spend a lot of money for select pieces of jadeite can be divided into three groups: (1) collectors of all types of jadeite colours: green, violet, inky, yellow, red, colourless and so on, including special (Fig. 5), unique (Fig. 6) and top collector's items (Fig. 7), (2) buyers who want to invest money. They are hunting for natural jadeite with a better quality and reasonable price, and (3) individual buyers who want to use the goods as gifts or personal property. Most of them are chasing green jadeite or highly translucent, nearly colourless jadeite. They ask for single stones or for large quantities, e.g. to be used at selling parties or for Chinese New Year gifts.



Figure 5. Charming pair of chili pendants, orange-yellow jadeite carvings, a true speciality item. Photo courtesy DuaSun Collection.



Figure 6. A unique jadeite fish with very fine texture and green colour grading into orangey red (length ca. 3 cm), a special collector's item. Photo courtesy DuaSun Collection.



Figure 7. Exclusive violet (or lavender) jadeite saddle ring, an outstanding example of a rare collector's item. Photo courtesy DuaSun Collection.

Chinese people are getting richer and richer. They can spend more and more money to collect jadeite, especially high and top-quality goods. At the end of 2010, there were 55,000 billionaires and 875,000 multimillionaires in China, and the number keeps growing fast (www.china.com, www.sina.com). As a result, jadeite trading in China will become more and more prosperous.

Acknowledgements

The author expresses her heartfelt thanks to G.eorge Bosshart, Horgen-Zürich, Switzerland, for continued support and technical advice with the abstract as well as to her husband Gordon Duan for the development of the pyramid and support with the script and to her assistants Yu Wang and Karl Zhang for market surveys.

References

- Anon. (2004): Ancient Tea-horse trails. ISBN 7-5032-2342-1.
 Bosshart G. (2006) : Old and new Jade roads from the Jadeite jade mines in Upper Burma to the vast market-places of Chinese cities. Proceedings 1st International Gem and Jewelry Conference, Gem and Jewelry Institute, Bangkok. 43.
 China Cartographic Publishing House (1996): Atlas of China. 1st ed., 41. ISBN 7-5031-1868-7.
 Hughes R.,W., Galibert O., Bosshart G., Ward F., Thet Oo, Smith M., Tay T.S., Harlow G.E. (2000) : Burmese Jade – The inscrutable gem. *Gems & Gemology* 36 (1), 2-26.
www.sina.com
www.mmtimes.com

Fancy sapphires from Deniyaya deposit, southern Sri Lanka

Chakkaphan Suthirat^{1,2*}, Sasipim Pumpeng¹, Wilawan Atichat¹ and Gamini Zoysa³

1. The Gem and Jewelry Institute of Thailand (GIT), Faculty of Science, Chulalongkorn University, Bangkok 10330 Thailand

2. Department of Geology, Faculty of Science, Chulalongkorn University, Bangkok 10330 Thailand

3. Mincraft Company, Mount Lavinia, Sri Lanka

*Corresponding Email: c.sutthirat@gmail.com;

Deniyaya area is located in the highly potential gem deposits of Sri Lanka (e.g., Dissanayake and Rupasinghe, 1993; Cooray, 1994). Geologically, it is situated in the terrain of Highland Complex (HC) which is extensively formed by Proterozoic metamorphic rocks, mainly belonging to granulite facies (Mathavan et al., 2000). Secondary deposits appear to be the most potential where alluvia have been derived from the primary sources. New gem deposits have been discovered and mined particularly along the Gin Ganga River (see Fig. 1) and Mederapitiya for a couple of years. Chrysoberyls (including cat's eye and alexandrite), sapphires and zircons appear to be the main gem materials (Fig. 2) accumulated along with sand and gravel in palaeo-channels. Sapphire collection (see Fig. 3) was emphasized in this study. It contains a variety of colours ranging from colourless to pale blue, violet, purple and pink. Colourless and pale blue sapphires appear to be the most abundant whereas pink sapphires are rare. Moreover, colour patches are commonly present in these stones. Their weights range from 0.14 to 2.9 ct. Gem-mological properties were collected; accordingly, these stones fall within the common ranges of corundum. They mostly show fluorescent colours of orange to orangey red and deep red under long wave ultraviolet; on the other hand, they are mostly inert or fluoresce pale orange under short wave ultraviolet radiation.



Figure 1. An alluvial deposit along the Gin Ganya River in Deniyaya, Southern Sri Lanka.



Figure 2. Chrysoberyls associated with sapphires in the alluvium of Deniyaya.



Figure 3. Sapphire assemblage from Deniyaya deposit showing a variety of colours from colourless to pale blue, violet, purple and pink. Note that some crystal forms still remain.

FTIR spectra of these samples show significant absorptions due to AlOOH clusters, particularly around the regions of 3473-3453, 2875-2788 and 2134-1994 cm^{-1} (see Fig. 4). UV-VIS-NIR absorption spectra clearly show differences between colour varieties; however, iron absorptions appear in all varieties, even in colourless stones. Chromium absorptions are usually observed in violet, purple and pink varieties; on the other hand, Fe/Ti absorptions are common in pale blue stones. These observations are compatible with chemical analyses.

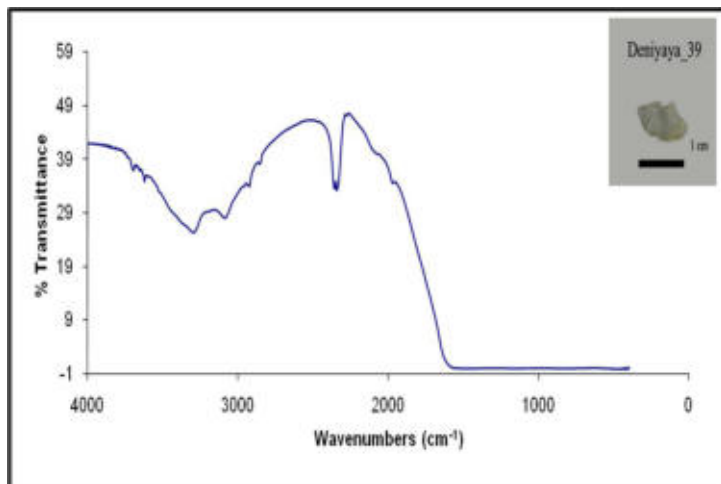


Figure 4. FTIR spectrum of a sapphire sample from Deniyaya deposit

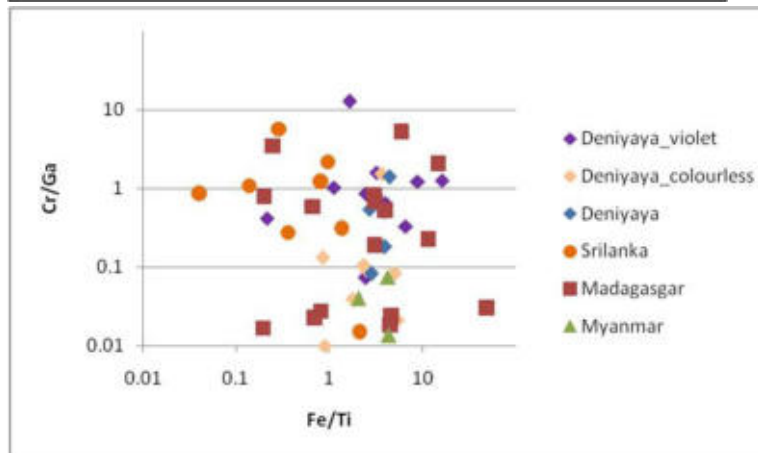


Figure 5. Plot of Fe/Ti against Cr/Ga in comparison with sapphires from famous deposits.

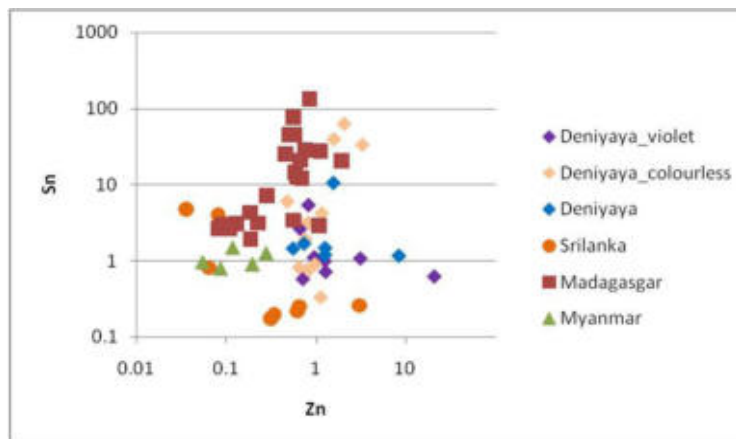


Figure 6. Plot of Zn versus Sn in comparison with sapphires from other places.

Internal features were investigated under the microscope and some inclusions were also identified using a Raman spectroscope at GIT. Tiny needles and cloud inclusions, the most typical, usually align along crystallographic planes within three directions. Fluid inclusions are also common and CO₂ gas bubbles sometimes can be recognized in two-phase inclusions. Mineral inclusions found in these samples are apatite, rutile, mica and amphibole, identified by Raman spectrometry.

Chemical analyses of these stones were carried out using an Energy Dispersive X-ray Fluorescence (EDXRF) Spectrometer and a Laser Ablation-Inductively Coupled Plasma-Mass Spectrometer (LA-ICP-MS), based at GIT. Qualitative EDXRF analyses show that iron and titanium in all colour varieties appear to be higher than the other trace elements whereas chromium contents rise up in violet, purple and pink varieties. The other trace elements are negligible. Regarding LA-ICP-MS analyses, these quantitative trace analyses are applied for identification of geographic origin. Variation plots among trace elements were taken and placed in comparison with sapphires of other main deposits of the world including some of Sri Lanka, using GIT's database (see Figures 3 and 4). In general, Deniyaya sapphires have trace compositions falling within the ranges of Sri Lankan sapphires and they are different, e.g., by a slightly lower Sn content and higher Cr/Ga ratio, from the other world deposits. The Zn vs Sn diagram is slightly more diagnostic than the Cr/Ga vs Fe/Ti diagram. The data overlap, however, is considerable in both diagrams.

References

- Cooray, P.G. 1994. Introduction of the Geology of Sri Lanka. 2nd Revised Edition. National Museum of Sri Lanka Publication.
- Dissanayake, C.B. and Rupasinghe, M.S. 1993. New gem localities of Sri Lanka. I.G.C. Volume of Resources Geology, 16: 271-275.
- Mathavan, V., Kalubandara, S.T. and Fernando, G.W.A. 2000. Occurrences of two types of gem deposition in the Okkampitiya gem field, Sri Lanka. *Journal of Gemmology*, 27(2): 65-72.

Bicoloured sapphires from basaltic and metamorphic affiliations

Panjawan Thanasuthipitak¹, Piyanart Kulsrisuwan¹, Gamini Zoysa² and Theerapongs Thanasuthipitak¹

¹ Gemmology Program, Department of Geological Sciences, Chiang Mai University, Chiang Mai 50200, THAILAND
panjawan@cmu.ac.th

² Mincraft Co., Sri Lanka

Materials and Methods

In this study, 20 basaltic bicoloured sapphire from Chanthaburi, Thailand and Diego Suarez, Madagascar (10 each) were characterized and compared with 10 metamorphic bicoloured sapphire from Sri Lanka, using analytical techniques including EPMA, UV-Vis-NIR and FTIR.

Gemmological Properties

Colour: Rough Diego Suarez samples viewed parallel to c axis show characteristic core-rim bicolour consisting of yellowish green to greenish yellow core and blue rim with sharp contact (Fig 1). Bicoloured Chanthaburi sapphires are cut stones, most of them show colour zoning of blue and green bands (Fig 2). Sri Lankan cut samples are of various colours ranging from blue and yellow, blue and yellowish green, blue and colourless, dark green and yellowish green, to purple and blue (Fig 3).



Figure 1 Diego Suarez Sapphires

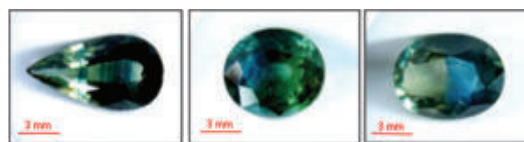


Figure 2 Chanthaburi sapphires



Figure 3 Sri Lankan sapphires

The gemmological properties of these bicoloured sapphires are recorded in Table 1. Generally, there are no variations in their characteristics and colour, except the fluorescence reaction, between the corundum of both genetic associations.

Properties	Chanthaburi samples	Diego Suarez samples	Sri Lankan samples
S.G.	3.97-4.02	3.95-4.01	3.95-4.02
R.I. n_o n_e	1.770-1.772 1.762-1.764	1.768-1.772 1.760-1.764	1.767-1.771 1.759-1.763
Birefringence	0.008	0.008	0.008
UV fluorescence LWUV SWUV	Inert Inert	Inert Inert	Inert Inert, rarely weak to moderate orangey red
Internal features	- fingerprints - silk (TiO ₂) along colour bands - strong colour zoning	- fingerprints - fractures - lots of small negative crystals - strong colour zoning	- fingerprints - silk - colour zoning - negative crystals - twinning - small dark mineral inclusions

Table 1. Gemmological properties of the studied sapphires.

Chemical composition

Quantitative electron-microprobe analyses were performed on some selected samples. In each sample, 3 points were analysed for each colour. The result showed that the chromophore Fe in both colours (blue and yellow or green) was higher in the basaltic samples as shown in Table 2.

Samples	Fe ₂ O ₃ (weight %)	
	Blue	Yellow, Yellow Green
Chanthaburi	0.24-1.08 (0.62 ave.)	0.17-0.87 (0.49 ave.)
Diego Suarez	0.66-0.92 (0.96 ave.)	0.73-1.17 (0.91 ave.)
Sri Lanka	0.01-0.53 (0.17 ave.)	0.01-0.41 (0.33 ave.)

Table 2. Fe contents in blue and yellow portion in sapphires from 3 localities.

Cr was detected in some samples, but the highest concentration was found in the violet part of the Sri Lankan sample with 0.20-0.32 weight% Cr₂O₃. TiO₂ was not detected in Chanthaburi sapphire, but could be found in the Diego Suarez with slightly higher concentration in the blue area (0.045-0.115 weight% TiO₂). In the Sri Lankan samples, TiO₂ contents are also very low with around 0.01-0.05 weight% except the purplish sample with high Cr₂O₃ where higher TiO₂ (0.15-0.20 weight%) was detected.

The V and Ga concentrations in both igneous and metamorphic samples were generally low. The highest V₂O₃ contents, up to 0.06 weight%, were measured in the purplish Sri Lankan samples. Rarely, the Ga₂O₃ concentration found was 0.10 weight%.

Spectroscopy

UV-Vis-NIR absorption characteristic spectra (Fig. 4) of Chanthaburi and Diego Suarez sapphires in both blue and yellow portions are quite similar, dominated by three essential absorption mechanisms:

- Fe³⁺ bands in the ultraviolet region (377, 388 nm) and visible region (450 nm)
- Fe²⁺ - Ti⁴⁺ IVCT broad bands in visible region (500-700 nm)
- Fe²⁺ - Fe³⁺ IVCT broad bands toward the near infrared (700-1000 nm).

These are typical of sapphires from basaltic fields influenced by high Fe content, particularly the Fe²⁺/Fe³⁺ IVCT bands which is in agreement with those reported by many workers (Levinson and Cook, 1994; Schwarz et al.,

1996; Khunkaew, 2004; Singbamroong, 2004; Thanasuthipitak et al., 2009). Generally, the absorption of Fe^{2+} - Ti^{4+} IVCT and Fe^{2+} - Fe^{3+} IVCT are more pronounced in the blue than in the yellow areas of the basaltic sapphires from the two areas. The Fe^{2+} - Fe^{3+} (colour-causing) mechanism is absent in most of the Sri Lankan sapphires. The FTIR spectra in the mid-infrared region between 4000 and 1500 cm^{-1} of all samples are very similar with common OH peak positioned at 3309 cm^{-1} (Smith, 2006). Only the purplish Sri Lankan sample show two maxima peaking at 3309 and 3232 cm^{-1} with combination of weaker peaks at 3394 and 3186 cm^{-1} of unknown phases (Fig.5).

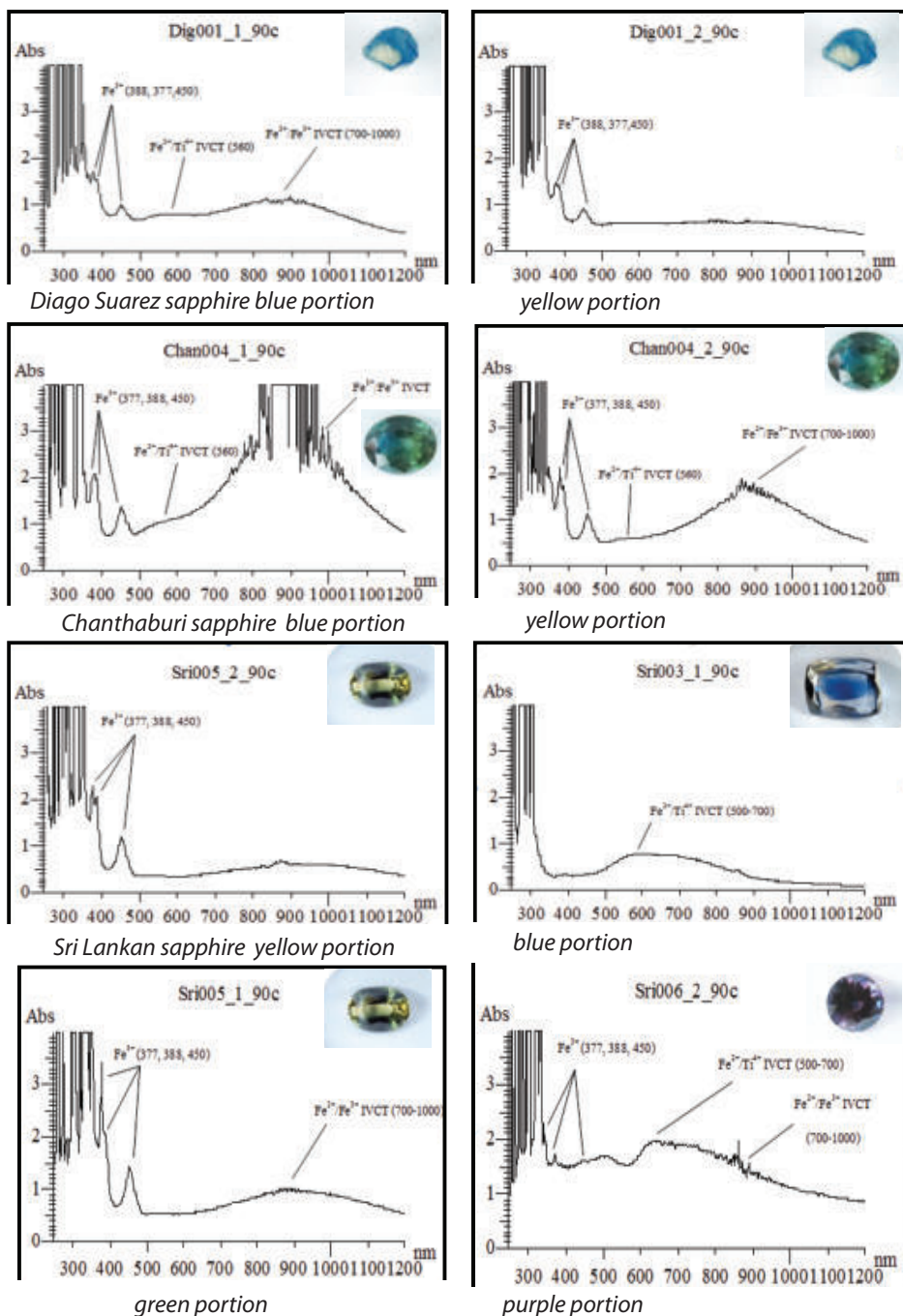


Figure 4. UV-Vis-NIR absorption spectra of the studied sapphires.

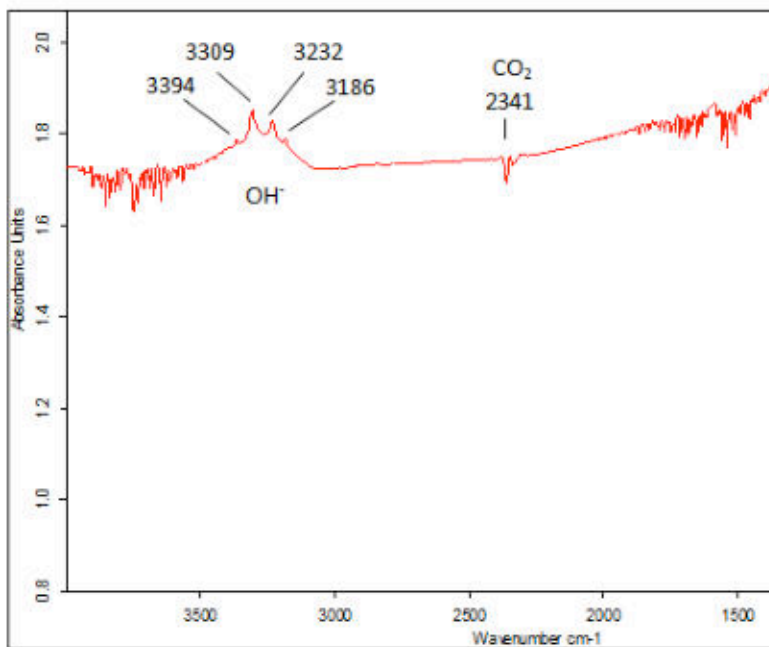


Figure 5. FTIR spectrum of purplish Sri Lankan sapphire

In conclusion, the bicoloured sapphires from basaltic sources, commonly display yellow or green and blue colour while those from metamorphic source can be found in more colour variation. The gemmological properties, inclusions and infrared spectral characteristic of the studied samples from both igneous and metamorphic sources can not easily be distinguished. However, the chromophore Fe_2O_3 content and the absorption spectra might be used as evidence in distinguishing these bicoloured sapphires.

References

- Khunkaew, Y., 2004, Spectroscopy of Thai Corundum, Master thesis, Chaing Mai University, Thailand, 137 p.
- Levinson, A.A. and Cook, F.A., 1994, Gem Corundum in Alkali Basalt: Origin and Occurrence, *Gems&Gemology*, Vol.30, No.4, pp. 253-262.
- Schwarz, D., Petsch, E.J. and Kanis, J., 1996, Sapphire from The Andranondambo Region, Madagascar, *Gems & Gemology*, Vol. 32, No. 2, pp. 80-99.
- Singbamroong, S., 2004, Spectroscopy of Lao Corundum ; Master thesis, Chaing Mai University, Thailand, 137 p.
- Smith, C.P., 2006, Infrared Spectra of Gem Corundum, *Gems&Gemology*, Vol. 42, No. 3, pp. 92-93.
- Thanasuthipitak, P., Worawitratnanagul, P. and Thanasuthipitak, T., 2009, Fe-Ti Variation in Blue Sapphires of magmatic and metamorphic Affiliations, *Proceeding of the 31st International Gemmological Conferences, Arusha, Tanzania*, pp. 67-69.

The History
of the International
Gemmological Conference

1952 - 2009



BIBOA, Forefather of the IGC.

The early “foundation stone” of the IGC was basically laid during a congress in April 1926 in Amsterdam. At the time the commercialization of cultured pearls required written rules of ethics, hence, members at the Amsterdam congress organized the International Federation of Associations of Manufacturers, Craftsmen, Wholesalers and Retailers of Jewellery and Gold and Silverware (BIBOA) (Bureau international pour la Bijouterie, Orfèvrerie, Argenterie).

This was followed with a congress of experts at the Hague during December 1926 and later with the 1st International Conference in Paris during January, 1928, where the name “cultured pearl” was proposed. Other resolutions favoured a minimum of 0.3 mm for holes drilled in pearls, to encourage governments to legalize the metric carat, study the problems of gemstone control, harmonization of standards for precious metals and steps toward the removal of luxury taxes.

The 2nd International Conference was also held in Paris, during October 1928, where 19 resolutions were adopted regarding cultured pearl names, the description of origin of rubies other than Burmese, the establishment of laboratories for control in different countries, which could cooperate with one another, the development of informative “propaganda” concerning precious stones and pearls and other resolutions..

From 1928 onward, a congress was held regularly, in advance prepared by well known international gemmological experts.

The next congress was held during May 1929 at the Hague, where all previous resolutions were reiterated in order to have these applied by every country.

The subsequent congress was held in London during May 1930, where 24 resolutions were adopted. These resolutions reaffirmed the importance to establish national gem testing laboratories empowered to examine both pearls and precious stones, using as model existing laboratories in Berlin, London, Paris and Vienna.

The adopted standards were 950/1000 for platinum, 750/1000 (18 Karat) and 585/1000 (14 K) for gold, while discussions continued for gold of 8 or 9 Karats. The silver standard was set at 800/1000.

The next International Conference was held at The Hague during May 1931, during which the enforcement of the various resolutions was examined. Members expressed regret at the absence of a testing laboratory in the USA. They also decided to use a standardized nomenclature for precious and “semi-precious” stones.

Members at the congress, held in Rome during May 1933, approved the definition of the diamond and the names “synthetic stones” and “imitations” (presented by Germany after research by Prof. K. Schlossmacher)

The following International Conference was held in The Hague during May 1934 and 13 members attended, representing Great Britain, Germany, France, Italy and Switzerland. Prof. Schlossmacher and Mr. G. Göbel were appointed as editors for the publication of an official nomenclature of gemstones.

However, during the summer of 1934 the Gemological Institute of America (GIA) published its own classification and nomenclature for precious stones, independent of the nomenclature list which would be published by BIBOA the following year.

The next International Conference was held in Berlin, during August 1935. Members encouraged the testing laboratories to remain in constant collaboration with each other at a time when the first synthetic emeralds were appearing on the market.

The members also adopted the statutes of the BIBOA

The subsequent congress was held at The Hague during May 1936. The gem traders present acclaimed the cooperation between laboratories and encouraged laboratory directors to meet each other during a special technical conference from which all commercial delegates would be excluded.

The first such technical conference took place during January 1937 at Aix-la-Chapelle with B.W. Anderson, G. Göbel and K. Schlossmacher present.

Thus began the international gemmological meetings.

The next International Conference was held in Paris in 1937 and during the 7th congress held in Lucerne, June 1938, the adoption of the BIBOA nomenclature by various countries was examined, as well as the purity of diamonds and standards for precious metals.

The following International Conference was scheduled to be at Prague during May 1939, but was changed for Luxembourg during the following September. However, due to the outbreak of war this event was also cancelled.

During the war years a congress took place at Munich during September 1942, which was attended by Dr. Gübelin (Lucerne), Dr. Harting (Berlin), K. Brenner (Vienna), A. Begeer (Holland) and Mrs. Cavenago-Bignami (Milan).

Discussed were topics concerning the international nomenclature, research on pearls and precious stones and the use of x-rays in gemmology.

After the war informal contacts resulted in a BIBOA board meeting on 15th June 1948, attended by members of Belgium, France, Great Britain, Italy, Holland and Switzerland.

The purpose of this meeting, where also Dr. Gübelin and Mr. Göbel were present, was to resume the work of BIBOA and to arrange a conference of experts.

This took place in Paris, during October 1948 where resolutions and directives published before the war (Lucerne, 1938) were taken up again.

The commission on "Diamonds, Pearls and Precious Stones" now planned the establishment of a permanent sub-committee of scientists. With this decision, the IGC began to acquire their present form.

The following participants were present during this Paris Meeting:

Mr. Göbel, (FR), director of the Public Service for Control of Precious Stones, Mr. F. Wolff (BE) from the editorial board of Technica, Mr. A. Selwyn (GB), from the Research Centre of Gold, Silver and the Jewellery Industries, Mr. K. Siess (A) director of the Austrian Research Centre for Precious Stones, Mr. J. Bolman (NL), gemmologist, and Dr. E. Gübelin, representing the European Federation of Gemmological Associations.

The next technical conference was held at Scheveningen (The Hague) during September 1950, but before (on 7th April) it was decided at a BIBOA board meeting in Brussels to allow Germany to participate again at this technical conference.

The participants formed a technical sub-committee which role should be –as specified by the chairman of BIBOA–

to advise the professional delegates. The chairman observed, however, that this sub-committee had already been in existence since the meeting at Aix-la-Chapelle (Aachen) on 9th January 1937.

Prof. Schlossmacher, who had organized the nomenclature list, chaired this commission and secretary was Mr. Göbel (France).

From now on technical meetings were annually and the next meeting was held at Idar-Oberstein during 3rd to 5th April 1951.

The agenda included nomenclature lists (both international and American), diamonds (characteristics, clarity and colour according to the USA system being set up), new synthetic stones (synthetic emeralds, synthetic diamonds, synthetic star ruby), new processes (artificial colouring), laboratory methods, x-rays of pearls and the lay-out of examination reports.

The following members attended this scientific meeting: Prof. Schlossmacher (G), Mr. Anderson (GB), Dr. Gübelin (CH), Mr. Wolff (BE), Mr. Bonebakker (NL), Mr. Tillander (SF), Mr. Strömdahl (S) and Mr. Dragsted (DK).

A list was drawn up of other gemmological institutes in the hope they would also attend these technical meetings in future, namely Mr. Shipley (Los Angeles), Mr. Crowningshield (New York), Mrs. Cavenago-Bignami (Milan), Mr. Rose (Hamburg), and Mr. Raub (G). In addition the hope was expressed that the Diamond Institute of Johannesburg and scientists of Norway and Australia will also attend.

At this point, the future framework of the I.G.C. was established.

At the London scientific congress during May 1951, new Articles of Association were drawn up, in which the gem associations participating in the BIBOA were replaced by the National Federal Committees, hence the newly proposed name of BIBOAH was adopted (Confédération Internationale des Associations de l'Industrie, de l'Artisanat et du Commerce des Diamonds, Perles et Pierres Precieuses, Bijouterie, Joaillerie, Orfèvrerie et Horlogerie). Later, this became CIBJO (Confédération Internationale de la Bijouterie, Joaillerie et Orfèvrerie).

At the Brussels meeting, during January 1952, BIBOAH was defined as an international public service organisation for liaison, information and direction to the industry, in order to "truly serve humanity".

The Brussels meeting was followed by a technical conference at Locarno during October, 1952.

At this conference Dr. Gübelin proposed the creation of a "Committee of an International Gemmological Association" consisting of one member per country, being the director of a laboratory or a gemmologist such as present at the Locarno meeting. The conference was attended by seven members.

Agreement of this proposal was later considered (Milan, 1960) to be the founding of the IGC and this Locarno meeting to be the the first IGC and the conferences from the 9th (in Helsinki) onwards are numbered on this basis.

1st IGC in Amsterdam

The first IGC meeting took place in Amsterdam, from 5th-7th October 1953, in the Netherlands and each country was represented by two delegates. Those attending were Great Britain, France, Germany, Switzerland, Norway, Finland and The Netherlands.

The creation of an international gemmological association was envisaged, while other discussions concerned conoscopy, magnetism, inclusions and the history of mineralogy.

Visits were organized to a diamond cutting factory, to the mineralogical and geological museum in Leiden and to an exhibition of gems ("Gems 53") at the Hague. The foundations of IGC were at this time securely laid. Fourteen delegates attended the conference.

The 2nd European IGC was held in Copenhagen from the 4th to the 7th October 1954.

Participants saw the Danish crown jewels, the mineralogical museum and the laboratory of gemmology. A farewell dinner was given by the Danish Goldsmiths' Guild. Ten delegates attended the conference.

The 3rd IGC was held in London from 3rd to 7th October 1955.

It was here that the official name I.G.C. was employed for the first time. France and Switzerland were represented by one representative each, while the six other participating countries, namely Denmark, England, Germany, Holland, Norway and Sweden had two each. For the first time, the working sessions took up the entire week. Visits, alternating with technical sessions, were made to the Natural History Museum, the British Museum, the Gemmological Laboratory of the London Chamber of Commerce and to Windsor Castle. The conference ended with a farewell dinner at the Goldsmith' Hall. Fourteen delegates attended the conference.

The 4th IGC was held in Munich from 25th to 29th September 1956.

It was here that also Spanish and Italian representatives participated for the first time. Eleven delegates attended the conference.

The 5th IGC was held in Oslo from the 1st to 4th October 1957.

Delegates from 11 different countries attended the Conference. Museum visits and social functions, in particular those organized by the Oslo City Hall, alternating with technical sessions. Special notepaper with IGC logo was provided by the organizers. Seventeen delegates attended the conference.

The 6th IGC was held in Paris from the 6th to 10th October 1958.

Delegates from two new countries attended for the first time, namely Austria and the USA. Great Britain sent three delegates. Visits were organized to the "Cabinet des Medailles", to Chantilly (where the pink Condé diamond was specially displayed for the members of the Conference), to the mineralogical laboratory of the Sorbonne and to the gemmological laboratory of the Chambre de Commerce et d'Industrie de Paris (CCIP). A farewell reception was given by the CCIP at the head quarters building. It was then decided that henceforth the IGC would be held every two years. Nineteen delegates attended the conference.

The 7th IGC was held in Milan from the 10th to 18th October 1960

But the Italian delegates called it the 8th IGC as they considered the meeting at Locarno in 1952 as the 1st IGC. Although two new countries had been invited, namely Australia and Brazil and had accepted, their representatives were unable to come to Italy. Great Britain sent 5 delegates. Social programmes were organized by the CCI

of Milan, the City Hall of Milan, the CCI of Alexandria and the National Museum of Science and Technology. On the last day, October 8th, an excursion was organized to Valenza, Aqui and Alexandria. Twenty six delegates attended the conference.

The 9th IGC was held in Helsinki during 4th to 8th October 1962.

In between the technical sessions, a one-day study trip was organized in order to have a break between the great number of technical sessions. Nineteen delegates attended the conference.

The 10th IGC was held in Vienna from the 4th to 8th October 1964.

Discussed were details regarding maw-sit-sit and the identification of cultured pearls with an organic implant. The question of new synthetics (synthetic emeralds by Gilson and Zerfass, symerald of Lech-leitner) and the issue of diamond grading were discussed at length. Twelve delegates attended the conference.

The 11th IGC was held in Barcelona from 2nd to 6th October 1966.

Main subject of discussion was the study of gem inclusions, emphasized during work sessions. Belgium and Australia were represented for the first time. Among the social activities were the reception at the City Hall and various cocktail parties. Also a visit to an exhibition of jewels created by local jewellers was on the programme. The Post-Conference excursion was to the Heusch imitation-pearl factory at Majorca. Twenty two delegates attended the conference.

The 12th IGC was held in Stockholm from 6th to 10th October 1968 with a welcoming reception on Sun 6th.

The King of Sweden's jade collection was exhibited to the conference participants at the Royal Palace who were also invited to an evening at the Stockholm Opera. Gemmological subjects discussed included a description of Chatham synthetic rubies produced by the flux fusion process, how to describe these and quantify colour. It was agreed that presentations in future not exceed 30 minutes in order to allow time for discussion and that abstracts of the talks would be given to the organizers as information to all participants. Twenty nine members attended the conference, including a new member from Southern Rhodesia.

The 13th IGC was held in Brussels from 27th September to 1st October 1970.

This time new delegates joined from Japan, Canada and Kenya. The Belgium Society of Gemmology gave a welcome reception at the Westbury Hotel. Apart from the technical sessions Dr. Gübelin showed his film "Mogok, la Vallée des Rubis". On October 1st a trip was organized to Antwerp to visit the Diamond Cutting Centre. During the evening the conference ended with a dinner at the Westbury hotel. Thirty four delegates attended the conference.

The 14th IGC was held at Vitznau (Switzerland)

From 25th to 28th September 1972 at an hotel located on the Lake of the Four Cantons, far from any urban centre. During the technical sessions Prof. Strunz discussed modern mineralogical classification as applied to gems. This was the year when an artificially coloured diamond of 104.52 carats, the "Deepdene", was discussed at length. This is considered the largest golden/yellow irradiated diamond in the world IGC members approved the determination "artificially coloured", previously obtained by Dr. Gübelin (Nov. 1969 and June 1971) B.W. Anderson (June 1971) and by R. Crowningshield (Sept. 1971).

On Tuesday a picnic excursion was organized to Mount Rigi. At the end of the technical sessions on Thursday 28th a farewell lunch was given and there-after all participants left by boat to Lucerne. Twenty nine delegates attended the conference.

The 15th IGC was held in Washington from 5th to 9th October 1975.

This was the first conference outside Europe. New participants came from South Africa (new diamond cuts) and Brazil (irradiation of beryl to make it blue, "halbanite"). This was the year two new flux fusion products were described: synthetic alexandrite and synthetic ruby by Kashan. The farewell dinner was held in the Gem Hall at the Smithsonian Institute, sitting next to the famous "Hope" diamond. Twenty seven delegates attended the conference.

The 16th IGC was held in The Hague from 9th to 13th October 1977.

During the technical sessions an interesting ladies' programme was also organized. Tuesday afternoon participants went to the Mineralogical Museum at Leyden University and were invited to a cocktail by the Organization of gold-, silver- and watch trade and industry at the Museum. On Wednesday evening the Dutch Diamond Publicity Committee invited all participants to a Dutch Diamond Evening at the Old-Wassenaar Castle. Two delegates reported here on Diamond Quality Grading in the U.S.A. and fancy-colour diamonds. A farewell lunch was held on Thursday 13th October. Thirty eight delegates attended the conference.

The 17th IGC was held in Idar-Oberstein from 23rd to 27th September 1979.

The welcome reception was at the Diamant- and Edelsteinbörse on Sunday evening and the technical/poster sessions were from Monday to Thursday. During this period a visit to the gemstone museum in Idar was organized and on Wednesday afternoon, at the German Gemmological Training Centre, demonstrations and teaching techniques were explained. This was the year of "korite", a fossil extracted from an occurrence of *Placentoceras meeki* and of "taprobanite" which was later (1984) determined to be a variety of taaffeite. The Japanese delegates mentioned that 90% of Thai sapphires were being locally heat-treated (treatment usually lasting 7 to 8 hours). The Australian delegate mentioned that yellow and green sapphires were also treated in Australia. Not to be outdone, the Idar-Oberstein lapidaries showed their own furnaces to the IGC members and gave glimpses of their dye treatments. A farewell lunch was offered by Mrs. Bank at their home with traditional Brazilian food. Forty two delegates attended the conference.

The 18th IGC was held in Japan from 7th to 14th November 1981.

An open conference day was organized for Japanese gemmologists in Tokyo before the conference itself and another open conference was held in Kyoto, after the IGC conference. This time representatives came from China, Korea, Hong Kong, USSR, Singapore, Sri Lanka and Taiwan. Participants enjoyed the opening ceremony, on Sunday evening which included local folk-dances. The technical/poster sessions were from 9th to 12th November with an interesting film session during one evening. Thursday, after lunch, all participants left by train to the Miyako hotel in Kyoto. From here excursions were organized to the Mikimoto pearl farms and to the fresh-water pearl farms at Lake Biwa. The farewell party was particularly sumptuous. Forty four delegates attended the conference and a 57 page "Collected abstracts" was published.



Group photo at the 18th IGC in Japan

The 19th IGC Conference was held in Sri Lanka (Beruwela)

A tropical beach location, from 30th October to 5th November 1983. The opening ceremony was a traditional Oil Lamp ceremony, symbol of wisdom, prosperity, good health and friendship. Technical sessions were held from 1st to 4th November with a full day excursion, on the Wednesday, to the interesting gemstone mining area at Ratnapura. The farewell dinner was hosted by the Gemmological Association of Sri Lanka and all participants enjoyed the cultural show. Twenty three delegates attended the conference.

The 20th IGC was held in Australia (Sydney) from 29th September to 5th October 1985.

At the Manly Pacific International hotel near Sydney and opened with an ice-breaker cocktail party on Sunday evening. Interesting social tours were organized for spouses and guests during the conference. Many technical sessions were held between Monday and Friday on which day the conference ended with a farewell party and closing speech by Dr. Gübelin. During the last day, rules were adopted to specify the role and the holding of the meetings, to nominate a number of "international members", to take steps to avoid commercial intrusions in the debates, to require that each delegate has some publication to his name and to produce collected abstracts following each conference. It also was reiterated that the official language is English and that the aim of the IGC is to promote gemmology through institutes and laboratories of various countries. The Post-Conference excursion started on Sunday morning by bus to Dubbo with a visit to the Wellington limestone caves. The tour continued the next day to the Lightning Ridge Opal Field, source of black opals. After 2 days participants went to the Inverell-

Glen Innes district to visit sapphire deposits and mines, where they also spent 2 full days. A “Collected Abstract” was published and thirty seven delegates attended the conference.



The 21st IGC was held in Brazil (Rio de Janeiro) from 20th September to 4th October 1987

The opening ceremony was at hotel Atlantico Sul with dinner and entertainment. The technical sessions were held from Monday 21st to Thursday 24th September and an interesting social programme was organized for spouses and guests during this period. A farewell dinner was given on Thursday evening. The Post-Conference excursion was through parts of Minas Gerais, hence, all participants flew from Rio to Belo Horizonte on Saturday 26th. From here visits were organized to the Sampaio and Boa Vista diamond mines.



Other highlights during the following excursion days were: the Tejucana diamond dredging operation, visit to the Urubu and Marambaia pegmatite mines, in Governador Valadares a visit to the Ailton Barbosa mineral collection and the Itabira (Belmont) emerald mine. A short second excursion was to Ouro Preto to visit the famous Capão Imperial Topaz mine. A well presented document of the "Transactions of the XXI International Gemmological Conference Brazil 1987" (131 pages) was given to all participants. Thirty nine delegates attended the conference.

The 22nd IGC was held in Italy at Tremezzo (Lake Como) from 23th to 29th September 1989

The Post-Conference excursion was from 30th September to 8th October. The official opening was on Sunday evening by courtesy of the Municipality of Tremezzo and the conference and technical sessions were also held at the Tremezzo Palace Grand Hotel. The organizing committee had a most interesting tour/entertainment programme prepared for spouses/guests during the technical session period. Before the conference, an open scientific session was held in Milano for Italian gemmologists. During both the scientific session and the following excursion, entertainment was sponsored by the CCI of Milan, Tremezzo City Hall, Carrara CCI and the Roberto Cusi Co.



Group photo at the 22nd Tremezzo, 1989.

The Post-Conference tour from September 30th to October 8th started with a bus trip to Rapallo and from there a boat cruise to Portofino (by courtesy of Lalla and Roberto Cusi). Other highlights of the tour were a visit to Volterra, the ancient Etruscan town with the Etruscan Museum Guarnacci, the Carrara marble quarries and sculpture workshop, as well as the Marble Museum and marble saw-mill. In Firenze the group visited the "The opificio delle Pietre Dure" and in Sorrento/Torre del Greco the famous Coral Museum and coral factories. Saturday 7th was devoted to a trip to Rome and visit to the Cappella Sistina and the Vatican Museum. The excursion ended with a return trip to Milan. Noteworthy is the introduction of the IGC logo, designed by the well known artist Roberto Sambonet and manufactured as a gold jacket pin by the Roberto Cusi Co. and presented to each delegate. Forty three delegates attended the conference, who all received a copy of the 63 page "Scientific Program and Abstracts".

The 23rd IGC was held in South Africa (Stellenbosch) from 5th to 18th October 1991.

The Pre-Conference Tour was from 5th to 13th October and the technical sessions from 14th to 18th October. The official opening was on Sunday evening with a welcome cocktail at the Public Library Hall at Stellenbosch. All technical sessions were held at the same locality. During this period an interesting social program was arranged for spouses and guests to a winery, Kirstenbosch botanical gardens, Cape Point, Groot Drakenstein, Stellenbosch University, etc. On Wednesday evening, after the technical sessions, the Mayor of Stellenbosch invited the participants to a cocktail party at the Town Hall.



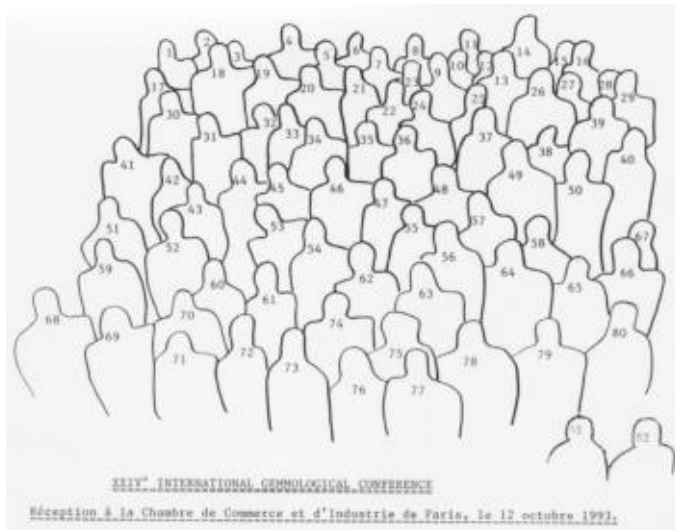
The Pre-Conference Tour started at the Johannesburg airport on Saturday 5th October from where participants were transported to a local hotel. The principal sponsor during this tour was De Beers Group, who assisted during visits to diamond mines (Premier diamond mine), Big Hole (Kimberley) and alluvial diamond diggings at the Orange River. The Chamber of Mines arranged a visit to a gold mine on the famous Witwatersrand and lunch by invitation of the Mine Manager. On Saturday morning all participants flew from Kimberley to Cape Town to attend the Conference. A booklet with abstracts and address list of all participants was made available. Twenty seven delegates attended the conference.

The 24th IGC Conference was held in Paris during the 2nd – 15th October 1993.

Technical sessions were between 11th and 15th October. The pre-conference gemmological/geological excursion started with a train journey to Lyon on Saturday 2nd October and all participants were issued with a well prepared 62 page tour guide, describing in great detail all activities during this excursion (including four pages on the famous Beaujolais vineyards and wines). During the excursion various museums were visited (mining museum St. Pierre la Palud, Natural Sciences Museum Grenoble). Also visited was a synthetic corundum factory in Jarrie and in Lyon a visit was organized to a jewellery factory and the "School of Jewellery".

The very interesting geological/mineralogical volcanic region of Le Puy was well worth visiting. Sunday 10th October a sightseeing tour of Paris/Versailles was organized and during the evening the participants enjoyed a welcome cocktail. At the end of the technical sessions, on Friday evening 15th a Farewell Dinner was held at the famous "Le Printemps".

Last but not least the organizing committee had also arranged a very interesting ladies' programme.



24th IGC reception at the Chamber of Commerce in Paris

1.M.Brandm (Paris) 2.F.Bouqueau (Paris) 3. M-P Bouqueau (Paris) 4. J-R Mossmann (Paris) 5. D..Piat 6.A. Mossmann-Bouquillon (Paris) 7. B. Lasnier (Fr.) 8. A. Brand (Paris) 9.E. Fritsch 10. R.Signet (Australia) 11.J.Shida (Japan) 12. C.Sapalski (Spain) 13. G.Browne (Australia) 14.H.Meyer (USA) 15. Muriel Saul 16. E.Gübelin 17. Madame Cambournac (Paris) 18. B. Cambournac (Pres.Chamber /Commerce) 19. Prof. H.Curien (Paris) 20. D.Schwarz (Switzerland) 21. A.Schwarz. 22. F.Fayette (Canada) 23. P.Entremont (Paris) 24. J.Saul (Paris) 25. G.Bosshart (Switzerland) 26. A.Levinson (Canada) 27. F.Pough (USA) 28. D.Piat (Paris) 29. M-L.Dele (Fr.) 30.J-P.Poirot (Paris) 31.N.Haralyi (Brasil) 32. C.Sevdermish (Israel) 33.M.Sevdermish 34. H.Pienaar (S.Africa) 35. C.Moreaux (Belgium) 36. C.Pienaar 37.H.Hänni (Switzerland) 38.S.Ehrman (India) 39.R.Kane (USA) 40.H.Kane 41.G.Bukin (Russia) 42. M.Superchi (Italy) 43. C.Farina (Italy) 44.C.Petrella (Brasil) 45G.Tombs (Australia) 46. J-M.Dereppe (Belgium) 47. J.Tombs 48.M-C. Cusi-Lamperti (Italy) 49. G.Graziani (Italy) 50. I.Estive-Madrid (Spain) 51. E.Bukina (Russia) 52. G.Zoysa (Sri Lanka) 53. V.Balitsky (Russia) 54. I.Eliezri (Israel) 55. L.Kanis (Germany) 56. J.Kanis 57.R.Cusi (Italy) 58.C.Duchemin (Paris) 59. E.Buhtiarova (Russia) 60. T.Vitalis (Paris) 61. S.Eliezri (Israel) 62. H.Tllander (Finland) 63. J.Ponahlo (Austria) 64. K.Schmetzer (Germany) 65. S.Tombs (Australia) 66.R.Harding (England) 67.J.Harding 68. U.Henn (Germany) 69. G.Becker (Germany) 70. H.Bank (Germany) 71. I.Bank 72.M.Jobbins (England) 73. A.Jobbins 74. J.Koivula (USA) 75. K.Koivula 76. S.Scarratt (Thailand) 77. K.Scarratt 78. A.Chikayama (Japan) 79. C.Poirot (Fr.) 80. Ph.Maitrallet (Paris) 81. Madame J.C.. Penauille (Paris) 82.J-C Penauille (member of C.C.I.P.).

The 25th IGC Conference was held in Thailand during 20th October – 5th November 1995.

Delegates arrived at the Holiday Inn Crowne Plaza hotel in Bangkok on Friday, 20th October. The following day was an Open Conference Day for the gem industry in Bangkok, where several IGC members gave talks throughout the day. The welcome dinner and opening ceremony took place that evening. On Saturday morning a visit was arranged to the Grand Palace, including Wat Pra Kaew with its famous "Emerald Buddha". After lunch all delegates, observers and their spouses travelled to the Rayong Resort hotel (appr. 3 hours by bus). The Conference presentations took place between Monday 23rd and Friday 27th October. The only "break" was on Wednesday afternoon when participants and guests went to Pathaya to visit fruit gardens, and Nong Nuch village. A seafood dinner was enjoyed at the Nang Nuai restaurant and the evening ended with the Alcazar Show in Pathaya. The Gala Dinner, on October 28th, was at the Rayong Resort hotel. During the Conference guests were entertained with a visit to the islands of the coast of Rayong, a visit to the Kao Chamao Waterfall, Kao Wong Park, a speed boat tour to coral islands and a visit to Bo Rai border town and alluvial ruby mine. They also witnessed an eclipse of the sun. Proceedings of the abstracts regrettably were not issued.



Group photo at the 25th IGC at the Rayong Resort Hotel, Thailand

The organizing committee had also arranged a splendid 4 days' excursion to the Chiang Mai region to visit an orchid farm and elephant camp. Near the Myanmar border a jade cutting factory and the famous ruby market were visited. A boat trip on the Mekong river at the Golden Triangle was fascinating and so was the visit to Hill Tribe villages in Doi.

The 26th IGC was held in Idar-Oberstein from 27th September to 3rd October 1997.

A Post-Conference excursion was organized between 4th and 11th October to a region of Eastern Germany. On Sunday 27th the conference participants went by bus to the Hambachtal Conference Centre, where they enjoyed a welcome dinner. The technical and poster sessions were held at the same centre between 29th September and 2nd October and ended with an original Spießbraten dinner. On October 3rd a full day excursion was organized to the volcanic Eifel region, well known for hauyne, sanidine and olivine occurrences. The day ended with a gala dinner. The participants of the Post-Conference excursion from October 4th to 11th visited the Thuringen/Saxony region with, among others, the porcelain industry of Meissen, the University of Jena with the optical museum, the mining museum of Freiberg and the famous "Green Vault" of Dresden. An 87 page "Abstract Volume" was published, including a list of all participants.



Group photo at the 26th IGC at the Gemmological Institute in Idar.

The 27th IGC was held in India between 25th September to 1st October 1999

The Pre-Conference excursion was from 19th to 24th September with a Post-Conference excursion from 2nd to 7th October. Highlights of the Pre-Conference excursion were visits to the Zeolite quarries of Jalgaon and the famous Ajanta Caves (200 B.C. to 600 A.D.). The Conference opened on Friday morning 24th September with an International Gemmological Seminar for local gemmologists and the local jewellery trade. The inauguration dinner was held at the famous Taj Mahal hotel in Bombay. All delegates, spouses and their guests left by plane for Goa on Sunday morning where the technical/poster sessions were held at the luxury "Cidade de Goa" hotel between 27th to 30th September. In between, on Wednesday afternoon, an excursion was arranged to Veling, Mangeshi temples and old Goa churches. The day ended with a boat cruise on the river Mandovi. During the conference a cultural/entertainment programme was organized every day for the spouses and guests of the delegates /observers. The conference ended with a gala dinner on the Friday evening with a "Glimpses of India Show" at the Cidade de Goa hotel.



Group photo at the 27th IGC in Goa, India

Saturday morning participants flew back to Bombay on their way home and with a flight from Goa to Bangalore the remaining participants started their Post-Conference Tour to the state of Karnataka from 2nd to 7th October. Highlights of this tour were a visit to the famous 12th Century temples of Belur and Halebeedu and to see the world's tallest monolithic statue of Lord Bahubali at Shravanabelagola. Also visited were ruby mines at Chena-patna and the cutting workshops, as well as a silk emporium and a wooden handicraft manufacturing centre. On October 7th all participants returned to Bombay. A Gemmologists Handbook was presented to all participants, issued by the Forum of Indian Gemmologists for Scientific Studies, including abstracts of all presentations and list of delegates.

The 28th IGC was held in Spain (Madrid) from 6th to 12th October 2001.

Saturday 6th was an Open Conference Day to interact with the Spanish Gem Trade & Industry and several IGC members gave talks. Also most delegates/observers, spouses and guests arrived that day at Madrid. There was a full-day excursion on Sunday 7th October to Segovia and a visit to the El Escorial monastery. The day ended with the official inauguration of the 28th IGC and Welcome dinner. The technical/poster sessions took place between 8th to 11th October at the CEE. For spouses and guests an interesting programme was organized daily. Friday 12th October is a Holiday in Spain called the Spanish Day. Hence, all participants went by bus to the Ranch Los

Arcos del Rey for a Spanish horse demonstration and enjoyed a typical “Tapas” lunch and classical Spanish music. The gala-dinner and closing of the conference was during the evening at the restaurant Pedro Larumbe.



Group photo at the 28th IGC in Madrid

Highlights of the Pre-Conference Tour, from 3rd to 5th October, were a visit to Arnedo to see the Dinosaur foot-prints and the visit to the mine at Navajun in the Rioja region, with quarries of the perfect pyrite cubes, some up to 20 cm. The Post-Conference Excursion was from 14th to 21st October and the first stop was at Villanueva, a new sapphire occurrence in marble. In the afternoon a visit was made to the medieval city of Toledo. Other highlights during this excursion were a visit to the historic cinnabar mine at Almadén, granite quarries at Quintana de la Serena with cutting/polishing factories, visit to skarn minerals at Jérez de los Caballeros, the Parador of Cáceres (a 14th c. Palace), a visit to rose quartz occurrences in pegmatites near Plasencia and to Salamanca with the oldest university in Spain. The organizing committee published “Extended Abstracts” (109 pages), a conference programme with a list of all delegates/observers and detailed Pre- and Post-Conference programmes.

The 29th IGC was held in China (Wuhan) from 12th to 18th September 2004.

The conference was planned for 2003 but had to be postponed due to bird flu risk. The executive meeting took place on October 12th and the opening ceremony, with Chinese dances, was at the University of Geosciences on the 13th September. During the technical/poster sessions two tours were organized, namely to the Plait Bell Museum, where the 2400 year old tomb of Marquis Li is exhibited together with many bronze ritual vessels, weapons, etc. and specially of interest is a whole Plait Bell of 65 pieces with a total weight of 2500 kg and still operational. Also a jade workshop was visited. The other tour was to freshwater pearl farms at Donggen, ca. 60 km from Wuhan, where approximately 90 tons of cultured freshwater pearls are produced annually. The organizing committee had also arranged an interesting programme for the accompanying spouses and guests during the conference. The closing ceremony took place at the University during the afternoon of September 17th, followed with a banquet at a local restaurant. The Pre-Conference excursion was from 10th to 12th September and included a visit to the diamond bourse and jewellery market in Shanghai, pearl farms and market in Suzhou and a night-time visit to a turquoise mine in Maanshan.

The Post-Conference excursion was from 18th to 23rd September. Participants flew from Wuhan to Jinan and from there travelled by bus to the Changle basalt-type sapphire occurrences, visited the Zibo-Mengyin diamond mine, and Confucius temples at Qufu and then participants flew to Beijing where a visit was organized to the national gemmological testing centre. The afternoon of September 21st was reserved for a visit to the Imperial Pa-

lace. On 22nd bus ride to Zhangjiakou to visit the Damaping peridot diggings and jewellery factory, and on 23rd climb of the Great Wall and short visit to the Ming graves. Delegates were given an extensive 220 page handbook, containing all abstracts, list of delegates/observers, details of the Wuhan and Hong Kong Institute of Gemology and other interesting gemstone information.



The 30th IGC was held in Moscow from July 15th – 19th 2007

It was arranged by Prof. Dr. Vladimir S. Balitsky. The Academy of Sciences managed the conference which commenced with a pleasant ice-breaker on a tourist boat on the Moscow River. However, the attendants badly missed all dinners and evening entertainment, which were the courtesy of the organizing hosts at all previous conferences. Not even a gala dinner in honour of the 30th IGC Jubilee was offered. The meetings took place in the impressive Presidium Building of the Russian Academy of Sciences and included a substantial poster session. The conference
problems, a
major cons



Group photo at the 30th IGC in Moscow

Half-day excursions included a visit to the Diamond Treasury which, with its diamonds and oversized nuggets

of gold and platinum, was the highlight of the conference. Other visits included the Weapons Hall (Oruzheinaya Palata), the Pushkin Art Museum and the Tretyakov Art Gallery.

A pre-conference field trip, July 11-14, to the Sakha-Yakutia diamond area including visits to the Internationalnaya mine (to the -720 m level) and unique Kimberlite museum was capably organized by Y.P. Solodova and Maria S. Alferova. An enjoyable post-conference tour organized by E.P. Melnikov, L.E. Serkova, Warren Boyd and M.S. Alferova to the Urals consisted of visits to the Malyshevo Emerald Mines (underground), the Novo-Karkodinskoye demantoid deposit, the Urals Geological Mining Academy Museum as well as a city tour of Ekaterinburg in which memories of the Tsar and his family were very much present. Other field trips included St. Petersburg and visits to the modern Arkhangelskaya open-pit diamond mine and sorting room in the Lomonossov area which were particularly interesting.

The 31st IGC was held in Arusha, Tanzania, from 9 till 14 October 2009

It was convened by Dr. John M. Saul and Mark Saul. Virtually all participants stayed at the Arusha Hotel where the conference itself was held, providing good opportunities for exchanges in comfortable Western style surroundings. An ice-breaker the evening of October 9th was attended by about 200 people including the District Commissioner and numerous journalists. Dinners were organized in different hotels or lodges each evening. Presentations the following days were grouped into sections: 1) Pearls, 2) Coloured Gems (East Africa, Ethiopia & Madagascar), 3) Coloured Gems (General), 4) Coloured Gems (Asia & Europe), 5) Diamonds, and 6) Treatments & Laboratory Determinations. There was no poster session but a few posters concerning East African gems were put up in the meeting room itself.



Group photo at the 31st IGC in Arusha

The field trips were efficiently run and included visits to the TanzaniteOne Mine at Merelani and the Longido Ruby Mine, with several participants going underground at both. At Longido, permission was obtained to collect freely from the decades-old tailings piles. A third trip was made to diggings that had commenced a few weeks previous at the emerald and alexandrite deposit at Lake Manyara. Game drives to Arusha National Park and elsewhere allowed participants to view a great variety of animals. Some delegates then visited the Ngorongoro crater (spectacular wildlife scenes) and crossed the Serengeti Park, driving on to the vast Williamson Diamond Mine where they were very graciously received. Others flew to southern Tanzania to visit Swala Gem Traders' Mahenge spinel deposit. Extended Abstracts were issued in an 87 page publication.

Outlook

After 31 International Gemmological Conferences, it is clear that this is the longest surviving conference in this field to remain in its original format. During its history, invited delegates have been present from 33 countries: Australia, Austria, Belgium, Brazil, Canada, China, Czech Republic, Denmark, England, Finland, France, Germany, Greece, Hong Kong, India, Israel, Italy, Japan, Kenya, Korea, Netherlands, Norway, Russia, Singapore, South Africa, Spain, Sri Lanka, Sweden, Switzerland, Taiwan, USA and Zimbabwe.

IGC Rules and Operating Procedures.

During the 20th IGC, which was held at Sydney on October, 1985, the following rules and operating procedures were agreed for future meetings of the IGC:

1. Prime objective is the exchange of gemmological experiences,
2. Gemmology is to be the platform for all topics and to be regarded as the principal theme.
3. It was decided that attendance at all further Conferences should be by invitation and determined, where necessary, by the Conference Secretary and the Executive Committee.
4. Each country with a gemmological association should send two official delegates of which one may be a director of the national gemmological laboratory (where appropriate).
5. All delegates are to be encouraged to present papers, but this would not be mandatory.
6. All delegates must have a publishing record and all papers at IGC meetings must be presented in English, both written or spoken.
7. The Conference to keep foremost in mind the prime objectives and avoid dilution/confusion of this objective which, if not maintained, could result in a bland organization without any status or credibility.
8. No peripheral commercial activity and there should be no blatant sponsorship of any kind.
9. Secretary to act as clearing house with regards the relevant gemmological information of a material nature, especially in respect of new synthetics.
10. Promote the development of gemmology through educational institutes and laboratories in various countries. agreed at Sydney,
11. The following nine Honorary Members were elected by the members present:
Dr. E. Gübelin, (Switzerland) Prof. A. Chikayama, (Japan) Mr. R.T. Liddicoat, (USA), Mr. R. Crowningshield (USA), Mr. M. Masso, (Spain), Mr. O. Dragsted, (Sweden), Dr. F.H. Pough, (USA), Mr. O. Chalmers (Australia) and Dr. J.M. Saul. (Kenya).

During the 29th IGC in Wuhan (China), the above rules and standard procedures were discussed again and the following details were adopted:

Membership, honorary members, who are senior members of the IGC, are elected by delegates on an as-required basis.

Delegates, who are elected from observers, on the recommendation of the Executive Committee, from those observers who have presented (in English) worthwhile presentations (either lectures, and/or posters) at three successive IGC meetings before becoming eligible for election as a delegate.

Observers, internationally recognised gemmologists who are invited to attend IGC meetings on the invitation of either the Executive Committee, Delegate/s from the country in which they are resident, or the Conference Secretary of the country in which the IGC meeting is to be held.

Applications for Observer status, which shall be supported by a pertinent CV and list of publications, should be

submitted to the Executive Committee for consideration before any invitation to attend an IGC is offered by the Conference Secretary.

Executive, the day-to-day administration and decision making of the IGC shall be overseen by an Executive Committee that meets formally at IGC meetings, and in between meetings conducts the routine business of the IGC by e-mail. Following nomination, new members of the Executive Committee shall be elected by a majority vote of delegates at the business meeting that follows each IGC,

From time to time, the Executive Committee shall elect a Chairman (woman) and a Honorary Secretary who will be responsible for detailed administration and the distribution of decisions of the Executive Committee to Honorary Members and Delegates.

Written minutes shall be kept for all meetings of the Executive Committee and general business meetings of delegates. Copies of these minutes shall be circulated by the Honorary Secretary to eligible Honorary Members and Delegates.

IGC Meetings should be held every two years in a host country approved by Honorary Members and Delegates. Historically these meetings have been held in odd calendar years.

IGC meetings should be timed so as not to clash with other meetings (e.g. IMA meetings) that delegates are likely to attend.

The venue for IGC meetings should alternate between European and non-European countries.

A country wishing to host an IGC meeting shall submit their proposal first to the Executive Committee and then formally present their proposal to delegates. The decision to accept or reject a proposal to host an IGC meeting will be made by majority vote of Honorary Members and Delegates present at the IGC business meeting or electronically if an IGC meeting is not being held at the time a decision needs to be made.

Countries hosting IGC meetings shall establish their own administrative structures to ensure the efficient planning and operation of the IGC. Cost involved in hosting an IGC shall be met by the Registration Fees paid by Honorary Members, Delegates and Observers attending the meeting, and financially sponsored from private, institutional and government sources. Day-to-day administration for an IGC shall be the responsibility of an elected Conference Secretary, who shall be either an Honorary Member or Delegate of the IGC.

General responsibilities of the Conference Secretary of each IGC include:

- Planning and implementation for the IGC of:
 - pre-conference activities
 - post-conference activities
 - the formal IGC conference
 - associated cultural activities and events
 - guest entertainment program
 - all finances
 - receipt and compilation of abstracts of papers
 - publication of proceedings of IGC conference
 - implementation of poster presentations
- Obtaining the necessary government permissions and other political factors
- Organisation of formalities required for different foreign visitors in the host country, e.g. visas, special permissions, etc.

Attendance at IGC meetings, of Delegates and Observers from countries other than the host country, shall be restricted to a maximum of five registrations per country. This restriction does not include Honorary Members.

Each IGC shall consist of a minimum of:

1. Two to three day pre- and post-conference study excursions to areas and facilities of gemmological interest.
2. A one-day session, prior to the IGC, at which previously nominated delegates and/or observers will be invited to give presentations to gemmologist members of the country hosting the IGC.
3. A five-day professional conference that shall consist of:
 - formal papers of 15 minutes duration, followed by 5 minutes of questions and answers.
 - Poster presentations shall be scheduled independently so that adequate time is allowed for each poster to be presented by its author/s and then have its content available for discussion by interested delegates.
4. A business meeting for delegates of a maximum of 1 hour duration that traditionally follows closure of the IGC professional conference.
5. A one-hour general discussion session to allow Honorary Members, Delegates and Observers time to exchange opinions on future directions of the IGC.

To minimise duplication of content, the titles and brief outlines of all papers, which an Honorary Member, Delegate or Observer plans to present at an IGC meeting, shall be submitted to the Executive Committee for approval.

Illustrations used for presentations at IGC meetings shall be presented in CD ROM (not laptop computer), 35 mm slide, or OH projector formats.

If feasible, future meetings of the IGC should be held at the hotel/institution in which the accommodation for Honorary Members, Delegates and Observers has been arranged by the host country's organizing committee.

If sufficient seating is available at the venue/s for future IGC lectures, gemmology students from the country hosting the IGC shall be encouraged to attend lectures presented at that IGC.

At the Arusha IGC, during October, 2009, the Executive Committee acknowledged the contribution of the past Execo members and four of them were awarded an honorary membership of IGC, namely Alan Jobbins, Prof. Ichiro Sunagawa, Dr. Jan Kanis and Prof. Herman Bank.

The Executive Committee also agreed that all matters concerning the IGC should continue to cc e-mail of the senior Execo members.

During the Arusha committee meeting Mr. Tay Thye Sun mentioned that he has been secretary of IGC for two terms now and indicated that he would like to step down. Mr. Gamini Zoysa proposed Dr. Jayshree Panjekar as the new secretary and the Execo voted for her unanimously.

During a discussion at the Arusha Execo meeting Mr. Gamini Zoysa said he prefers to keep the IGC as simple as possible so as to facilitate the working of the Execo. He compared the previous IGC to now, at that time there were only 25 members attending the conference and that administration and logistics was kept very simple. Over the years, IGC has grown into a larger group, which has created administrative and logistic problems for the organizers of the conferences.

Following an unpleasant experience at the TanzaniteOne mine, it was decided that delegates in future will have privileged access to mines, exhibitions etc., whenever the number of visitors is limited by the host(s).

It was also confirmed at Arusha that the next IGC venue will be Switzerland (Interlaken) and John Saul handed over the IGC flag to Michael Krzemnicki under applause from delegates and observers.

What started as a meeting of eight European gemmologists in 1952, the IGC has grown into a large circle of friends representing some thirty nationalities.

These meetings have gradually widened to include also representatives of gemmological laboratories with its goal to expand gemmological knowledge world-wide.

Jan Kanis

Veitsrodt, Germany, April, 2011 / rev. 13 June 2011

Acknowledgements

I thank Dr. John Saul for his summary contribution of the Moscow and Arusha IGC meetings and Mr. Alan Jobbins and Mr. George Bosshart for their assistance as editors and contributors. Last but not least a great source of information was the publication "Origin of the IGC" issued during the 24th IGC in Paris (1993).